Gene-Environment Interactions In Myopia

A thesis submitted to Cardiff University for the degree of Doctor of Philosophy

By

Yu Huang

School of Optometry and Vision Sciences
Cardiff University

August 2018

Supervised by Prof Jeremy A. Guggenheim,
Prof Jonathan T. Erichsen

Acknowledgement

It has been almost 4 years since I start my PhD, during these years, I have moved from Hong Kong to Cardiff, met many people who gave me lots of help and finally, ended my PhD with satisfaction and gratefulness.

Firstly, I would like to express my deepest gratitude to my supervisor, Professor Jeremy Guggenheim, who guided me in the myopia research world with his broad knowledge, patience and British humour. As a modest man, he never saves his praises to his students, and always encourages us to think creatively and to work hard. It is my great honour to study with him, a wise man, a life mentor and a role model.

Meanwhile, I am heartily thankful to my supervisor Professor Jonathan Ericson for his insightful academic and career suggestion. I would also like to thank my thesis advisor Professor David Whitaker sincerely for providing me with lots of helpful suggestions.

It has been my great privilege and pleasure to be able to work with Rupal, Neema, Alfred and Denis, who gave me warm support and encouragement for my study and daily life in the past few years. In addition, I owe earnest thankfulness to Asma, Nikki, Lindsay, Grant, James, Kathy, Sharon and Aysha, I would not have enjoyed my PhD life so much without their friendship. And I would also extend my gratitude to the staff members at the School of Optometry and Vision Science: Tony, Sue, Phil, Luke and Judith, for their generous help in all matters.

During my stay in Hong Kong, it is a pleasure to thank Dr Chea-Su Kee and Professor Shea-Ping Yip from the Hong Kong Polytechnic University, both of whom provided me with lots of support and suggestions when I started my experiments. I also would like to thank KK, Panfeng, Xiao Hu, Bian Bian, Bing Jie, Rachel and Samantha from PolyU, for their help with lab work and daily life.

Last but not the least, I owe my greatest gratitude to my family. They gave me endless love and understanding, and most importantly, they taught me to be a person with an unwavering and noble personality. Only with their support, can I realize my dream and become the person I would like to be.

Summary

Myopia, as a common ocular disorder, is caused by both genetic and environmental factors. Conventional genome-wide association studies (GWAS) in humans have limited power to detect myopia genes partly due to the complex interplay between genes and environment. Here, I performed a GWAS in a sample of chicks with form deprivation (FD) myopia, aiming to reduce environmental complexity and increase the statistical power to detect genetic variants that confer susceptibility to this environmentally-induced myopia phenotype.

The degree of FD myopia was quantified by measuring the treatment-induced changes in axial length (ΔAXL) and mean spherical equivalent (ΔMSE). Body weight, sex, and batch were evaluated as potential confounding factors. To reduce costs, chicks in the phenotype extremes (lowest or highest ΔAXL, within each batch) were selected for genotyping.

To identify genetic variants conferring susceptibility to myopia, GWA analyses for ΔAXL and ΔMSE were applied to the genotype data. After adjusting for confounding factors, genetic variant rs317386235, located between the genes PRKAR2B and PIK3CG exceeded the Bonferroni corrected significance threshold for ΔAXL.

To complement the GWAS findings, an RNA sequencing transcriptomics analysis was performed, using retinal tissue from the treated and control eyes of chicks with high or low-susceptibility to myopia. This revealed 516 differentially-expressed genes, identified using a combination of three analysis tools.

In order to discover more about the biological function underlying the GWAS and transcriptomics analysis results, pathway analyses were conducted. The pathway analysis implicated gene sets relating to circadian rhythms, extracellular matrix (ECM) and structural remodelling, energy generation, oxidative stress, glycometabolism and lipid metabolism.

Table of Contents

List of Figures

List of Tables

List of abbreviations

ACD	Anterior Chamber Depth	GWAS	Genome-Wide Association Studies
AD	Autosomal Dominant	het-so	Heterozygous Strength Offset
AL-CR	Axial Length - Corneal Radius Ratio	het-so-otv	Heterozygous Strength Offset off Target Variant
ALSPAC	Avon Longitudinal Study of Parents and Children	HGF	Hepatocyte Growth Factor
APL	Association in the Presence of Linkage	hom-ro	Homozygous Ration Offset
		HWE	Hardy-Weinberg Equilibrium
AR	Autosomal Recessive	IBW	Initial Body Weight
ATOM	Atropine for the Treatment of Myopia	ILM	Internal Limiting Membrane
		IOP	Intraocular Pressure
AXL	Axial Length	IV	Instrumental Variable
BC	Before Century	KEGG	Kyoto Encyclopedia of Genes and Genomes
BMI	Body Mass Index		
bp	base pair	LD	Linkage Disequilibrium
BP	Biological Process	LIM	Lense-Induced Myopia
BrM	Bruch's Membrane	LT	Lens Thickness
BRS	Baseline Refractive Status	MAF	Minor Allele Frequency
C	Control	MDS	Multidimensional Scaling
CC	Cellular Component	MF	Molecular Function
CHD	Chromo Helicase DNA-binding	MR	Mendelian Randomization
CPM	Counts Per Million	MSE	Mean Spherical Equivalent
cr	Call Rate	NES	Normalized Enrichment Score
CREAM	Consortium for Refractive Error and Myopia	NHANES	National Health and Nutrition Examination Survey
CT	Corneal Thickness	NMDA	N-methyl-d-aspartic acid
D	Dioptre	ORA	Over-Representation Analysis
ddNTPs	di-deoxynucleotidetriphosphates	PCA	Principal Components Analysis
DEG	Differentially-Expressed Genes	PCR	Polymerase Chain Reaction
DOPAC	3,4-dihydroxyphenylacetic acid	PDT	Pedigree Disequilibrium Test
DQC	Dish Quality Control	PKAs	protein kinase family
ECM	Extra Cellular Matrix	QC	Quality Control
eQTLs	expression QTLs	QTL	Quantitative Trait Loci
FBW	Final Body Weight	RE	Refractive Error
FCS	Functional Class Scoring	RFLP	Restriction Fragment Length Polymorphism
FD	Form Deprivation		
FDM	Form-Deprivation Myopia	SE	Spherical Equivalent
FDR	False Discovery Rate	SNP	Single Nucleotide Polymorphism
FFQ	Food Frequency Questionnaire	SNV	Single-Nucleotide Variant
fld	Fisher's Linear Discriminant	T	Treated
G × E	Gene-Environment Interactions	TDT	Transmission Disequilibrium Test
GLM	General Linear Model	USA	United State of America
GO	Gene Ontology	VA	Visual Acuity
GRM	Genetic Relationship Matrix	VCD	Vitreous Chamber Depth
GSEA	Gene Set Enrichment Analysis	VDR	Vitamin D Receptor

Chapter 1 Introduction

1.1 Definitions

Myopia, also known as nearsightedness, is a highly prevalent ophthalmic disorder which is known to have affected people for more than a thousand years. It is believed that Aristotle (384-321 BC) was the first person to distinguish between the conditions of myopia and hyperopia, when both of these words had not yet been invented. Many years later, some people found that they could see things more clearly by partially closing their eyes, so the Greeks created the word *myopos* – a combination of *myein* ('to close') and *ops* ('eye') – to describe this condition (1). At this stage, people's understanding of myopia only related to their subjective feelings; there was no systematic theory of its aetiology. With the development of modern science, an objective and systematic definition of myopia became widely accepted, which specifies myopia as a condition of the unaccommodated eye where parallel light focuses in front of, instead of on, the retina (2) (Figure 1.1).

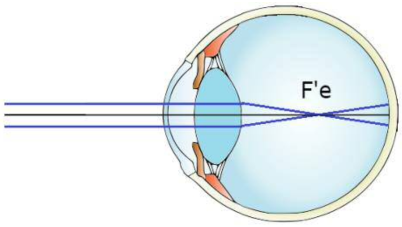

Figure 1.1. In the myopic eye, parallel light focuses in front of the retina.
F'e represents the power of the eye (3).

1.2 The prevalence of myopia – from the past to the present

The prevalence of myopia has increased during the past 2-4 decades, especially in Southeast Asian countries. In China, where one-fourth of the world's population lives, the overall prevalence of reduced visual acuity (VA) in children (most of which is caused by myopia) had been increasing from 1985 to 2010. Among teenagers aged 7 to 18 year-old, the prevalence of reduced VA was 28.6% in 1985. Gradually it rose to 38.6% in 1991, 41.0% in 1995, 38.5% in 2000, 49.5% in 2005, and 56.8% in 2010, with the reduced VA being more widely observed in urban areas than in rural areas (4). In another similar study in Guangzhou, China, from 1988 to 2007, the same trend was seen: the prevalence rate of myopia continued to increase and the proportion of moderate and severe myopia rose among grade 1–12 students (5). In Taiwan, from 1983 to 2000, five surveys pertaining to ocular refraction of 7 to 18 year-old students were conducted, and an increase in myopia prevalence was observed (6). Another convincing study performed in Singapore investigated 18–19 year-old male conscripts for nearly 20 years and found in later birth cohorts, there was a significant increase in the prevalence of myopia (7).

In other parts of the world, the myopia rate has risen steadily in the last few decades. In the Middle East region, Dayan et al. (8) conducted a retrospective study and found that between 1990 and 2002, the overall prevalence of myopia increased from 20.3% to 28.3% in young Israeli adults. In European countries, like Finland and Sweden, the same trend was reported. In Finland, the prevalence of myopia was <10% among adults born during the first three decades of the 20th century, whereas there was a rapid rise in the prevalence during the second half of the 20th century, reaching 21–30%. Although the prevalence of myopia did not change significantly in 7 year-old children, it doubled in 15 year-old teenagers over the past half-century (9). In the Goteborg area of Sweden, among 12 to 13 year-old school children, Villarreal et al. (10) found 49.7% of children were myopic. They concluded that the tendency towards myopisation in the teenage population in Goteborg was similar to that found in other parts of the world. A recent meta-analysis for refractive error in adults across Europe was done by Williams (11). In this study, fifteen population-based cohort and cross-sectional studies generated from 1990 to 2013 were combined for analysis. After stratifying the 61,946 individuals by age, a higher prevalence of myopia was found in the younger age groups, which suggested an increasing myopia rate in more recent years (11); Figure 1.2.

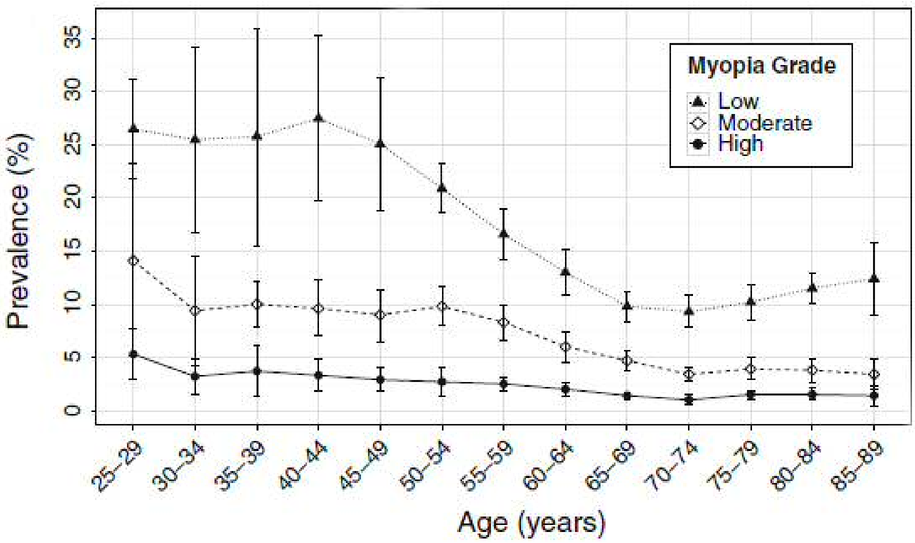

Figure 1.2. Prevalence of myopia in European adults.
The prevalence of myopia according to age (with 95 % confidence intervals). Low myopia was defined as -3D < SE ⩽ −0.75D, moderate myopia −6D < SE ⩽ −3D, high myopia SE ⩽ −6D (SE, spherical equivalent; D, Dioptres; taken from Williams et al, page 312.(11)).

In the USA, approximately 25% of individuals aged 12 to 54 year-old were myopic in the 1980s, while in 2004 the myopia prevalence increased to ~33% in people aged 20

(12, 13). According to the population-based National Health and Nutrition Examination Survey (NHANES), the myopia prevalence was substantially higher in 1999–2004 than in 1971–72 for non-Hispanic participants (14).

In the Southern Hemisphere, a similar trend has also been observed. The Blue Mountains Eye Study (15) and the Melbourne Visual Impairment Project (16) both reported a decrease in myopia prevalence with increasing older age. Rose and colleagues (17) summarized a series of studies from both USA and Australia and suggested that the decreasing myopia prevalence in elder cohorts was not purely caused by increasing presbyopia prevalence with age (Figure 1.3).

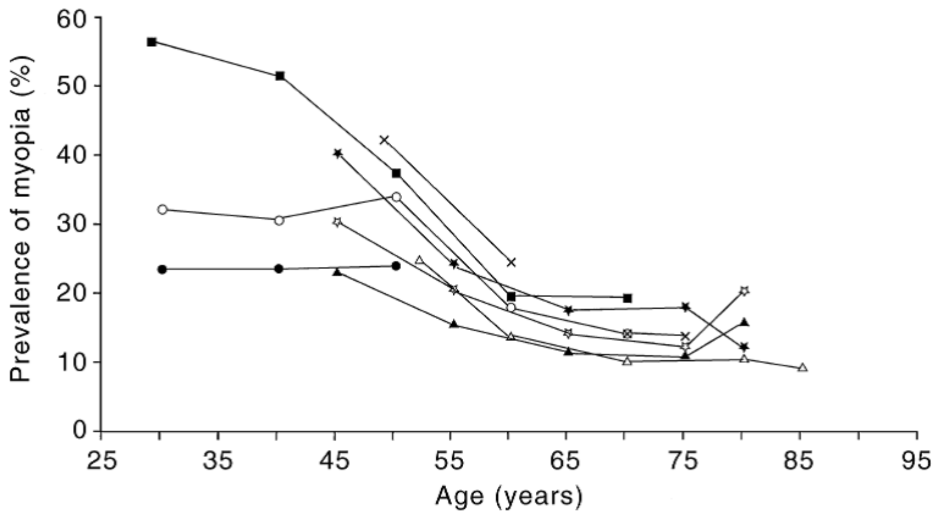

●, National Health and Nutrition Examination Survey (NHANES);
O, NHANES, data as recalculated by Mutti and Zadnik;
×, Beaver Dam Eye Study;
■, Framingham Offspring Eye Study;
★, Baltimore Eye Survey, non-African American subjects;
☆, Baltimore Eye Survey, African American subjects;
△, Blue Mountains Eye Study;
▲, Melbourne Visual Impairment Project.

Figure 1.3. The prevalence of myopia in age cohorts older than 25 years in epidemiological studies in the USA and Australia *(Taken from Rose et al, page 118. (17)).*

Most epidemiology studies show a tendency towards a rising prevalence of myopia regardless of demographic differences. An exception is the study in Denmark by Jacobsen et al. (18), who reported a significant decrease in the myopia prevalence rate amongst Danish conscripts in 2004 compared with 1964. However, in this study, the comparability has been questioned since in different years the methodologies were different. Meanwhile, a study comparing the differences in myopia prevalence between 1996-1997 and 2009-2010 in young Singaporean males found similar myopia prevalence rates between the two periods, but the high myopia and refractive astigmatism rates increased (19). Thus, overall, the world has experienced an increasing prevalence of myopia in recent decades.

1.3 The prevalence of myopia – from the east to the west

The prevalence of myopia varies markedly with geographic location and ethnicity; individuals of Han Chinese ancestry show the highest prevalence while Africans show the lowest prevalence. For example, in 2014, the prevalence of myopia among 7-18 year-old Beijing students was 64.9% ($-0.5 \leq$ SE) (20), in France 2013, among teenagers (10 to 19 year-old), it was 42% (21); in 2003 South Africa, the prevalence was only 4% among 5-15 year-old children (22). Studies performed in countries with multi-ethnicity also found the Chinese were most susceptible to myopia. In Singapore, the odds of becoming myopic was 2.04 times higher in Chinese compared to Malays (23). In Australia, 39.5% of the East Asian children were myopic, compared to 4.6% in European Caucasian and 6.1% in Middle Eastern individuals (24). In the USA, Asians again had the highest rate of myopia (18.5%), followed by Hispanics (13.2%). African and white Americans had the lowest myopia rate (6.6% and4.4%, respectively) (25); Pan et al. (26) had summarized the worldwide prevalence of myopia in children and concluded that Chinese children had a higher myopia prevalence than European children (Figure 1.4).

Figure 1.4. Prevalence of myopia in different countries or ethnicities. *(Modified from (26))*

1.4 Impact of myopia

It is noteworthy that not just the prevalence of myopia is increasing, the severity of the disorder is also increasing. According to previous studies (6, 19), along with the increasing prevalence rate of myopia, a concomitant increasing shift towards higher degrees of myopia has been observed. Holden et al. (27) predicted that by 2050, 49.8% of the global population might be myopic and around 1/5 of the myopes might eventually become high myopes. If this rapidly increasing trend is not suspended, an increase in corrected and uncorrected refractive error and visual impairment will be expected.

The complications of high myopia will be the main cause of visual impairment. There is evidence that the risk of myopic macular degeneration (28, 29), retinal detachment (30, 31), retinal atrophy (32), glaucoma (33) and cataract (34) are all greater in highly myopic eyes. Furthermore, in East Asian countries, myopic macular degeneration is now the leading cause of monocular blindness (35, 36). This global trend will also lead to an economic burden. To manage patients with vision impairment, it is estimated the cost will be 202 billion USD each year globally (37).

1.5 Aetiology of myopia

The aetiology of myopia is complicated. Since Cohn (38) suggested that going to school increases the risk of myopia, reading and other forms of near work have been implicated in causing axial myopia. However, twin-based, family-based and population-based studies have shown convincing evidence that refractive error also has a genetic cause. It is now widely accepted that a complex interplay between genetic factors and environmental factors drives the development of myopia (39). However, how exactly genes and the environment interact with each other is still an area of active research.

1.5.1 The genetic theory

1.5.1.1 Heritability of myopia

Heritability is defined as the genetic contribution to a population's phenotypic variance. For myopia, it had long been observed that myopic parents tended to have myopic children, which suggested the condition is heritable. However, it was not until people began to study twins and families that the heritability of refractive error could be estimated quantitatively. In these studies, the theoretical level of genetic sharing (kinship) between family members is estimated. For example, the kinship between monozygotic twins is 1, between dizygotic twins is 0.5, and between parents and offspring is 0.5. Heritability can be estimated using the correlation coefficient of the difference in phenotype between family members divided by their kinship. However, this estimation is prone to bias, since it does not account for the fact that individuals in a family typically share the same environment.

Recently, it has become possible to estimate the genetic similarity between pairs of individuals much more precisely, allowing for the study of sets of essentially unrelated individuals. For example, after genome-wide genotyping, single nucleotide polymorphism (SNP) genotypes can be used to calculate the genetic similarity between every pair of individuals in a population, building up a genetic relationship matrix (GRM) describing their kinship. A heritability estimate (called the "SNP heritability"; h^2_{SNP}) can be calculated based on the GRM and phenotype information. In family-based studies, the heritability of refractive error has been estimated at between 0.10 and 0.70, while twin studies have generally yielded higher estimates of between 0.50 and 0.96 (40). For axial length, the estimated heritability varies from 0.20 to 0.95 (41). Such relatively high heritability implies that genetic factors play a major role in the aetiology of myopia. However, the SNP heritability for ocular traits is estimated to be lower. For example, in studies examining 15-year-old participants of the Avon Longitudinal Study of Parents and Children (ALSPAC), $h^2_{SNP} = 0.28$ for refractive error (42), $h^2_{SNP} = 0.46$ for axial length (43) and $h^2_{SNP} = 0.42$ for corneal curvature (43). The difference between heritability estimated from SNPs and from twins is called missing heritability and the underlying reason for the underestimation using SNPs will be discussed in Chapter 4, section 4.1.1.

Heritability analysis estimates the effect of genes as a whole in explaining inter-individual variation in refractive error; it does not identify specific genes or loci connected with the trait. Hence, further studies such as linkage analysis or genome-wide association studies (GWAS) are needed.

1.5.1.2 Linkage studies and candidate regions

Genetic linkage analysis is a method based on Mendelian genetics designed to identify a particular region of the genome that co-segregates with a specific disease phenotype. Familial occurrence of myopia within one or more pedigrees showing a monogenic pattern of phenotype segregation is necessary to perform linkage analysis. In familial myopia, among all the regions following Mendelian modes of inheritance that have been reported to date, the autosomal dominant (AD) mode is the most frequent pattern (40). This is likely because linkage analysis is more powerful in AD pedigrees than recessive pedigrees, and because AD pedigrees are usually easier to ascertain.

In 1990, Schwartz et al. (44) performed a linkage study in a family with Bornholm Eye Disease (a Mendelian disorder featuring high myopia, amblyopia, and deuteranopia) and identified a locus on the X chromosome which showed strong evidence that it might be linked to this disease for the first time. This gene locus was named *MYP1* (Table 1.1). Since then many regions harbouring myopia genes have been reported: in 1998, Young and her colleagues (45, 46) used linkage analysis to discover two gene loci that linked to high myopia, named *MYP2* and *MYP3*. These were the first AD gene loci for non-syndromic high myopia. In 2002, Naiglin et al. (47) recruited 23 high myopia families with at least one person affected and found a novel locus on chromosome 7q36 linked to myopia, which they named *MYP4*. However, in 2008, Paget et al. (48, 49) studied 26 high myopic families including those Naiglin et al. (47) had analyzed and found no significant linkage to chromosome 7q36. Instead, they found chromosome 7q15 (*MYP17*) showed significant linkage, and this result was replicated in the same year (49). The discordance among different studies could be caused by the difference in sample size or genotyping error.

It was not until 2004 that linkage analysis was first applied to mild or moderate myopia pedigrees. High myopia was hypothesized to be a genetic disease caused by a rare mutation which directly led to the uncontrollable elongation of the eye. Inheritance of such a mutation would yield a high prevalence of high-grade myopia in the family. Linkage analysis provides a method to identify such mutations. However, mild or moderate cases of myopia were believed to be ‘complex’ (multifactorial) quantitative traits, which were difficult to investigate by linkage analysis (for statistical reasons, linkage analysis has extremely low power to detect small genetic effects). A research team from the USA performed a genome scan for common-myopia susceptibility loci for the first time among an Ashkenazi Jewish sample of multiplex pedigrees and found Chromosome 22q12 (*MYP6*) was statistically significantly linked to the disease (50). At the same time, another study used 221 dizygotic twin pairs and performed a genome-wide linkage scan which located 4 regions linked to refractive error, including chromosome 11p13 (*MYP7*), chromosome 3q26 (*MYP8*), chromosome 4q12 (*MYP9*), and chromosome 8p12 (*MYP10*) (51). These studies implied that linkage analysis could also be used to identify quantitative trait loci (QTLs) influencing refractive error.

Similar methods to those described above were used between 2004-2006 to identify 3 additional loci: *MYP11*, *MYP12* and *MYP13* (52-54). In 2006, Wojciechowski et al. (55) measured refractive error in 49 multigenerational Ashkenazi Jewish families with at least 2 affected persons, which were previously studied by Stambolian et al. (50). Instead of using microsatellite polymorphisms as genetic markers, they used SNPs as markers and performed a QTL linkage analyses; they identified a novel QTL for ocular refraction on the short arm of chromosome 1(*MYP14*) (55). Later, *MYP15* (chromosome 10q21.1) (56), *MYP16* (chromosome 5p15.33-p15.2) (57), *MYP18* (chromosome 14q22.1-q24.2) (58) and *MYP19* (chromosome 5p15.1-p13.3) (59) were identified. The above loci were all autosomal dominant except *MYP18* (chromosome 14q22.1-q24.2), which showed autosomal recessive inheritance. To date, more than 24 loci have been identified by family-based linkage studies.

A major innovation took place in 2011, when Shi et al. (60) conducted a GWAS in 419 high myopia cases and 669 controls from a Han Chinese cohort, and then identified a variant at 13q12.12 that was significantly associated with high myopia. They subsequently added four additional SNPs –rs9510902, rs3794338, rs7325450, and rs7331047 –which were in the same LD block with rs9318086 and rs1886970 according to the Han Chinese Beijing in the HapMap database, and all these SNPs showed a significant association with high myopia. The most strongly associated haplotype corresponded to a 1.35-fold increased risk of high myopia. This was the first myopia study to identify a linkage block by GWAS but not using linkage analysis. In the same year, the same group used exome sequencing to identify a mutation responsible for causing high myopia (61). (Table 1.1)

Table 1.1 Myopia gene loci identified by linkage analysis.

Symbol	Inheritance	Map location	Research subjects	Country	Referenc
MYP1	XR	Xq28	Pedigrees	Danish	Schwartz
MYP2	AD	18p11.31	Pedigrees	American and Chinese	Young et
MYP3	AD	12q21-q23	A large pedigree	German/Italian	Young et
MYP4	AD	7q36	Pedigrees	French and Algerian	Naiglin e
MYP5	AD	17q21-q22	A large pedigree	English/Canada	Paluru et
MYP6	AD/QTL	22ql2	Large pedigrees	Ashkenazi Jewish descent	Stamboli
MYP7	QTL	11p13	Dizygotic twin pairs	Britain	Hammon
MYP8	QTL	3q26	Dizygotic twin pairs	Britain	Hammon
MYP9	QTL	4q12	Dizygotic twin pairs	Britain	Hammon
MYP10	QTL/AD	8p23	Dizygotic twin pairs	Britain	Hammon
MYP11	AD	4q22-q27	A large pedigree	Chinese	Zhang et
MYP12	AD	2q37.1	A large pedigree	American	Paluru et
MYP13	XR	Xq23-q25	A large pedigree	Chinese	Zhang et
MYP14	QTL	1p36	Pedigrees	Ashkenazi Jewish descent	Wojciech
MYP15	AD	10q21.1	A large pedigree	Hutterite population from South Dakota	Nallasam
MYP16	AD	5p15.33-p15.2	Large pedigrees	Hong Kong Chinese	Lam et a
MYP17	QTL	7p15	Pedigrees	French and Algerian	Paget et
MYP18	AR	14q22.1-q24.2	Pedigrees	Chinese	Yang et a
MYP19	AD	5p15.1-p13.3	Pedigrees	Chinese	Ma et al.

1.5.1.3 Association studies and GWAS

Genetic association is found when genotypes within a population co-occur with a phenotypic trait with statistical significance. Generally speaking, association studies can be conducted with large cohorts of families, population-based samples of unrelated subjects, or groups of unrelated cases and controls. Unlike linkage studies, which have high power to detect rare disease-causing variants, association studies have high power to detect common disease-causing variants. They rely on the fact that individuals who carry the risk allele of a specific gene variant will have a slightly increased risk of getting the corresponding disease (accordingly, the frequency of the risk allele will be higher in cases than in controls). Association studies have contributed a wealth of new findings in myopia genetics research. (Figure 1.5)

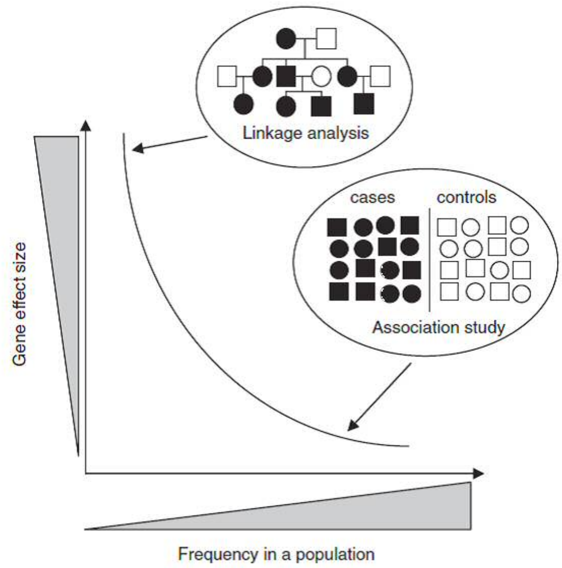

Figure 1.5. Gene effect size and frequency in the population for different study designs(63).
For linkage analysis, it is assumed that the disease is inherited in a Mendelian manner and is caused by a genetic variant with a large effect but low frequency. For an association study, diseases are considered to be common, and to be caused by gene variants exhibiting small effects but with high frequency (Taken from Tang et al. page10 (63)).

1.5.1.3.1 Family-based association study

According to the law of independent assortment ('Mendel's Second Law'), alleles at a locus will be transmitted randomly from parents to an offspring, which means the probability of transmitting either of the two alleles will be 0.5 vs. 0.5. For a specific phenotype, a genetic association will occur when transmission of the alleles deviates from random occurrence (so-called 'transmission disequilibrium'). The most common approach to test for this genetic association is the transmission disequilibrium test

(TDT), which tests for distortion (or disequilibrium) in the inheritance of an allele from heterozygous parents to affected offspring in terms of the McNemar Chi-squared test (64). Accordingly, the typical study design for a family-based association study will be the use of family 'trios' containing one affected child with two parents (only heterozygous parents are actually used in the test).

This family-based association study design has been applied in myopia research, albeit infrequently. In 2000, Li and colleagues (65) found out that *HLA-DQB1* might be associated with the progression of pathological myopia by using a restriction fragment length polymorphism (RFLP) as a genetic marker. This study applied family-based association analysis and a transmission disequilibrium test to 58 individuals from 8 families with 23 affected individuals. Similar methods but with more families and new genetic markers like SNPs were used in later studies; subsequently, more loci associated with myopia were detected. In 2006, Han et al. (66) performed a family-based association study in 128 nuclear families which contained 133 severely myopic offspring; a variant in the hepatocyte growth factor gene (*HGF*) was found to be associated with the condition. Similar methods were used by the same research team in demonstrating that a genetic variant in the paired box 6 (*PAX6*) gene was also associated with high myopia in southern Han Chinese (67). In 2009, Yanovitch et al. (68) sought to replicate the association between *HGF* and myopia. They recruited 146 multiplex families consisting of 649 Caucasian subjects and measured their refractive status. After genotyping 'haplotype-tagging' SNPs within *HGF*, they analyzed data with two family-based association methods: the pedigree disequilibrium test (PDT) and the association in the presence of linkage (APL) test and found a significant association with mild to moderate myopia compared to emmetropia. An association between extreme high myopia and the *HGF* gene variants was also reported (68). In the same year, Metlapally et al. (69) used families recruited from the USA and UK to identify that *COL2A1*, but not *COL1A1*, variants were associated with refractive error.

1.5.1.3.2 Population-based association study

Currently, the most widely used genetic association method is the population-based association study design. In this kind of study, the sample is a set of unrelated individuals. A direct association test between a genetic marker and the phenotype is done. Either the phenotype can be analyzed as a continuous trait, or subjects can be assigned as cases or controls. According to the scale of genetic association, population-based association studies can be categorized as shown in Table 1.2 (70).

*Table 1.2. **Association study design**. Reproduced from (70).*

Type	Description
Candidate polymorphism	Focus on an individual polymorphism, e.g. a single SNP, which is suspected of being involved in disease causation.
Candidate gene	Focus on 5–50 SNPs within a gene. The candidate gene can be chosen from a prior linkage study or a functional candidate.
Fine mapping	Focus on a candidate region of 1–10 Mb, typically involving several hundred SNPs. The candidate region might have been identified by a previous linkage study and contain 5–50 genes on average.
Genome-wide	Focus on the whole genome, and require ⩾300,000 well-chosen SNPs. The main purpose is to identify common causal variants throughout the whole genome.

Small-scale association studies can test for association in a single gene region and are relatively cheap to fund. For example, in 2009, Nishizaki et al. (71) performed association study using 39 SNPs distributed around a previously reported myopia susceptibility gene and suggested that a SNP (rs2839471) - located in the frequent recombinant region within the *UMODL1* gene – was associated with high myopia in the Japanese population. One previous exome sequencing study in 2011 reported linkage between *ZNF644* (*MYP21*) and high myopia (61), and then in 2014, by candidate gene association study, five novel *ZNF644* high myopia susceptibility variants were identified in the Chinese Han population (72). In 2012, Hysi et al. (73) reported an association between *SERPINI2* gene variants and refractive error in a European birth cohort. In this study, they genotyped 1536 SNPs that covered 3 myopia linkage peaks in 590 individuals. In another study the vitamin D receptor (VDR) was chosen as a candidate gene; SNPs within this gene region were tested for association with myopia (74). Four SNPs within VDR: rs2853559, rs2239182, rs3819545and rs2853559 were significantly associated with both high and mild to moderate myopia in a multivariate analysis.

With improvements in genotyping technology, performing whole genome genotyping or sequencing is becoming cheaper. Meanwhile, the completion of the HapMap Project and the 1000 Genomes Project provided a detailed reference panel for the human genome. By genotyping the whole genome with a high-density array of SNPs and then imputation of additional non-genotyped variants, scientists now have the chance to capture the variations of QTLs that contribute tiny effects to a trait. By

adding all these effects together, the contribution of these loci markers to the variation of the phenotype (heritability) can be calculated.
The first large-scale GWAS study of myopia was conducted in 2009 by Nakanishi et al. (75). In order to identify genetic variations which might be implicated in pathological myopia, they performed a two-stage GWAS. After analyzing 411,777 SNPs with 830 cases and 1,911 general population controls, they set P-values smaller than 10e-4 as their threshold and identified 22 associated SNPs. By testing for association in the second stage and combining the results, they identified a single locus at chromosome 11q24.1, which showed an association with the disease. Hysi et al. (76) reported that the transcription initiation site of *RASGRF1* was related to myopia, while Solouki et al. (77) reported a significant association at chromosome 15q14 (rs634990, P = 2.21 × 10e-14) near the *GJD2* gene, which was expressed in the retina, and was considered a strong candidate. In 2013, two very large GWAS were published, which identified a total of nearly 40 gene loci associated with refractive error. One of the studies was carried out by the Consortium for Refractive Error and Myopia (CREAM) group (78). At the time, it was the largest myopia GWAS meta-analysis using data from 32 studies from Europe, the USA, Australia and Asia. In their study, they first identified 18 distinct genomic regions strongly associated with myopia in European ancestry populations and then tested these results in Asian cohorts and found 10 showed evidence of association. To explore more loci, they carried out a gene-based analysis and identified eight additional loci. In all, 26 new loci associated with refractive error were identified. In another study, a genome-wide survival analysis study was carried out by Kiefer et al. (79). In their study, based on the assumption that SNPs with a large effect size will be associated with an earlier age-of-onset of myopia, they used a Cox proportional hazards model with age of onset of myopia as the endpoint and identified 20 new loci. Compared to a case-control study, this study was believed to have higher power, and furthermore, its results suggested that there might be similar genetic factors underlying myopia age of onset and refractive error. The most recent GWAS for myopia, which was performed with 106,086 European ancestry cases and 85,757 European ancestry controls, identified 51 association hits with the phenotype ‘self-reported nearsightedness’ (80).

To date, 16 genome-wide studies related to refractive error and axial length have been reported, with more than 170 SNPs related to these phenotypes being identified. (Please refer to http://www.ebi.ac.uk/gwas/search?query=myopia for more details about the 16 GWAS for refractive error.)

Although genome-wide association studies have tremendously advanced our understanding of the genetic factors in myopia, to date only a small fraction of the variation in refractive error can be explained by the variants identified (78). To get more precise results, studies in larger populations are needed.

1.5.1.4 DNA sequencing

DNA sequencing is a more comprehensive method to detect DNA variants compared to genotyping. In DNA sequencing, every base is assessed, and thus, rare mutations will be captured. The application of this technique to explore relatively rare myopia mutations has become more popular. Several mutations causing high myopia have been identified by exome and whole genome sequencing in pedigrees showing monogenic transmission. For instance, Guo et al. (81) studied a 3-generation Chinese family in which 5 members were affected by high myopia. They identified a mutation in the *SLC39A5* gene. Jin et al. (82) performed trio-based exome sequencing in family trios and identified 29 de novo single-nucleotide variant (SNV) mutations in early-onset high myopia, some of which may be causal. Sun et al. (83) carried out exome sequencing in 298 probands with early-onset high myopia, and reported 34 potentially pathogenic mutations in 71 probands. Among the reported genes, 11 had been implicated in myopia development in previous studies.

1.5.1.5 Comparison between linkage analyses, family-based association study, GWAS and sequencing

Linkage studies, association studies and DNA sequencing studies for myopia research all have the potential to provide evidence for the role of genetic factors in myopia development. These research methods should be applied to different datasets because they each have their own strengths and weaknesses.

Linkage analysis performs optimally when the trait is a simple Mendelian disease (driven by one rare causal gene), and data from a large family pedigree are available. The main limitation of linkage analysis is that it can only identify a candidate region, which requires follow-up studies to fine map the candidate genes at the locus.

Compared to linkage analysis, association studies have a vastly better resolution, i.e. they can pinpoint individual genes, rather than highlighting a large chromosomal region that may contain hundreds of genes. However, GWAS results are not always reliable due to population stratification, and because so many variants are tested, their results need to be replicated in independent samples even for loci with very low P-values (84). Figure 1.6 illustrates the potential for false positive association in GWAS caused by population stratification (85).

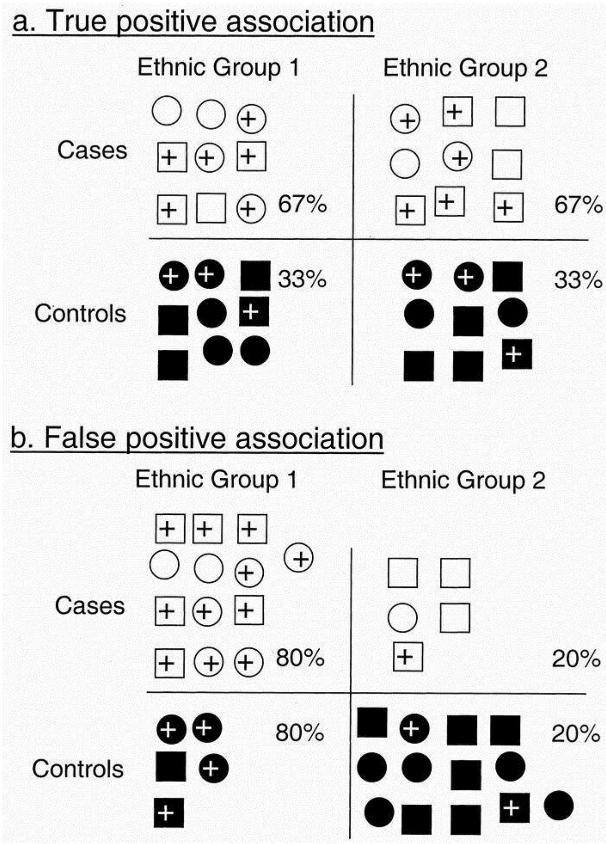

Figure 1.6. Illustration of Population stratification (85).
The white shapes represent cases, and the black shapes represent controls. Association test is carried out for a putative risk allele – the plus sign (+). In a and b, the proportions of individuals carrying the risk allele are doubled in the case population compared to the control population. In a, true-positive association: in either ethnic group, the greater frequency of the risk alleles is observed in cases than in the controls. In b, false-positive association due to the mixture of ethnicities, 80% of ethnic group 1 and 20% of ethnic group 2 carry the risk allele in both of the cases and controls. However, while mixing the population, the overall risk allele frequency in the cases is twice greater than the controls. This false positive association is caused by population stratification: the target allele is more prevalent in ethnic group 1, meanwhile ethnic group 1 is overrepresented in the cases. (Taken from Hirschhorn et al., page 60 (85))

Family-based association studies require family trios and require at least one of the parents to be heterozygous, which makes the recruitment of participants more difficult than for GWAS studies. However, family-based association studies are robust against population stratification. Table 1.3 summarized the features of linkage analysis, family-based association study and GWAS (63).

It is now straightforward to identify mutations for monogenic diseases using whole genome sequencing. The limiting factor in applying these methods to high myopia is that pedigrees showing monogenic inheritance are very rare – instead, most cases of high myopia appear to be polygenic.

Table 1.3. Summary of linkage analysis, family-based association studies and GWAS. *Reproduced from (63)*

	Linkage analysis	Family-based association study	GWAS
Study population	Large pedigrees with many affected subjects	Small nuclear families including cases and their parents; TDT requires heterozygous parents	Unrelated individuals
Mode of inheritance	Assumption of mode of inheritance (AD, AR and X-linked)	Additive model	Additive model
Statistical power	High for Mendelian diseases Low for complex diseases	Low for Mendelian diseases Lower than case-controlled study for alleles with small genetic effects	Low for Mendelian diseases in small numbers of pedigrees High for detecting small genetic effects in complex disease
Advantages	Highest power for Mendelian diseases More efficient using a genome scan approach	Presence of internal control to avoid the potential for population stratification	Systematic assessment across the genome Convenient sample collection, e.g. population-based sampling
Disadvantages	Need to ascertain suitable pedigrees Limited by genetic heterogeneity if present	Need to ascertain large numbers of nuclear families; Recruitment more difficult than case-controlled studies, especially for late-onset diseases	False positive association due to ethnically mismatched cases and controls (population stratification)

AD – autosomal dominant; AR – autosomal recessive

1.5.2 Environmental factors

Myopia was first thought to be an environmentally-determined disorder, as proposed by Cohn (38). He observed that children began to get myopic only after they went to school, and therefore concluded that it was going to school and overuse of the eyes that made people myopic. After he announced his findings, many studies focused on the environmental factors that might trigger the onset or progression of myopia. Epidemiologists have found many important risk factors that directly or indirectly associated with the development of myopia.

1.5.2.1 Near work and education

With industrialization and modernization, people begin to spend more and more time performing indoor activities such as reading, writing, and watching electronic screens. This near work was suggested to be the leading cause both for myopia onset and progression. Time spent reading (86, 87) - as well as reading distance - are indeed risk factors for myopia. In 2011, Muhamedagic et al. (88) recruited 100 myopic students and performed a retrospective-prospective study. They found that the time spent performing near work had a statistically significant impact on both subjective and objective visual acuity examinations. To explore a potential hypothesis regarding the underlying mechanism, Ghosh et al. (89) used an optical biometer to investigate the change of eye biometrics after a 10-minute near task performed in downward gaze. Axial length increased post-task, accompanied by choroidal thinning. These findings thus provide an interesting new biological mechanism through which near work/down gaze may link to myopia development. A cross-sectional study was conducted in Singapore, which recruited 1005 school children aged 7 to 9 years. After adjusting for several factors, children who read more than two books per week had an odds ratio for myopia of 3.05 (95% CI, 1.80-5.18). However, children who read for more than 2 hours per day or with more than 8 diopter hours, had an odds ratio for myopia not significantly different to one (OR=1.50; 95% CI.0.87-2.25 and OR=1.04;95%CI,0.61-1.78, respectively) (90). Importantly, several studies have observed only a weak or even absent association between near work and myopia (91). In two studies, one in Singapore and another in Orinda, near work such as reading was not associated with myopia development (92, 93). More research is needed to identify the cause of the different findings in studies of near work and myopia.

Usually, studies of near work have examined school-age children, while studies investigating the role of education have tended to analyze a wider age range. Education has been reported to be a risk factor for myopia development in many studies. A population-based cross-sectional study in Germany found both the prevalence and magnitude of myopia were associated with education level (94). Williams et al. (11) pointed out that increasing education levels were associated with an increasing prevalence of myopia in Europe (although education alone could not fully explain the trend of the increasing prevalence of myopia over recent decades).

Interestingly, a recent Mendelian Randomization (MR) study suggested a causal role for education in myopia development (95). The estimated causal effect was significantly higher than the conventionally-observed effect, suggesting that other environmental influences partially buffer against the adverse causal effect of education.

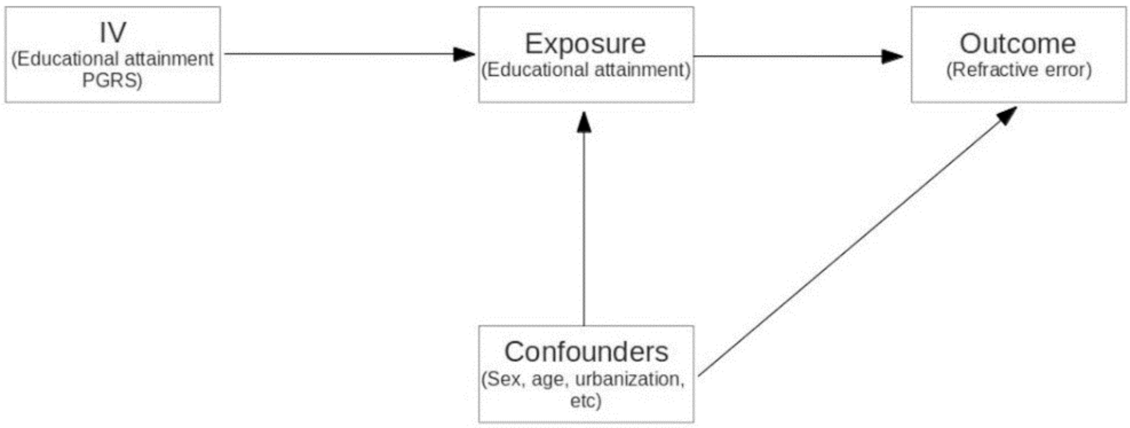

Figure 1.7 Mendelian randomization assumptions in a study examining the relationship between education and myopia *(Taken from Cuellar-Partida (95)). "(1) Educational attainment polygenic risk score (instrumental variable, IV) is robustly associated with educational attainment (exposure variable); (2) IV is only associated with refractive error (outcome variable) via educational attainment (exposure variable); (3) IV is not associated to the confounders." (Taken from Cuellar-Partida, page 12, (95),)*

1.5.2.2 Time spent outdoors

Time spent in outdoor activities is another environmental factor related to refractive error. In 2013, He and Xiang (96) finished a 3-year randomized controlled trial (RCT) among grade 1 children from 12 primary schools. In their study, the intervention group had an additional 40-minute class of outdoor activities, and parents were involved to encourage their children to have outdoor activities. After 3 years of intervention, compared to the control group, the cumulative incidence rate of myopia was significantly lower, the myopia progression was significantly slower, although the axial length change was similar. In another RCT performed in Taiwan (97), 571 students participated. Among them, 333 students were encouraged to spend time outdoors during recess, which in total was approximately 6.7 hours of time outdoor per week. After 1 year of follow up, the myopia incidence rate was reduced and the myopic shift was lower in the intervention group, all of which suggested a significant role of outdoor activities in myopia control.

For other studies, Sherwin and colleagues pooled the results from 7 cross-sectional studies to perform a meta-analysis and found that each additional hour of outdoor activities per week was associated with a reduction in the odds of myopia by 2% (98). Rose et al. (99) reported higher levels of total time spent outdoors, rather than sport, were related to less myopia and a more positive mean refraction; Jin et al. (100) suggested that outdoor activities are a potential prophylactic measure which could prevent the onset of myopia. A prospective cohort by Guggenheim et al. also showed a similar result that increasing time spent outside is associated with a reduced incidence of myopia (101).

The underlying mechanism of this effect is not well understood, however, the 'light-dopamine' theory is the best supported. During time outdoors, the increased light intensity will stimulate the release of dopamine, a neuromodulator which has been shown in animal models to be associated with reduced experimentally-induced eye elongation (102).

However, not all studies have observed an association between outdoor activities and myopia. In one study, Bei et al. (103) recruited 1892 school-age children in Xichang, China, to examine the relationship between near work, outdoor activity and myopia. After adjusting for age, sex and parental education, neither time spent on near work nor time outdoors were associated with myopia. Although lack of accuracy in the self-assessment of time outdoors is a limitation of this school-based study, it still questions the true nature of the association between outdoor activity and myopia. Another study investigated 874 full sibling families (i.e. families in which each child within a family has the same parents) and conducted a heritability analysis. After adjusting for sex and ethnicity, the heritability of myopia was approximately 73%. After further adjusting for time spent outdoors and time spent reading, the heritability was essentially unchanged, suggesting that outdoor activities (and near work) did not account significantly for the difference in refractive error between siblings (104).

1.5.2.3 Diet and physical activity

When evaluating environmental risk factors that potentially increase the incidence of myopia, lifestyle factors such as diet and physical activity may be relevant. In most societies, individuals typically take in more nutrition than is actually needed. The excess protein, fat, and cholesterol not only leads to overweight or other metabolic diseases, but may also be related to the development of myopia. As early as 1956, Gardiner proposed that diet might be a risk factor for myopia. By comparing the diets between 33 progressing myopes and 251 stable myopes, Gardiner reported that stable myopes consumed more protein but less fat and carbohydrate than the progressing myopes (105). Forty - four years later, Cordain et al. (106) speculated that a high glycemic load and the resulting hyperinsulinaemia might cause rapid scleral growth via insulin-related growth factors. More recently still, Lim et al. (107) applied a comprehensive food frequency questionnaire (FFQ) to school-age students to assess the relationship between dietary factors and refractive error. They found that higher saturated fat as well as cholesterol intake were associated with longer axial length although not with severity of myopia. However, in a 1993 study, Edwards et al. (108) compared the diets of 24 myopes and 68 non-myopes and reported that myopes had lower protein, energy, fat, and cholesterol intake. These inconsistencies between the findings of these studies are likely to be the result of differences in sample size as well as the methods of dietary assessment.

As well as these studies examining protein or fat intake, some researchers have focused on vitamin D. Studies in Korea and Australia reported an association between serum vitamin D level and myopia, however, other researchers attributed this association to differences in outdoor activity, which would increase serum levels of vitamin D (109-111). A recent Mendelian randomization study also supported this idea: Cuellar-Partida et al. (112) analyzed data for 37,382 and 8,376 adult participants of European and Asian ancestry, respectively, and used SNPs with known effects on vitamin D concentration as instrumental variables. The study found essentially no relationship between the IVs and refractive error, suggesting vitamin D levels were not causally associated with myopia development.

Some studies report that myopes spend less time engaged in sports (93, 113). However, such studies typically did not distinguish whether this sporting activity occurred outdoors or indoors. In 2008, Rose et al. (99) separately investigated indoor versus outdoor activities and reported that time spent outdoors was much more strongly associated with refractive error than time spent indoors or physical activity. Indeed, indoor sports activity was not associated with myopia. A study conducted by Guggenheim et al. (101) also suggested that the association between myopia and 'sports/ outdoor activities' was due mainly to time outdoors rather than physical activity. In the latter study, time outdoors was assessed using a questionnaire and physical activity was assessed using activity monitors.

1.5.2.4 Physical stature and social status

As a component of the whole body, the growth of eyes is co-ordinated with the growth of the body (i.e. height or stature). Saw et al. (114) examined the association of birth parameters with biometry and refraction in Singapore Chinese children and found that birth weight, birth length, head circumference and gestational age were related to axial eye length. However, these parameters were not associated with refraction. A research group in Australia conducted a similar study and reached the same conclusion (115). Northstone et al. (116) did a further study on body stature growth trajectories during childhood and reported that, during the linear phase of height increase (2.5 to 10 year-old), faster-growing children had a small increased risk of myopia by the time they reached 11 to 15 in age.

In addition to physical characteristics, specific aspects related to social and demographic status have also shown an association with myopia. It was reported that in Australia and Beijing, school-age children living in rural districts had a lower risk of becoming myopic (20, 117, 118). High education level, non-manual worker status, and higher income were all associated with the prevalence of myopia (119-122). It has been suggested that these associations derive from genetic or lifestyle factors.

1.5.2.5 Parental factors

Certain parental characteristics have been recognized as potential risk factors for myopia, such as maternal age, parental education level, parental smoking, gestational age, breastfeeding, and birth order (123-126). However, these studies may have been biased by confounders such as socioeconomic status and education.

In all, there is convincing evidence that environmental factors influence the development of myopia. However, although epidemiologists have discovered a diverse array of environmental risk factors, together they explain only a small proportion of the inter-subject variation in refractive error (127).

1.5.3 Gene-environment interactions

Although much evidence supports a role for both genes and environmental factors in myopia development, the involvement of gene-environment interactions ($G \times E$) is less well understood. In one novel twin study of 114 monozygotic twin pairs, Lyhne et al. (128) detected a significant correlation between the sum of the intra-pairwise refractions and the absolute difference in intra-pairwise refraction (Figure 1.8).

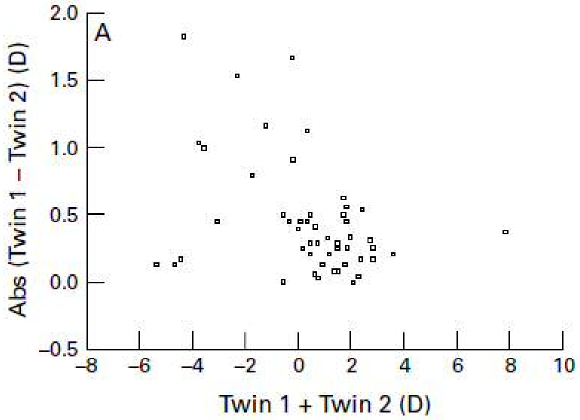

Figure 1.8. Gene-environment Interaction for ocular refraction (128).
The x-axis shows the sum of ocular refraction of each monozygotic twin pair, which reflects the effect of shared genes and common environment. The y-axis represents the variance between monozygotic twin pairs that reflects the effects of purely environmental differences. A correlation was observed (r = −0.32, P <0.05), which is evidence of an interaction (Taken from Lyhne et al. page 1475, (128)).

The method was proposed by Jinks and Fulker (129), based on the theory that the individual environmental difference could be estimated by variation between MZ twins, whereas the sum of MZ twins' scores could represent the shared genetic effect and the shared common environment effect. However, this method does not provide a quantitative measurement of gene-environment interaction. In another study, Saw et al. (130) reported that an interaction between parental myopia and near work influenced the risk of moderate to high myopia (SE < -3.00 D) in Singaporean children.

These two studies provide evidence of G × E in myopia. However, they were designed to detect general effects rather than the influence of specific genes. To discover which genes interact with a specific environmental factor, detailed genotyping and careful measurement of the environmental risk factor of interest are needed. This topic is discussed in more detail in Chapter 4, section 1.

1.6 Treatment interventions for myopia

The most popular method used to improve the visual quality of myopic patients is prescribing concave spectacle lenses, which is economical and convenient. However, this approach is not a treatment of the underlying cause, but simply a way to remove the symptoms of myopia. Refractive surgery and contact lenses are also effective in treating the symptoms of blurred vision but do not address the high risk of ocular pathology in myopic eyes (due to glaucoma, retinal detachment and chorioretinal atrophy).

There are several therapeutic contact lenses, which were designed based on the theory that fully correcting the central vision but imposing myopic defocus on the peripheral retina would slow down axial length elongation and myopia progression (131-133). Ortho-K contact lenses, which re-shape the cornea during overnight wear, provide clear vision in the daytime. Clinical trials suggest that wearing Ortho-K lenses slows the progression of myopia (134, 135). Other lens types including bifocal or multifocal contact lenses also showed the effect of controlling myopia progression (136-138). However, the potential of having contact lens-associated infectious keratitis is one of the factors limiting their adoption.

In recent years, using muscarinic receptor antagonists such as atropine is considered to be the first-tier therapeutic method. Clinical experiments conducted in many countries, including Singapore (139), China (140), Rotterdam (141), and the USA (142) all suggested topical atropine treatment could slow down the progression of myopia. In the Singapore-based Atropine for the Treatment of Myopia (ATOM2) clinical trial, the effect of different atropine concentrations (0.5%, 0.1%, and 0.01%) was compared. It was found that increasing atropine concentration was positively correlated with the therapeutic effect, however, it was also potentially related to an increased incidence of side effects, such as allergic conjunctivitis, photophobia and near blur. Chia et al. (139) suggested 0.01% atropine for controlling myopia progression with minimal side effects.

Although many methods have been tested, and many others are being developed, none is fully effective at halting the incidence of myopia and preventing future progression. Thus, new or improved therapeutic intervention strategies are needed.

1.7 Animal models of myopia

As early as 1977, Wiesel and Roviola (143) found that monocularly or binocularly suturing the eyelid of neonatal monkeys could induce myopia and enlarge the lid-sutured eye. Since then, different animal models have been evaluated to examine their response to the deprivation of sharp vision (so-called “form deprivation” [FD]). It has been found that myopia can be induced by FD in tree shrew (144), monkey (143), chick (145), kestrel (146), marmoset (147), rabbit (148), mouse (149), guinea pig (150) and fish (151).

As with form deprivation, minus lens wear can induce myopia in juvenile animals. In 1988, Schaeffel et al. (152) imposed a serious of lenses ranging from +4D to -8D to young chicks eyes, and both hyperopia and myopia could be induced. A similar effect was also observed in tree shrew (153), guinea pig (154), mouse (155), marmoset (156) and fish (157).

Comparing these models to the process of myopia development in humans, they are similar in many ways. Firstly, both experimental myopia and human myopia show similar characteristic features. For example, in both animal models and humans, the myopic eyes tend to have an increased axial length, particularly as regards the vitreous chamber depth (158, 159), as well as retinal, choroidal and scleral thinning (150, 160-162). Secondly, both animal models and humans exhibit a susceptible period for myopia at younger ages (158, 163, 164). Moreover, form deprivation myopia has also been reported to occur in human infants with congenital cataract or disorders of the eyelids (165).

The discovery of experimentally-induced myopia was a milestone in myopia research history. The availability of animal models has allowed researchers to manipulate experimental conditions and investigate their effects on myopic eye growth, and to take physiological measurements and tissue samples of myopic animals to learn more about the mechanisms controlling refractive development.

1.7.1 Key findings from animal experiments

1.7.1.1 Light intensity and wavelength

Light intensity is important for emmetropisation. It was found that just increasing the ambient illuminance level reduced the effects of form deprivation. In chicks, exposure to bright light (15,000 lux) 5 hours per day retarded the development of form-deprivation myopia (FDM) by roughly 60% (166), and with increasing light intensities, lesser myopic refraction and shorter axial length were found (167). For short-duration bright light exposure, the effect depended on the time of day of the exposure, with maximum impact occurring with exposure at mid-day (168). Similar findings have been observed in rhesus monkeys (169). Bright light can also influence the rate of lens-induced myopia development (170).

Apart from light intensity, the wavelength of the light is another important factor. Chicks reared in red light became more myopic than those reared in blue light (171). However, rhesus monkeys reared under red light remain more hyperopic than those reared in blue light (172), and the same phenomenon was observed in tree shrews (173). The wavelength effects might be explained by longitudinal chromatic aberration (LCA), which means long wavelength (“red”) light is focused farther from a lens than short wavelength (“blue”) light is. Thus, red light will produce hyperopic defocus if the medium wavelengths ("yellow") of white light are focused on the retina (173).

Furthermore, light flicker frequency is also found to be related to myopia development. Di et al. (174) reared guinea pigs under flicker with a flash rate of 5, 1, 0.5, 0.25 or 0.1Hz, and found 0.5Hz flicker maximally induced myopia. In another study in chicks treated with ±10 D or 0 D lenses, or without lenses, a temporal modulation of flicker-induced a myopic shift, with 1Hz flicker having the strongest impact (175).

1.7.1.2 Signalling pathways and molecules

Signalling pathways and molecules involved in myopia development are of interest to many researchers. To date, signalling molecules including dopamine, melatonin, ZENK, and retinoic acid have been reported to be involved in experimentally-induced myopia.

Dopamine

In 1989 Stone and colleagues (176) first reported a decrease of dopamine and its metabolite 3,4-dihydroxyphenylacetic acid (DOPAC) in FD eyes. Since then the mechanism of dopamine's effect on eye growth has been studied widely. In rhesus monkeys (177), guinea pigs (178), and tree shrews (179), activation of retinal dopamine receptor 2 (D2 receptor) was found to reduce the degree of FD-induced myopia development. In eyes recovering from FD, dopamine, DOPAC and the DOPAC/dopamine ratio increased rapidly within 2 days (180).

Light intensity and both spatial and temporal contrast also affect retinal dopamine levels. Megaw et al. (181) reported that an increase in light intensity increased the dopamine level and dopaminergic activity in chick vitreous. Feldkaemper and colleagues (182) reported that, compared to eyes treated with frosted diffusers, eyes covered with neutral density filters (which only reduce light level but keep Michelson contrast constant), had a higher level of DOPAC. Thus, both luminance and spatial contrast in the retina image are connected to dopamine release.

ZENK

ZENK, also known as early growth response protein 1 (Egr-1), nerve growth factor-induced protein A (NGFI-A), zinc finger protein 225 (zif268), tis8, cef5, and Krox24, was found to be up-regulated in retinal amacrine cells when plus lens defocus was imposed. In contrast, ZENK was found to be down-regulated in FD or minus lens-treated eyes. In chick retina, the glucagon amacrine cells contribute mostly to the

regulation of ZENK under defocus condition (183), which suggests that glucagon cells might guide ocular growth.
To better understand the role of ZENK in eye growth, Schippert and colleagues (184) studied refractive development in ZENK knockout mice. It was found that knocking out ZENK mainly influenced axial length since mice experienced a myopic shift due to having longer eyes, while lack of ZENK had only minor effects on anterior chamber depth and corneal curvature.

1.7.2 Comparison between different animals

The ideal animal model for myopia research would be an animal that spontaneously develops myopia without any experimental intervention, which is the situation in humans. However, spontaneously-occurring myopia is rare in natural animal populations. It has been reported that rhinoceroses (185), thoroughbreds horses (186), and certain dog breeds (187-189) have a high prevalence of myopia. However, conducting experiments on these animals might require a great deal of space and very high financial support. Jiang et al. (190) found a wild-type guinea pig strain (Cavia porcellus) which 28 out of 220 of them had spontaneous axial myopia (less than -1.5D in both eyes). However, after visual function measurement using an optomotor drum, they also showed that the affected animals displayed deficits in pupil responses and accommodation.

The various animal models of myopia have different features that make some models better suited for addressing specific research questions than others. A summary of different animal models (191) is listed below in Table 1.4.

Table 1.4. Summary of different animal models of myopia. *Reproduced from Schaeffel & Feldkaemper (1*

Animal model	**Character features**	
	Advantages	**Disadvantages**
Chick	1. Relatively large eyes (8 to 14 mm); 2. Rapid eye growth; 3. Highly sensitive control of refractive state by retinal image quality and focus; 4. Excellent optics (diffraction-limited at 2.0mm pupils); 5. Active accommodation (about 17 D); 6. High visual acuity (7 cycles/degree); 7. Easy drug delivery by intravitreal injection; 8. Friendly, co-operative nature; 9. Inexpensive and easy to keep.	1. Lack of a fovea; 2. Differences in sc 3. Different mecha lenticular) comp 4. Differences in ci
Tree Shrew	1. Closely related to humans; 2. Can induce myopia by FD and negative lenses, and eye growth is modulated to compensate for defocus; 3. Single layered sclera, similar to human.	1. Lack of a fovea; 2. Longer treatmen 3. No clear indicat 4. More complex ha
Primates	1. Closely related to humans; 2. Parallel ocular anatomy with human, such as their retinal vascular structure and fovea are similar to humans;	1. Limited availabi 2. Longer treatmen 3. High expense fo
Guinea pigs	1. Easy to maintain and breed, “friendly” and co-operative; 2. Large pupils and reasonably large eyes (axial length 8.0 mm); 3. Easy to perform measurements.	1. Lower visual acu 2. Lack of evidence
Mouse	1. Well-established animal model for a range of human diseases with a wealth of knowledge on its biochemistry and genetics; 2. Lots of well-established transgenic versions; 3. Easily obtained and bred.	1. Small eye size (a 2. Difficult to meas 3. Poor optics, no a 4. Difficult to indu 5. Not as friendly a

1.7.3 Interventions for inducing myopia

1.7.3.1. Form-deprivation myopia (FDM)

Myopia can be induced by continuously blocking an eye's sharp vision; so-called 'form-deprivation myopia' (FDM). In an animal undergoing form deprivation, the illuminance level will be different in the treated eye versus the control eye, and the contrast and sharpness of the image projected onto the retina will be reduced. Under this stimulation, eyes show a reduced expression level of dopamine and ZENK, thinning of the choroid, and an increase in axial length. One of the features of FDM is that there is no plane of focus, which means there is no end point for the eyes to grow towards. Hence form-deprived eyes become progressively more and more myopic with time. In animals treated with FD, some might be very susceptible while the others might be less sensitive. The 'open-loop' character of FD, therefore, maximizes the variance in the degree of induced myopia among treated animals.

1.7.3.2. Lens-induced myopia (LIM)

Placing a minus lens in front of the eye causes the image to focus behind the retina. This signals the eye to accelerate its growth rate such that the retina moves towards the focal plane, i.e. producing an increase in axial length. This process is presumed to mimic the natural emmetropisation process during eye development, which guides the positioning of the retina relative to the image focal plane. Unlike FDM, LIM does not markedly reduce the illuminance level, and the image quality may be improved immediately by accommodation. In chicks, the accommodation ability is greater than in man, at approximately 20 D (192, 193). An intervention to eliminate the ability to accommodate did not prevent LIM from occurring, although it did impair its accuracy (194). Importantly, the accelerated growth of axial length will stop when the eye has compensated for the refractive power of the imposed lens. This 'closed-loop' characteristic, therefore, leads to limited variability in the final refractive state of animals undergoing LIM once full compensation for the lens has occurred.

1.8 Overview of the research design strategy for the PhD project

A selective breeding experiment carried out in chicks by Chen et al. (195) provided strong evidence that genetic factors regulate susceptibility to FDM. The aim of this PhD project was to build on this finding in order to discover some of the genes that mediate this genetic susceptibility to myopia. The chosen study design was a GWAS in a chick population treated by monocular FD based on the hypothesis that a GWAS is able to identify genetic loci conferring myopia susceptibility in an animal population exposed to a myopia-inducing environmental stimulus (For more details, please refer to Chapter 4, section 4.1.2). Monocular FD treatment was selected in preference to binocular FD since the within-animal monocular treatment design provides a more sensitive measure of the effect of the treatment (196).

1.8.1 Animal selection for the PhD project

The chick was selected as the animal model for this study for the following reasons. First, chicks rely on vision as their primary sense; thus chicks have relatively large eyes and a highly developed visual system (197, 198). The large eye size of the chick would facilitate accurate measurement of the degree of experimentally-induced myopia in each individual animal. Second, chicks are a well-established animal model for myopia. Like human eyes, chicks are typically mildly hyperopic soon after they are hatched (born) and undergo emmetropization during juvenile development. Post-hatch ocular growth is relatively fast in chicks, about 100 μm per day, and FD causes rapid and robust myopia development in chicks (199, 200). Third, genetic variation has already been shown to modify susceptibility to FDM in chicks in the selective breeding experiment of Chen et al. (195). Thus, searching for genes associated with chick FDM is feasible. Finally, chicks are inexpensive and easy to keep. In this study, a large number of animals are needed, and thus the economical cost makes chicks a good choice.

1.8.2 Method to induce myopia

1.8.2.1 Form-deprivation myopia vs. lens-induced myopia

In this study, FD was selected to induce myopia. Compared to the ‘closed loop’ LIM paradigm, FD is an ‘open-loop’ treatment and therefore has the advantage that highly-susceptible individuals could not fully compensate for the treatment stimulus.

1.8.2.2 Method of attaching occluders to produce form deprivation

Instead of using a matched pair of Velcro rings (201), sutures were selected to fix the occluder in place in front of the eye. There are several advantages of using sutures. Firstly, compared to Velcro, sutures provide better fixation of the occluder (occluders attached with sutures very rarely fell off). Secondly, occluders attached using Velcro can prevent moisture from evaporating, which can ‘mist up’ the occluder. Sutures provide tiny gaps that allow airiness between the occluder and the underlying feathers and avoided this problem. Moreover, sutures were considered more humane since they prevented the adverse tissue reaction to the glue used to attach the Velcro, which can result in tissue inflammation around the eye. By cutting the suture knots, sutures could be quickly removed without detectable tissue damage, to allow eye measurements to be carried out.

1.8.2.3 Age and duration of form deprivation

Myopia can be induced in chicks from the day of hatch to at least 1 year of age, although the magnitude of the response to FD declines rapidly with age (202). Here, a period of FD of 4 days was selected, beginning when the chicks were 7 days old. Under this regimen, the degree of induced myopia had not yet reached its plateau, and the inter-animal variability in response to FD was known to be sufficient to distinguish differences in genetic susceptibility (195). Chickens reach sexual maturity at approximately 6 months of age and can live for 20 years, therefore the FD period in this experiment corresponds to the neonatal period in children.

1.8.3 Method to assess the degree of FD myopia

In this study, both spherical equivalent (SE) of the chick eye and axial length were recorded. Measurement of treatment-induced axial elongation was selected as the method for quantifying the degree of induced myopia in each chick (Chapter 2, section 2.2.3). According to previous studies (203, 204), FD would cause enlargement of the whole eye in chicks, with the major contribution from vitreous chamber elongation, accompanied by crystalline lens thickening and anterior chamber deepening/corneal flattening. Ocular component dimensions can be measured more reproducibly than the refractive error in chicks (i.e. the coefficient of variation of repeat readings is lower for A-scan ultrasonography measurements than for retinoscopy measurements). Therefore, ocular biometry was selected as a more precise measure of the degree of induced myopia than the retinoscopy findings. Of the ocular component dimensions, the change in axial length shows a closer correlation to the degree of induced myopia than does the change in vitreous chamber depth in chicks (205) Therefore, treatment-induced axial elongation was selected as the main outcome measure.

1.8.4 Method used to measure axial length

A-scan ultrasonography is a diagnostic test used in optometry or ophthalmology. This technique is widely used by myopia researchers to measure the degree of treatment-induced axial elongation in animal models (191). Although more accurate techniques have become available for measuring axial length in recent years (206) the new instruments are expensive. The most accurate meanwhile cost-effective technique available to us was A-scan ultrasonography.

When ultrasound waves travel from one medium to another of a different density, an echo will bounce back when the ultrasound beam strikes the interface. In an A-scan device, sound waves of a specific frequency are emitted from a probe tip driven by electrical pulses, causing a crystal element to vibrate. As the sound beam passes through the eye, it is partially reflected back at each interface of different acoustic impedance, forming a series of echoes. These echoes are detected by the probe tip (this time, the sound vibration is converted into an electrical signal). From the front to the back of the eye, the echoes correspond to the interfaces of: air/anterior corneal surface, the posterior corneal surface/aqueous interface, the aqueous/anterior lens surface, the posterior lens capsule/anterior vitreous, the posterior vitreous/retinal surface, the retina/choroid interface and the choroid/anterior scleral surface (Figure 1.9).

Waveform peaks reflected from the eye can be displayed along an x-axis of time. The velocity of sound varies when it passes medium with different density and thus, the ocular component dimension can be calculated by a simple formula:

$$\text{Distance} = \text{Velocity} \times \text{Time}$$

Waveform peak heights can be used to gauge the quality of the measurement. Peak height is not only affected by the difference in density at the interface but also by the alignment of the ultrasound beam and the visual axis. Sound waves can be reflected and refracted in the same way as light rays; if they are parallel with the visual axis and perpendicular to the corneal vertex, sound waves will be maximally reflected back towards the probe.

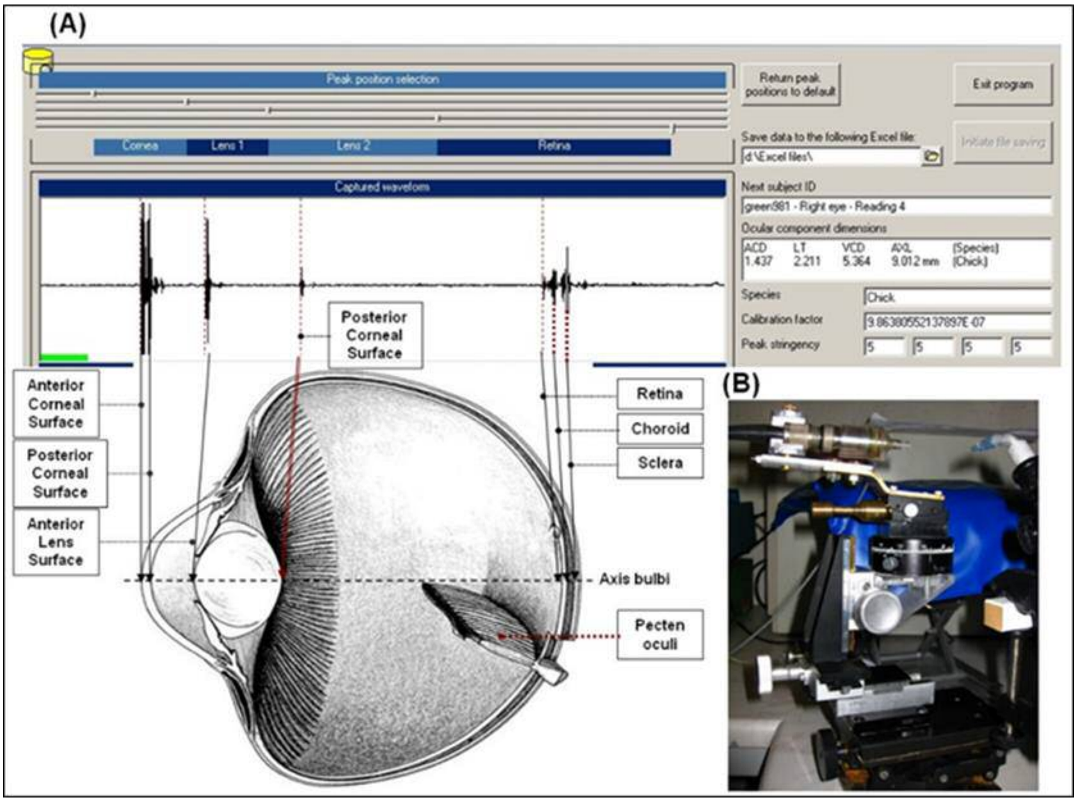

Figure 1.9. High-frequency A-scan ultrasonography system and holding device (205).
(A) Explanation of A-scan echo spikes in ultrasonography and the corresponding ocular component of the chick eye. (B) Custom-made holding device, with animal position fixing holder and a holder for the transducer (Taken from Chen, page 39,(205)).

1.8.5 Method used to measure spherical equivalent

Retinoscopy is a technique to obtain an objective measurement of the refractive error of the eye. When a light beam passes through a lens and is projected onto a screen, if the focal plane is between the lens and the screen, the reflex will move opposite to the light source (an ‘against’ movement); on the contrary, if the focal plane is behind the screen, the reflex will move with the light source (a ‘with’ movement); while if the focal plane is exactly on the screen, the reflex will stay still (“neutralized”). The same principle is utilised in retinoscopy. Through a peephole in the retinoscope mirror, the observer can determine if the refractive power of the eye it is too strong (indicating myopia) or too weak (hyperopia). The refractive error of the eye can be corrected by adding minus or plus lenses until a neutral point is achieved.

1.8.6 Method to detect gene loci influencing susceptibility to form deprivation myopia

In this study, GWAS was selected as the optimal method for this project. Details explaining how the GWAS was performed in chicks and selection of the genotyping platform will be discussed in Chapter 4, section 4.1.4.

In this study, instead of genotyping all chicks that were phenotyped, a 'selective genotyping' strategy was used, in which only chicks that exhibited extreme phenotypes were genotyped (in this study, extreme high and low FD-induced axial elongation). The selective genotyping strategy was designed to reduce the cost but retain sufficient statistical power. This issue is discussed in Chapter 4, section 4.4.8.

Chapter 2 Material and methods

2.1 Material

2.1.1 Experimental animal

The animal experiments were carried out at Hong Kong Polytechnic University. The experiments complied with the Animals (Control of Experiments) Ordinance Chapter 340 of the Hong Kong Department of Health. White Leghorn chicks (*Gallus gallus domestics*) were used as the myopia model. Chicks were obtained from specific-pathogen-free (SPF) eggs obtained from a local supplier (Tin Hang Tech Ltd, China) and hatched in batches of approximately 20 per week. It was assumed that chicks from the company were randomly mated as part of a very large population of chicks and hence that the chicks would exhibit sufficient genetic diversity to permit genetic association mapping.

2.1.2 Occluders

Translucent occluders for depriving the eye of form vision were made from a sheet of 0.8 mm-thick polypropylene with an absorbance of 0.07 log units. The polypropylene sheet was cut into 2x2 cm squares, heated for 20 seconds at 180°C and compression moulded into appropriately sized hemispheres. A mechanical punch was used to remove extraneous material, leaving a 2-3mm rim around the edge of the occluder. The edges were smoothed by sandpaper. Four holes (0.4 mm diameter) were drilled in the occluder rim, at positions corresponding to 12, 4, 6 and 8 o'clock, to allow the occluder to be sutured in position.

2.2 Method

2.2.1 Myopia model: Form deprivation

After hatching, chicks were reared in wire-mesh cages with a suspended infrared heat lamp controlling the temperature to 25°C under a 12/12 hr light/dark diurnal cycle (lights providing 500 lux illumination were turned on at 7 am and off at 7 pm). They were given access to water and fed commercial chick starter ad libitum.

On day 7 after hatching, chicks were monocularly form deprived. The treated eye was alternatively selected between right and left eye. Chicks were anaesthetized by intramuscular injection of ketamine 50 mg/kg and xylazine 3.5 mg/kg. A translucent occluder was affixed to the periorbital skin surrounding the orbit of the treated eye using 3-4 sutures in the 12, 4, and 8 o'clock positions (195). The treated eye was observed after recovery from anaesthesia to confirm it locates in the middle of the lens and it could open freely.

2.2.2 Measurement and quantification of eye parameters

2.2.2.1 High-frequency A-scan ultrasonography

Prior to FD when chicks were 7 days old ('baseline'), A-scan ultrasonography was performed on both eyes of the anaesthetized chicks. After the 4-day treatment period, when chicks were 11 days old, the occluder was temporarily removed to perform A-scan ultrasonography for a second time. During the measurements, the eyelids of the anaesthetized chicks were kept open with a speculum. The ultrasound system was calibrated each day, prior to use, by measuring an aluminium block of known dimensions.

The A-scan system consisted of 4 parts: 1) a 20 MHz transducer of focal length 25 mm; 2) a 15 mm saline stand-off with autoclaved saline being perfused at a rate of 0.15 ml/min; 3) a Panametrics model 5073PR pulser-receiver; 4)a personal computer fitted with an Acqiris DP-110 data acquisition card. Waveforms were sampled at 100 MHz, and for each measurement, 50 waveforms were taken and the average value was calculated. The resolution of the A-scan was 10 μm (203). For each eye, 3 to 6 measurements were performed, data would be taken only if the difference between two measurements was smaller than 0.05 mm. The average value of all the measurements was used for further analysis.

Two custom-made holding devices were used to assist the alignment of the ultrasound probe with the visual axis of the chick's eye. The first device consisted of a platform to hold the chick and maintain its head in a fixed position. The second was an opto-mechanical stage used to control the position of the ultrasound probe, which allowed translational movements along the X, Y and Z axes, plus rotational movement in the vertical (pitch) and horizontal (yaw) axes. When clear echo spikes exhibited an amplitude size profile: cornea > anterior lens > posterior lens and retina < choroid < sclera, it was assumed that the alignment of the probe to the visual axis was optimal. Dimensions of each eye component were analysed in real-time using a custom-written software according to the formula given in Chapter 1, section 1.8.4, by assuming an ultrasound velocity of 1.6078 mm/μs in the lens and 1.5340 mm/μs in the other ocular media (158). The average value of the three highest readings was used in the data analysis. The measurements included: corneal thickness (CT), anterior chamber depth (ACD), lens thickness (LT) vitreous chamber depth (VCD) and axial length (AXL).

2.2.2.2 Retinoscopy

Streak retinoscopy was performed on both eyes of awake chicks at the 11 days-old assessment, before anaesthesia and A-scan measurements. Cycloplegic eye drops were not used because, unlike in mammals, avian ciliary muscle is striated not smooth muscle and is controlled primarily by nicotinic receptors. A minus-power lens bar and a plus-power lens bar were clamped upright to a bench and positioned at a 'working distance' of 33 cm (3.00 D) from a marker position where the retinoscope was held. Retinoscopy was performed under dim illumination, and chicks were gently restrained such that each eye in turn was positioned approximately in the middle of the correction lens and perpendicular to the light beam of the retinoscope. Spherical refractive error was measured in both the horizontal and vertical meridians and entered into a custom-designed database program that converted values to sphere and cylinder powers automatically.

Retinoscopy measurement in small eyes such as those of the chick is subject to a source of systematic bias (in the direction of hypermetropia) known as the 'small eye artefact of retinoscopy' (207). The bias arises from light being reflected from the retina/vitreous interface rather than the retinal photoreceptor layer. No account was taken of the small eye artefact in this study, because the primary interest was in the relative refractive error between treated and control eyes, not their absolute refractive error.

Chicks have both cornea and lens accommodation (208). Accommodation by chicks during retinoscopy was evident as a fluctuation in the measurement and constriction of the pupil. Therefore, to increase measurement accuracy, a dark and quiet environment was created, and measurements were performed once the pupil size was maximal.

2.2.2.3 Quantification of eye parameters

To quantify the change in ocular dimensions due to FD, the following formulae were used:

Change in CT (ΔCT) = $\Delta CT_T - \Delta CT_C$

Change in ACD (ΔACD) = $\Delta ACD_T - \Delta ACD_C$

Change in LT (ΔLT) = $\Delta LT_T - \Delta LT_C$

Change in VCD (ΔVCD) = $\Delta VCD_T - \Delta VCD_C$

Change in AXL (ΔAXL) = $\Delta AXL_T - \Delta AXL_C$

Where,

Change in CT of treated eye (ΔCT_T) = CT (after FD) - CT (baseline) in treated eye

Change in CT of control eye (ΔCT_C) = CT (after FD) - CT (baseline) in control eye

Change in ACD of treated eye (ΔACD_T) = ACD (after FD) - ACD (baseline) in treated eye

Change in ACD of control eye (ΔACD_C) = ACD (after FD) - ACD (baseline) in control eye

Change in LT of treated eye (ΔLT_T) = LT (after FD) - LT (baseline) in treated eye

Change in LT of control eye (ΔLT_C) = LT (after FD) - LT (baseline) in control eye

Change in VCD of treated eye (ΔVCD_T) = VCD (after FD) - VCD (baseline) in treated eye

Change in VCD of control eye (ΔVCD_C) = VCD (after FD) - VCD (baseline) in control eye

Change in AXL of treated eye (ΔAXL_T) = AXL (after FD) - AXL (baseline) in treated eye

Change in AXL of control eye (ΔAXL_C) = AXL (after FD) - AXL (baseline) in control eye

The actual mean spherical equivalent (MSE) was calculated using the following formula:

MSE = Sphere + 1/2 Cylinder – 3 Dioptres

Where 3 Dioptres corresponds to the working distance of 33cm. In this study, since the working distance was consistent, it was not corrected.

2.2.3 Measurement of body weight

Body weight was measured on day 4 and day 11 using a digital balance, before anaesthesia, as an indicator of the chick's health status. Chicks with extremely low body weight on day 4 (< 30 g) were excluded from the study.

2.2.4 Biological sample collection

In pilot experiments, it was found that the neural retina strongly adhered to the RPE layer if the chick was sacrificed immediately after a sodium pentobarbital overdose during anaesthesia with ketamine/xylazine. However, it was found that if the chick was sacrificed by CO_2 asphyxiation without prior anaesthesia, the neural retina would swell and become edematous over the next few minutes, which allowed it to be isolated easily. The reason for the tight adherence of the retina and choroid after ketamine/xylazine anaesthesia and sodium pentobarbital sacrifice, versus the ease of separation after CO_2 asphyxiation was unclear. One possible explanation is that during the process of cell death, N-methyl-d-aspartic acid (NMDA) receptors are activated, producing an influx of Ca^{2+}. Ketamine may deactivate the NMDA receptors in retinal cells, producing a neuroprotective effect which may postpone cell death and oedema (209-211). Furthermore, ketamine itself could directly reduce cell swelling subsequent to anoxia-hypoxia, which may help maintain the normal tight adherence between the neural retina and the RPE. (212) Xylazine is an alpha-2 adrenergic agonist, and it has both analgesic and sedative properties (213). It was found that ketamine/xylazine combination could protect rat photoreceptor cells against apoptosis induced by strong light (211).

Applying ketamine/xylazine combination prevented collection of a retina sample free from the adherent choroid. Consequently, this study followed a protocol whereby after the ultrasound measurements had been completed at the 11 days-old assessment, the occluder was re-fixed in position, the chick was allowed to recover from the anaesthesia and returned to its home cage. After one further day of form deprivation, animals were sacrificed by CO_2 asphyxiation, and then blood samples were collected, and retinal dissections were performed 7 minutes after death.

2.2.4.1 Blood sample collection

After the chick was sacrificed, cardiocentesis was performed to obtain a blood sample (> 1ml). Before performing cardiocentesis, a 3ml syringe with a 21g needle was prefilled with 50 µl of 200 mM EDTA as an anticoagulant. The feathers and skin of the chest were disinfected with ethanol, and the needle was inserted perpendicular to the chest cavity along the upper edge of the sternum to obtain the blood sample. After collection, the syringe was inverted several times to disperse the EDTA. For each chick, two 1 ml blood samples were collected and were stored at -20°C in 1.5 ml screw-cap centrifuge tubes for approximately 10 days (prior to DNA extraction).

2.2.4.2 Retina sample collection

After collecting the blood sample, retina samples from both the treated and control eyes were collected. The feathers and skin around the orbit were disinfected with ethanol, and the eyes were removed and placed on an ice-cooled aluminium plate. Each eye was sectioned along the equator and the anterior segment discarded. The neural retina from the posterior hemisphere was carefully separated from the pigment epithelial layer using fine forceps. Neural retina samples were transferred to a 1.5 ml screw-cap vial containing 150 µl of 'RNALater' solution and stored frozen after the tissue was fully saturated, and then were stored at -20°C.

2.2.5 Nucleic acid extractions

2.2.5.1 DNA extraction

Unlike humans, chick red blood cells possess nuclei, thus DNA can easily be extracted from whole blood. After thawing blood samples to room temperature, DNA was extracted with the following protocol:

i. A 15µl aliquot of each blood sample was mixed with 800µl TES solution (250mM Tris, 25mM EDTA and 2% Sodium dodecyl sulfate, pH=8.0) by gentle trituration until the solution was homogeneous.
ii. 1.5µl RNase solution (100mg/ml stock, RNase A, Qiagen Ltd.) was added and the mixture was incubated at 37°C for 30 minutes.
iii. After cooling the solution to room temperature, 200µl of cold ammonium acetate (7.5M, 4°C) and 100µl chloroform were added. The sample was vortex mixed for 20 seconds and centrifuged at 14,000g for 3 minutes.
iv. The upper liquid phase was transferred to a fresh 1.5ml tube. DNA was precipitated by adding 700µl cold isopropanol, mixed gently, and centrifuged at 14,000g for 2 minutes.
v. The pellet was washed with 200µl 70% ethanol, and air dried for 15 minutes.
vi. The DNA pellet was then re-suspended in 100µl TE solution (10mM Tris, 1mM EDTA) by incubation overnight at 37°C.

2.2.5.2 DNA concentration measurement

DNA was used for genotyping, which required a concentration of 50 µg/µl. Thus, the concentration of DNA was measured using a spectrophotometer.

i. The spectrophotometer (GeneQuant II, Pharmacia Biotech Ltd.) was calibrated with deionized water and a reference sample (50 µg/µl calf thymus DNA in water).
ii. 5µl of chick genomic DNA was diluted in 995ul autoclaved deionized water and mixed by vortexing.
iii. The absorbance at 260 nm and 280 nm was recorded (OD260 and OD280, respectively). Any sample with an OD260/OD280 ratio less than 1.8 was re-extracted.
iv. DNA was diluted to 50 µg/µl with Te solution (10mM Tris, 0.1mM EDTA).

2.2.5.3 RNA extraction

RNA was extracted using the RNase-free DNase set (Qiagen#79254) and RNeasy mini kit (Qiagen#74101) following the manufacturer's instructions:

i. Retina samples in RNAlater were allowed to warm to room temperature, removed from the RNAlater solution, and frozen in liquid nitrogen.
ii. The frozen sample was powdered using a freezer mill (Dismembrator, Braun Biotech Ltd) at 1600rpm for 2 minutes together with 100µl buffer RLT-DTT from the Qiagen kit.
iii. For complete homogenization, another 250µl buffer RLT-DTT was added and dismembratation was continued for a further 5 minutes.
iv. After collecting the tissue suspension in a 1.5ml tube, it was centrifuged at 12000rpm for 3 minutes.
v. The supernatant was transferred to a fresh tube, mixed with 350µl 70% ethanol, applied to an RNeasy spin column, followed by a wash step.
vi. Contaminating DNA was degraded by applying 80µl Buffer RDD-DNase-I to the spin column and incubating at room temperature for 10 minutes.
vii. After 2 further wash steps, the RNA was eluted in 35µl water.

2.2.5.4 RNA quality test

The quality of the extracted RNA was tested by gel electrophoresis.

i. 100ml of 1% agarose in 1× running buffer ('SB buffer', 36mM boric acid, pH 8.0) was heated to boiling point, cooled to 55°C and poured into a gel mould.
ii. A 10µl RNA sample was premixed with 2µl 6× loading buffer (New England BioLabs, #B7025S) and 0.25µl SYBR gold stain (Thermo-Fisher, #10358492).
iii. A 10µl sample was loaded into the well, and electrophoresis was carried out for 15 minutes at 120 volts.
iv. The gel was photographed under UV light.

Approximately 70-80% of RNA in tissues is ribosomal RNA (rRNA), which is composed of 5.8S, 18S and 28S subunits. The latter two subunits are readily visualised on 1% agarose electrophoresis gels (Figure 2.1), while 5.8s rRNA is selectively excluded during the extraction procedure due to its low molecular weight. The presence of strongly-staining 18S and 28S bands was taken as evidence of good RNA integrity.

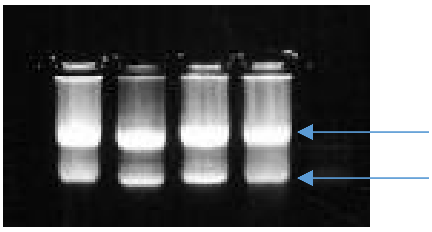

Figure 2.1. RNA electrophoresis showing the 28S and 18S ribosomal subunits (upper and lower bands, respectively).

2.2.6 Polymerase chain reaction (PCR) sexing test

To test the quality of the extracted DNA and simultaneously test the sex of the chicks, a PCR-based assay was performed, based on the following mechanism:
Male chicks carry two copies of the Z chromosome whilst females carry one Z and one W chromosome. Based on the sequence of the CHD (Chromo Helicase DNA-binding) gene, which is present on both Z and W chromosomes, the sexes can be inferred by performing an allele-specific PCR (214). For this assay, 3 PCR primers were used (Table 2.1): a forward primer that is complementary to both the Z and W chromosome CHD gene sequence. The other two primers are reverse primers specific for the Z and W chromosome copies of CHD, respectively. The two reverse primers were designed to yield PCR products of markedly different size when combined with the forward primer (322 vs. 418bp). After PCR and electrophoresis, male chicks show one band while females show two bands (Figure 2.2). This 3-primer allele-specific PCR method is faster than previously-published methods, which require a restriction enzyme digestion step.

The PCR reaction was performed as follows:

i. A 20μl 'master mixture' was prepared for each sample, comprising: 5.0μl chick DNA, 2.0μl 10× PCR Buffer (New England BioLabs), 0.4μl 0.2mM of each dNTP (New England BioLabs), 1.0 μl 1μM forward primer, 1.0μl 1μM of each reverse primer, 9.4μl water and 0.2μl (1.0 unit) Taq DNA polymerase (New England BioLabs).
ii. Samples were placed in the thermal cycler (MJ Research Dyad PCR Dual Block), with a setting of heating at 95°C for 5 min, following by 35 cycles of 94°C for 1 minute, 67°C for 1 minute and 72°C for 1 minute.

PCR products were visualised using agarose gel electrophoresis:

i. 100ml of molten 1.5% agarose in 1× running buffer ('SB buffer', 36mM boric acid, pH 8.0) was poured into a gel mould.
ii. 10μl PCR product was premixed with 2μl 6× loading buffer (New England BioLabs, #B7025S) and 0.25μl SYBR gold stain (Thermo-Fisher, #10358492).

iii. 10µl of the PCR product mixture was loaded into an electrophoresis well and run for 15 minutes at 150 volts.

iv. The gel was photographed under UV light.

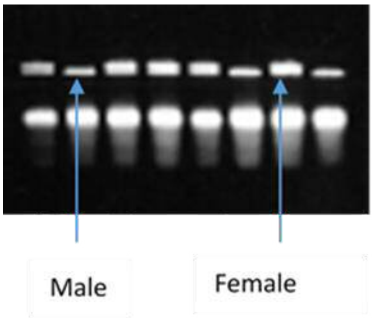

Figure 2.2. Chick sexing using allele-specific PCR and gel electrophoresis. *Female DNA samples yield 2 bands, male samples 1 band. The samples shown were classified as (left to right): F, M, F, F, F, M, F, M. The bright bands at the bottom of the gel are primer-dimer artefacts.*

Table 2.1 Allele-specific PCR primer information.

	Chromosome	
	CHD(Z)	
Forward primer	CCCAGAGRTACCTGTTTTGCACAGT	CCCAGAGR
Reverse primer	CTGGTTAAAATTATTACAGTGTGGGTACAGTTT	GAGCCCCCT
PCR product size (bp)	322bp	
Detailed information	**Galgal4:Z:51129165:51130709** TTACTAAAATAAGAAATATTTATGAATGTGTTAATGACTGCAATTCTG GGTTGTGTTGTCTTCATGCCTTTGATTAAGCATCTGTGGTGTTTTT AAACACAATAATTGATGACTTTTAGAAAGTACTTTCAGCCCTGAAGT ATACCTGAGTGCCGTATATTTTGTGTTACTGGTTAAAATTATTACAGT GTGGGTACAGTTTATAGATGCATAAAATACAGAACTTAGTTTCCCTA AAATACTAGCTGCTAAGCCATATTTAAATAAAGCCATGTATTTACTACA TATGTTCTGATGCATAAGGTGGCGAACTTTTCCAATATGGATGAAGA TGATATTGAGTTGGAACCAGAAAGAAATTCAAGAAATTGGGAAGAA ATCATCCCAGAATCCCAACGGAGAAGGATAGAGGAGGAGGAAAGA CAAAAAGAACTTGAAGAAATATACATGCTCCCGAGGATGAGAAACT GTGCAAAACAGGTACCTCTGGGTTTTGACTGTCTTGCGTCTTTATG TTGATATTTTCATTTGAGTTTTTGCCTTTTTTCCCCCTTCTCTGAAT TCATATTTTTGTCAGGCTAGATAAGACTTTACTATGTTTGAGATAATC ATGTGGTTTTGAATTCTCATGCTGAAATTCCA	**CHD-W chrW_JH375235_** TACATTAACTTGAATGTTCA TTAAACAACAGTTGCACAG ATATTAATTAACTTTTAAAAT ATCTTGAATGGAACGTATGT GATGTTGCTTCATGAAGTAT AAAATATGCCATTCCAAACT TGTTTAAATAAAATCATGTAT ACATAAGGTAGCTAACTTTT GAACCAGAACAAAATCTAAG TCAGTGGCGACGAATAGAA GAAATATATATGCTTCCAAGA TGGGTTCTGACTGATTTTT GACTTGTACTTTTGTGTTGT ATATTTTTATGGACTAGGTA

2.3 Statistics

All the statistical analysis were performed using R version 3.4.2. The statistical methods and packages are described in each chapter.

2.4 Ethical statement

This work was approved by the Animal Subjects Ethics Sub-committee of The Hong Kong Polytechnic University. The care and use of the animals in this experiments were in compliance with the ARVO Statement for the Use of Animals in Ophthalmic and Vision Research.

2.6 Flowchart of the experiment design

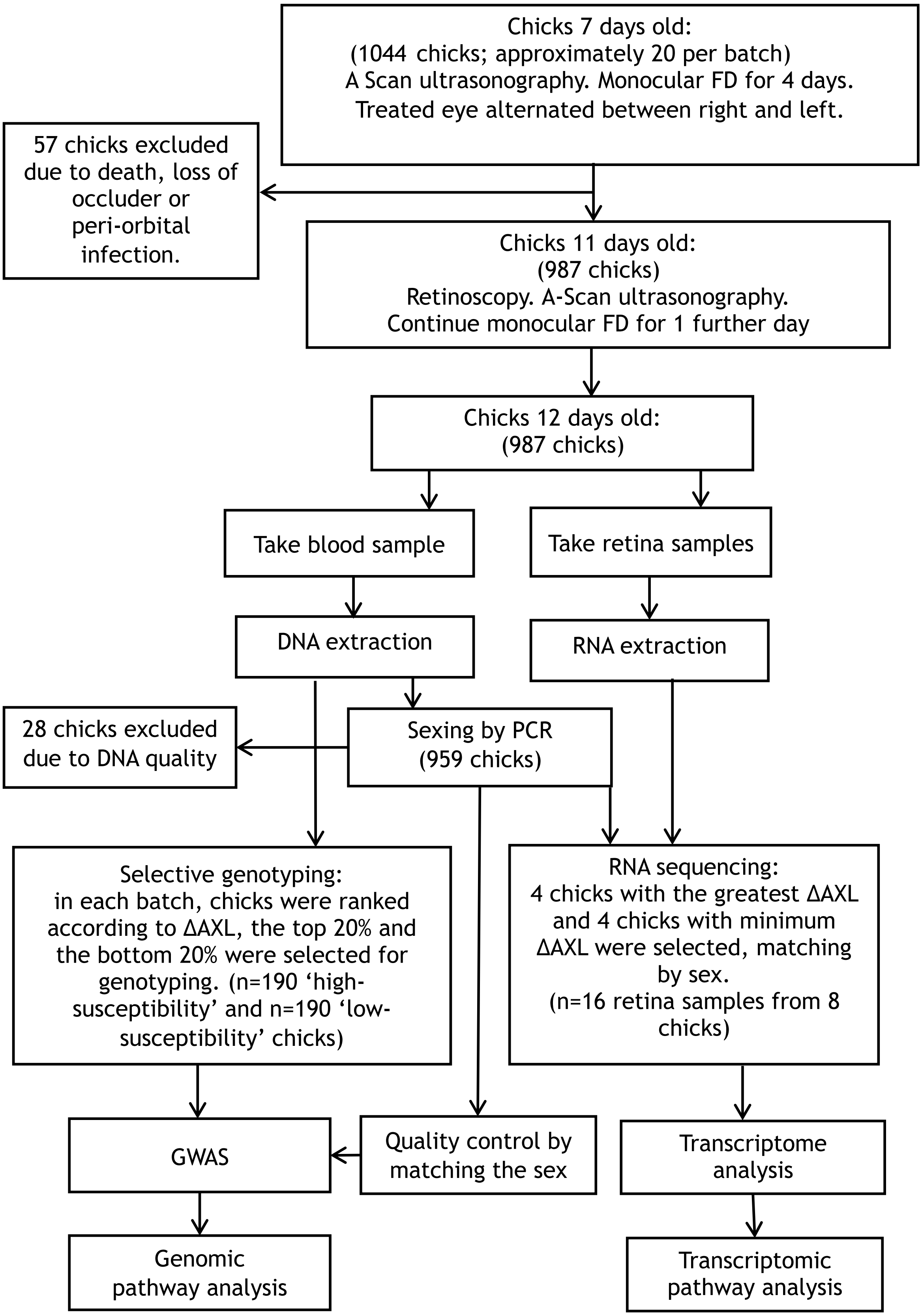

Chapter 3 Characteristics of myopia in form deprived chicks

3.1 Introduction

Epidemiology studies have identified a series of risk factors for myopia such as education level (94, 215), socioeconomic status (215) and time spent outdoors (101). Apart from these modifiable environmental risk factors, other biological traits such as height and sex have also been found to be related to ocular traits. This chapter focuses on the identification of potentially confounding factors associated with myopia in the chick form deprivation (FD) model, in order to control for their effects and thus increase statistical power in the subsequent chick myopia susceptibility GWAS (Chapter 4).

3.1.1 Height

Height, as a quantitative trait, has been found to be associated with eye size: many studies have reported that taller people have larger eyes (216-219). In a population-based cross-sectional survey of Singapore Chinese adults, after controlling for confounding factors (age, sex, education, occupation, housing type, income, and weight), it was found that taller persons tended to have longer axial lengths, deeper anterior chambers, thinner lenses, longer vitreous chambers, and flatter corneas, although refractive status was independent of stature (217). Another cross-sectional study focussing on the relationship between anthropometric determinants and ocular biometry among Singapore Chinese students revealed that 7-9 year-old children of taller stature had eyes with longer axial lengths, along with deeper vitreous chambers, thinner lenses, deeper anterior chambers, flatter corneas and more negative refractive errors (218). Similar results were found in a study of Chinese twins (219) and in the Singapore Malay Eye Study (220). Studies in European cohorts have reached similar conclusions. A survey of 790 Finnish twins revealed that the myopic subjects were taller compared to the non-myopic subjects, among males (221). However, an association between height and refractive error has not been observed in all studies. Rosner et al. (222) conducted an investigation among 106,926 male military recruits aged 17 to 19 years, and found that those who were highly myopic were slightly shorter compared to those with mild myopia and non-myopes. Another study of 3,294 Danish conscripts found no relationship between height and myopia (18). Sharma's (223) study of 14 year-old students and Jung's (224) study of 19 year-old Korean males also found no association between height and refractive error (Table 3.1).

3.1.2 Body weight and body mass index (BMI)

Body weight is another important biological characteristic that reflects body size. In many studies that investigated the relationship between stature and myopia, body weight and BMI were also considered along with height. Studies conducted in the UK (225), USA (226) and Finland (227) in the 1950-1980's all reported that heavier body weight was associated with a more myopic refractive error. In recent years, studies that addressed this question were performed in Israel (222), Croatia (228), Myanmar (229), Taiwan (230), Japan (231), Singapore (217, 218, 220), Korea (224) and India (232). Nonetheless, evidence for an association between body weight and myopia was conflicting. Studies in Croatia (228), Singapore (217) and Japan (231) suggested body weight was positively related to axial length; in the Myanmar study (229), heavier persons had longer axial lengths but tended to be less myopic; the study of 106,926 Israeli males (222) found non-myopes were heavier than severe myopes; the studies conducted in Taiwan (230) and Korea (224) found no correlation between body weight and myopia (Table 3.1).

3.1.3 Sex

Sex has been found to be associated with myopia. An early survey of myopia prevalence in the USA revealed that, across all age groups, the prevalence of myopia in females was higher than in males (12). This result was replicated in several other studies (227, 233-235). A recent multi-centre study conducted on 469 children who were 6-11 years old revealed that female sex was an independent risk factor for myopia after adjusting for age, ethnicity and other confounding factors; girls developed -0.16 D ($P < 0.01$) more myopia than boys after three years of observation (236). However, in the same study, there was no association between sex and axial length elongation, indicating a complex relationship. Lu et al. (103) performed a study of 1,892 adolescent students (average age 14.6 years) in rural China. They found that girls had worse uncorrected vision than boys and that girls spent more time on homework and reading and less time on outdoor activities and playing video games. After accounting for age, parental education, near work and outdoor activity, there was no difference in refractive error between the sexes.

Many other studies did not find an association between myopia and gender. A study of 307 Danish children found no difference between the sexes in myopia rate, refractive error, or best-corrected visual acuity (237). However, the boys had longer axial lengths, deeper anterior chamber depths and flatter corneas (237). Richter's (238) study of 4,071 Chinese American participants also confirmed these findings: refractive status was similar between the two sexes, but males had longer axial lengths. Similar results were reported in the Tanjong Pagar Survey (239) and the Liwan Eye Study (240).

In some studies, female sex was found to be related to a lower prevalence of myopia. In the Singapore Longitudinal Aging Study (241), male gender was associated with a higher rate of myopia after adjusting for race, age, height, education, diabetes and hypertension. The Blue Mountains Eye Study, which examined individuals aged 49-97 year-old, identified that women were slightly more hyperopic than men, after adjusting for age (15). Shimizu et al.'s (242) study of a Japanese cohort suggested that women were more hyperopic than men (Table 3.2).

Table 3.1. Prior studies investigating the association between height, weight, BMI and ocular biometry/myopia in human subjects

Study	Date	Population (Sample size)	Age	Height	Weight	BMI	Covariates
Gardiner (225)	1954	England (463)	3 ~ 16	Taller in myopes Rapid growth rate with fast myopia development	Heavier in myopes	NA	NA
Krause (227)	1982	Finland (1939)	up to 15	Taller in those wearing spectacles (Girls)	Heavier in those wearing spectacles (Girls)	NA	Social status
Teikari (221)	1987	Finland (790)	30 ~ 31	Taller in myopes (male only)	N.S.	Smaller in myopes	height, weight, BMI
Rosner (222)	1995	Israeli (106926 male)	17 ~ 19	Shorter in severe myopes	Lighter in severe myopes	Smaller in myopes	Sex, education, intelligence
Wong (a) (217)	2001	Singapore (951)	40 ~ 79	N.S. with RE	+ RE	+ RE	Age, sex, education, SES and weight or height
Saw (218)	2002	Singapore Chinese (1449)	7 ~ 9	- RE + AXL, VCD, CC, AL-CR	+ RE -VCD	N.S.	Age, gender, parental myopia, books read per week, school, Height, weight, BMI
Shimizu (242)	2003	Japan (2168)	40 ~ 79	N.S.	+ RE (males only)	NA	For body stature: age, education, smoking, social status, diabetics, hypertension
Selović (228)	2005	Croatia (1600)	6 ~ 16	+ AXL	+ AXL	NA	NA
Wu (229)	2007	Myanmar (2418)	≥ 40	-N.S. with RE + AXL,ACD,VCD, CC and CT	+ RE + AXL, ACD, VCD , CC and CT	+ RE	Age and sex
Jacobsen (18)	2007	Danish (4681 male)	19.3	–N.S.	–N.S.	–N.S.	NA

Lee (243)	2009	USA (1968)	50 ~ 100	+ AXL	NA	NA	For height, adjusted for age, gender, education; For Sex, adjusted for age
Lim (220)	2010	Singapore and Malay (2788)	40 ~ 80	+ AXL,CC	+ AXL,CC	NA	Age, sex, education, height, weight, number of reading hours, diabetes, and current smoking
Sharma (223)	2010	Chinese (1371)	14.5	N.S.	N.S.	NA	Age, height, and parental education
Zhang (219)	2011	China (565)	7 ~15	+ AXL	NA	NA	Sex, age and sex age interaction
Jung (224)	2012	South Korea (23616 male)	19	N.S. with RE	N.S. with RE	N.S. with RE	Multivariate model include education, height, weight and BMI
Huang (230)	2014	Taiwan (88)	7 ~ 9	N.S. with RE + AXL	N.S.	NA	Sex and age
Roy (232)	2015	India (152)	7 ~ 15	+ AXL, ACD, VCD	–N.S.	+ RE	NA
Terasaki (231)	2017	Japan (122)	8 ~ 9	N.S.	+ AXL	+ AXL	Sex and parental myopia

Note: '+' indicates a positive correlation, '-' indicates a negative correlation, for example, '+ RE' means positively associated with the trait-of-interest; AXL, VCD, CC, CT, AL-CR, RE are abbreviations for axial length, vitreous chamber depth, corneal curvature, corneal thickness, axial length - corneal radius ratio, refractive error, respectively. N.S. – none significant.

Table 3.2.Prior studies investigating the association between sex and ocular biometry/myopia in human subjects.

Study	Date	Population (sample size)	Age	Sex	Covariates
Angle (235)	1980	USA	12 ~ 17	Females more often myopic	NA
Krause (227)	1982	Finland (1939)	up to 15	Females wore spectacles more often	Social status
Sperduto (12)	1983	USA (9882)	12 ~ 54	Females more often myopic	NA
Wang (233)	1994	USA (4533)	43 ~ 84	Females more often myopic	Age
Attebo (15)	1999	Australia (3654)	49 ~ 79	Males were more myopic	Age
Wong (b) (239)	2001	Singapore (1717)	40 ~ 79	Non - significant with RE Males had longer AXL	Age
Midelfart (234)	2002	Norway (3137)	20 ~ 45	Females more often myopic	NA
Shimizu (242)	2003	Japan (2168)	40 ~ 79	Males were more often myopic	NA
Hyman (236)	2005	USA (469) (mixed ethnic)	6 ~ 11	Males had slower myopia progression	Age, ethnicity, BRS, treatment, interaction between BRS and treatment
He (240)	2009	Guangzhou China (1269)	> 50	Non - significant with RE Males had longer AXL	Age
Lu (103)	2009	Xichang China (1829)	14.6	Girls had worse VA and a higher myopia rate Non - significant (after adjusted for covariates)	Age, parental education, near work, outdoor activity
Lee (243)	2009	USA (1968)	50 ~ 100	Men had longer AXL, flatter CR and deeper ACD	Age
Tan (241)	2011	Singapore (1835)	55 ~ 85	Male were more often myopic	Race, age, height, education, diabetes, hypertension
Huang (230)	2014	Taiwan (88)	7 ~ 9	Non - significant	Age
Roy (232)	2014	India (152)	7 ~ 15	Non - significant	NA
Lundberg (237)	2017	Danmark (307)	14 ~ 17	Non - significant with RE Males had longer AXL	NA
Richter (238)	2017	Chinese American (4071)	60.5	Non - significant with RE Males had longer AXL	Age, height
Terasaki (231)	2017	Japan (122)	8 ~ 9	Males had longer AXL	Parental Myopia

Abbreviations: AXL, RE, BRS represent axial length, refractive error and baseline refractive status, respectively.

3.1.4 The influence of body weight and sex on animal ocular biometry.

Stature (height), body weight and sex have also been considered as potential confounders for variation of animal ocular component dimensions.

The difference in eye size between animal species is related to differences in body size. Moreover, within the same animal species, body weight has also been found to be related to eye size in fish (157), mice (244) and birds (245). In herring, eye diameter increases allometrically with body length and the cubic root of body weight (246). To understand the relationship between body size and eye size, Zhou and William (247) did an experiment in mice. The eyes of approximately 700 mice from 26 BXD strains (recombinant inbred mice strains derived from crossing C57BL/6 (B) and DBA/2 (D) mice) were examined, and it was found that eye weight was positively associated with brain weight and body weight, while sex had no independent effect if body weight was accounted for.

It was reported that eye traits were related to sex. In mice, after adjusting for body weight, eyes of female mice were proportionally larger than male mice (247) ; according to Puk et al. (248), the sex-related differences of ocular parameters were not obvious in every strain of mice, but only significant in C57BL/6J and 129S2/SvPasCrl strain mice; however, in many studies, sex had no effect on eye size or myopia development. In Murphy et al.'s study (249), the refractive error of 240 dogs of various breeds was measured, and a tendency towards myopia was found in several breeds, but sex was not correlated with refractive error (249). Black et al.'s (189) study on canine inherited myopia also supported Murphy's finding. In form deprived tree shrews, the level of induced myopia was not statistically different between the sexes (250). According to Valentini et al. (251), in neonatal foal, the ocular parameters were not influenced by sex.

In many myopia experiments using chick models, body stature and sex have been considered. Zhu et al. (252) found that, during form deprivation, male chickens had deeper anterior chambers and were more susceptible to form deprivation. In Guggenheim et al.'s study (203), myopia was induced in 3 strains of chicks. Male chicks showed a 0.2mm increase in the vitreous chamber and axial length elongation as compared to female chicks, however, the level of induced myopia was similar between the sexes. A later study conducted by Chen et al. (253) reported that sex explained 6.4% of the variation in FD-induced VCD elongation, but that sex did not affect the degree of induced myopia. Body weight, as an indicator of eye size, showed no association with myopia development (253). In Schmid and Wildsoet's (204) study of White Leghorn chickens form deprived by lid suturing, susceptibility to myopia was not associated with sex.

3.2 Methods

3.2.1 Experiment models

The procedures used to induce myopia in chicks and to determine the sex of chicks are described in Chapter 2, sections 2.1 and 2.2.

3.2.2 Statistical Analysis

The frequency distribution of the eye size parameters, initial body weight (IBW) and final body weight (FBW) were tested for normality by using the Kolmogorov-Smirnov test. Because the data for the level of induced myopia (ΔMSE) and for IBW were not normally distributed, the Spearman correlation coefficient was used to test the relationship between ΔMSE versus ΔAXL, and IBW versus FBW. Comparisons between treated versus control eye, or right versus left eye, ocular component dimensions were made using paired *t*-tests. Either the 2-sample *t*-test or the Mann–Whitney U test was used to test the difference between the sexes, according to the normality of the data.

To examine potentially confounding factors that might influence myopia susceptibility, multivariate linear regression analyses were carried out, with myopia susceptibility (ΔAXL or ΔMSE) as the dependent variable and the following phenotypic characteristics as independent variables: sex, hatch-to-hatch variability ('batch effect'), initial body weight (IBW), final body weight after treatment (FBW), interaction between sex and IBW (sex × IBW) and interaction between sex and FBW (sex × FBW). There was a high correlation between IBW and FBW ($R = 0.83$, $P < 2.2e-16$; Figure 3.1), IBW and FBW were tested in different models to avoid collinearity. Meanwhile, since a subsample of chicks was selected for genotyping, the above potential confounding factors were also tested in this subsample of selected chicks. The R packages '*qqplot2*' and '*coefplot*' were used to produce the figures in this chapter. The statistical models tested were as follows:

Testing confounding factors for ΔAXL in all 959 chicks:

```
Model 1: ΔAXL ~ sex + batch + IBW + (sex × IBW)
Model 2: ΔAXL ~ sex + batch + FBW + (sex × FBW)
```

Testing confounding factors for ΔMSE in all 959 chicks:

```
Model 1: ΔMSE ~ sex + batch + IBW + (sex × IBW)
Model 2: ΔMSE ~ sex + batch + FBW + (sex × FBW)
```

Testing confounding factors for ΔAXL in the 380 selected chicks:

```
Model 1: ΔAXL ~ sex + batch + FBW + (sex × FBW)
Model 2: ΔAXL ~ sex + FBW + (sex × FBW)
```

Model 3: logit(case/control status) ~ $e^{\beta 0 + (\beta 1 \times Batch) + (\beta 2 \times Sex) + (\beta 3 \times FBW) + (\beta 4 \times Sex \times FBW)}$

Model 4: logit(case/control status) ~ $e^{\beta 0 + (\beta 1 \times Sex) + (\beta 2 \times FBW) + (\beta 3 \times Sex \times FBW)}$

Testing confounding factors for ΔMSE in the 380 selected chicks:

```
Model 1: ΔMSE ~ sex + batch+ FBW + (sex × FBW)
Model 2: ΔMSE ~ sex + FBW + (sex × FBW)
```

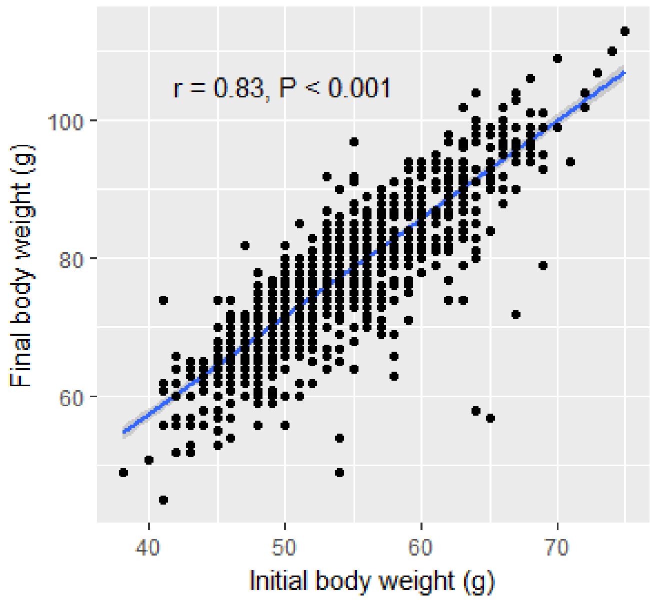

Figure 3.1.Relationship between IBW and FBW. (n=959)

3.3 Results

3.3.1 Characteristics of chick traits prior to form deprivation

A total of 987 chicks from 48 batches were form deprived. Among all the chicks, 959 of them had sex information while 38 chicks had poor quality DNA and could not be sexed. PCR sex-testing revealed that 501 (52%) were male and 458 (48%) female. On day 7, before the treatment, mean body weight of the chicks was 54.26 ± 6.36g (mean ± standard deviation), and the mean body weight of male and female chicks was 54.33 ± 6.18g and 54.19 ± 6.55g, respectively; there was no difference between male and female chick body weight (P=0.72; Table 3.3). However, when comparing the eye parameters, male chicks had longer eyes compared to female chicks in both right and left eyes (Table 3.3). In the right eyes, for example, the mean axial length was 8.74 ± 0.16mm in males while it was 8.59 ± 0.16mm in females (P<0.01). Similar differences were also observed for ACD, LT and VCD for both eyes. When comparing the right eye with the left eye, irrespective of sex, the right eye was found to be slightly longer on average than the left eye for ACD, LT, VCD and AXL (all P<0.01; Table 3.3). In general, it was found that the initial body weight was positively associated with the initial AXL (e.g. r = 0.45, P < 0.01 in the right eye, Figure 3.2).

Table 3.3. Chick parameters on day 7, before form deprivation

		Male mean ± SD (n=501)	**Female mean ± SD (n=458)**	**All mean ± SD (n =959)**	**P-value (M vs. F)**
IBW(g)		54.33±6.18	54.19±6.55	54.26±6.36	0.72
ACD (mm)	Right eye	1.38±0.04	1.35±0.04	1.37±0.04	**<0.001**
	Left eye	1.38±0.04	1.35±0.04	1.36±0.04	**<0.001**
	P-value (R vs. L)	**<0.001**	**<0.001**	**<0.001**	
LT (mm)	Right eye	2.00±0.05	1.97±0.05	1.98±0.05	**<0.001**
	Left eye	1.99±0.05	1.96±0.06	1.98±0.05	**<0.001**
	P-value (R vs. L)	**<0.001**	**0.007**	**<0.001**	
VCD (mm)	Right eye	5.36±0.14	5.27±0.14	5.32±0.14	**<0.001**
	Left eye	5.32±0.14	5.24±0.14	5.28±0.14	**<0.001**
	P-value (R vs. L)	**<0.001**	**<0.001**	**<0.001**	
AXL (mm)	Right eye	8.74±0.16	8.59±0.16	8.67±0.18	**<0.001**
	Left eye	8.69±0.16	8.55±0.16	8.62±0.18	**<0.001**
	P-value (R vs. L)	**<0.001**	**<0.001**	**<0.001**	

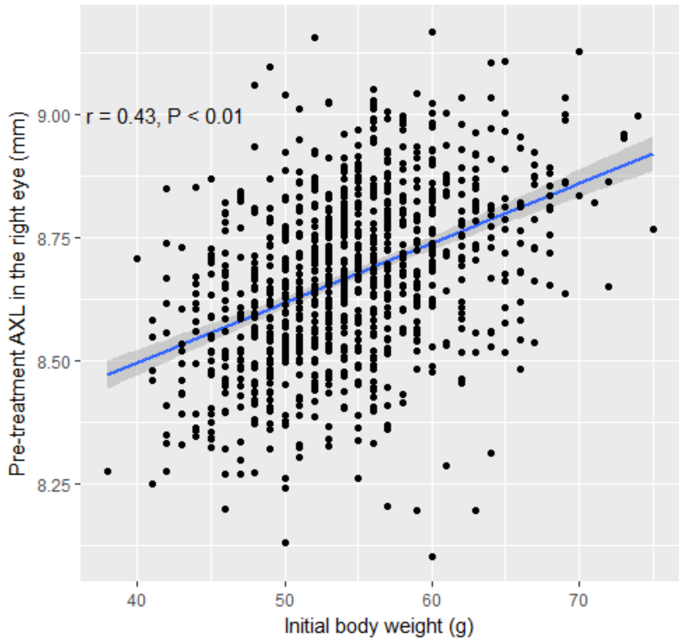

Figure 3.2.Correlation between pre-treatment AXL in the right eye and initial body weight (IBW) in the full sample (n=959).

3.3.2 Characteristics of chick traits after form deprivation

After monocular form deprivation for 4 days, the average body weight was 77.72 ± 10.54g, which again was not different between the sexes (P = 0.42). Average AXL in control eyes was 9.02 ± 0.21mm, and males had longer eyes compared to females (9.10 ± 0.19mm vs. 8.94 ± 0.20mm, P < 2.2e-16). In treated eyes, the average AXL elongated to 9.57±0.28mm; the difference in absolute AXL between male and female treated eyes was 0.16 mm (P < 2.2e-16). The average axial elongation (ΔAXL) due to FD was 0.55 ± 0.17 mm, with male and female chicks showing similar responses (P= 0.80; Table 3.4).

For mean spherical equivalent (MSE; analysed without subtracting the retinoscopy working distance), the average MSE in control eyes was 6.50 ± 1.05 D and, on average, female chicks were more hyperopic than male chicks (6.62 ± 1.00 D vs. 6.42 ± 0.91 D, P < 0.001; Table 3.4). In treated eyes, male chicks were slightly more myopic than female chicks, but the difference was not statistically significant (-4.22 ± 3.08 D in male and -4.10 ± 2.95 D in females, P = 0.56). Treated eyes were more myopic than control eyes: (-4.16 ± 3.02 D vs. 6.52 ± 0.96 D, P < 2.2e 16). The level of induced myopia was similar in males and females (-10.64 ± 3.07 D in males and -10.73 ± 2.97 D in females, P = 0.64; Table3.4).

Table 3.4. Chick parameters after FD for 4 days in the full sample (n=959).

		Male mean ± SD (n=501)	**Female mean ± SD (n=458)**	**All Mean ± SD**	**P-value (M vs. F)**
FBW (g)		77.98±10.6	77.43±10.48	77.72±10.54	0.42
ACD (mm)	control eye	1.46±0.04	1.43±0.04	1.45±0.04	**<0.001**
	treated eye	1.57±0.08	1.53±0.08	1.55±0.08	**<0.001**
	P-value (T vs C)	**<0.001**	**<0.001**	**<0.001**	
ΔACD		0.11±0.07	0.10±0.06	0.10±0.06	0.08
LT (mm)	control eye	2.15±0.05	2.11±0.04	2.13±0.05	**<0.001**
	treated eye	2.15±0.05	2.12±0.05	2.14±0.05	**<0.001**
	P-value (T vs C)	**<0.001**	**<0.001**	**<0.001**	
ΔLT		0.004±0.04	0.01±0.04	0.01±0.04	0.34
VCD (mm)	control eye	5.49±0.17	5.40±0.17	5.45±0.17	**<0.001**
	treated eye	5.93±0.22	5.84±0.22	5.88±0.22	**<0.001**
	P-value (T vs C)	**<0.001**	**<0.001**	**<0.001**	
ΔVCD		0.43±0.14	0.44±0.14	0.44±0.14	0.17
AXL (mm)	control eye	9.10±0.19	8.94±0.2	9.02±0.21	**<0.001**
	treated eye	9.65±0.27	9.49±0.27	9.57±0.28	**<0.001**
	P-value (T vs C)	**<0.001**	**<0.001**	**<0.001**	
ΔAXL		0.54±0.17	0.55±0.17	0.55±0.17	0.80
MSE (D)	control eye	6.42±0.91	6.62±1.00	6.52±0.96	**<0.001**
	treated eye	-4.22±3.08	-4.10±2.95	-4.16±3.02	0.56
	P-value (T vs C)	**<0.001**	**<0.001**	**<0.001**	
ΔMSE		-10.64±3.07	-10.73±2.97	-10.68±3.02	0.64

A further comparison between the right eye and the left eye was performed. After FD, in treated eyes, right eyes were slightly longer and more myopic than the left eyes ($P < 0.01$ and $P = 7.0e-4$ respectively); in control eyes, right eyes were longer than left eyes ($P = 0.04$), while the corresponding MSE levels were not asymmetric ($P = 0.6$).Furthermore, right eyes were more susceptible to FD-induced myopia than the left eyes. (Table 3.5)

Table 3.5. Comparison of ocular parameters in right versus left eyes after 5 days of FD. Values are presented as mean ± SD

	Chicks whose right eye is treated eye (n=485)	**Chicks whose left eye is treated eye (n=474)**	**P**
AXL in treated eye	9.62 ± 0.28	9.52 ± 0.27	**<0.001**
AXL in control eye	9.01 ± 0.21	9.04 ± 0.20	**0.04**
MSE in treated eye	-4.49 ± 2.87	-3.81 ± 3.13	**<0.001**
MSE in control eye	6.54 ± 1.02	6.50 ± 0.89	0.6
ΔAXL	0.56 ± 0.17	0.53 ± 0.17	**0.004**
ΔMSE	-11.03 ± 2.9	-10.31 ± 3.1	**<0.001**

The relationship between body weight and eye parameters after FD was also investigated. Among all of the 959 chicks, final body weight was found to be correlated with change in AXL and MSE (r=0.22, P < 0.001 and r=-0.09, p = 0.004 respectively). A similar correlation was also identified between the change in body weight and myopia susceptibility, whereas the correlation coefficients were slightly smaller (r=0.21, P < 0.001 and r=-0.08, p = 0.01, respectively) (Figure 3.3).

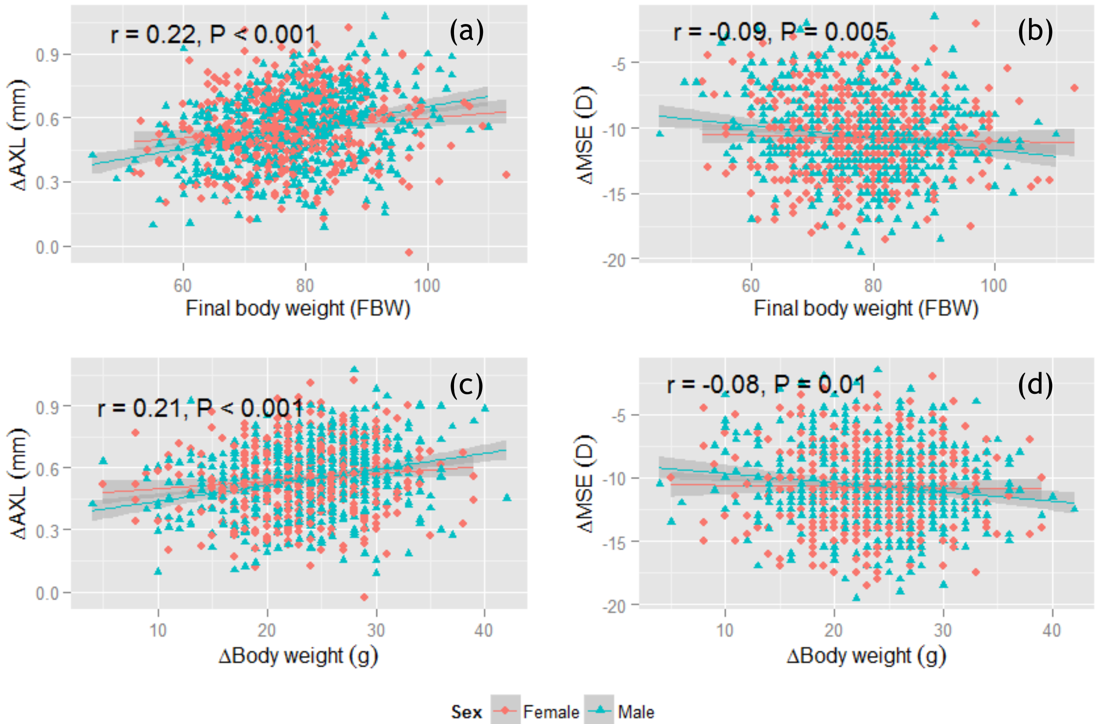

Figure 3.3.Correlation between body weight and myopia susceptibility after FD (n=959).

The body weight correlation coefficients shown are sex-averaged values. Correlation between (a) final body weight and ΔAXL; (b) final body weight and ΔMSE; (c) change in body weight and ΔAXL. (d) change in body weight and ΔMSE.

3.3.3 Myopia susceptibility in response to form deprivation (full study sample)

The parameters ΔAXL and ΔMSE were analysed separately as indicators of myopia progression among the 959 chicks. ΔAXL was selected as the main outcome measure (Chapter 1, section 1.8.3), with ΔMSE analysed additionally to guard against important findings being missed.

3.3.3.1 Chick characteristics associated with treatment-induced axial elongation (full study sample)

Two multivariate linear regression models were used to test for the confounding factors for ΔAXL (Chapter 3, section 3.2.2; n=959 chicks).

In the first model, sex, batch, IBW and sex × IBW were tested. In this model, sex, batch, and the interaction between sex and IBW were associated with ΔAXL (Figure 3.4, Table 3.6). In the multivariate model, male chicks had a ΔAXL that was approximately 0.2mm shorter than female chicks, however, this was countered by a sex × IBW interaction. Certain batches (specifically, batches 1, 30, 31, and 43) developed less AXL elongation (by approximately -0.1mm). In totality, the covariates explained 3.2% of the variation in ΔAXL.

In the second model, sex, batch, FBW and sex × FBW were tested. In this model, sex, batch, FBW and sex × FBW were associated with ΔAXL, with similar effect sizes to those observed in the first model (Figure 3.4, Table 3.6). The second model explained 5.8% of the variance in ΔAXL.

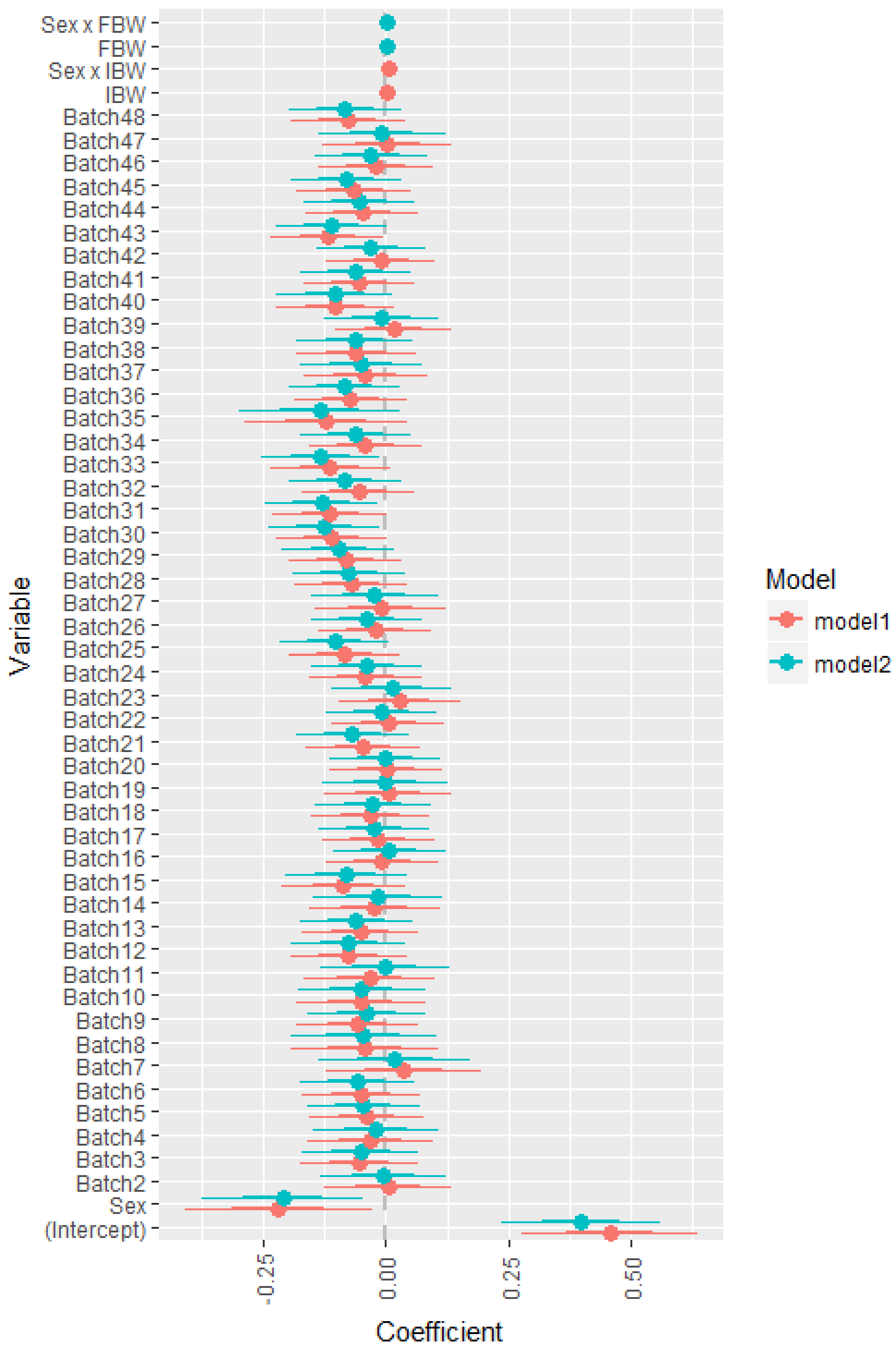

Figure 3.4.Coefficient plot showing the relationship between ΔAXL and confounding factors (full study sample).

Table 3.6.Relationship between ΔAXL and confounding factors (full study sample).

	Dependent Variable:			
	ΔAXL			
Independent variable	**Model 1**		**Model 2**	
	B (95% confidence interval)		**B (95% confidence interval)**	
Sex (female as reference)				
Male	**-0.220****	**(-0.407, -0.034)**	**-0.211****	**(-0.371, -0.051)**
Batch (Batch 1 as reference category)				
Batch2	0.004	(-0.123, 0.131)	-0.007	(-0.132, 0.119)
Batch3	-0.055	(-0.173, 0.064)	-0.051	(-0.168, 0.066)
Batch4	-0.032	(-0.159, 0.095)	-0.021	(-0.146, 0.104)
Batch5	-0.04	(-0.154, 0.074)	-0.046	(-0.158, 0.066)
Batch6	-0.051	(-0.168, 0.066)	-0.059	(-0.174, 0.055)
Batch7	0.037	(-0.117, 0.192)	0.017	(-0.135, 0.170)
Batch8	-0.044	(-0.192, 0.104)	-0.047	(-0.193, 0.099)
Batch9	-0.058	(-0.179, 0.062)	-0.041	(-0.160, 0.078)
Batch10	-0.052	(-0.182, 0.077)	-0.05	(-0.178, 0.077)
Batch11	-0.033	(-0.164, 0.097)	-0.002	(-0.132, 0.127)
Batch12	-0.077	(-0.193, 0.040)	-0.075	(-0.190, 0.039)
Batch13	-0.052	(-0.167, 0.064)	-0.061	(-0.175, 0.053)
Batch14	-0.023	(-0.155, 0.109)	-0.017	(-0.146, 0.113)
Batch15	-0.087	(-0.211, 0.037)	-0.081	(-0.203, 0.040)
Batch16	-0.008	(-0.122, 0.107)	0.007	(-0.106, 0.119)
Batch17	-0.016	(-0.129, 0.096)	-0.025	(-0.136, 0.086)
Batch18	-0.032	(-0.150, 0.085)	-0.026	(-0.141, 0.088)
Batch19	0.004	(-0.123, 0.131)	-0.003	(-0.128, 0.122)
Batch20	0.001	(-0.112, 0.114)	-0.001	(-0.113, 0.111)
Batch21	-0.048	(-0.161, 0.066)	-0.068	(-0.180, 0.044)
Batch22	0.005	(-0.108, 0.117)	-0.011	(-0.122, 0.100)
Batch23	0.027	(-0.094, 0.149)	0.012	(-0.108, 0.131)
Batch24	-0.041	(-0.153, 0.070)	-0.039	(-0.149, 0.072)
Batch25	-0.084	(-0.195, 0.026)	-0.106*	(-0.215, 0.004)
Batch26	-0.022	(-0.135, 0.091)	-0.04	(-0.151, 0.071)
Batch27	-0.011	(-0.141, 0.119)	-0.024	(-0.152, 0.103)
Batch28	-0.071	(-0.186, 0.043)	-0.076	(-0.189, 0.037)
Batch29	-0.083	(-0.197, 0.032)	-0.097*	(-0.209, 0.016)
Batch30	**-0.112****	**(-0.223, -0.001)**	**-0.127****	**(-0.236, -0.017)**
Batch31	**-0.115****	**(-0.229, -0.001)**	**-0.131****	**(-0.244, -0.018)**
Batch32	-0.057	(-0.170, 0.057)	-0.084	(-0.196, 0.028)
Batch33	-0.114*	(-0.234, 0.006)	**-0.135****	**(-0.254, -0.017)**
Batch34	-0.042	(-0.154, 0.070)	-0.063	(-0.174, 0.047)
Batch35	-0.121	(-0.284, 0.042)	-0.135*	(-0.296, 0.025)
Batch36	-0.072	(-0.184, 0.041)	-0.084	(-0.195, 0.027)
Batch37	-0.042	(-0.167, 0.083)	-0.051	(-0.174, 0.072)

Batch38	-0.061	(-0.180, 0.059)	-0.064	(-0.181, 0.054)
Batch39	0.016	(-0.102, 0.133)	-0.009	(-0.125, 0.106)
Batch40	-0.104*	(-0.222, 0.014)	-0.104*	(-0.220, 0.012)
Batch41	-0.055	(-0.167, 0.057)	-0.062	(-0.172, 0.048)
Batch42	-0.011	(-0.122, 0.100)	-0.03	(-0.139, 0.078)
Batch43	**-0.119****	**(-0.232, -0.006)**	**-0.113****	**(-0.223, -0.002)**
Batch44	-0.049	(-0.162, 0.065)	-0.056	(-0.167, 0.056)
Batch45	-0.066	(-0.180, 0.048)	-0.081	(-0.194, 0.031)
Batch46	-0.021	(-0.137, 0.095)	-0.031	(-0.145, 0.082)
Batch47	0.002	(-0.127, 0.131)	-0.009	(-0.136, 0.119)
Batch48	-0.078	(-0.192, 0.037)	-0.083	(-0.196, 0.029)
IBW	0.003*	(-0.0001, 0.005)		
Interaction (Female × IBW as reference)				
Male × IBW	**0.004****	**(0.001, 0.007)**		
FBW			**0.003*****	**(0.001, 0.004)**
Interaction (Female × FBW as reference)				
Male × FBW			**0.003****	**(0.001, 0.005)**
Constant	**0.456*****	**(0.280, 0.632)**	**0.397*****	**(0.240, 0.555)**
Observations	958		958	
R^2	0.083		0.107	
Adjusted R^2	0.032		0.058	
Residual Std. Error (df = 907)	0.168		0.165	
F Statistic (df = 50; 907)	**1.637*****		**2.180*****	

Note:*p<0.1; **p<0.05; ***p<0.01

3.3.3.2. Chick characteristics associated with the treatment-induced degree of myopia (full study sample).

In the full study sample (n=959 chicks), there was a high correlation between change in MSE and change in AXL (r = 0.74, P < 0.001; Figure3.5).

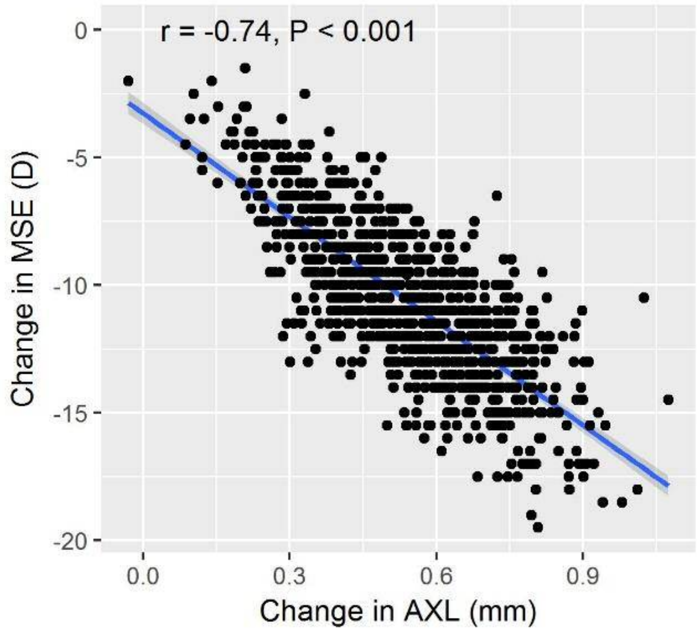

Figure 3.5.Relationship between change in MSE and change in AXL in 959 chicks.

Two multivariate linear regression models were used to test for confounding factors for ΔMSE. In the first model, only the batch effect term was associated with ΔMSE (Figure 3.6, Table 3.7); more than half of the batches showed evidence of less myopia susceptibility than in the reference batch (batch 1). In model 2, both batch and FBW were associated with ΔMSE, while sex and the interaction between sex and FBW were not. Models 1 and 2 explained similar proportions of the variance in ΔMSE (model 1: adjusted R^2 = 7.2%, model 2: adjusted R^2 = 8.8%; Figure 3.6, Table 3.7)

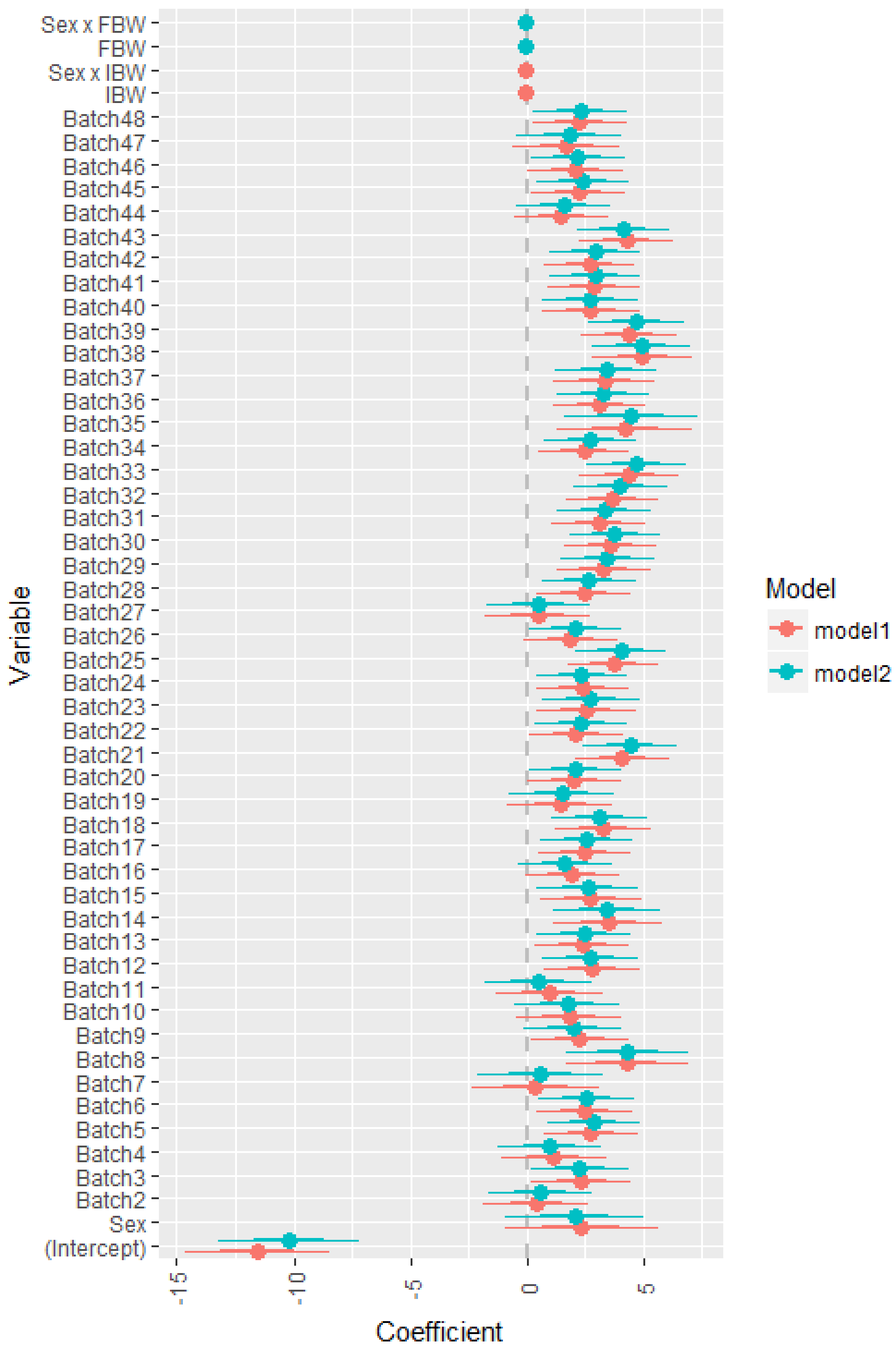

Figure 3.6.Coefficient plot showing the relationship between ΔMSE and confounding factors (n=959).

Table 3.7. Relationship between ΔMSE and confounding factors (n=959).

	Dependent Variable:			
	ΔMSE			
Independent variable	Model 1		Model 2	
	B (95% confidence interval)		B (95% confidence interval)	
Sex (female as reference)				
Male	2.347	**(-0.899, 5.594)**	2.047	(-0.860, 4.954)
Batch (Batch 1 as reference category)				
Batch2	0.398	(-1.803, 2.600)	0.594	(-1.592, 2.780)
Batch3	**2.333****	**(0.252, 4.414)**	**2.266****	**(0.205, 4.326)**
Batch4	1.153	(-1.046, 3.352)	0.984	(-1.198, 3.165)
Batch5	**2.733*****	**(0.763, 4.703)**	**2.854*****	**(0.901, 4.807)**
Batch6	**2.493****	**(0.466, 4.519)**	**2.556****	**(0.557, 4.556)**
Batch7	0.368	(-2.314, 3.049)	0.584	(-2.067, 3.235)
Batch8	**4.263*****	**(1.699, 6.826)**	**4.314*****	**(1.773, 6.855)**
Batch9	**2.275****	**(0.185, 4.365)**	1.981*	(-0.094, 4.057)
Batch10	1.807	(-0.436, 4.051)	1.741	(-0.483, 3.965)
Batch11	0.954	(-1.307, 3.214)	0.463	(-1.790, 2.717)
Batch12	**2.760*****	**(0.742, 4.778)**	**2.719*****	**(0.722, 4.717)**
Batch13	**2.367****	**(0.363, 4.370)**	**2.452****	**(0.472, 4.431)**
Batch14	**3.497*****	**(1.207, 5.786)**	**3.425*****	**(1.159, 5.690)**
Batch15	**2.729****	**(0.583, 4.875)**	**2.608****	**(0.487, 4.730)**
Batch16	1.925*	(-0.056, 3.906)	1.642	(-0.324, 3.608)
Batch17	**2.468****	**(0.516, 4.420)**	**2.570*****	**(0.636, 4.503)**
Batch18	**3.275*****	**(1.240, 5.311)**	**3.106*****	**(1.103, 5.110)**
Batch19	1.424	(-0.779, 3.626)	1.487	(-0.692, 3.667)
Batch20	**2.028****	**(0.063, 3.993)**	**2.050****	**(0.102, 3.998)**
Batch21	**4.100*****	**(2.138, 6.062)**	**4.430*****	**(2.476, 6.385)**
Batch22	**2.116****	**(0.165, 4.067)**	**2.323****	**(0.390, 4.257)**
Batch23	**2.539****	**(0.436, 4.642)**	**2.750*****	**(0.663, 4.836)**
Batch24	**2.385****	**(0.433, 4.338)**	**2.357****	**(0.422, 4.293)**
Batch25	**3.724*****	**(1.807, 5.640)**	**4.037*****	**(2.128, 5.945)**
Batch26	1.869*	(-0.088, 3.826)	**2.071****	**(0.138, 4.004)**
Batch27	0.464	(-1.750, 2.678)	0.502	(-1.681, 2.685)
Batch28	**2.447****	**(0.452, 4.443)**	**2.651*****	**(0.670, 4.631)**
Batch29	**3.289*****	**(1.309, 5.270)**	**3.452*****	**(1.489, 5.415)**
Batch30	**3.594*****	**(1.667, 5.521)**	**3.770*****	**(1.861, 5.678)**
Batch31	**3.091*****	**(1.112, 5.069)**	**3.314*****	**(1.350, 5.278)**
Batch32	**3.657*****	**(1.693, 5.620)**	**4.022*****	**(2.069, 5.975)**
Batch33	**4.390*****	**(2.309, 6.470)**	**4.694*****	**(2.630, 6.757)**
Batch34	**2.441****	**(0.504, 4.378)**	**2.724*****	**(0.800, 4.648)**
Batch35	**4.207*****	**(1.381, 7.034)**	**4.463*****	**(1.659, 7.267)**
Batch36	**3.129*****	**(1.177, 5.080)**	**3.297*****	**(1.361, 5.233)**
Batch37	**3.316*****	**(1.149, 5.483)**	**3.416*****	**(1.273, 5.560)**
Batch38	**4.937*****	**(2.844, 7.029)**	**4.911*****	**(2.845, 6.977)**

Batch39	**4.394*** **	**(2.361, 6.427)**	**4.711*** **	**(2.695, 6.726)**
Batch40	**2.754*** **	**(0.705, 4.803)**	**2.709*** **	**(0.687, 4.731)**
Batch41	**2.844*** **	**(0.906, 4.782)**	**2.915*** **	**(0.995, 4.835)**
Batch42	**2.677*** **	**(0.759, 4.594)**	**2.916*** **	**(1.018, 4.814)**
Batch43	**4.263*** **	**(2.309, 6.216)**	**4.133*** **	**(2.202, 6.063)**
Batch44	1.482	(-0.484, 3.448)	1.567	(-0.381, 3.514)
Batch45	**2.209** **	**(0.227, 4.191)**	**2.397** **	**(0.435, 4.359)**
Batch46	**2.068** **	**(0.063, 4.073)**	**2.161** **	**(0.181, 4.141)**
Batch47	1.704	(-0.538, 3.945)	1.827	(-0.393, 4.047)
Batch48	**2.250** **	**(0.265, 4.234)**	**2.283** **	**(0.317, 4.248)**
IBW	-0.034	(-0.080, 0.013)		
Interaction (Female × IBW as reference)				
Male × IBW	-0.042	(-0.101, 0.018)		
FBW			**-0.042*** **	**(-0.074, -0.011)**
Interaction (Female × FBW as reference)				
Male × FBW			-0.025	(-0.062, 0.012)
Constant	**-11.56*** **	**(-14.614, -8.505)**	**-10.20*** **	**(-13.125, -7.275)**
Observations	955		955	
R^2	0.121		0.136	
Adjusted R^2	0.072		0.088	
Residual Std. Error (df = 904)	2.909		2.884	
F Statistic (df = 50; 904)	**2.481*** **		**2.837*** **	

Note: *p<0.1; **p<0.05; ***p<0.01

3.3.4 Phenotypic characteristics of chicks selected for genotyping

To reduce costs, not all of the chicks were genotyped; instead, only chicks in the myopia susceptibility phenotype extremes were genotyped (see Chapter 4, section 4.4.8). Chick selection was based on the phenotype ΔAXL, rather than ΔMSE (see Chapter 1, section 1.8.3). Thus, it was planned that the chicks would be ranked according to ΔAXL, and the top 20% and the bottom 20% of the full sample selected for genotyping. However, according to the results above (section 3.3.3.1), there was a batch effect. Therefore, in order to avoid bias from the batch effect, instead of selecting chicks from the whole population at once, chicks were selected within each batch separately. Thus, from within each batch, the 20% of the chicks with largest treatment-induced AXL change and the 20% with the smallest change were selected. A total number of 380 chicks, comprising 190 chicks with a relatively low ΔAXL and 190 with a relatively high ΔAXL, were selected for genotyping (Figure 3.7). For the low ΔAXL chicks, the average ΔAXL was 0.31 ± 0.08 mm while for high ΔAXL chicks, the average ΔAXL was 0.78 ± 0.08 mm (Figure 3.8a). The difference in ΔAXL between high and low chicks was 0.47 mm (P < 2.2e-16). The average ΔMSE was -13.55 ± 2.29D in the high ΔAXL subsample and -7.14 ± 2.29D in the low ΔAXL subsample. The difference of ΔMSE between the selected chicks was 6.41D ($P < 2.2e-16$). (Figure 3.8b)

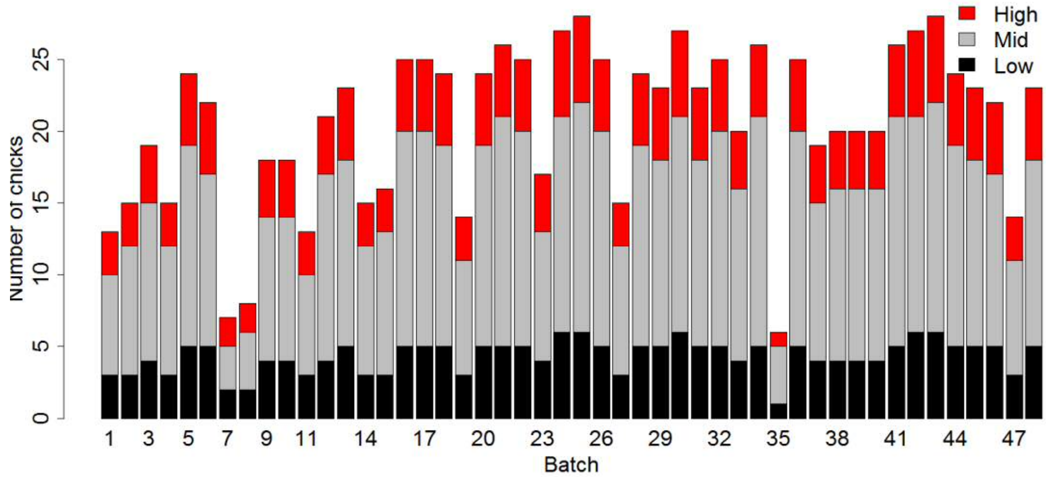

Figure 3.7. Number of chicks selected from each batch.
A total of 48 batches of chicks were examined. Each bar represents the number of chicks in the batch, with the red section and the black section representing the number of high ΔAXL and low ΔAXL chicks selected, respectively. The total sample size=959.

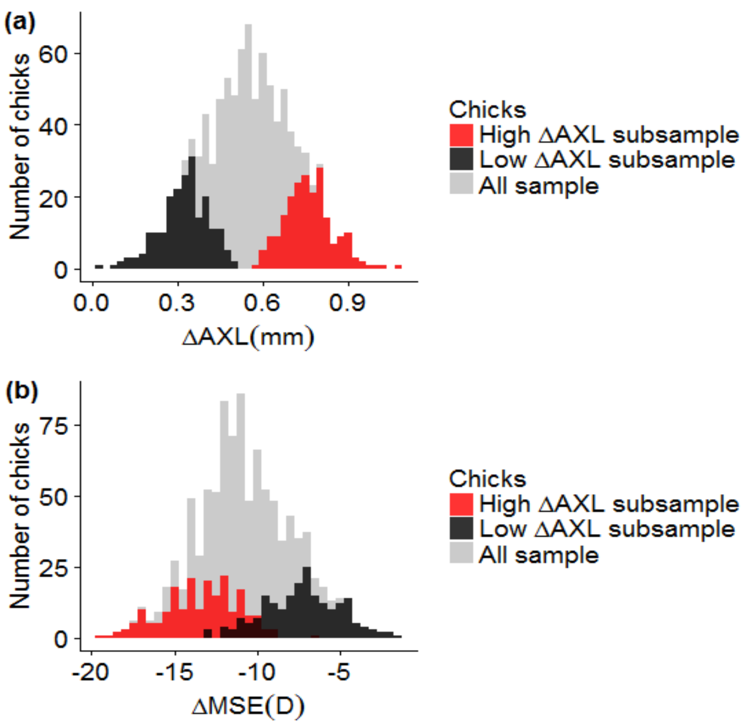

Figure 3.8. Phenotype distribution in selected chicks.
Red bars represent chicks in the high ΔAXL subsample, black bars represent chicks in the low ΔAXL subsample, and grey bars represent all chicks. Panel (a) shows the distribution of ΔAXL and panel (b) the distribution of ΔMSE. The total sample size=959.

3.3.5 Myopia susceptibility in response to form deprivation in selected chicks

According to the analyses described above (section 3.3.3), the FBW of chicks explained more of the variance in ΔAXL than did IBW, hence FBW and sex would be considered in the following analysis. The main difference between selected chicks and the full sample was the adjustment for batch effect. To explore if these were also true in the chicks after selection by batch, the relationship of potential confounders was re-evaluated in the 380 selected chicks.

3.3.5.1 Chick characteristics associated with treatment-induced axial elongation (selected sample, n=380)

As before, two multivariate linear regression and two logistic regression models were fitted (see section 3.2.2), with ΔAXL as the dependent variable (n=380). The results are shown in Table 3.7.

In model 1, sex, FBW, and the interaction between sex and FBW were associated with ΔAXL. There was no evidence for a batch effect, consistent with chicks being selected within each batch separately. In model 2, which was similar to model 1 except that a term for batch effects was not included, sex and the interaction between sex and FBW were associated with ΔAXL. Model 2 explained more of the variance in ΔAXL than model 1 (model 1, adjusted R^2 = 3.2%; model 2, adjusted R^2 = 9.8%; Figure 3.9, Table 3.8).

In model 3, case/control status (i.e. high ΔAXL versus low ΔAXL) was associated with sex and the interaction between sex and FBW. Again, no batch effect was observed. In model 4 which did not contain a term for batch effects,) the model fit was better than model 3: model 3, Akaike information criterion –-AIC = 565.6; model 4, AIC = 494.3, Figure 3.9, Table 3.8.

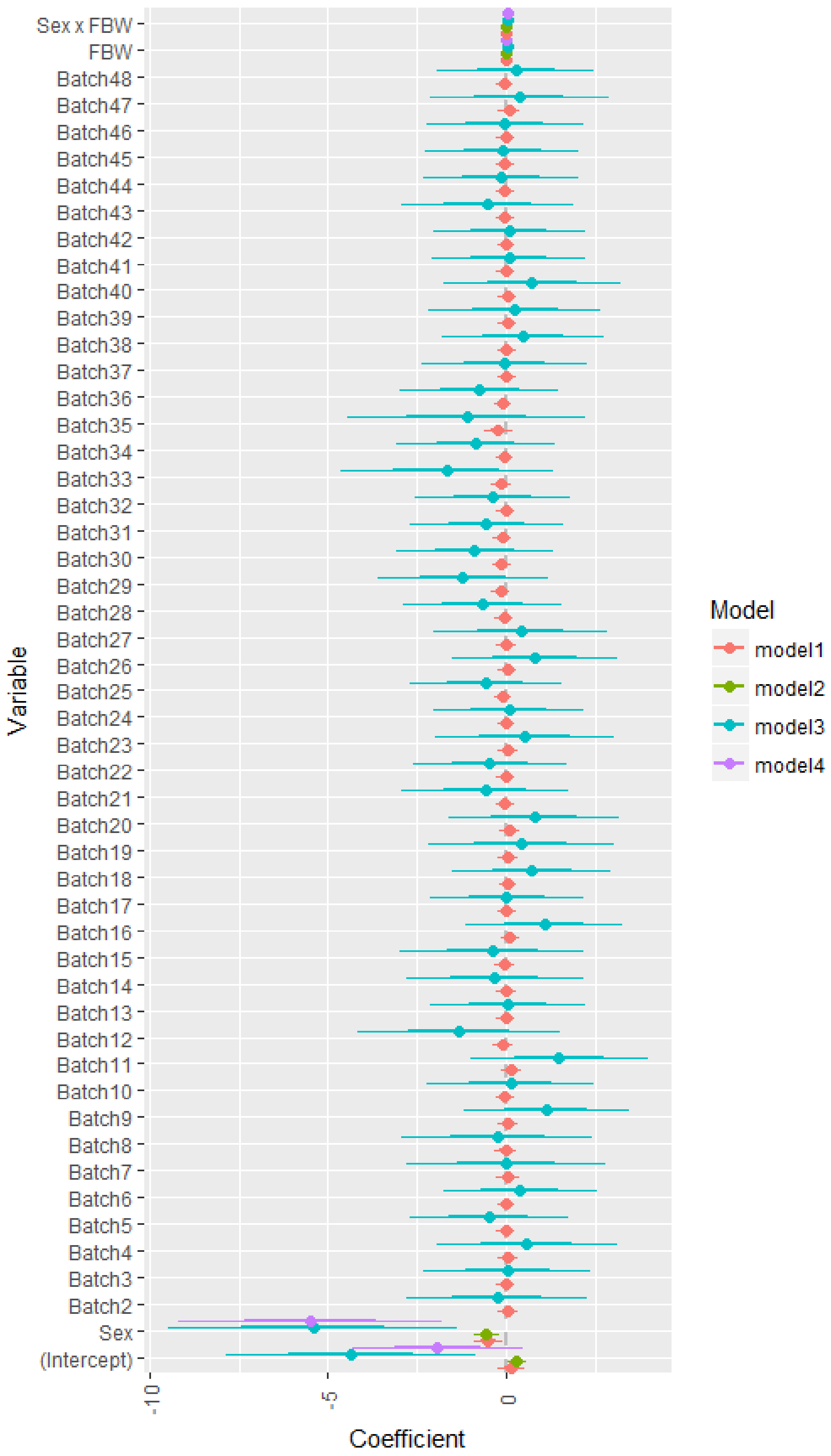

Figure 3.9.Coefficient plot showing the relationship between ΔAXL and confounding factors (selected chicks, n = 380).

Table 3.8.Relationship between ΔAXL and confounding factors (selected chicks, n = 380).

Independent variable	Dependent Variable							
	ΔAXL Linear regression				Case-control status Logistic regression			
	Model 1		Model 2		Model 3		Model 4	
	B (95% confidence interval)		B (95% confidence interval)		B (95% confidence interval)		B (95% confidence interval)	
Sex (Female as reference)								
Male	**-0.503****	**(-0.905, -0.101)**	**-0.543*****	**(-0.903, -0.184)**	**-5.421*****	**(-9.399, -1.442)**	**-5.497*****	**(-9.100, -1.893)**
Batch (Batch 1 as reference category)								
Batch2	0.045	(-0.245, 0.334)			-0.253	(-2.754, 2.248)		
Batch3	-0.007	(-0.272, 0.258)			0.036	(-2.272, 2.345)		
Batch4	0.048	(-0.243, 0.339)			0.581	(-1.911, 3.073)		
Batch5	-0.017	(-0.268, 0.234)			-0.476	(-2.666, 1.714)		
Batch6	0.004	(-0.242, 0.250)			0.395	(-1.718, 2.509)		
Batch7	0.052	(-0.255, 0.359)			0.008	(-2.715, 2.731)		
Batch8	-0.009	(-0.315, 0.298)			-0.248	(-2.858, 2.361)		
Batch9	0.05	(-0.209, 0.309)			1.121	(-1.156, 3.399)		
Batch10	-0.028	(-0.294, 0.237)			0.126	(-2.164, 2.417)		
Batch11	0.154	(-0.124, 0.431)			1.495	(-0.938, 3.929)		
Batch12	-0.102	(-0.391, 0.188)			-1.34	(-4.128, 1.448)		
Batch13	-0.008	(-0.253, 0.238)			0.059	(-2.063, 2.181)		
Batch14	0.01	(-0.265, 0.284)			-0.315	(-2.754, 2.123)		
Batch15	-0.05	(-0.340, 0.241)			-0.378	(-2.910, 2.155)		
Batch16	0.106	(-0.144, 0.356)			1.08	(-1.079, 3.240)		
Batch17	0.021	(-0.225, 0.266)			0.025	(-2.104, 2.154)		
Batch18	0.056	(-0.192, 0.304)			0.731	(-1.454, 2.916)		

Batch19	0.054	(-0.234, 0.341)	0.429	(-2.123, 2.982)
Batch20	0.103	(-0.161, 0.368)	0.789	(-1.556, 3.135)
Batch21	-0.032	(-0.295, 0.231)	-0.581	(-2.878, 1.715)
Batch22	-0.007	(-0.253, 0.239)	-0.447	(-2.564, 1.671)
Batch23	0.053	(-0.222, 0.329)	0.53	(-1.948, 3.009)
Batch24	0.012	(-0.226, 0.251)	0.087	(-1.984, 2.158)
Batch25	-0.075	(-0.314, 0.163)	-0.58	(-2.664, 1.504)
Batch26	0.041	(-0.215, 0.297)	0.812	(-1.477, 3.101)
Batch27	0.006	(-0.269, 0.282)	0.419	(-1.967, 2.804)
Batch28	-0.06	(-0.306, 0.186)	-0.661	(-2.860, 1.539)
Batch29	-0.153	(-0.418, 0.112)	-1.215	(-3.572, 1.143)
Batch30	-0.116	(-0.361, 0.130)	-0.873	(-3.019, 1.272)
Batch31	-0.102	(-0.348, 0.143)	-0.542	(-2.641, 1.558)
Batch32	-0.014	(-0.261, 0.232)	-0.384	(-2.533, 1.766)
Batch33	-0.129	(-0.418, 0.160)	-1.659	(-4.583, 1.264)
Batch34	-0.042	(-0.291, 0.206)	-0.853	(-3.025, 1.318)
Batch35	-0.226	(-0.617, 0.165)	-1.108	(-4.378, 2.162)
Batch36	-0.089	(-0.336, 0.157)	-0.74	(-2.916, 1.436)
Batch37	0.022	(-0.236, 0.279)	-0.041	(-2.314, 2.232)
Batch38	0.019	(-0.239, 0.277)	0.49	(-1.735, 2.714)
Batch39	0.035	(-0.229, 0.299)	0.247	(-2.115, 2.609)
Batch40	0.031	(-0.236, 0.298)	0.738	(-1.699, 3.176)
Batch41	-0.015	(-0.261, 0.231)	0.084	(-2.027, 2.195)
Batch42	0.022	(-0.216, 0.259)	0.089	(-2.000, 2.177)
Batch43	-0.034	(-0.292, 0.224)	-0.511	(-2.893, 1.870)

Batch44	-0.025	(-0.270, 0.221)			-0.133	(-2.271, 2.004)		
Batch45	-0.028	(-0.274, 0.219)			-0.107	(-2.236, 2.022)		
Batch46	-0.013	(-0.259, 0.232)			-0.035	(-2.188, 2.118)		
Batch47	0.085	(-0.204, 0.373)			0.382	(-2.084, 2.848)		
Batch48	-0.035	(-0.283, 0.212)			0.283	(-1.881, 2.448)		
FBW	**0.005****	**(0.001, 0.010)**	0.003*	(-0.0003, 0.007)	**0.057*****	**(0.018, 0.095)**	0.025	(-0.005, 0.055)
Interaction (Female × FBW as reference)								
Male × FBW	**0.006****	**(0.001, 0.011)**	**0.007*****	**(0.002, 0.011)**	**0.068*****	**(0.017, 0.118)**	**0.069*****	(0.023, 0.115)
Constant	0.139	(-0.245, 0.524)	**0.307****	**(0.039, 0.575)**	**-4.348****	**(-7.781, -0.915)**	-1.918	(-4.269, 0.432)
Observations	380		380		380		380	
R^2	0.16		0.105		/		/	
Adjusted R^2	0.032		0.098		/		/	
Log Likelihood	/		/		-231.788		-243.175	
Akaike information criterion	/		/		565.575		494.349	
Residual Stander Error	0.242 (df = 329)		0.234 (df = 376)		/		/	
F Statistic	1.25 (df = 50; 329)		14.693*** (df = 3; 376)		/		/	

Note: *p<0.1; **p<0.05; ***p<0.01

3.3.5.2 Chick characteristics associated with treatment-induced degree of myopia (selected sample, n=380)

Chick characteristics associated with ΔMSE in the selected sample were tested in two multiple linear regression models (see section 3.2.2). In the first model, ΔMSE was associated with the batch, despite the chicks having been selected within each batch separately (Figure 3.10, Table 3.9). A reason for this may be that although ΔMSE and ΔAXL are highly correlated, they have different relationships with potential confounders (see Table 3.6 versus Table3.7). Sex and FBW were also associated with ΔMSE. In the second model 2 (in which a batch effect was not included), sex and the interaction between sex and FBW were associated with ΔMSE. Model 1 and model 2 explained a similar proportion of the variance in ΔMSE (model 1, adjusted R^2 = 5.0%; model 2, adjusted R^2 = 5.9%; Figure 3.10, Table 3.9) suggesting that the influence of batch was minimal.

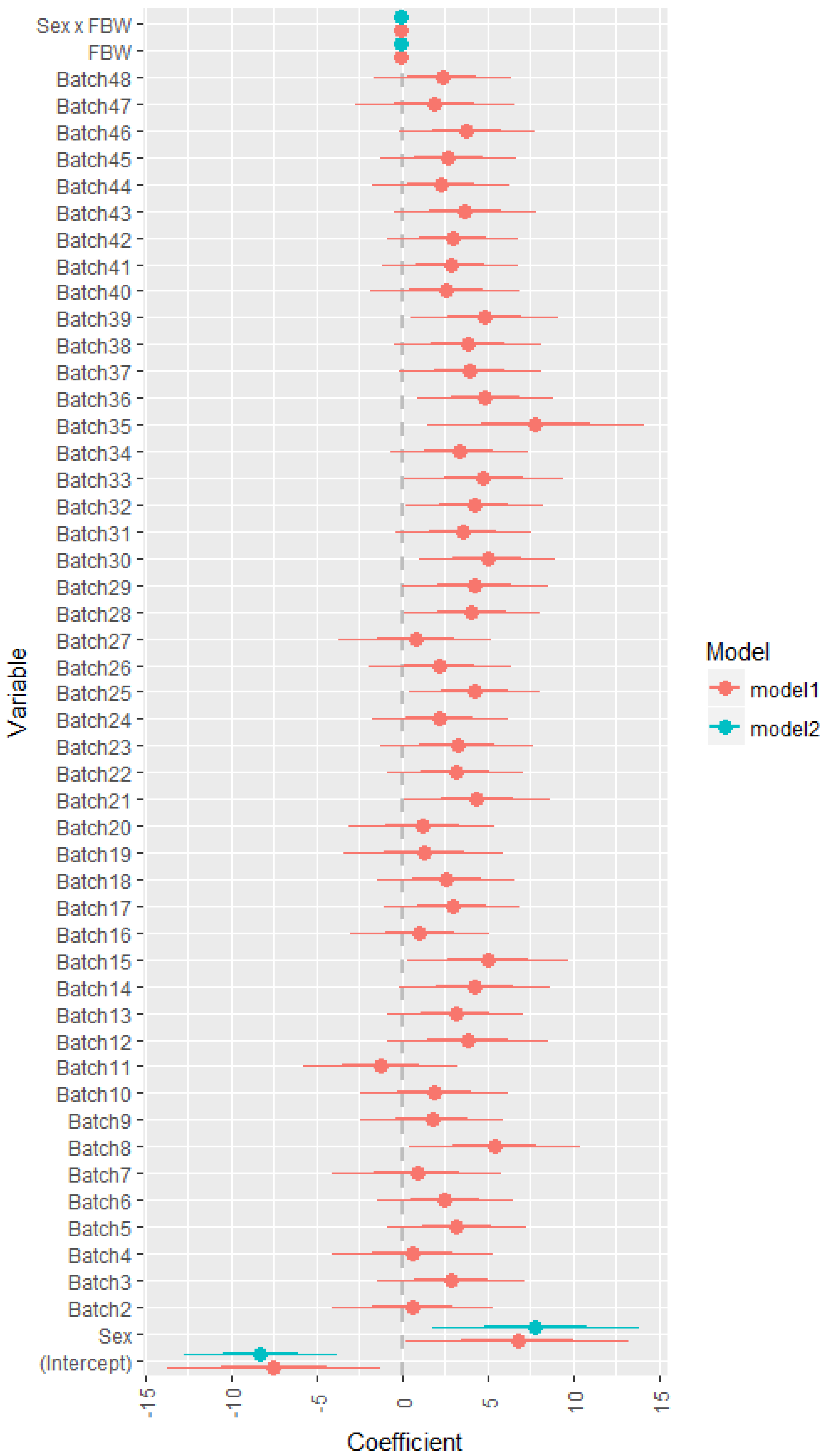

Figure 3.10.Coefficient plot showing the relationship between ΔMSE and confounding factors (selected chicks, n = 380).

Table 3.9. Relationship between ΔMSE and confounding factors (selected chicks, n=380).

Independent variable	Dependent Variable: ΔMSE			
	Model 1		Model 2	
	B (95% confidence interval)		B (95% confidence interval)	
Sex (female as reference)				
Male	**6.730****	**(0.354, 13.105)**	**7.799*****	**(1.914, 13.685)**
Batch (Batch 1 as reference category)				
Batch2	0.577	(-4.011, 5.165)		
Batch3	2.857	(-1.352, 7.066)		
Batch4	0.587	(-4.026, 5.201)		
Batch5	3.177	(-0.803, 7.158)		
Batch6	2.508	(-1.400, 6.416)		
Batch7	0.863	(-4.005, 5.731)		
Batch8	**5.405****	**(0.546, 10.265)**		
Batch9	1.746	(-2.364, 5.857)		
Batch10	1.904	(-2.308, 6.117)		
Batch11	-1.242	(-5.644, 3.160)		
Batch12	3.827	(-0.761, 8.415)		
Batch13	3.111	(-0.786, 7.007)		
Batch14	4.232*	(-0.122, 8.587)		
Batch15	**5.045****	**(0.435, 9.655)**		
Batch16	1.045	(-2.919, 5.010)		
Batch17	2.926	(-0.971, 6.823)		
Batch18	2.589	(-1.347, 6.525)		
Batch19	1.28	(-3.281, 5.841)		
Batch20	1.176	(-3.017, 5.369)		
Batch21	**4.372****	**(0.203, 8.542)**		
Batch22	3.131	(-0.767, 7.029)		
Batch23	3.209	(-1.160, 7.578)		
Batch24	2.22	(-1.622, 6.062)		
Batch25	**4.231****	**(0.447, 8.016)**		
Batch26	2.197	(-1.870, 6.264)		
Batch27	0.792	(-3.579, 5.163)		
Batch28	**4.054****	**(0.149, 7.960)**		
Batch29	**4.263****	**(0.060, 8.466)**		
Batch30	**4.991****	**(1.099, 8.883)**		
Batch31	3.564*	(-0.332, 7.460)		
Batch32	**4.213****	**(0.307, 8.120)**		
Batch33	**4.765****	**(0.185, 9.346)**		
Batch34	3.317*	(-0.623, 7.256)		
Batch35	**7.779****	**(1.578, 13.980)**		
Batch36	**4.854****	**(0.950, 8.759)**		
Batch37	3.948*	(-0.132, 8.029)		
Batch38	3.804*	(-0.406, 8.014)		

Batch39	**4.828****	**(0.638, 9.017)**		
Batch40	2.523	(-1.710, 6.755)		
Batch41	2.832	(-1.066, 6.730)		
Batch42	2.952	(-0.816, 6.721)		
Batch43	3.666*	(-0.426, 7.757)		
Batch44	2.274	(-1.619, 6.168)		
Batch45	2.707	(-1.202, 6.616)		
Batch46	3.762*	(-0.134, 7.658)		
Batch47	1.898	(-2.675, 6.471)		
Batch48	2.351	(-1.575, 6.277)		
FBW	**-0.079****	**(-0.147, -0.011)**	-0.031	(-0.087, 0.026)
Interaction (Female × FBW as reference)				
Male × FBW	-0.079*	(-0.160, 0.002)	**-0.091****	**(-0.166, -0.017)**
Constant	**-7.482****	**(-13.580, -1.384)**	**-8.266*****	**(-12.651, -3.880)**
Observations	378		378	
R2	0.176		0.067	
Adjusted R2	0.05		0.059	
Residual Std. Error	3.840 (df = 327)		3.821 (df = 374)	
F Statistic	1.397** (df = 50; 327)		8.892*** (df = 3; 374)	

Note: *p<0.1; **p<0.05; ***p<0.01

3.4 Discussion

3.4.1 Relationships between body weight, sex and ocular parameters before FD

In 7 day-old chicks examined, before FD was imposed, body weight was around 54 g, and there was a positive correlation between body weight and axial length, i.e. on average, the heavier the chick, the larger the eye (Figure 3.2). In humans, a positive correlation between axial length and body stature has also been observed (Table 3.1). Thus, the growth of the eye in the 'normal' environment is tuned to stature. Interestingly, there was no difference between male and female chicks in pre-treatment body weight, but it was observed that male chicks had deeper anterior chambers, thicker crystalline lenses, longer vitreous chambers, and longer resultant axial lengths (Table 3.3). (Note that for the ACD, the means and standard deviations reported in Table 3.3 are identical in the right and left eyes when presented to 2 decimal places. However, given the large sample size and the use of a paired *t*-test comparison, the difference between fellow eyes was statistically significant). These findings confirmed those of previous studies (252, 253) and indicated that the difference in eye size between male and female chicks is not simply caused by differences in body weight, but by other mechanisms related to sex (253).

3.4.2 In FD environment, body weight, sex and ocular parameters

After 4 days of FD treatment, all of the ocular components enlarged and body weight increased. As in the 7 day-old chicks, there was not yet any difference in body weight between the sexes, but male ocular components remained larger than those of females in both control eyes and treated eyes (Table 3.4).

The average ΔAXL was similar between female and male chicks (according to a simple, univariate *t*-test; Table 3.4). Interestingly, when sex was tested in a multivariate regression model that included terms for body weight and a sex-by-body weight interaction, it became apparent that there was a complex relationship between sex, body weight, and ΔAXL. Such a phenomenon of a difference between univariate and multivariate analysis is not uncommon (254, 255). Indeed, Wang et al. (256) have suggested that the selection of covariates should not merely be based on univariate analysis screening, since this may miss important covariates and lead to biased effect estimates. In view of the interaction between sex and body weight, it was decided that both parameters should be included as covariates in the subsequent GWAS (Chapter 4).

Spherical equivalent refractive error in control eyes differed between females and males, yet not in treated eyes. Conversely, the absolute axial length in treated eyes was longer in male chicks, but absolute MSE was similar in the two sexes. When using ΔMSE as the indicator of myopia susceptibility, there was no evidence of an influence of sex in either univariate or multivariate analysis. Likewise, Chen et al. (253) found that ΔAXL was greater in male chicks, but the corresponding ΔMSE was similar. These results indicated that the anterior segment, e.g. corneal curvature, might be different between female and male chicks, both before and after FD.

Many studies in humans have reported a difference in corneal curvature or asphericity between the sexes (257-259). Males tend to have flatter corneas than females, which counteracts the tendency for male eyes to be longer. In chick myopia studies, researchers have sometimes found that chicks develop a flatter cornea and deeper anterior chamber after FD (198, 260), however other studies reported that corneal curvature was minimally affected by FD (261). According to Troilo et al. (262), for marmosets of different age groups treated with monocular FD, corneal curvature changes were only observed in 0-39 day-old marmosets.

Body weight was also associated with myopia susceptibility. In the multivariate regression models, both IBW and FBW were found to be associated with ΔAXL, while only FBW was associated with ΔMSE (Table 3.6, 3.7).

In human studies, a child's growth trajectory may be associated with myopia. For example in a study of 6,815 children, height and weight growth trajectories at early ages were positively associated with axial length and corneal curvature at later ages (116). In a study examining 510 inbred chicks, it was found, after being adjusting for sex, that body weight, body length and head width predicted 45-49% of the variation in eye weight, axial length and corneal radius (263). These studies suggest that shared genetic variants contribute to eye size and body stature, however, whether the genes that regulate myopia susceptibility also regulate body stature is still unclear.

In previous studies, Schmid and Wildsoet (204) found similar susceptibility to FD-induced myopia in female and male chicks, while Chen et al., Guggenheim et al. and Zhu et al. (203, 252, 253) found that the increase of eye size in response to FD was greater in male chicks. None of these prior studies included a sex-by-body weight interaction in their analysis models, as the present did. This, coupled with differences across White Leghorn strains, and the choice of ΔMSE or ΔAXL to quantify myopia susceptibility may explain the conflicting findings in the literature.

As summarized in Table 3.2, some studies have reported female sex to be a risk factor for myopia in humans. My study also suggested that the response to FD differs between the sexes in chicks. Sex hormone receptors were found in various ocular tissues such as cornea, lens and retina, and changes in sex hormone levels in women have been shown to influence corneal thickness (264, 265). More research would be needed to uncover the underlying mechanisms for the sex and body weight differences in susceptibility to form deprivation myopia that I observed.

3.4.3 Differences between right and left eyes

An interesting finding in this study was that right eyes were longer than left eyes, as has been reported previously (266). In normal, untreated chicks, all of the ocular components were asymmetric in size between the right and left eyes. To further investigate this phenomenon, eye parameters after FD were analyzed and our results confirmed previous findings (Table 3.5). One possible explanation is that the visual pathways in avians are fully separated, i.e. decussation at the optic chiasm is complete. Thus visual processing from the two eyes is conducted in different cerebral hemispheres (the binocular field of view is much lower than in animals with forward-facing eyes). Avian eyes may have evolved subtly different functions/preferences for looking at different targets, which may finally influence the anatomy of the eyes (267). For instance, in another study, which investigated food search ability in monocularly occluded chicks, it was found that chicks using their left eyes performed poorly compared to chicks using their right eyes (268). However, during this experiment, eye parameters were always measured in the right first, hence the left eye would experience a relatively longer exposure to the ketamine/xylazine anaesthetic before being measured. A time-dependent reduction of intraocular pressure (IOP) has been observed after anaesthesia in rabbits (269) and mice (270), and therefore such a time-dependent decrease in IOP might have caused a decrease AXL (271). Further work is required to determine whether this potential explanation is correct.

3.5 Conclusions

In this experiment, ocular phenotyping was performed in chicks before and after FD treatment. Before treatment, it was found that male chicks had slightly longer axial lengths compared to female chicks and that they were less hyperopic than females. After FD, axial length was still longer in male chicks, however, refractive error in treated eyes was found to be similar between the sexes. A batch effect was found significant in this study, and sex and body weight were also found to subtly influence susceptibility to FDM. It was concluded that chicks chosen for genotyping should be selected separately within each batch, and that sex and body weight should be included as covariates in the subsequent GWA analysis for myopia susceptibility.

Chapter 4 A genome-wide association study (GWAS) of FD myopia chicks

4.1 Introduction

In Chapter 3, confounding factors for myopia susceptibility were identified. In this chapter, a GWAS in the FDM chick population was carried out.

It has been 8 years since the first GWAS for refractive error was published (75). Although this method has been successfully applied to identify genetic risk factors for myopia in many studies (77, 78, 272), there are still some limitations. A recent study suggested that all commonly-occurring genetic variants together could only explain 25-35% of the variance in refractive error (42). In the same study, the environmental factors, time spent outdoors and time spent reading (ascertained at age 8 using questionnaires), each explained less than 1% of the variance (42). Therefore, either current analysis models are strongly deficient, additional as-yet unidentified risk factors are involved, or a more complicated interplay of the known risk factors needs to be considered.

4.1.1 Missing heritability and gene-environment interaction

A major contribution by gene-environment interactions (GxE) would be one explanation for the so-called 'Missing Heritability' of myopia (i.e. the gap between the heritability estimated in twin/family studies and the heritability explained by currently identified genetic variants). In a GWAS, factoring in the influence of environmental risk factors and GxE in the statistical model can increase interpretability and the heritability estimated by SNPs. For example, in a GWAS model that includes a GxE effect, it is easy to understand if both the main genetic effect (G) and the GxE effect are significant, the proportion of phenotype variance explained by (G + GxE) will typically be more than by G only. More importantly, sometimes the main genetic effect may not be detected while the GxE could be significant (Figure 4.1). In this situation, if the main G effect is the only consideration, a large proportion of phenotype explained by genetic factors (heritability) is missed.

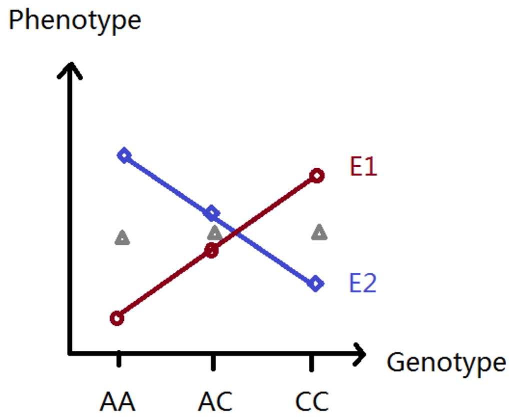

Figure 4.1. Example of a significant GxE effect yet non-significant G effect. *The x-axis represents the different genotypes; the grey triangles indicate the means of the main genetic effect. For the three genotypes, their mean effect is similar, so there might be no observable genetic effect in a standard GWAS. E1 and E2 indicate two different environments, which modify the genetic risk; a strong GxE effect can be observed. The slope of E1 is positively related with the phenotype, while the slope of E2 is negatively related with the phenotype.*

Among the published studies focusing on the role of GxE influencing myopia, only a limited number have reported significant findings. One study, which analysed 40,036 adults from 25 studies of European ancestry and 10,315 adults from 9 studies of Asian ancestry, reported an interaction effect between education level and genetic variants close to the *AREG*, *GABRR1* and *PDE10A* genes (273). Another study in 4461 children, which examined 39 genetic variants previously reported to be (directly) associated with refractive error in prior GWAS, found that only 5 variants showed nominal evidence of interactions with near work, and that none showed convincing evidence of an interaction with time spent outdoors (274). For other studies (see below), due to lack of sample size, an interaction effect was difficult to identify. In a myopia candidate gene replication study, 30 SNPs within or near matrix metalloproteinase gene coding regions were tested for association with ocular refraction in 1,913 people. GxE with education level were also evaluated. While no marker met the statistical significance threshold after stringent multiple-testing correction, one marker was marginally significant (275). One ALSPAC study investigated whether childhood longitudinal refractive error trajectories varied depending on the interaction effect between APLP2 gene variants and time spent on near work or time spent outdoors; only time engaged in near work showed evidence of an interaction (276).

4.1.2 Hypothesis – an animal model to detect G × E interactions

Detecting GxE is difficult when individuals within a population are exposed to highly variable lifestyles (277-279). Reducing the complexity of environmental exposures can increase the power to detect GxE effects (280). However, in human studies, it is not feasible to control the variability in environmental exposures. Performing carefully-controlled animal experiments under simple and uniform environments, therefore, provide an attractive alternative (280). Thus, I tested the following hypothesis: if a GWAS was performed in an animal population exposed to a myopia-inducing environmental stimulus, genetic loci conferring myopia susceptibility in that particular environment could be identified.

4.1.3 Comparison between GWAS in chicks and GWAS in human

There are several differences between conducting a GWAS in chicks and in humans. First, the composition of the genome is different. Chicks have 76 autosomal and 2 sex chromosomes, while humans have 44 autosomal and 2 sex chromosomes. Unlike in primates, male chicks are the homogametic sex (ZZ) and females are the heterogametic sex (ZW). Second, there is no imputation reference panel available for the chick genome. By contrast in human GWA studies, large-scale scientific endeavours such as the 1000 Genomes Project have provided fine-scale reference panels for the human genome, making high-density imputation feasible.

4.1.4 Genotyping techniques

Currently, there are two main companies that offer technologies for high-throughput genotyping of human and non-human samples: Affymetrix and Illumina. Both companies have their own genotyping platforms and associated techniques.

For Affymetrix, there are two genotyping technologies, Axiom genotyping technology and GeneChip technology while Illumina mainly uses BeadChip technology. Figure 4.2 illustrates these three genotyping technologies in detail. Comparing all these methods, the main feature of the Axiom technique is that it uses a DNA ligase enzyme to connect a biotinylated probe with the capture probe. The DNA ligase will recognize the adjacent DNA sequence, which ensures high-fidelity complementation (281). The GeneChip approach, by contrast, purely relies on perfect hybridization between the capture probe and target DNA sequence (282, 283). While for the Illumina bead array, a DNA polymerase-catalyzed single-base extension method is used to detect the genotype (283).

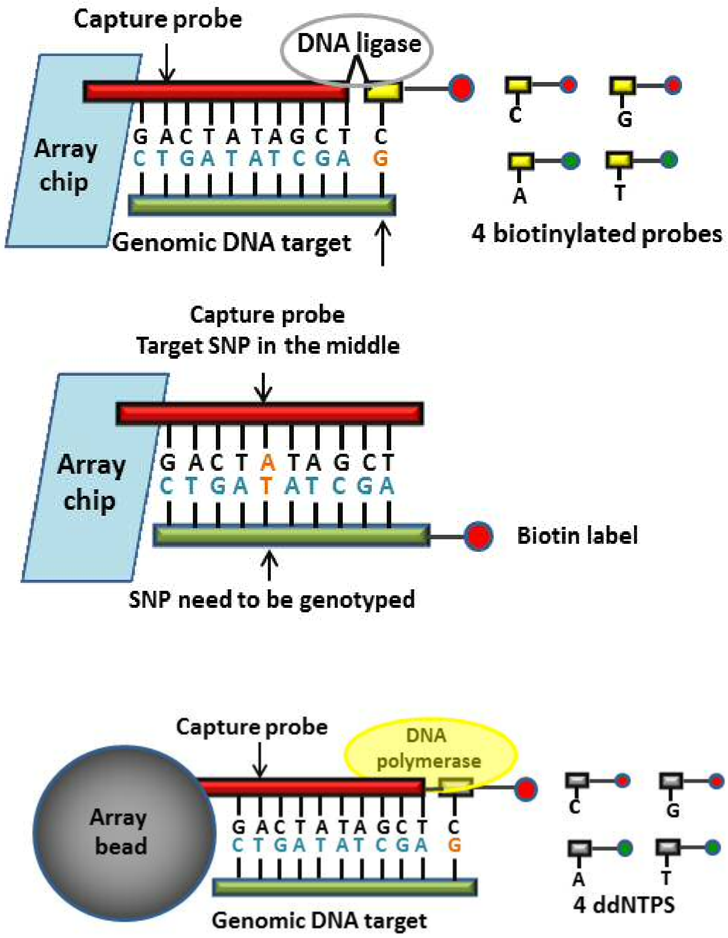

(a)

(b)

(c)

Figure 4.2. An explanation of genotyping techniques.
(a). Illustration of Affymetrix Axiom technique. The capture probe (red bar) hybridizes with the target DNA fragment (green bar), and 1 of 4 biotinylated probes hybridizes with the target SNP. A DNA ligase then links the biotinylated probe to the capture probe to detect the genotype. (b). Illustration of GeneChip technique. The complementary target SNP is placed in the middle of the capture probe. Genotyping is based on a perfect match between the capture probe and target DNA fragment. (c). Illustration of the Illumina technique. The captures probe is attached to a bead (grey disc). The capture probe hybridizes with the target DNA sequence preceding the target SNP. It then incorporates one of the 4 ddNTPs and the genotype is detected by a single-base extension reaction.

In addition to the difference in chip manufacture process and the genotyping technology, another distinction involves the two platforms' SNP-selection strategies. For human genotyping chips, Illumina's probes are mainly selected from haplotype-tagging 'tagSNPs' which are identified by the International HapMap Consortium. For Affymetrix, except for the tagSNPs which account for half of the array probes, the rest are ‘unbiased SNPs chosen to cover the genome while accommodating sequence restraints imposed by the assay itself’ (284).

4.1.5 Selection of chick genotyping platform

For chicken data, both companies have designed genotyping chips: the Illumina 3k chicken SNP array (285), the Illumina 12,945 SNP chip (286), the Illumina 18k chip (287), the Illumina 60K chicken SNP chip (288) and the Affymetrix high-density 600K SNP genotyping array (289). Fu et.al (290) studied the LD pattern of broiler chickens using the 60k chip; using the same type of chip, Luo analyzed the antibody response to Newcastle disease virus (291); Morota et.al (292) analyzed QTL for body weight, ultrasound area of breast meat (BM) and hen house production using the Affymetrix 600k chip while Abdollahi – Arpanahi et.al (293) calculated the SNP heritability of these three traits.

Although the two chips have been widely used, they differ in coverage and SNP-selection strategies. The Illumina chip was constructed using genetic data from only two 'broiler' chickens and two 'layer' chickens (288), while the Affymetrix array employed genetic data from twenty-four chicken lines, including fifteen commercial lines, eight experimental inbred layers and one unselected layer line (289). The Affymetrix chip covers more chick lines and contains almost 10 times more SNPs than the Illumina 60K chip. This allows a better resolution of chicken genome compared to the lower density chips (294), hence, in the current study, the Affymetrix (Axiom) chip was selected.

4.2 Method

4.2.1 Sample size

To minimize 'batch effects', the 20 per cent of chicks with the largest treatment-induced AXL change and the 20 per cent with the smallest change were selected from each batch. A total of 380 chicks (190 from the high and low tail of the induced-myopia frequency distribution) were selected for genotyping (please refer to Chapter 3, section 3.3.4).

4.2.2 Genotyping

DNA samples were sent to Aros-Eurofins Ltd for genotyping on the 600K Affymetrix Axiom Chicken Genotyping Array (Affymetrix, Inc. Santa Clara, CA, USA). The DNA extraction process is described in Chapter 2, section 2.5.1. Since the genotyping was to be performed in 96-well plates, the 380 DNA samples were randomly assigned to the wells of four 96-well plates (in order to avoid 'plate effects' from confounding the statistical analyses). One well of each plate was assigned an "internal duplicate" sample for the purpose of quality control. The genotyping process carried out by the company was as follows (295):

i. Total DNA was amplified, and then randomly fragmented into 25 to 125 bp fragments.
ii. Fragments were precipitated and then resuspended.
iii. The suspension was hybridized to the Affymetrix Axiom Chicken Genotyping Array.
iv. The hybridized chip was washed under stringent conditions and thus, background noise caused by random ligation events was reduced.
v. Four different biotinylated probes were added and the second hybridization was performed.
vi. The DNA ligase was added to specifically link the biotinylated probes to the chip surface.
vii. After ligation, the arrays were stained and imaged on the GeneTitan™ Multi-Channel Instrument, so that the genotype of each SNP could be recorded.

The working flow is shown in Figure 4.3.

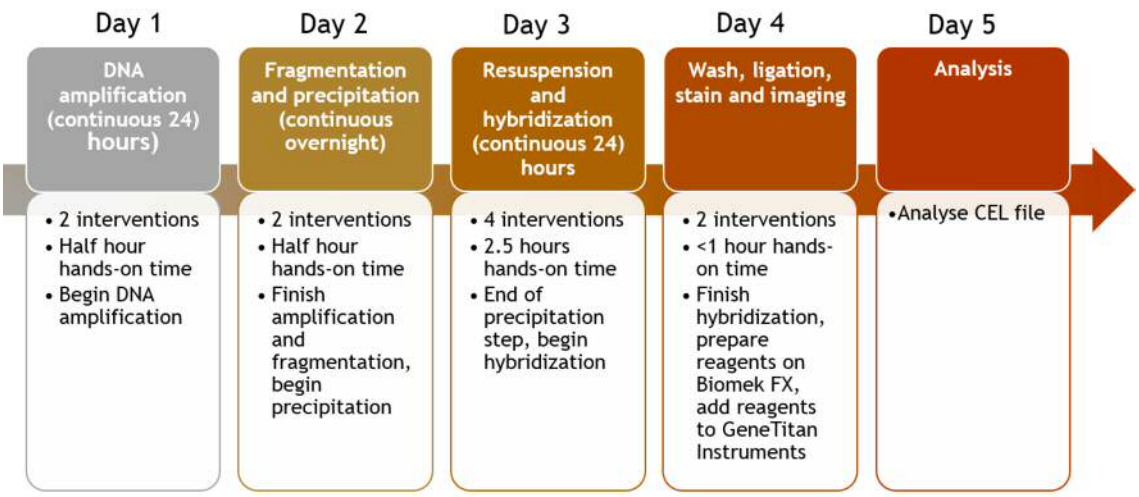

Figure 4.3. Workflow of the Affymetrix genotyping process (296).
Five days' workflow is illustrated from left to right.

4.2.3 Quality control

Of the 380 genotyped samples, 4 were duplicate DNA samples included for the purpose of quality control (QC); one pair of duplicates was included on each of the four 96-well plates used for genotyping.

4.2.3.1 Quality Control carried out by the genotyping company

Dish quality control (DQC) for all samples and SNP quality control (QC) for 20001 SNPs were performed by the company. All samples passed DQC, with a threshold of DQC not smaller than 0.82 and sample call rate not smaller than 97%. For SNP QC, the threshold was set as call rate (cr) -cutoff ⩾ 97, Fisher's linear discriminant (fld)-cutoff ⩾ 3.6, Heterozygous Strength Offset (het-so)-cutoff ⩾ −0.1, Heterozygous Strength Offset off target variant (het-so-otv)-cutoff ⩾ −0.3, homozygous ratio offset (hom-ro)-1-cutoff ⩾ 0.6. After QC by the genotyping company, genotypes for 580,961 SNPs were released.

4.2.3.2 Additional Quality Control procedures

Additional quality control (QC)was carried out using PLINK v1.90 (297).

Marker-based QC included several criteria:

1) Remove SNPs with a call rate less than 95%.

SNP call rate is defined as the proportion of individuals in the study for which the corresponding SNP information is not missing. A call rate of 95% for a certain SNP means that 95% of the individuals have data for this SNP. In most published GWA studies, SNPs with a call rate less than 95% are removed, though some studies have chosen higher thresholds (e.g. 99%) for rare mutations (298). This step was designed to remove SNPs that were poorly genotyped (some SNPs are inherently difficult to genotype due to the surrounding DNA sequence).

2) Remove or merge duplicate SNPs.

When multiple variants share the same genomic position and allele codes, they are likely to be duplicates. In published GWA studies, they are either merged or removed to reduce the false positive rate. In this study, duplicates were removed.

3) Remove SNPs with no annotation information.

Chicks have 38 pairs of autosomes and 1 pair of sex chromosomes; some of the chromosomes are small in comparison to mammalian chromosomes. SNPs in these "micro-chromosomes" may lack detailed annotation information, such as rs ID, bp coordinate or allele codes. To increase power and reduce the false positive rate, SNPs lacking annotation information were not included in the GWAS.

4) SNPs on sex chromosomes were not included.

In chicks, males carry two copies of the Z chromosome whilst females carry one Z and one W chromosome. Hence, the conventional additive model used in GWAS cannot be applied to the sex chromosomes. Although studies performing GWAS including the sex chromosomes have been reported for chicks (299, 300), the present study had limited power, thus only the autosomes were considered.

5) Power calculation and minor allele frequency (MAF).
To calculate the statistical power, the software package Quanto (301) was utilized. According to previous GWAS for human myopia, statistical power was sufficient to identify variants that contributed ~0.01 D of change in refractive error (78). Based on the sample size and experimental design of this study (Table 4.1), it was found that testing SNPs with a MAF <10% would provide insufficient statistical power. For example, to detect a SNP with more than 80% power, using MAF 5% was able to detect an effect of increasing AXL by 0.05mm per copy of the risk allele, while a SNP with MAF 10% would yield an effect 0.04mm, which is more powerful. In this study, MAF ⩾ 10% was selected as the criterion for choosing SNPs.

6) Hardy-Weinberg equilibrium (HWE) test was not performed in this study.
Genotyping errors can cause SNPs to fail a test for HWE. However, in this study, chicks with extreme phenotypes were selected for genotyping and the chicks were partially inbred. Therefore SNPs with genotypes that did not conform to HWE were *not* excluded.

Table 4.1. Power estimation calculated using Quanto, based on different effect sizes (β) and MAFs.

MAF	β	Power	R^2
0.05	0.01	0.0879	0.0003
	0.02	0.207	0.0013
	0.03	0.4015	0.003
	0.04	0.6261	0.0053
	0.05	0.8143	0.0082
	0.06	0.9289	0.0118
	0.07	0.9795	0.0161
	0.08	0.9956	0.021
	0.09	0.9993	0.0266
	0.1	0.9999	0.0329
0.1	0.01	0.1229	0.0006
	0.02	0.3482	0.0025
	0.03	0.6538	0.0056
	0.04	0.8818	0.01
	0.05	0.9759	0.0156
	0.06	0.9972	0.0224
	0.07	0.9998	0.0305
	0.08	0.9999	0.0399
	0.09	0.9999	0.0504
	0.1	0.9999	0.0623

Sample-based QC included the following criteria:

1) Exclude chicks whose PCR-determined sex conflicted with the genotyping chip-inferred sex.

In this study, sex was identified by PCR (Chapter 2, section 2.6). To ensure the samples were not mixed up during the preparation stage, a comparison between PCR-determined sex and genotyping chip-inferred sex was necessary. Samples were removed if there was a sex mismatch (however, there were none).

2) Remove samples with a call rate of < 95%.

The sample call rate is defined as the fraction of called SNPs in each sample over the total number of SNPs in the dataset. The sex chromosomes were not included while calculating the call rate due to unequal information between different sexes. If the sample call rate is too low, it infers the sample quality is not good enough. In this study, the threshold for excluding samples with a low call rate is 95%, which is applied in most GWAS.

3) Remove chicks with extreme heterozygosity.

Heterozygosity for an individual refers to the fraction of loci within an individual that is heterozygous. Usually, heterozygosity varies among different ethnic groups but is relatively stable within a single ethnic group. If an individual's heterozygosity deviates from the average level in a population with the same ethnic background, it could be due to inbreeding or sample contamination (e.g. 2 DNA samples being pipetted into the same well of a 96-well plate). Heterozygosity outliers (+/- 5 standard deviations from the mean level) were excluded.

4) Remove internal duplicate samples.

For each 96 well plate, one duplicate sample was intentionally included to estimate the reproducibility rate within a 96 well plate, and to quantify the reproducibility of the genotyping process. One of each pair of duplicate samples was removed.

5) Estimation of kinship coefficients.

Kinship is a confounding factor in GWAS that can increase the false positive rate of tests of association (302). In this study, since the chicks were partially inbred, it was necessary to estimate their relatedness. The effects of relatedness can be corrected by genomic control or by including a genetic relatedness matrix in the association test model. Since there were several ways to control the genetic relatedness among the chicks, to maximise the sample size in order to gain maximal power, no samples were excluded in this study on the grounds of relatedness.

Marker-based QC was performed first in order to retain as many samples as possible. However, in some instances, sample QC must be done prior to marker QC. For example, sex inconsistency between the report from genotyping chip and the result from PCR must be checked before removing SNPs from sex chromosomes, and the sample call rate must be checked before filtering by MAF because the purpose of testing sample call rate is to ensure the quality of DNA samples. Unless there is a technical problem with specific SNPs (i.e. those with a low call rate), including more SNPs in sample call rate analysis will provide more confidence. Taking these factors into consideration, the QC procedure adopted is shown in the flowchart (Figure 4.4).

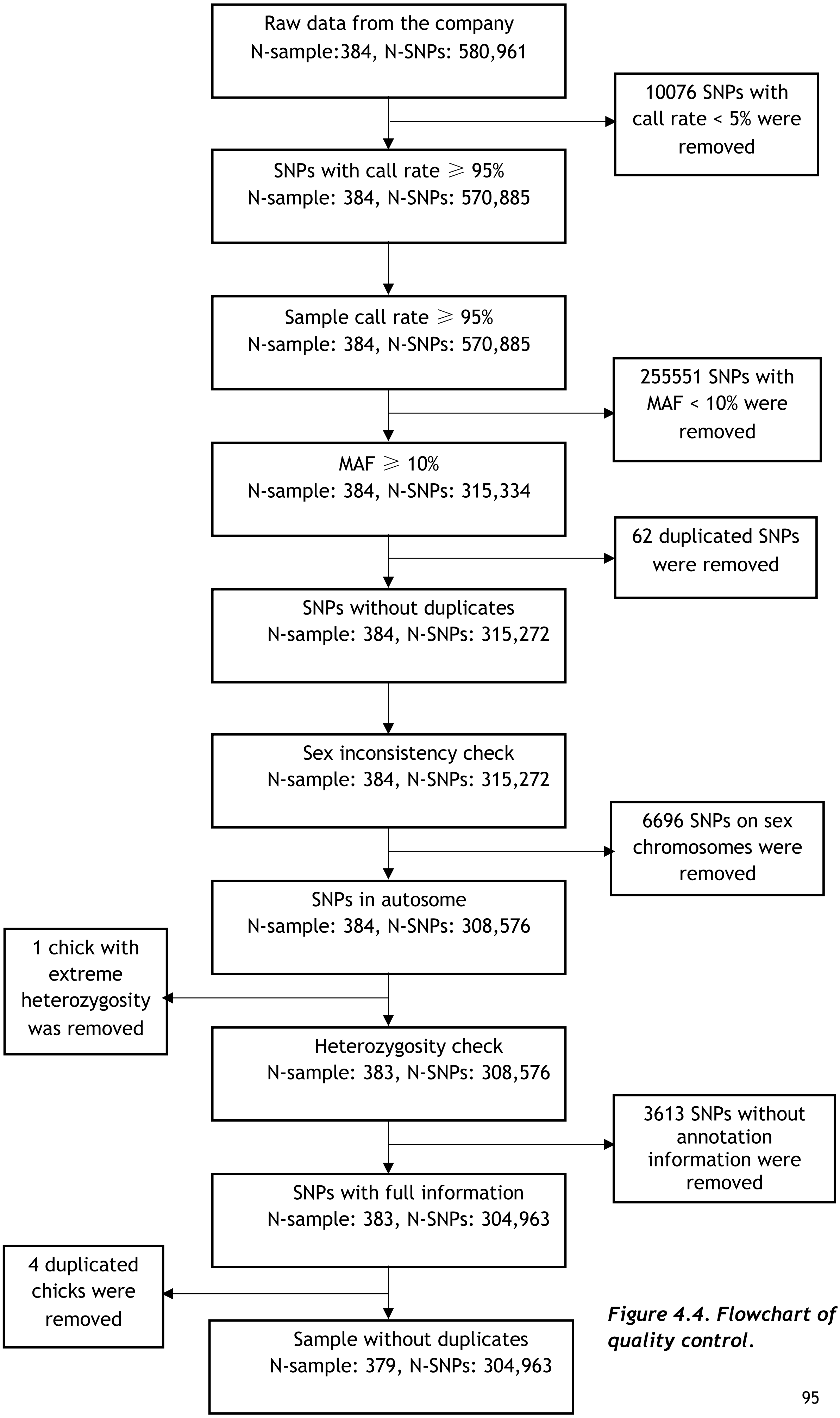

Figure 4.4. Flowchart of quality control.

4.2.4 Association analysis

In this study, PLINK served as the primary analytical tool. Single-locus association tests were performed for each marker; genotypes were coded as 0, 1, or 2 according to the number of minor alleles carried. A trend test for association was conducted within different statistical models and both phenotypes – change in AXL (ΔAXL) and change in MSE (ΔMSE) – were tested separately in independent models. For each phenotype, different regression models were designed as follows:

```
Model 1: Residual-ΔAXL ~ SNP + plate number
```

After adjusting for sex, final body weight and sex-body weight interaction (sex × body weight), the ΔAXL residuals were then analysed as a quantitative trait (dependent variable), with each SNP and plate number (a categorical variable, coded as 1, 2, 3 or 4) as the independent variable. Instead of using ΔAXL as a dependent variable and taking sex, FBW and a sex × FBW interaction term together with SNP into the model (`ΔAXL ~ Sex + FBW + Sex × FBW + SNP + plate number`), this two-step method has some advantages. It can control the confounding factors like sex and FBW, at the same time, it reduces the degrees of freedom in the regression model and improves the power. This approach is common in the genetics literature (303, 304).

```
Model 2: Residual-normalized-ΔAXL ~ SNP + plate number
```

Since ΔAXL was derived from extreme samples, the distribution of the trait was non-normal. Therefore, in the second model, the ΔAXL values were rank-normalized, regressed against sex, FBW and a sex × FBW interaction term, and the residuals taken as the phenotype. In this model, the phenotype was analysed as a quantitative trait, as above.

Model 3: logit(case/control status) ~ $e^{\beta 0 + (\beta 1 \times SNP) + (\beta 2 \times Sex) + (\beta 3 \times FBW) + (\beta 4 \times Sex \times FBW) + (\beta 5 \times plate\ number)}$

In the third model, ΔAXL was modelled as a binary (case/control) trait. Chicks selected from the low tail of the phenotype distribution (low ΔAXL) were assigned as controls while chicks with high ΔAXL were assigned as cases. In this model, sex, FBW, sex × FBW and plate number were included as covariates.

```
Model 4: Residual-normalized-ΔAXL ~ SNP + GRM + plate
number
```

The previous models did not include the GRM. Therefore, to correct for relatedness, results from the first three models needed to be corrected by the genomic control (λ_{GC}) method. However, this λ_{GC} method is overly conservative since LD is not considered. By contrast, in a mixed model, including GRM as a random effect can correct for relatedness while accounting for LD. GEMMA (305) was used to perform the mixed model association analysis.

The same sets of models were also applied for the ΔMSE phenotype, except that a logistic regression model was not included: the case/control status was based on the phenotype extremes. Thus this would be the same no matter whether AXL or MSE was considered. Therefore, in GWAS for MSE, the models were as follows:

```
Model 1: Residual-ΔMSE ~ SNP + plate number

Model 2: Residual-normalized-ΔMSE ~ SNP + plate number

Model 3: Residual-normalized-ΔMSE ~ SNP + GRM + plate
number
```

4.3 Results

4.3.1 Genotyping data quality

For the 580,961 SNPs that passed the QC filtering steps carried out by Aros/Eurofins, the average call rate was 99.5%. The average concordance rate for the 4 intentionally-included duplicate samples was also 99.5%. After quality control, 379 chicks and 304,936 SNPs with MAF ≥ 10% were analysed. A genome-wide significance threshold of 0.05/304,936=1.64e-07 was set according to a Bonferroni correction for testing 304,936 SNPs. However, this threshold would be highly conservative since SNPs in LD are not independent. A genetic relationship matrix was calculated for the selected chicks. The relatedness coefficients ranged from -0.10 to 0.34, with a median value of -0.00326 (Figure 4.5). To reduce false positive results due to the inflation of test statistics caused by relatedness (306), the genomic control inflation factor (λ_{GC}) was calculated based on the equation: λ_{GC} = median (χ^2)/0.456 (306), and genomic control correction was applied by correcting the χ^2 with λ_{GC} (χ^2 (adjusted) = χ^2 / λ_{GC}).

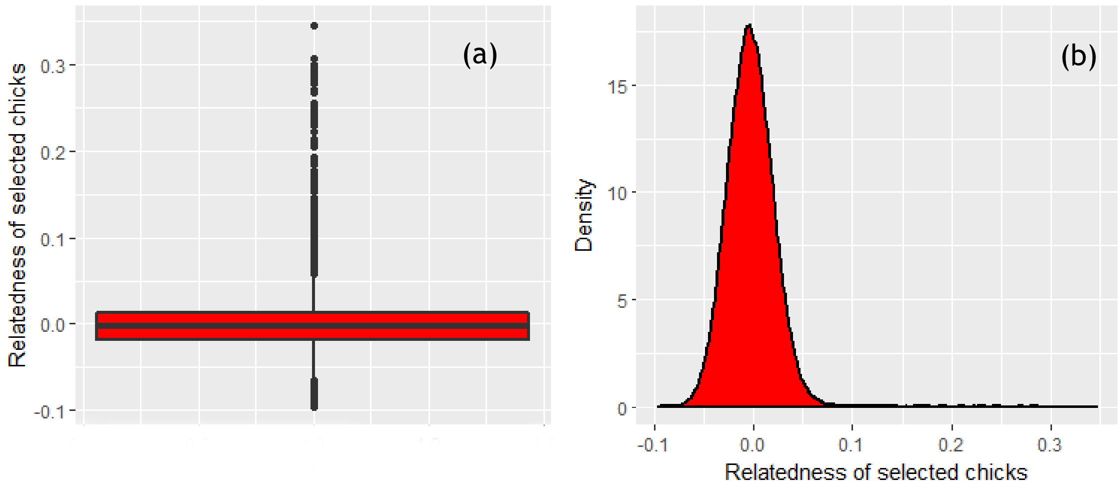

Figure 4.5. Relatedness coefficients of the genotyped samples.
(a) Box plot of the relatedness coefficients; (b) density plot showing the relatedness. Relatedness coefficients ranged from -0.10 to 0.34, with a median value of -0.00326.

4.3.2 GWAS for AXL

In the first model (`Residual-ΔAXL ~ SNP + plate number`), after adjusting for sex, final body weight and sex-body weight interaction, the residual of ΔAXL was considered as a dependent variable. In the association model, plate number was added as a covariate. After genomic control correction (λ_{GC} = 1.19), none of the SNPs reached the genome-wide significance threshold; however, 5 SNPs on chromosome 1 and 9 SNPs on chromosome 7 were found to exceed an arbitrary 'suggestive significance threshold' of 1.64e-05 (following Reed et al. (307), 100 times the genome-wide significance threshold was adopted as the suggestive association threshold). The most strongly associated SNPs on chromosome 1 were: rs317386235 (P = 9.67e-07) with β = -0.12, rs312695428 (P = 4.85e-06, β = -0.11), rs315478126 (P = 7.71e-06, β = -0.10), rs15195233 (P = 8.11e-06, β =-0.10) and rs316726738 (P = 1.46e-05, β =-0.10). On chromosome 7, the SNPs that reached the suggestive threshold were: rs316636360 (P = 1.04e-05, β = -0.09), rs313790665 (P = 1.08e-05, β = -0.09), rs313627312 (P = 1.14e-05, β = -0.08), rs16579210 (P = 1.14e-05, β = -0.08), rs312720765 (P = 1.40e-05, β = -0.08), rs14603638 (P = 1.40e-05, β = -0.08), rs314035281 (P = 1.46e-05, β = -0.08), rs317497540 (P = 1.48e-05, β = -0.08) and rs313006277 (P = 1.50e-05, β = -0.08) (Table 4.2, Figures 4.6 & 4.7).

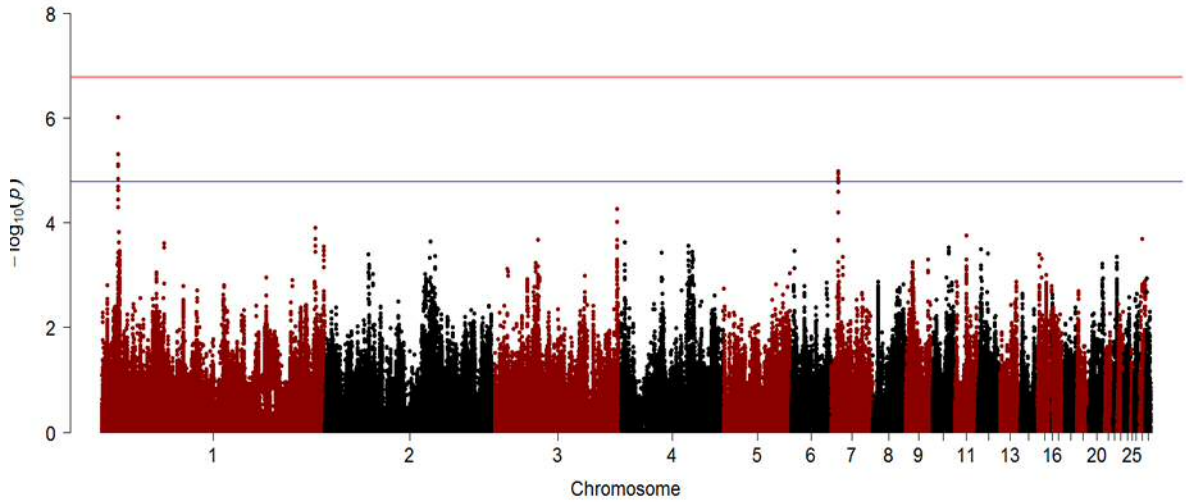

Figure 4.6. Manhattan plot for GWAS of non-normalized residual ΔAXL, after genomic control correction.
X-axis represents chromosome number and genomic position, y-axis represents minus log10 P-value. Red line represents the genome-wide significance threshold of 1.64e-07, blue line represents the genome-wide suggestive threshold of 1.64e-05.

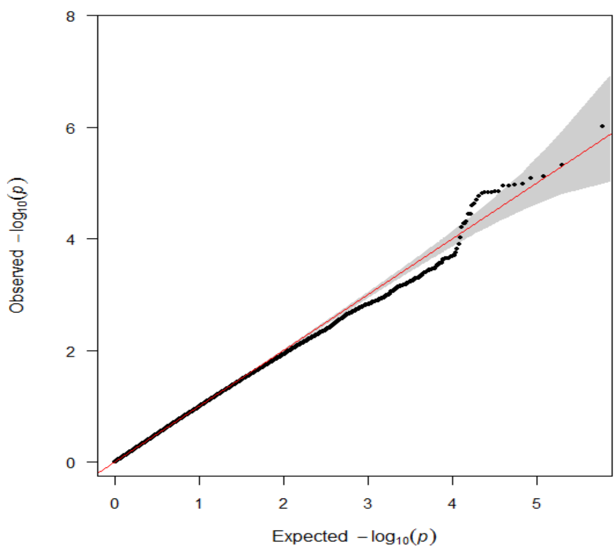

Figure 4.7. Q-Q plot for GWAS of non-normalized residual ΔAXL, after genomic control correction.

For the second model (`Residual-normalized-ΔAXL ~ SNP + plate number`), rank normalized ΔAXL values were adjusted for sex, FBW and sex × FBW, and the residuals of this model were analysed as a continuous trait. After genomic control correction (λ_{GC} = 1.16), SNP rs317386235 was again the most strongly associated marker and now exceeded the genome-wide significance threshold (P = 1.39e-07, β = -0.50). Another 9 SNPs – rs312695428, rs15195233, rs315398501, rs315478126, rs316320493, rs13829591, rs317899999, rs316726738 and rs313934866 in chromosome

1 - also exceeded the suggestive significance threshold (Table 4.2, Figures 4.8, 4.9 & 4.10). However, no signals from chromosome 7 exceed the suggestive threshold. All the SNPs at the chromosome 1 locus were in the region of the genes *PRKAR2B* and *PIK3CG*. After conditioning on the top SNP (rs31738623), the other SNPs no longer reached the suggestive threshold.

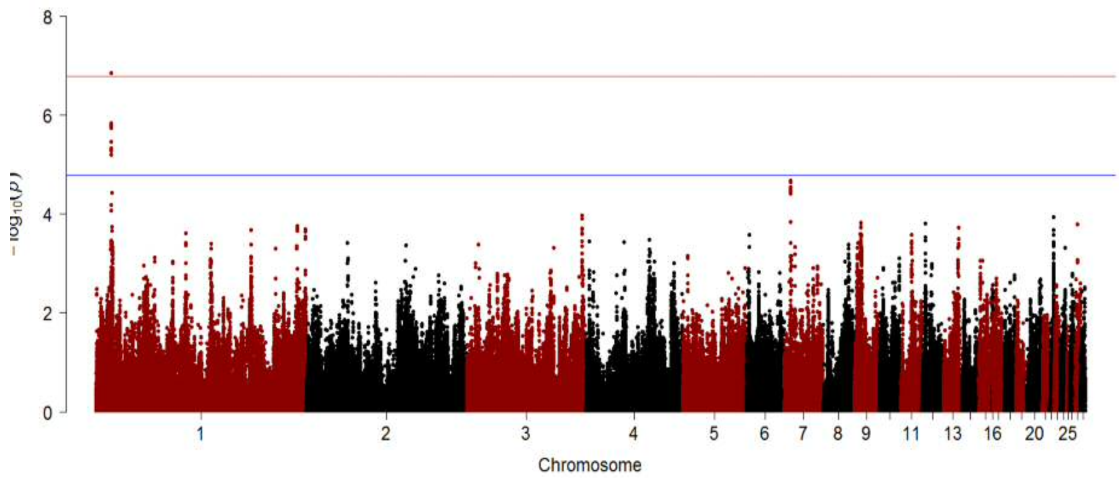

Figure 4.8. Manhattan plot for GWAS of residual from normalized ΔAXL, after genomic control correction.
X-axis represents chromosome number and genomic position, y-axis represents minus log10 P-value. Red line represents the genome-wide significance threshold of 1.64e-07, blue line represents the genome-wide suggestive threshold of 1.64e-05.

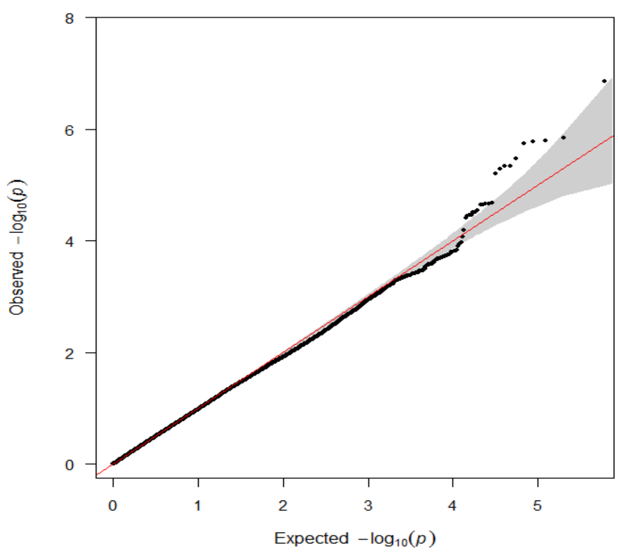

Figure 4.9. Q-Q plot for GWAS of residual from normalized ΔAXL, after genomic control correction.

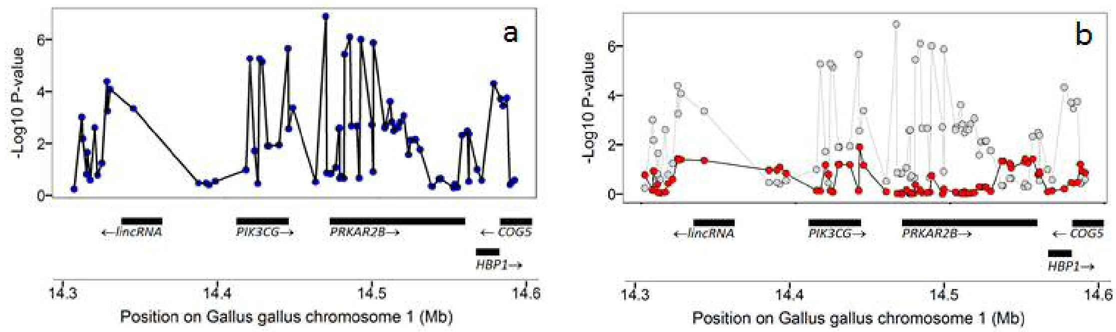

Figure 4.10. Regional plot for chromosome 1.
Plot (a) shows the top SNPs in chromosome 1 and it's mapping region. Plot (b) shows after conditioning on SNP rs317386235, the signals from other SNPs were no longer associated with the phenotype.

In the third model ($\text{logit(case/control status)} \sim e^{\beta 0 + (\beta 1 \times \text{SNP}) + (\beta 2 \times \text{Sex}) + (\beta 3 \times \text{FBW}) + (\beta 4 \times \text{Sex} \times \text{FBW}) + (\beta 5 \times \text{plate number})}$), ΔAXL was modelled as a binary trait. After GWA analysis and genomic control correction (λ_{GC} = 1.0), none of the SNPs reached the suggestive significance threshold (Table 4.2, Figures 4.11 & 4.12). However, the top SNP was still rs317386235 (P = 5.75e-05, OR = 0.38) from chromosome 1; the 9 next most significant SNPs were located on chromosome 7: rs316636360, rs313627312, rs16579210, rs313006277, rs313790665, rs312720765, rs14603638, rs314035281 and rs317497540.

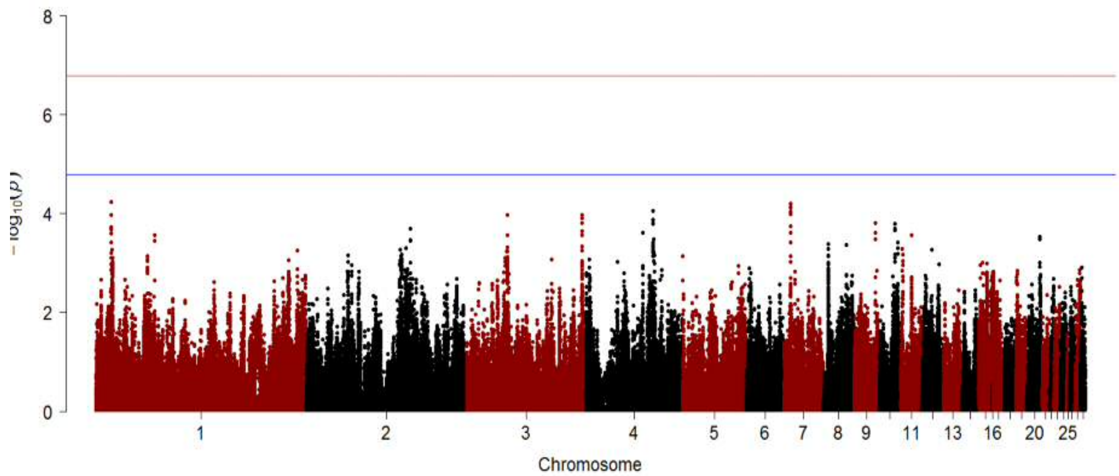

Figure 4.11. Manhattan plot for GWAS of ΔAXL modelled as a binary trait, after genomic control correction.
X-axis represents chromosome number and genomic position, y-axis represents minus log10 P-value. Red line represents the genome-wide significance threshold of 1.64e-07, blue line represents the genome-wide suggestive threshold of 1.64e-05.

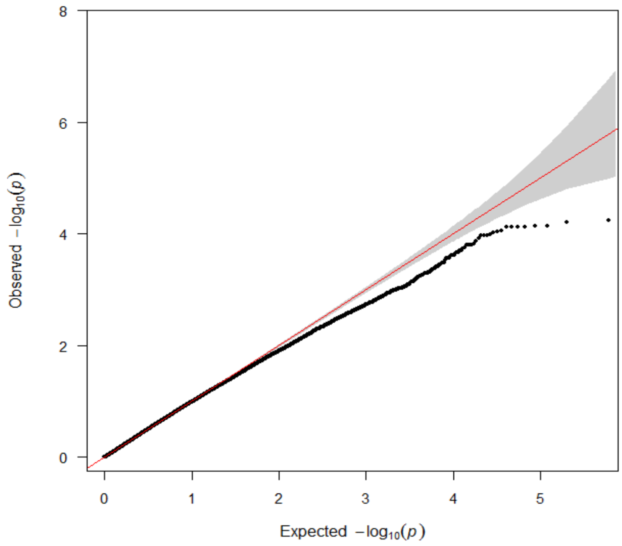

Figure 4.12. Q-Q plot for GWAS of ΔAXL modelled as a binary trait, after genomic control correction.

In the fourth model (`Residual-normalized-ΔAXL ~ SNP + GRM + plate number`), instead of using genomic control, a GRM was included as a random effect in a mixed model to correct for relatedness. In this model, the phenotype was the same as in model 2. A total of 14 SNPs reached the suggestive significance threshold (Table 4.2, Figure 4.13&4.14), and among them, rs317386235 on chromosome 1 also exceeded the genome-wide significance threshold (P = 9.54e-08, β = -0.49). Of the remaining 13 SNPs, 12 were in the same cluster as rs317386235 on chromosome 1, while the final SNP rs313633102 from chromosome 12 was just above the suggestive significance threshold (P = 1.62e-05, β = -0.29).

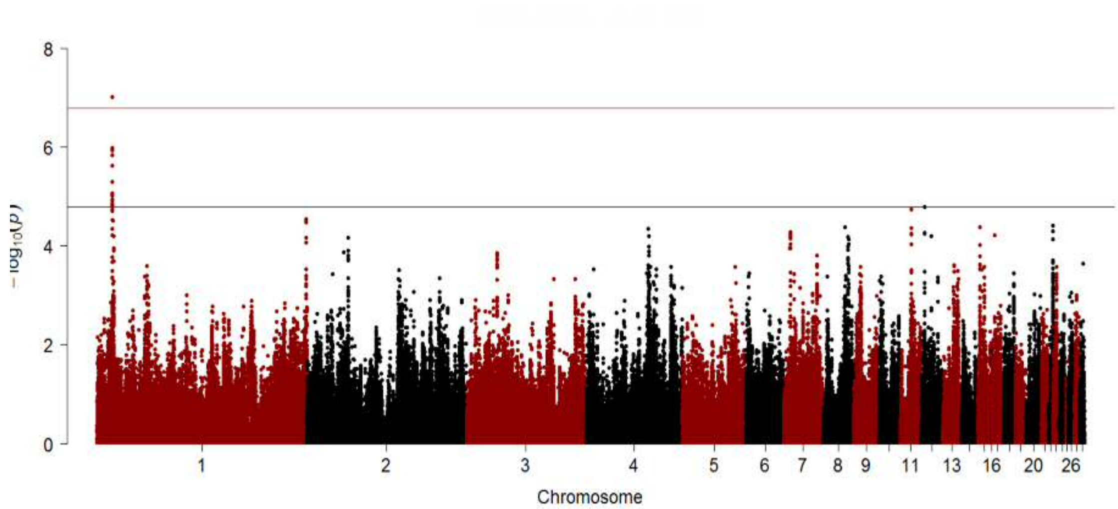

Figure 4.13. Manhattan plot for GWAS of residual from normalized ΔAXL, including GRM.

X-axis represents chromosome number and genomic position, y-axis represents minus log10 P-value. Red line represents the genome-wide significance threshold of 1.64e-07, blue line represents genome-wide suggestive threshold of 1.64e-05.

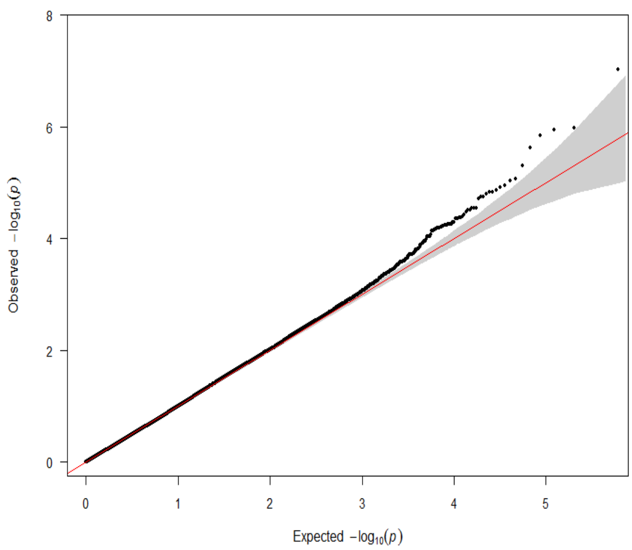

Figure 4.14. QQ plot for GWAS of residual from normalized ΔAXL, including GRM.

Table 4.2. All SNPs with minus log10 P-values exceeding suggestive significance threshold (P <1.64e-05

SNP	CHR	POS	MAF	Model 1		Model 2		Model 3		Model	
				β	P	β	P	OR	P	β	
rs312576845	1	13994774	0.31	-0.07	1.71e-03	-0.29	4.92e-04	0.61	9.72e-03	-0.34	1.
rs316320493	1	14109926	0.23	-0.09	2.37e-05	-0.41	3.40e-06	0.47	3.82e-04	-0.38	1.
rs315762686	1	14133858	0.40	0.07	4.65e-04	0.31	6.50e-05	1.61	7.36e-03	0.31	9.
rs316260627	1	14134122	0.28	0.06	2.23e-03	0.29	4.10e-04	1.53	2.17e-02	0.31	8.
rs313813218	1	14150933	0.30	0.06	1.87e-03	0.29	3.37e-04	1.54	1.77e-02	0.30	1.
rs13829591	1	14215009	0.23	-0.09	3.58e-05	-0.40	4.68e-06	0.48	7.94e-04	-0.37	2.
rs317899999	1	14221349	0.23	-0.09	3.58e-05	-0.40	4.68e-06	0.48	7.94e-04	-0.37	2.
rs313934866	1	14222991	0.23	-0.09	5.00e-05	-0.40	6.38e-06	0.49	1.05e-03	-0.36	4.
rs315398501	1	14239675	0.22	-0.10	1.99e-05	-0.43	1.64e-06	0.47	6.30e-04	-0.39	1.
rs13829565	1	14242687	0.32	0.06	1.05e-03	0.28	3.65e-04	1.61	7.23e-03	0.32	2.
rs317386235	1	14264125	0.19	-0.12	9.67e-07	-0.50	**1.39e-07**	0.38	5.75e-05	-0.49	**9.**
rs316726738	1	14276288	0.21	-0.10	1.46e-05	-0.42	5.14e-06	0.43	2.56e-04	-0.40	5.
rs312695428	1	14279681	0.21	-0.11	4.85e-06	-0.45	1.46e-06	0.40	1.07e-04	-0.43	1.
rs15195233	1	14286891	0.19	-0.10	8.11e-06	-0.45	1.59e-06	0.42	2.13e-04	-0.43	1.
rs315478126	1	14294877	0.21	-0.10	7.71e-06	-0.44	1.83e-06	0.42	1.87e-04	-0.43	1.
rs14792835	1	14355770	0.23	0.06	7.44e-03	0.26	2.59e-03	1.53	3.00e-02	0.31	1.
rs312799206	1	14356929	0.22	0.06	8.18e-03	0.26	3.14e-03	1.53	3.15e-02	0.32	1.
rs312720765	7	5837884	0.30	-0.08	1.40e-05	-0.33	3.10e-05	0.47	7.67e-05	-0.31	9.
rs14603638	7	5851886	0.30	-0.08	1.40e-05	-0.33	3.10e-05	0.47	7.67e-05	-0.31	9.
rs313790665	7	5856742	0.30	-0.09	1.08e-05	-0.33	2.10e-05	0.47	7.60e-05	-0.32	5.
rs316636360	7	5874170	0.30	-0.09	1.04e-05	-0.33	2.23e-05	0.47	6.20e-05	-0.32	6.
rs313627312	7	5874277	0.30	-0.08	1.14e-05	-0.33	2.21e-05	0.47	7.37e-05	-0.32	5.
rs16579210	7	5887049	0.30	-0.08	1.14e-05	-0.33	2.21e-05	0.47	7.37e-05	-0.32	5.
rs313006277	7	5895999	0.29	-0.08	1.50e-05	-0.33	3.53e-05	0.47	7.53e-05	-0.32	6.
rs314035281	7	5898250	0.3	-0.08	1.46e-05	-0.33	2.86e-05	0.47	9.25e-05	-0.31	6.
rs317497540	7	5903441	0.29	-0.08	1.48e-05	-0.34	2.25e-05	0.47	1.03e-04	-0.32	6.
rs313633102	12	3427410	0.45	-0.07	3.13e-04	-0.28	1.57e-04	0.59	2.74e-03	-0.29	1.

Note: CHR = chromosome; POS = position in base pair; OR = odds ratio. Genome-wide significance threshold = 1.64e-07,
1.64e-05.

4.3.3 GWAS for MSE

In the first model (`Residual-ΔMSE ~ SNP + plate number`), ΔMSE was first adjusted for sex, FBW and sex x FBW, and then the residuals from the regression model were used for association testing. After genomic control correction (λ_{GC} = 1.15), none of the SNPs reached the suggestive threshold. The top 10 SNPs were rs316850156 (P = 1.80e-05, ß = -1.72), rs312907731 (P = 2.42e-05, ß = -1.66) and rs317784343 (P = 8.13e-05, ß = -1.65) from chromosome 27, rs312972300 (P = 3.69e-05, ß =1.29) and rs317321618 (P = 4.62e-05, ß =1.27) from chromosome 20, rs315827399 (P = 5.68e-05, ß = -1.28) and rs315815227 (P = 6.83e-05,ß = 1.71) from chromosome 2, rs314929542 (P = 6.45e-05, ß = 1.45) from chromosome 15, rs14099455 (P = 6.63e-05,ß = 1.45) from chromosome 17 and rs313633102 (P = 7.39e-05,ß = -1.19) from chromosome 12 (Figures 4.15 & 4.16).

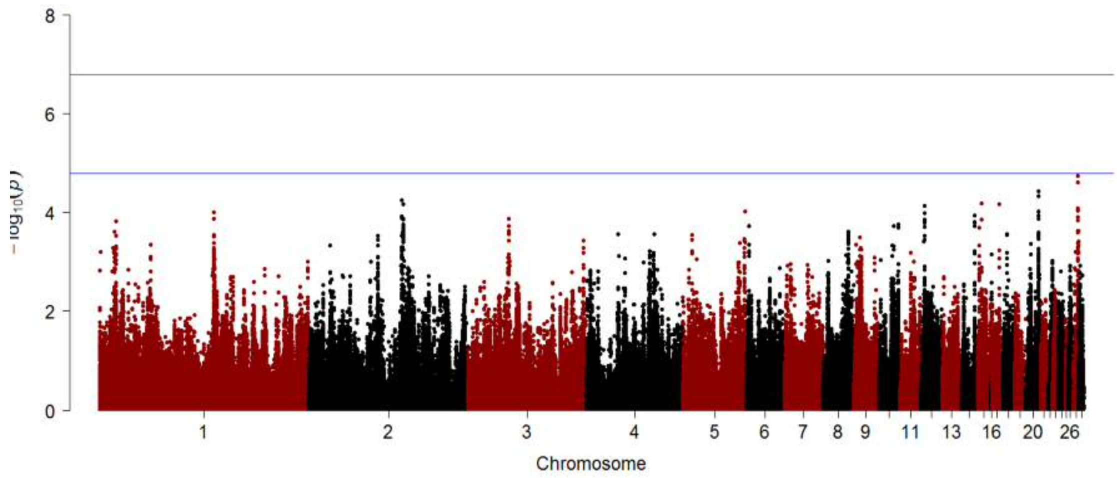

Figure 4.15. Manhattan plot for GWAS of non-normalized residual ΔMSE, after genomic control correction.
X-axis represents chromosome number and genomic position, y-axis represents minus log10 P-value. Red line represents the genome-wide significance threshold of 1.64e-07, blue line represents genome-wide suggestive threshold of 1.64e-05.

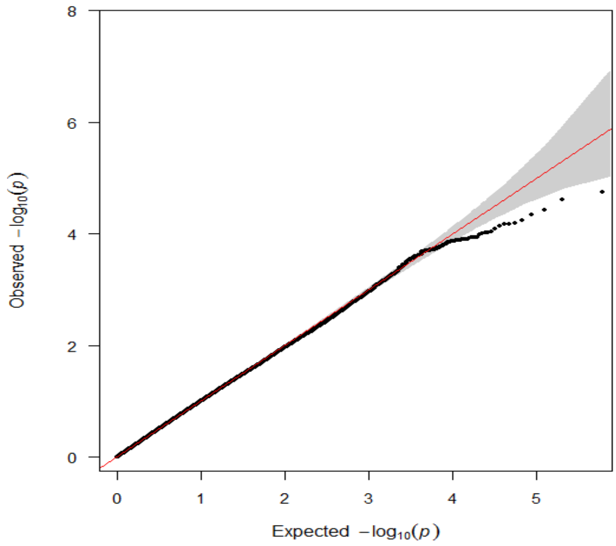

Figure 4.16. QQ plot for GWAS of un-normalized residual ΔMSE, after genomic control correction.

In the second model (`Residual-normalized-ΔMSE ~ SNP + plate number`), there were only two SNPs that reached the suggestive threshold after genomic control correction (λ_{GC} = 1.14), and no genome-wide significant SNPs. The two SNPs were rs316850156 and rs312907731 on chromosome 27, which had P-values of 1.15e-05 and 1.54e-05 respectively (Table 4.3, Figures 4.17 & 4.18).

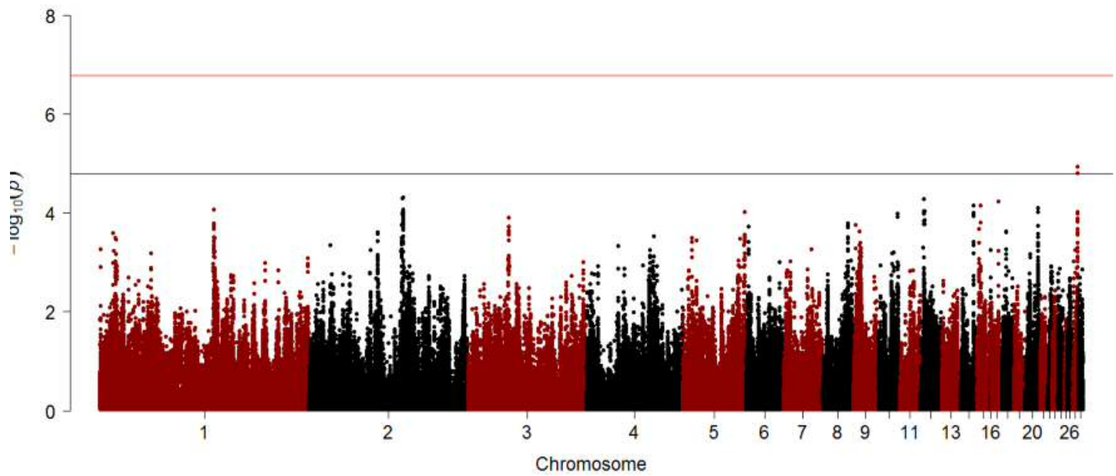

Figure 4.17. Manhattan plot for GWAS of residual from normalized ΔMSE, after genomic control correction.

X-axis represents chromosome number and genomic position, y-axis represents minus log10 P-value. Red line represents the genome-wide significance threshold of 1.64e-07, blue line represents genome-wide suggestive threshold of 1.64e-05.

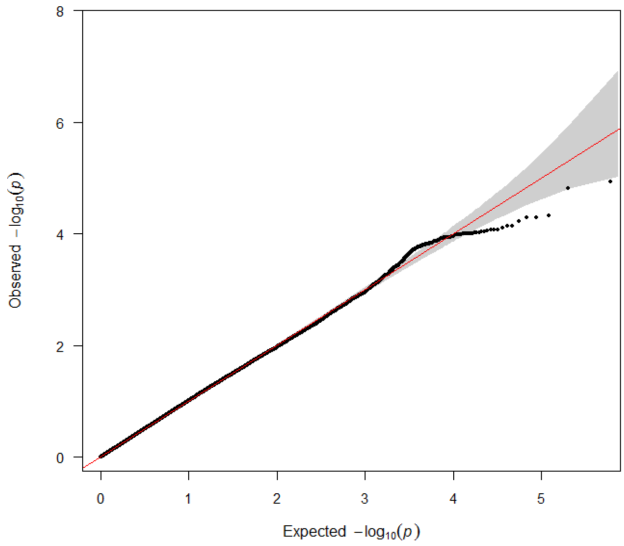

Figure 4.18. QQ plot for GWAS of residual from normalized ΔMSE, after genomic control correction.

In the third model (`Residual-normalized-ΔMSE ~ SNP + GRM + plate number`), in which the GRM was included, the residuals from the rank-normalized ΔMSE were used as the phenotype. No SNP reached the genome-wide significance threshold, however, 13 SNPs exceeded the suggestive threshold. Among the 13 SNPs, rs316720565 on chromosome 1 had the lowest P-value (P= 9.93e-07), followed by two nearby SNPs: rs10722203 (P= 1.46e-06, ß =-3.36) and rs13828835 (P= 2.53e-06, ß =-3.33). An independent (distantly-located) SNP on chromosome 1, rs13915147, also had a P-value less than the suggestive threshold. On chromosomes 3, 4 and 20, there were 3 clusters of strongly-associated SNPs, which were formed by rs313016590, rs312671401, rs16241712, rs13720406 and rs313789593 on chromosome 3, rs314184000 and rs14481912 on chromosome 4, and rs317266172 and rs316615987 from chromosome 20 (Table 4.3, Figures 4.19 & 4.20).

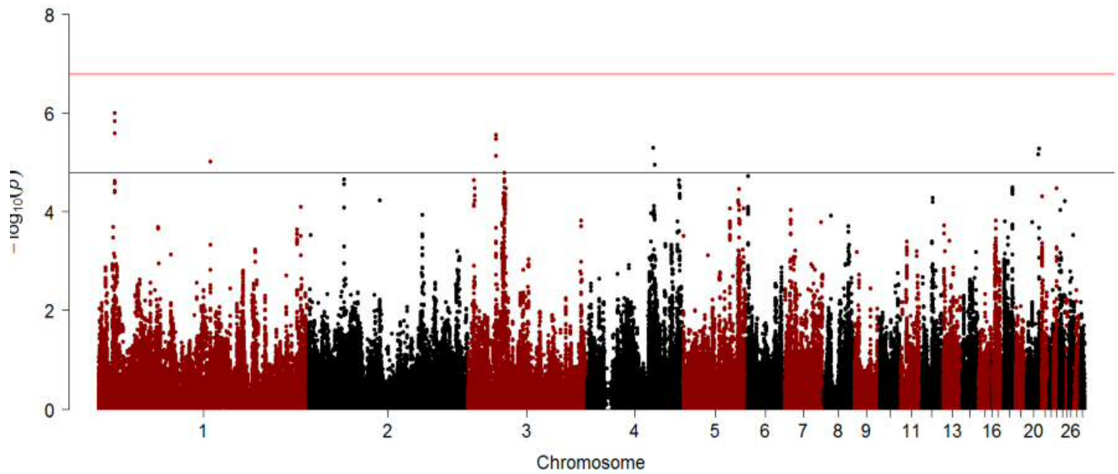

Figure 4.19. Manhattan plot for GWAS of residual from normalized ΔMSE, including GRM.

X-axis represents chromosome number and genomic position, y-axis represents minus log10 P-value. Red line represents the genome-wide significance threshold of 1.64e-07, blue line represents genome-wide suggestive threshold of 1.64e-05.

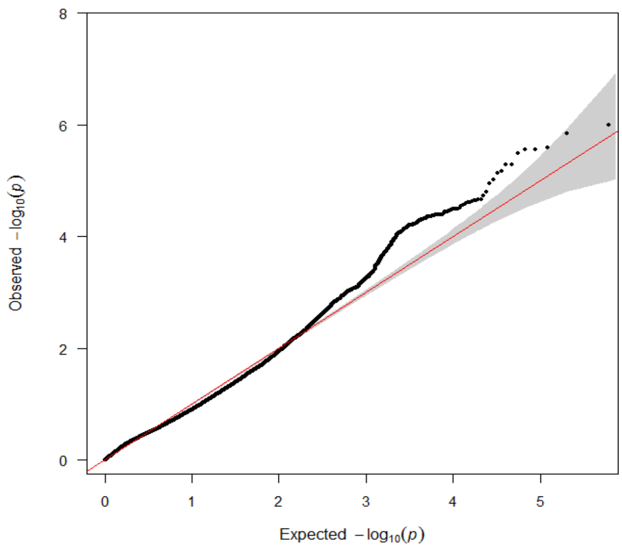

Figure 4.20. QQ plot for GWAS of residual from normalized ΔMSE, including GRM.

Table 4.3. All SNPs with minus log10 P-values exceeding suggestive significance threshold (P <1.64e-05)

SNP	CHR	POS	MAF	Model 1		Model 2		Model 3	
				β	P	β	P	β	
rs316720565	1	14766013	0.16	-0.71	0.09	-0.17	0.11	-3.50	9.9
rs10722203	1	14799410	0.17	-0.87	0.04	-0.21	0.04	-3.36	1.4
rs13828835	1	15071070	0.17	-0.50	0.24	-0.11	0.28	-3.33	2.5
rs13915147	1	103910210	0.14	-0.18	0.65	-0.02	0.84	-2.93	9.4
rs312671401	3	25956860	0.10	-0.68	0.20	-0.16	0.22	-4.17	2.7
rs16241712	3	25959747	0.10	-0.67	0.20	-0.16	0.22	-4.13	3.2
rs313016590	3	25962057	0.10	-0.65	0.22	-0.16	0.22	-4.19	2.7
rs13720406	3	25965464	0.11	-0.37	0.47	-0.08	0.52	-3.93	7.3
rs313789593	3	34223859	0.20	-0.53	0.17	-0.15	0.12	-2.84	1.6
rs314184000	4	62387547	0.13	-0.73	0.05	-0.19	0.04	-2.87	5.0
rs14481912	4	63352189	0.11	-1.12	0.02	-0.28	0.02	-3.58	1.1
rs316615987	20	11538043	0.11	-1.15	0.02	-0.28	0.02	-3.79	6.6
rs317266172	20	11848093	0.11	-1.17	0.02	-0.29	0.02	-3.86	5.1
rs312907731	27	4377267	0.17	-1.66	2.42e-05	-0.43	1.54e-05	0.20	0
rs316850156	27	4379502	0.16	-1.72	1.80e-05	-0.44	1.15e-05	0.19	0

4.3.4 Annotation of lead SNPs

The location and annotation of all SNPs reaching the suggestive significance threshold of 1.64e-05 identified by the GWAS are listed in Tables 4.2 and 4.3. For the 27 SNPs associated with ΔAXL, 23 of them were situated in the coding regions of 7 genes. The most strongly associated SNP in the ΔAXL quantitative trait GWAS analysis, rs317386235, is positioned upstream of the *PRKAR2B* gene on chromosome 1, while nearby SNPs rs316726738, rs312695428, rs15195233 and rs315478126 are situated in the coding region of the same gene. The next most strongly associated variants, rs13829591, rs317899999, rs313934866, rs315398501 and rs13829565, are positioned in the coding region of the *PIK3CG* gene on chromosome 1. Adjacent to the *PIK3CG* gene, rs316320493, rs315762686 with rs316260627 are situated in the coding region of *LOC107051631* on chromosome 1 with rs313813218 located between *LOC107051631* and *CCDC71L*. Another two SNPs, rs14792835 and rs312799206, are positioned in an intron region of H1B1, and another SNP, rs312576845, is located between *CDHR3* and *SYPL1*, all on chromosome 1. There was a cluster of associated SNPs on chromosome 7. Among them, rs14603638, rs313790665, rs316636360, rs313627312, rs16579210 and rs313006277 are situated in the *UGT1A1* gene, while rs317497540 is located in an intron of *UPS40*, with rs314035281 falling between these two genes. On chromosome 12, there was one SNP, rs313633102, in the coding region of *CENPP* (Table 4.2, Figure 4.21).

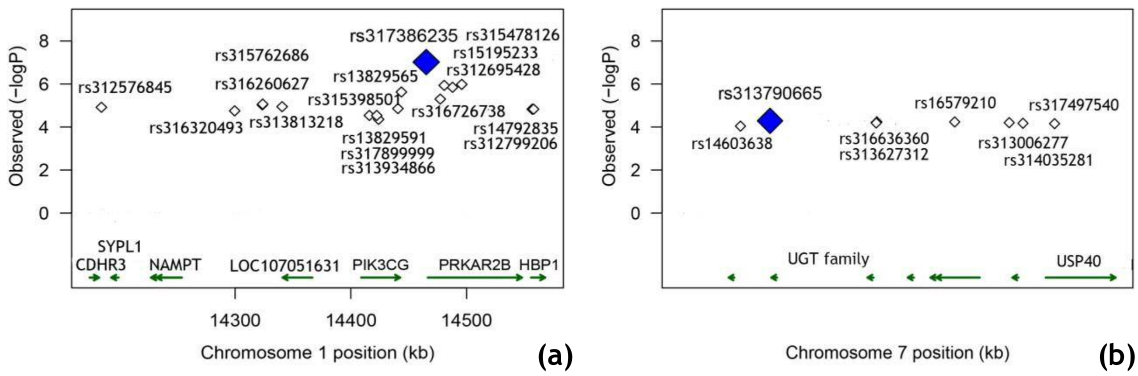

Figure 4.21.Regional plot for SNPs that reached the suggestive threshold in GWAS for ΔAXL.

Panel (a) shows the SNP cluster on chromosome 1, panel (b) shows the SNP cluster on chromosome 7.

Among the 15 SNPs that exceeded the suggestive threshold in the GWAS for ΔMSE, 4 of them – rs316720565, rs10722203, rs13828835 and rs13915147—are from chromosome 1 and are situated in intronic regions of *LAMB4*, *ERGIC2*, *C1H12ORF40* and *TIAM1*, respectively. On chromosome 3, rs312671401, rs16241712, rs313016590 and rs13720406 are clustered and positioned in gene *EPAS1*. Another SNP on chromosome3, rs313789593, is located upstream of *ZBTB18*. rs314184000, which falls within an intron of *ASAH1,* and rs14481912 which is located between *TUSC3* and *LOC107053248* are from chromosome 4. rs316615987 and rs317266172 are SNPs on chromosome 20, and map to the genes *VAPB* and *PMEPA1,* respectively. On chromosome 27, rs312907731 is situated in *CASC3*, while rs316850156 falls between *CASC3* and *RAPGEFL1* (Table 4.3).

4.4 Discussion

4.4.1 *PIK3CG*

The *PIK3CG* gene codes for PI3K (phosphoinositide 3-kinase) subunit gamma. PI3K is involved in diverse cellular activities such as cell growth, proliferation and survival (308). PI3K could influence eye growth in many ways, such as insulin-related refractive error development. One previous study (309) found that a PI3K inhibitor (Ly294002) could partially block the effect of insulin-induced overcompensation of negative lens wear in chicks. Meanwhile, it has also been suggested that insulin stimulates the PI3K/AKT pathway in normal and in plus lens wearing eyes of chicks (310). Another study suggested that PI3K participated in an inflammation mechanism that might play an important role in myopia progression (311).

4.4.2 *PRKAR2B*

The *PRKAR2B* gene codes for PKA regulatory subunit II beta. The cAMP-dependent protein kinase family (PKAs) are important kinases with roles in a wide range of cellular processes, including transcription, metabolism, cell cycle progression and apoptosis (312). During the process of cAMP-mediated activation of PKA, the inactive tetramer dissociates into a dimer of regulatory subunits and two active catalytic subunits. According to the type of regulatory subunit, PKA could be identified as type I or type II: *PRKAR2B* codes for a type II PKA regulatory β subunit (313).

PRKAR2B has previously been implicated in retinal signalling in emmetropisation (314). In an experiment carried out by Schaeffel and colleagues, chicks wore a positive lens over both eyes for 24 hours, and then retinal RNA was extracted for RNA microarray analysis and compared to retinal RNA from untreated control chicks. The mRNA expression of *PRKAR2B* was up-regulated 1.69-fold compared to control chicks (314). Moreover, in the retina, *PRKAR2B* was selectively expressed in type 3b bipolar cells in mice, although the specific role of this cell-type in transferring information was not clear (315). *PRKAR2B* is also found in many other tissues besides retina. In the brain, Leucine-rich repeat kinase 2 (LRRK2) interacts with PKAR2B protein, to negatively regulate PKA activity in response to dopamine receptor activation (316).

4.4.3 *UGT1A1*

UDP glucuronosyltransferase family 1 member A1 is encoded by the gene *UGT1A1*. A mutation in *UGT1A1* has been found to cause several diseases such as Cregler-Najjar Syndrome (317) and Gilbert Syndrome(318). *UGT1A1* is involved in the metabolism of retinol, in which all-trans-retinoate is converted to all-trans retinoyl β-glucuronide. Although there is no direct evidence about how the *UGT1A1* might affect visual system development, retinol and intermediates from the retinoid cycle are believed to have an impact on eye development and vision (319, 320). For myopia research, it was found that all-trans retinoic acid (RA) levels were increased in the retina of eyes with experimentally-induced myopia and reduced in eyes recovering from myopia or treated with plus lenses (150, 321, 322). Inhibition of retinal RA synthesis was also found to reduce the degree of myopia produced by FD in chicks (323). In the choroid, changes in the level of RA due to FD were found to be opposite to those in the retina (324). The disruption of *UGT1A1* could be a potential cause for abnormal RA metabolism, which might be a cause for myopia development.

4.4.4 *USP40*

Ubiquitin specific peptidase 40 (*USP40*) is encoded by the gene *USP40*. In a previous linkage analysis study of a high myopia pedigree, a high myopia locus (2q37) was mapped to a critical region between markers D2S1279 and D2S2205 on chromosome 2 at q37.1, where *USP40* is located. Thus, *USP40* is a promising candidate gene for high myopia (53).

4.4.5 *LAMB4*

The *LAMB4* gene encodes laminin subunit beta 4. Laminins are high molecular weight proteins of the extracellular matrix, which are expressed in basement membranes of the cornea, lens capsule, internal limiting membrane (ILM), Bruch's membrane (BrM) and many other eye tissues. They are one of the main components of the extracellular matrix, and are essential for stabilizing cellular structures and facilitating cell migration. In previous studies, laminin subunit alpha 1 (*LAMA1*) and subunit alpha 2 (*LAMA2*) were both found to be related to myopia development (78, 325). However, there are no studies of *LAMB4* and its relationship with eye development to date.

4.4.6 Different results from GWAS for AXL and MSE

In this GWA study, both the axial length and the mean spherical equivalent were tested as phenotypes. According to the GWAS results, there were no overlapping genes between these two phenotypes. There could be several reasons for these disparate results. First, the corneal curvature – another component that contributes to spherical equivalent – may also be sensitive to FD myopia. In one study in which chicks were monocularly form deprived for 14 days, the corneal curvature was flatter in treated vs. fellow eyes (260). However, the results of corneal changes have been inconsistent in other studies. In a study performed by Hayes et al., there was no significant difference in corneal curvature between FD and control eyes (326). Chen's (253) study also presented a similar conclusion. Chicks from different stains also showed different responses to FD. According to Troilo's study, 2 weeks of FD in the Cornell-K strain (K) results in less elongation of the VCD and flattening of the cornea yielding lower levels of induced myopia compared to the Washington H & N Strain (198).

Other species had different responses to FD. In a study of FDM in guinea pigs, after 6 days of diffuser wearing, the corneas of the treated eyes became steeper and the corneal power was greater than the fellow eyes (327). It suggested that the VCD was the initial dominant cause of the FDM in guinea pigs, but with longer FD periods, the corneal power begins to dominate. In macaque, FD might increase the corneal power (328, 329) while, in tree shrews, the corneal curvature is unaffected by FD (164, 330, 331).

Second, the measurement of the MSE may not be as accurate as the measurement of AL, which could reduce the statistical power to detect association signals. Cycloplegic refraction is rarely performed in chicks due to the ciliary muscle being striated rather than smooth and the very limited penetration of agents such as vecuronium bromide through the avian cornea. Retinoscopy under general anaesthesia (which relaxes accommodation in chicks) was ruled out since this necessitates the use of a speculum to hold open the eyelids, which can induce astigmatism. Thus, retinoscopy was performed on alert, awake chicks. Nevertheless, since chicks have a high amplitude of accommodation (over 25 D) and show wide fluctuations in accommodation, retinoscopy in chicks is technically challenging. This would have led to a degree of measurement error when assessing the refractive error of chicks.

Thirdly, the selection of chicks for GWAS was based on the change in AXL, not on the change in MSE. In the selected chicks, their ΔAXL corresponded to the phenotype extremes and therefore could be clearly separated into a high and low group (Figure 3.6a). By contrast, the ΔMSE of the selected chicks was more widely distributed, which meant that chicks with more moderate ΔMSE responses to FD were selected (Figure 3.6b). Thus, as a consequence of the limited sample size, a GWAS for ΔMSE may not have had sufficient power to detect genetic variants at a genome-wide significance level.

4.4.7 GRM and genomic control correction

Inflation of GWAS results can occur due to polygenicity (many small genetic effects), population stratification, and/or cryptic relatedness between samples. In the present study, the main concern was the relatedness among the chicks. To correct for this effect, in general, there are three methods: genomic control, mixed model analysis using a GRM, and LD score regression. Since LD score regression required an LD reference panel, which is not available for the chick, the other two methods were used in this study.

Genomic control. Under the null hypothesis, apart from a small number of SNPs that show a true association with the trait or disease, the test statistics for other SNPs should have chance levels of association with the trait; hence the observed P-value distribution should be equal to the null P-value distribution except for the low tail (306). Therefore, dividing the median x^2 of the observed test statistics by the theoretical median (x^2 = 0.456) under the null hypothesis, an inflation factor (called λ_{GC}) can be empirically determined. However, large-scale GWAS and meta-analyses indicate that there can be many causal variants for a particular disease or trait (polygenicity), which makes correcting by genomic control a conservative approach (332). In this study, although the sample size was small, there is still the concern of polygenicity of the trait. Hence, correcting by an inflation factor may not be the optimal method.

Mixed models with a GRM. The GRM approach was used for the association test by Yu et al. (333) to account for multiple levels of relatedness. Including a kinship matrix in a mixed model can reduce false positives and increase power (334). In the current study, the GRM accounted for relatedness amongst chicks, preventing overweighting of redundant information due to correlation structure. However, since the candidate marker is included in the GRM, this would lead to a small loss in power when testing the candidate SNP together with the GRM (334). GEMMA was used in this study because it computes an exact mixed model association test statistic with high computational efficiency (305).

4.4.8 Selective genotyping

Instead of performing a GWAS for the whole chick population (n=956), chicks with extreme phenotypes were selected for analysis (n=380). This strategy is based on the well-established theory that individuals in the phenotype extremes are enriched with trait-influencing alleles and/or alleles with large effects on the trait (335-337). Using this extreme phenotype selection approach increases statistical power when performing GWAS with a fixed sample size or fixed budget, making it economical (338).

4.4.9 Continuous vs. dichotomous phenotype coding

In this study, phenotypic data were analysed as both a continuous trait and a qualitative trait. When analysed as a continuous trait, there is uncertainty regarding whether the selective phenotype should be normalized prior to performing the GWAS analysis. Normalizing the phenotype would fit a basic assumption of linear regression, i.e. that the residuals in a linear regression should be normally distributed. However, during the process of normalization, the differences in phenotype between the two extremes are decreased. In this study, the results suggested that normalizing the phenotype increased statistical power (as judged by the QQ-plots under the assumption that association signals were true positives). Specifically, it was found that a larger number of genetic variants exceeded the suggestive significance threshold when ΔAXL was analysed as a quantitative trait compared to a dichotomous trait. The likely reason is that, in classifying ΔAXL as a dichotomous trait, information about the precise degree of myopia susceptibility is discarded (298, 335, 339).

4.4.10 Comparison of all models

In total, GWAS were performed using 7 different models for ΔAXL or ΔMSE. According to the QQ plots, the GWAS for ΔAXL using model 4 (Figure 4.14) was the optimal one. According to the theory that most genetic markers will not be associated with myopia susceptibility, for the majority of markers in a GWAS, the distribution of their p-values will be the same as that under the null hypothesis; these p-values would align with the diagonal in the QQ plot. Only a small proportion of SNPs from a GWAS are expected to have extremely small p-values and to deviate above the diagonal of the QQ plot at the tail of the p-value distribution. An early deviation of the observed p-value distribution from the QQ plot diagonal suggests a systematic bias (high false positive rate) of the model, while points mostly under the diagonal suggests a systematic overly stringent analysis has been carried out.

4.5 Conclusion

This study performed a GWAS in 379 chicks and identified one locus that was associated with myopia development at genome-wide significance. However, there were a number of limitations. Chicks were obtained from a commercial company with a large breeding colony, with the aim of minimizing relatedness between individuals. However, the genotypically-inferred kinship matrix showed a moderate level of relatedness (inbreeding) amongst the chicks. Relatedness inflates significance test P-values in a systematic manner (quantified by λ_{GC}), which complicated the analysis. A further important limitation is that chicks are phylogenetically distant from mammals, which makes the findings from chick studies of uncertain relevance to humans. Finally, owing to the relatively small sample size used, there was limited power to detect the genetic variants weakly associated with myopia susceptibility.

Chapter 5 Transcriptomic analysis of retinal gene expression in chicks developing form-deprivation myopia

5.1 Introduction

Performing GWAS can detect potential associations between genetic variants and a phenotype. However, even with large GWAS sample sizes, it is difficult to distinguish true causal variants from spurious signals due to LD. What's more, GWAS results usually provide little mechanistic insight, especially when the associated SNPs fall in noncoding areas. Indeed, even when SNPs are in coding areas, only if the loci are known to be translated into genes, and appropriate functional annotation information exists, can important pathways be identified. Another issue in GWAS is limited reproducibility. Sometimes, GWAS results are not replicated across studies or populations, leading to the report of false positives and suspicion of the validity of novel associations (340). To verify GWAS findings, apart from increasing the sample size and looking for replication from new GWAS studies, another approach is to verify the results in a different dimension, such as looking for complementary evidence from transcriptome, proteome, metabolome, or epigenome studies: the so-called 'systems genetics' approach.

Systems genetics considers the research target as a complicated biological network and shows a global view of the molecular architecture of complex traits (341). By integration or joint modelling, data from quantitative genetics is analysed with data from various high-throughput –omics platforms. Thus, results can be examined at different levels of biological organization, so that the underlying mechanisms and interactions between different aspects can be explored (341-343).

Among the different types of dataset that can be combined with GWAS results in systems genetics, transcriptomics is one of the most commonly selected –omics platforms. GWAS experiments provide the opportunity to identify potential causal variants at the DNA level, which is usually fixed (except for mutation) for each individual in all tissues during the whole lifetime of the organism, while transcriptomics provides dynamic observations linking genes to phenotypes. Compared to GWAS, there are two major benefits of transcriptome studies. First, transcriptomics is organ or tissue specific. For example, *DPYSL3* is a photoreceptor-specific gene that is only expressed in retina, while ζ-crystallin mRNA is only found in lens tissue (344, 345). Unlike GWA studies, which provide a general overview of disease pathogenesis, transcriptomic analysis of specific ocular tissues can provide complementary information. Second, expression patterns are time-dependent. They demonstrate which genes are actively expressed at given time-points, which will vary with external cues from the environment. For example, in one particular lens-induced myopia experiment (346), tree shrews wore a -5D lens over one eye for 2 days, 4 days or 11 days, and the mRNA expression patterns in the sclera were then analysed. The transcriptomics profiles were similar between the 2-day and 4-day treatment groups, but 3 genes showed down-regulated expression specifically in the 11-day treatment group (perhaps due to the eye having fully compensated to the lens by this stage of the experiment). These dynamic fluctuations could not have been detected through GWAS. What's more, transcriptomic analysis permit sub-gene level investigation, such as gene splicing analysis. This information is valuable, since variation in splicing can regulate protein function and cause phenotypic differences (347-349).

Transcriptome data can be analysed using a variety of methods. First, it can be used to test for association between a phenotype and gene expression level. In this scenario, one might postulate three potential causal relationships (341, 350): (a) the expression levels of the differentially-expressed genes are causal for the phenotype; (b) the phenotype causes the changes in expression level of the differentially-expressed genes; (c) there are confounding factors that influence both gene expression and phenotype. Second, transcriptomics data can be used to map gene expression levels to chromosomal loci. In this scenario, the expression information is considered as an 'intermediate phenotype'. Genetic variants associated with gene expression levels are termed eQTLs (expression QTLs). Co-localisation of phenotypic QTLs from GWAS and eQTLs from transcriptomics analyses implies that genetic variation in the region contributes to the phenotype via a change in expression level of the target genes (e.g. SNP $\rightarrow$ mRNA $\rightarrow$ phenotype, or equivalently, eQTL $\rightarrow$ eGene $\rightarrow$ phenotype). However, it should be noted that co-localisation of QTLs and eQTLs does not always signify a causal relationship (351). Thirdly, gene expression and GWAS information can be integrated by statistical modelling approaches, such as pathway analysis. The integrated modules are then tested for association with the phenotype (341, 350).

Transcriptomic data reflect tissue-specific and dynamic gene expression level changes that inherently carry functional information; such data are therefore ideal for studying G × E effects.

In this study, the transcriptome data originated from the retina. Emmetropisation is a visually-driven feedback process, which requires an image or light stimulation of the retina. Previous studies have shown that blocking the connection between the eye and visual cortex, either by severing the optic nerve or inhibition of ganglion cell action potentials with tetrodotoxin, does not prevent visual experience-dependent experimental myopia (163, 352, 353). These findings suggest that rather than emmetropisation being regulated by top-down signals from the brain completely, that the eye itself, at least partially, has the ability to regulate its rate of post-natal growth. A range of animal studies (354-359) suggest that the retinal processing of visual images signals a "stop" or "go" message to the sclera, via the choroid, in order to regulate eye elongation. Based on this evidence, the retina was selected as the target tissue for a transcriptomics study of differential gene expression in response to FDM. As discussed in section 5.4.2.2 below, transcriptomics studies have been widely utilised to investigate changes in gene expression in eyes developing experimentally-induced myopia (314, 360-362). An entirely novel aspect of the current experiment was the opportunity to examine differential retinal gene expression in chicks with either a high or low degree of susceptibility to FDM.

5.2 Methods

5.2.1 Overview and sample preparation

Gene expression profiling was carried out for both eyes (treated eye and control eye) of 8 chicks. The 8 chicks were selected from amongst the 380 chicks used in the GWAS experiment, with 4 selected as having a high degree of susceptibility to FDM and 4 chicks with low susceptibility. FDM treatment (section 2.1), tissue collection (section 2.4.2), and RNA extraction (section 2.5.3) are described in Chapter 2.

5.2.2 RNA sequencing and mapping

RNA sequencing and mapping were performed by Wales Gene Park Company. The company carried out library preparation using the Illumina TruSeq Stranded mRNA Library Prep Kit according to the manufacturer's protocol, and performed 75 bp paired-end sequencing on an Illumina HiSeq 2500 sequencer (30 million reads per sample). Before sequencing, RNA quality was analysed by the company using an Agilent Bioanalyzer to confirm that all samples had an RNA integrity value (RIV) no less than 8.

Briefly, the company's sequencing protocol had the following steps. Firstly, mRNA was purified by hybridizing with polyT-tailed beads; the purified mRNAs were released and sheared into 180-200bp fragments; the fragments were annealed to an arbitrary primer containing an upstream adapter sequence and reverse transcribed to yield first-strand cDNA, followed by synthesis of the reverse complement cDNA, to form double-stranded cDNA; paired-end adaptors (containing a further sequencing binding site and a barcode index) were then ligated to both ends of the double-stranded cDNA fragments. This is the cDNA library. Next, individual fragments were isolated in glass flow cells; the double-stranded cDNA fragments were denatured into single-stranded cDNA and PCR-amplified using primers matching the adapter sequence. Sequencing was performed using a 'sequencing by synthesis' approach using a primer targeting the 1st strand cDNA; for each extension cycle, di-deoxynucleotidetriphosphates (ddNTPs) labelled with different fluorophores were added to the buffer (note that ddNTPs cannot be extended any further, which halts the sequencing reaction after a single cycle of extension; note also that within each flow cell, only one ddNTP that matched with the template would be extended in each cycle); the newly-added ddNTPs were then excited by a light source, and the fluorescent signal emitted by each flow cell was recorded; the ligated fluorophors were then cleaved from the ddNTPs and washed away, and the ddNTPs converted to dNTPs (therefore allowing the next synthesis cycle to occur); after completely sequencing the 1st strand cDNA in this manner, the sequencing procedure was repeated for the 2nd (reverse) cDNA strands. Mapping: the sequences of all of the fragments were then assembled, and those with similar reads were clustered; forward and reversed reads were paired and converted to contiguous sequences; then they were aligned and mapped back to the reference genome (Gallus gallus-4.0). In the mapping step, alignment was performed by the HISTA2 program and transcript assembly was performed with the String Tie program. All of these steps were carried out by the Wales Gene Park company (Figure 5.1).

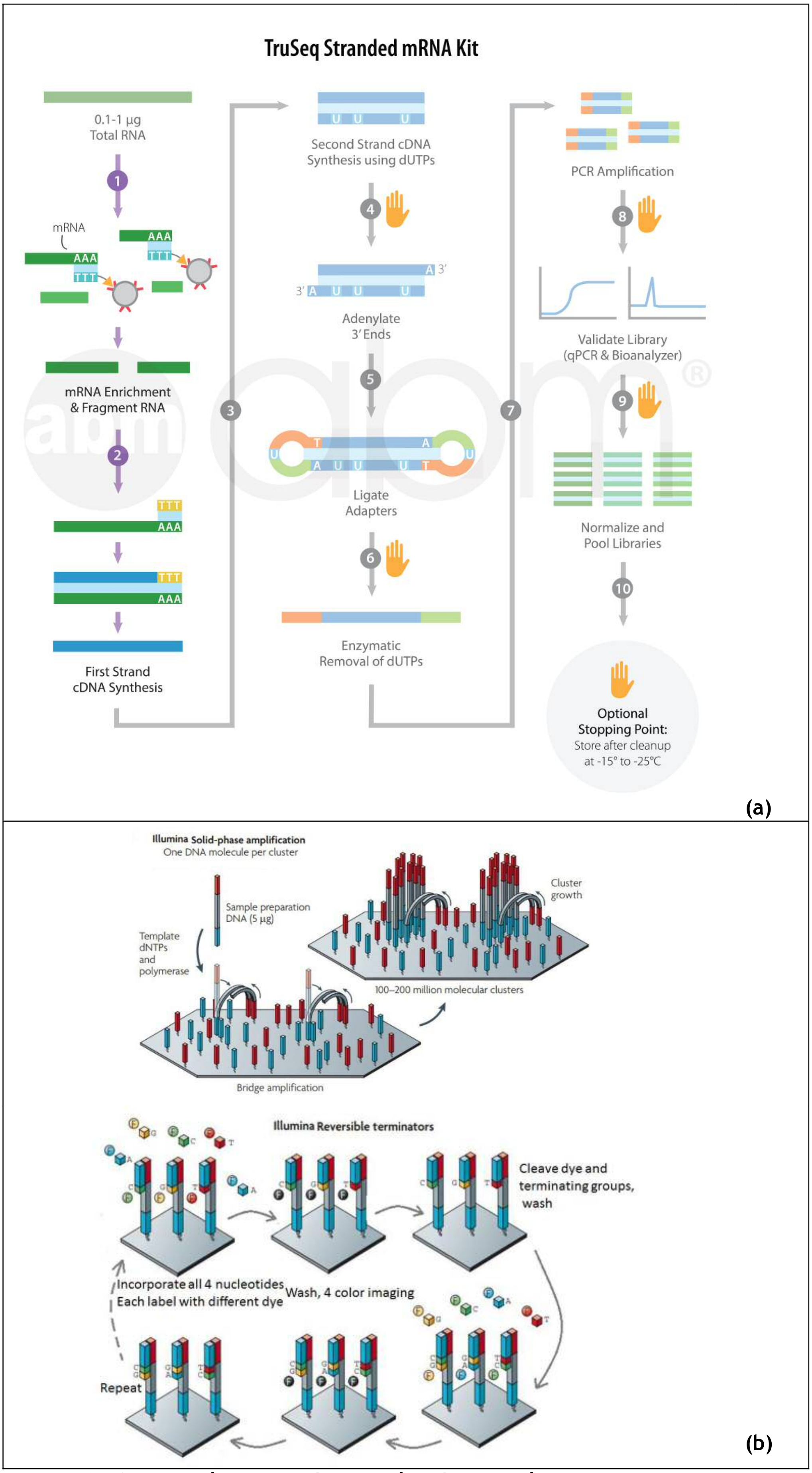

Figure 5.1. RNA-seq Using Next Generation Sequencing.
(a) Library preparation using TruSeq stranded kit (363); (b) Sequencing process (364).

5.2.3 Analysis pipeline

After count-based data were obtained (i.e. the number of reads mapping to each gene in the reference genome), further analyses were performed as follows:

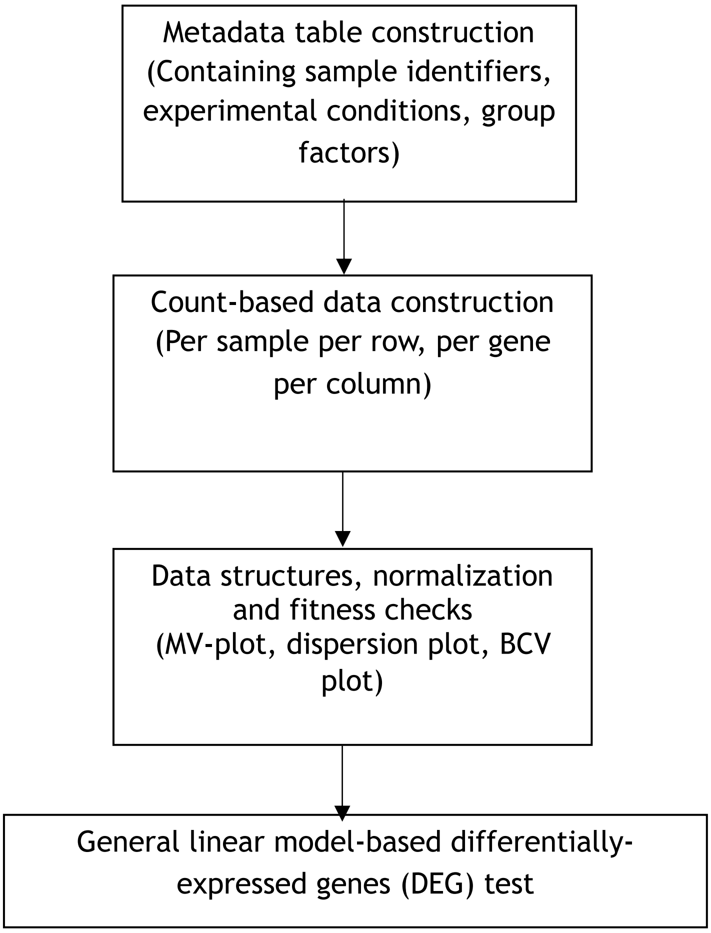

5.2.4 Statistical model

In recent studies, many software packages have been developed to analyse transcriptomics data and to identify differentially-expressed genes (DEG). Most packages make use of general linear models (GLMs). To identify DEGs between FDM vs. control eyes, and/or between High vs. Low myopia susceptibility group animals, several GLM models were used (in technical language, each model was chosen with a 'design matrix' that allowed the desired 'contrasts' to be specified and tested).

Model 1– Independent design

```
Expression Level ~ Sex + Treatment + Myopia_group
```

In the first model, the design matrix included contrasts for: (i) sex, (ii) treatment status (FDM vs. control), and (iii) myopia susceptibility group (High vs. Low). In this model, all 16 eyes were independent. The main purpose of this model was to detect differential expression between FDM vs. control eyes in an 'unpaired' manner, and to detect differential expression between the High vs. Low myopia groups independently of treatment status.

Model 2 – Paired design

```
Expression Level ~ 0 + Chick_ID + Treatment
```

In this model, the treated eye and control eye from the same chick were paired together to account for the similarity of the two eyes within the same chick (this is analogous to testing for differential expression between FDM vs. controls with a paired *t*-test). However, it was not possible to test the difference between the High vs. Low myopia groups independently using this paired model design, because there were linear dependencies between myopia group and Chick_ID (i.e. there would have been an infinite number of solutions for the best fit model, making it impossible to estimate the model coefficients).

Model 3 – Interaction design

```
Expression Level ~ 0 + Chick_ID + Treatment + Treatment × Mypoia_group
```

An interaction term (myopia group × treatment) was added to the paired-eye model in order to identify genes whose level of differential expression varied depending on whether they were in the High or Low myopia susceptibility group.

5.2.5 Software

For each model, three R packages were used to perform the above analyses: edgeR (365), DEseq2 (366) and Limma (367). All 3 packages take count-based data as input, however, while edgeR and DEseq2 model the data as a negative binomial distribution, Limma applies a transformation ('Voom') and models the data as a normal distribution. To synthesise results, the R package 'VennDiagram' (368) was used. The rationale for using 3 R packages for these analyses was to reduce type I errors and to examine the robustness of the findings.

Workflow for edgeR (369):

i. Exclude outliers and weakly expressed genes;
ii. Estimate normalization factors;
iii. Inspect relationships between samples (a multidimensional scaling (MDS) plot was used to visualise the similarity between samples);
iv. Estimate dispersion value;
v. Fit a GLM to the design matrix and dispersion estimate;
vi. Perform test on the contrast(s) of interest;

vii. Inspect and correct the p-values;
viii. Identify differentially-expressed genes at FDR <0.05.

Workflow for DEseq2 (369):

i. Estimate and inspect normalization factors;
ii. Inspect relationships between samples via a principal components analysis (PCA) plot;
iii. Estimate dispersion value;
iv. Fit linear model;
v. Perform test on contrast(s) of interest;
vi. Inspect and correct the p-values;
vii. Choose genes with adjusted p-values < 0.05.

Workflow for Limma (367):

i. Estimate and inspect normalization factors;
ii. Normalize read counts and estimate the mean-variance relationship;
iii. Perform voom transformation;
iv. Fit linear model;
v. Perform test on contrast(s) of interest;
vi. Inspect and correct the p-values;
vii. Choose genes with adjusted p-values < 0.05

5.2.6 Quality control

A total of 7341 genes had a detectable expression level in all 16 retinal RNAseq samples (30 M read depth). Gene expression data were inspected, and counts for 1 gene (*RN7SL1*) with extremely high expression level were removed, because extreme outliers could influence the power of edgeR, DEseq2 and Limma (370). Genes with less than 3 counts in any retina sample were also removed since the differentially-expressed gene tests are based on asymptotic statistics, hence for each sample and each gene, the transcripts or gene counts must not be too small (370). After filtering, 5688 transcripts were available for analysis and the frequency of mean counts per gene after filtering is shown in Figure 5.2a.

5.3 Results

5.3.1 Sample information and data structure overview

5.3.1.1 Sample information

A total of 16 eyes from 8 chicks were studied. Among these 8 chicks, 4 of them developed a high degree of myopia during the 4-day FDM treatment period (‘High’ group; mean ± SD treatment-induced axial elongation, 1.01 ± 0.057 mm) while the other 4 developed only a low degree of myopia ('Low' group; 0.079 ± 0.077 mm). Chicks were sex matched (2 males and 2 females in both the High and Low groups). Note that each chick's myopia susceptibility status was coded as a binary variable (High/Low) since the sample size was too small to permit an analysis using the continuous variable ΔAXL as the outcome variable. Information about the RNAseq samples is presented in Table 5.1.

5.3.1.2 Library size and normalization factors

After filtering, the library size of each sample ranged from 5,978,282 counts (sample green2054_Right) to 10,907,733 counts (sample white1495_Left). To account for this difference and make samples comparable, normalization factors were calculated before further analysis (Table 5.1).

5.3.2 Sample quality

To identify outlier samples, the relationship between samples was analysed. Before normalization, a principal components analysis (PCA) showed a low degree of similarity between samples (Figure 5.2b). After normalization, edgeR's multidimensional scaling (MDS) plot showed a trend of clustering between the pairs of eyes from the same individual chick (Figure 5.2c). In contrast, the DEseq2 PCA results suggested that sample white1495_left was an outlier (Figure 5.2d), and therefore, for subsequent analysis using DEseq2, samples white1495_right and white1495_left were removed.

Table 5.1.Sample information.

Sample ID	Sex	Myopia group	Chick ID	Treatment	AXL (mm)	MSE (D)	Library
white1587_Right	Female	High	white1587	Treated	1.41	-6.00	80006
white1587_Left	Female	High	white1587	Control	0.38	4.50	62849
green2006_Right	Female	Low	green2006	Control	0.31	5.50	67694
green2006_Left	Female	Low	green2006	Treated	0.43	0.50	79884
white1344_Right	Male	High	white1344	Control	0.37	6.50	82249
white1344_Left	Male	High	white1344	Treated	1.35	-12.00	93546
white1907_Right	Male	Low	white1907	Control	0.49	6.00	71064
white1907_Left	Male	Low	white1907	Treated	0.63	4.00	10377
green2054_Right	Female	High	green2054	Treated	1.46	-13.00	59782
green2054_Left	Female	High	green2054	Control	0.52	5.50	84953
white1495_Right	Male	Low	white1495	Treated	0.56	1.00	81688
white1495_Left	Male	Low	white1495	Control	0.47	5.5	10907
white1401_Right	Male	High	white1401	Treated	1.62	-8.00	67033
white1401_Left	Male	High	white1401	Control	0.55	6.50	76310
white1641_Right	Female	Low	white1641	Control	0.50	4.00	79467
white1641_Left	Female	Low	white1641	Treated	0.47	6.00	80802

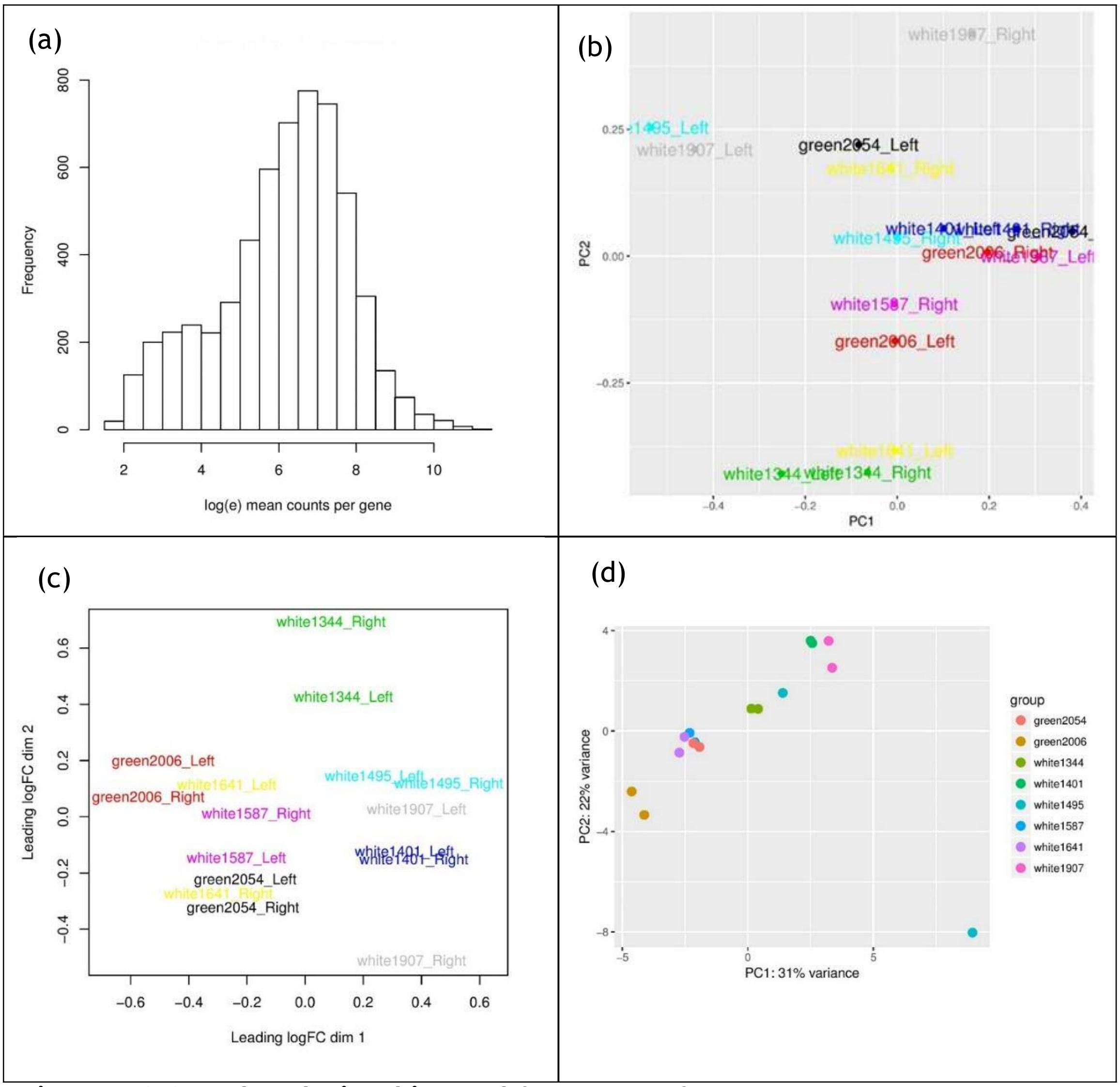

Figure 5.2.Sample relationships and frequency of mean counts per gene.
(a) Frequency of mean counts per gene after filtering; (b) Principle component analysis (PCA) before normalization; (c) Multi-Dimensional Scaling (MDS) plot from edgeR; (d) PCA by DESeq2.

5.3.3 Gene expression mean-variance plots

To investigate gene expression patterns, the mean and variance of the counts of each gene were analysed. The mean counts ranged from 5.25 counts to 72013 counts; the distribution of the mean counts (after log transformation) is shown in Figure 5.3. The variation in gene counts was generally larger than or equal to the mean count, ranging from 3.50 to 345081566. The mean-variation relationship before and after normalization is shown in Figure 5.3. Both plots confirmed that the variance was much larger than the mean value, suggesting the negative binomial model would be appropriate.

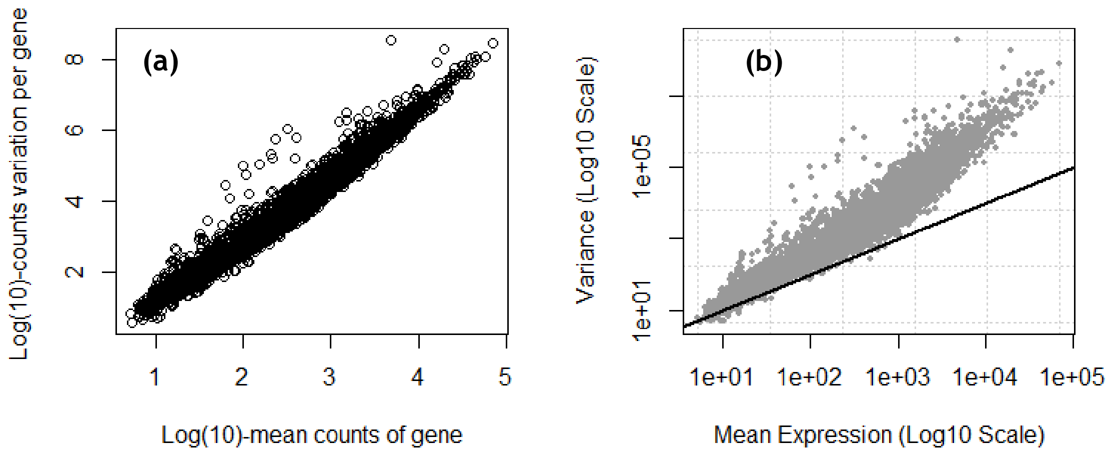

Figure 5.3. Mean-variance relationship.
(a) Before data normalization; (b) After data normalization

5.3.4 Dispersion estimation for different models

One of the most important steps in these analyses is estimating dispersion. Dispersion describes the variance of the gene counts in a negative binomial model. For each statistical model, dispersion was estimated by both edgeR and DESeq2 in order to fit the negative binomial distribution, while the mean-variance relationship was estimated by Limma (Figure 5.4). After this step, differentially expressed genes were identified using the various contrasts in Models 1-3.

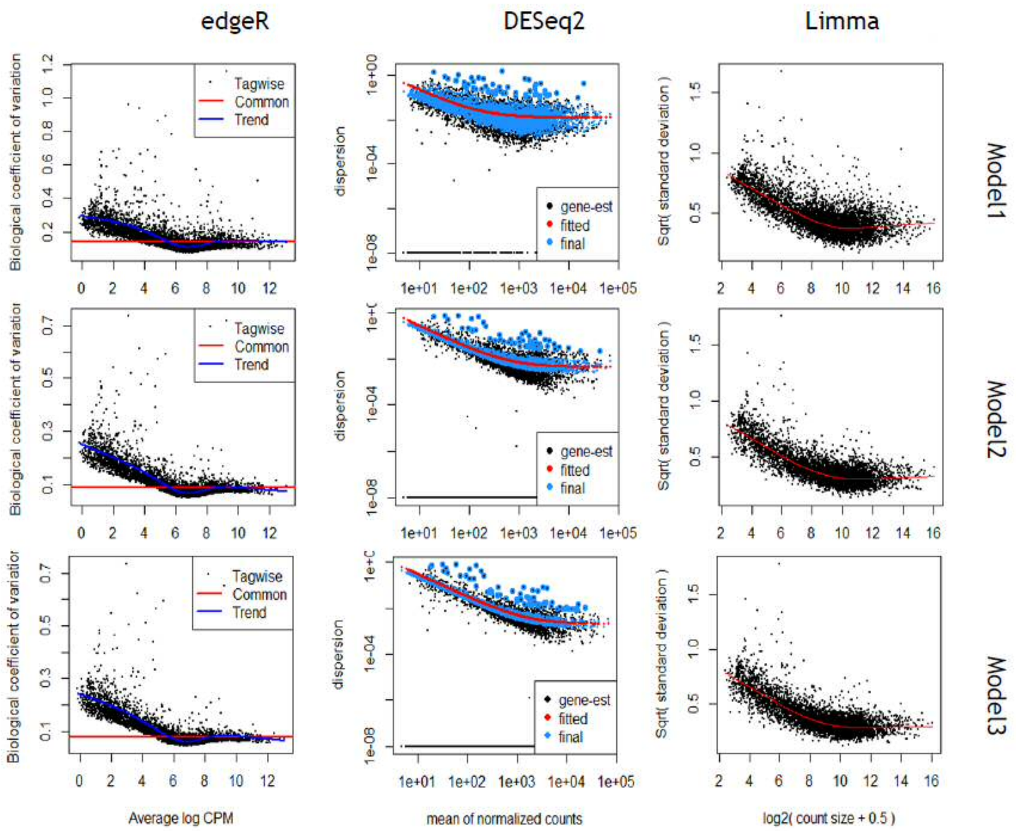

Figure 5.4. Dispersion plots generated by edgeR and DESeq2, and Mean-Variance plot by Limma after fitting the models.
edgeR's plotBCV illustrates the relationship between the biological coefficient of variation (BCV, square root of dispersion) versus the mean log counts per million (CPM); DESeq2's dispersion plot illustrates the relationship between the dispersion and the mean of normalized counts; Limma's mean-variance trend plot illustrates square-root of standard deviation versus count size on a log(2) scale.

5.3.4 Results for Model 1

In this model, sex, Treatment (FDM vs. control eye) and myopia susceptibility group (High vs. Low) were all considered.

5.3.4.1 DEG between FD eyes and control eyes

Twenty-two transcripts were differentially expressed between FD eyes and control eyes (FDR <0.05) using at least one of the software packages. Among these identified transcripts, DEseq2 identified 19 of them, edgeR identified 13, while Limma identified only 1. Only one gene, *UTS2B*, was identified by all 3 methods; 7 genes, *UNC5C, KCNA4, SIX3, VIP, SPRY4, DUSP4* and *MAFF* were identified by both edgeR and DESeq2. Two genes, *MSMO1* and *STARD4*, were up-regulated in FD treated eyes; the remaining 20 genes were down-regulated in FD eyes (Table 5.2, Figure 5.5).

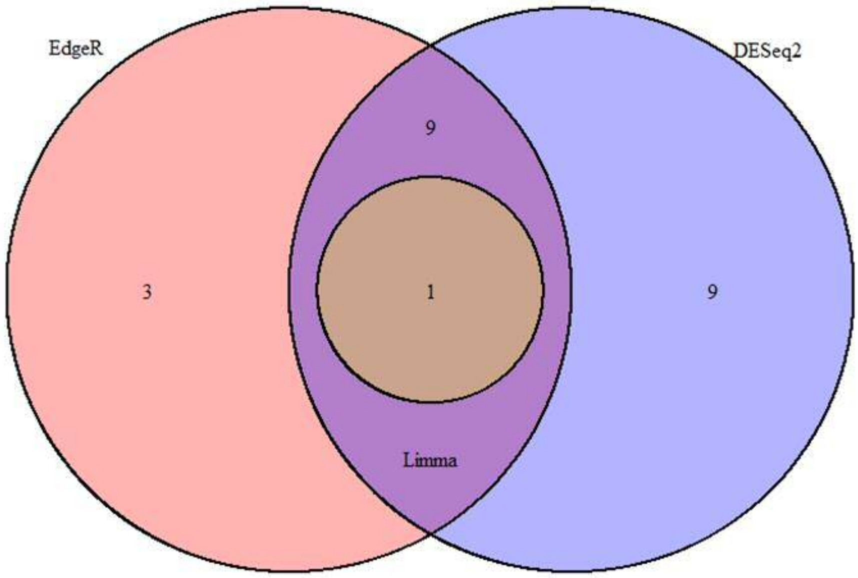

Figure 5.5. Venn-diagram showing overlap in differentially-expressed transcripts identification between FD and control eyes using analysis Model 1 with 3 software packages (edgeR, DEseq2, and Limma).

Table 5.2. Transcripts differentially expressed (FDR <0.05) between FD-treated eyes and control eyes
software packages.

Transcript ID	edgeR analysis		DEseq2 analysis		Limma analysis		Gene ID	Name
	logFC	FDR	log2FC	P-adj	logFC	P-adj		
NM_206989	-0.858	1.79e-04	-0.840	0.001	-0.858	0.009	*UTS2B*	Urotensin 2B
NM_204451	-0.314	0.004	-0.322	0.008	-0.316	0.078	*UNC5C*	unc-5 homolog C (C. e
NM_204851	-0.354	0.058	-0.328	0.008	-0.344	0.161	*SPON1*	Spondin 1
NM_204625	-0.238	0.063	-0.228	0.022	-0.239	0.126	*OPN4-1*	Photopigment melanop
NM_204899	-0.287	0.023	-0.288	0.022	-0.284	0.130	*KCNA4*	Potassium voltage-gated
NM_204364	-0.279	0.018	-0.269	0.024	-0.281	0.126	*SIX3*	SIX homeobox 3
NM_001177309	-1.011	0.004	-0.895	0.024	-1.068	0.130	*VIP*	Vasoactive intestinal p
NM_205366	-1.003	0.004	-0.890	0.024	-1.059	0.130	*VIP*	vasoactive intestinal p
NM_001079735	-0.908	0.004	-0.841	0.026	-0.887	0.126	*SPRY4*	Sprouty homolog 4 (Dr
NM_001079735_2	-0.898	0.004	-0.833	0.026	-0.878	0.126	*SPRY4*	Sprouty homolog 4 (Dr
NM_001006438	0.326	0.108	0.359	0.026	0.327	0.219	*MSMO1*	Methylsterol monooxy
NM_205455	-0.521	0.062	-0.563	0.033	-0.530	0.161	*TNS1*	Tensin 1
NM_001079742	0.296	0.108	0.314	0.033	0.296	0.161	*STARD4*	StAR-related lipid tran
NM_204838	-1.076	0.004	-1.039	0.034	-1.029	0.161	*DUSP4*	Dual specificity phospl
NM_204212	-0.336	0.160	-0.357	0.034	-0.336	0.258	*HK2*	Hexokinase 2
NM_204533	-0.238	0.188	-0.284	0.038	-0.242	0.258	*MAB21L1*	NM_204533
NM_204757	-0.547	0.017	-0.525	0.040	-0.556	0.127	*MAFF*	v-maf avian musculoap
NM_001305256_2	-0.877	0.353	-1.390	0.040	-0.808	0.391	*LOC420362*	NM_001305256
NM_205209	-0.251	0.222	-0.219	0.047	-0.251	0.161	*SLC2A1*	Solute carrier family 2
NM_001271902	-0.674	0.043	-0.700	0.115	-0.679	0.161	*GLI2*	GLI family zinc finger
NM_204114	-0.392	0.029	-0.353	0.117	-0.385	0.161	*DIO2*	Deiodinase iodothyron
NM_001324555	-0.383	0.042	-0.343	0.126	-0.377	0.161	*DIO2*	Deiodinase iodothyron

LogFC – log (10) fold of change; Log2FC – log (2) fold of change; P-adj – adjusted P- value.

(Table 5.3, Figure 5.6)

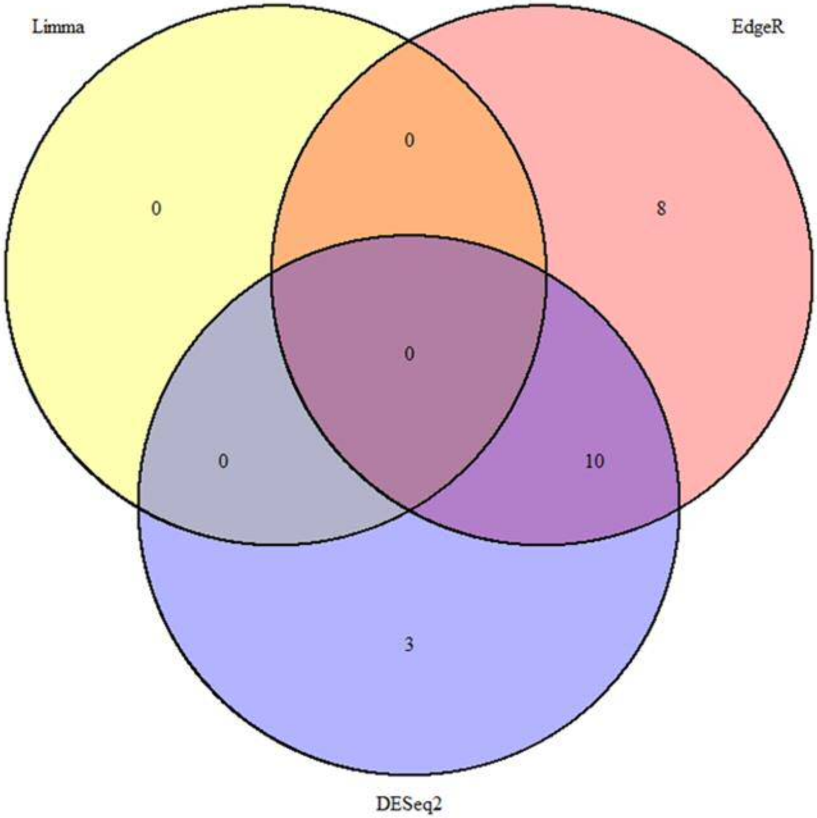

Figure 5.6.Venn-diagram showing overlap in identification of differentially-expressed transcripts between High vs. Low myopia groups using analysis Model 1, with 3 software packages (edgeR, DEseq2, and Limma).

Table 5.3. Transcripts differentially expressed (FDR <0.05) between High vs. Low myopia groups using packages.

Transcript ID	edgeR analysis		DEseq2 analysis		Limma analysis		Gene ID	Name
	logFC	FDR	log2FC	P-adj	logFC	P-adj		
NM_001012540	-0.278	0.024	-0.300	0.006	-0.278	0.307	*TTLL12*	Tubulin tyrosine ligase like
NM_001030697	0.744	0.031	0.867	0.028	0.785	0.322	*PIK3R5*	Phosphoinositide-3-kinase,
NM_001030697_2	0.747	0.001	0.835	0.006	0.757	0.307	*PIK3R5*	Phosphoinositide-3-kinase,
NM_001030697_3	0.747	0.039	0.866	0.043	0.786	0.339	*PIK3R5*	Phosphoinositide-3-kinase,
NM_001031409	-0.349	0.320	-0.463	0.046	-0.333	0.822	*EOGT*	EGF domain-specific O-link transferase
NM_001033643	-0.596	0.024	-0.677	0.014	-0.596	0.322	*CR1L*	Complement component (3
NM_001080888	0.292	0.031	0.208	0.080	0.296	0.322	*RCHY1*	NM _001080888
NM_001143931	-0.488	0.045	-0.530	0.074	-0.448	0.380	*TPCN3*	Two-pore calcium channel
NM_001199624	-0.356	0.027	-0.278	0.131	-0.347	0.322	*BTD*	Biotinidase
NM_001277827	1.442	0.024	1.093	0.328	1.402	0.574	*MYOZ2*	Myozenin 2
NM_001293134	0.659	0.039	0.737	0.043	0.625	0.339	*COL8A1*	Collagen, type VIII, alpha 1
NM_001318460	0.890	0.047	1.152	0.014	1.006	0.339	*TRPA1*	Transient receptor potentia
NM_204179	-3.668	0.014	-2.336	0.095	-1.875	0.998	*CRYBA2*	Crystallin, beta A2
NM_204204	0.457	0.029	0.434	0.190	0.452	0.339	*UGT8*	UDP glycosyltransferase 8
NM_204636	0.393	0.952	0.597	0.043	0.442	0.786	*MXRA8*	Matrix-remodelling associa
NM_204729	0.400	0.345	0.509	0.020	0.415	0.440	*RGN*	Regucalcin
NM_204935	0.829	0.039	0.956	0.050	0.763	0.462	*DCT*	Dopachrome tautomerase
NM_205112	0.895	0.024	1.033	0.020	0.801	0.380	*PMEL*	Premelanosome protein
NM_205280	0.542	0.029	0.428	0.279	0.530	0.380	*MBP*	Myelin basic protein
NM_205429	-0.633	0.024	-0.690	0.020	-0.651	0.322	*17.5*	NM_205429
NM_205501	-4.824	0.024	-1.870	0.327	-3.226	0.998	*ASL1*	Argininosuccinate lyase

LogFC – log (10) scale fold of change; Log2FC – log (2) scale fold of change; P-adj – adjusted P- value.

5.3.5 Results for Model 2

In this model, the design matrix was used to make a paired comparison between treated eyes and control eyes, with the aim of increasing the statistical power of the analysis. After re-estimating the dispersion and fitting the model to the data, a paired comparison was carried out. A total of 537 transcripts were found to be differentially expressed between FD eyes and control eyes. edgeR discovered 494 transcripts (adjusted P <0.05), while Limma and DESeq2 identified 327 and 282 transcripts, respectively. There were 205 transcripts that were identified by all 3 methods, 110 transcripts were commonly discovered by Limma and edgeR, 43 transcripts overlapped between edgeR and DESeq2, and only 3 transcripts were common only between Limma and DESeq2. Among the 537 transcripts, 269 transcripts were down-regulated and 268 up-regulated in FD-treated eyes (Appendix 5.1, Figure 5.7).

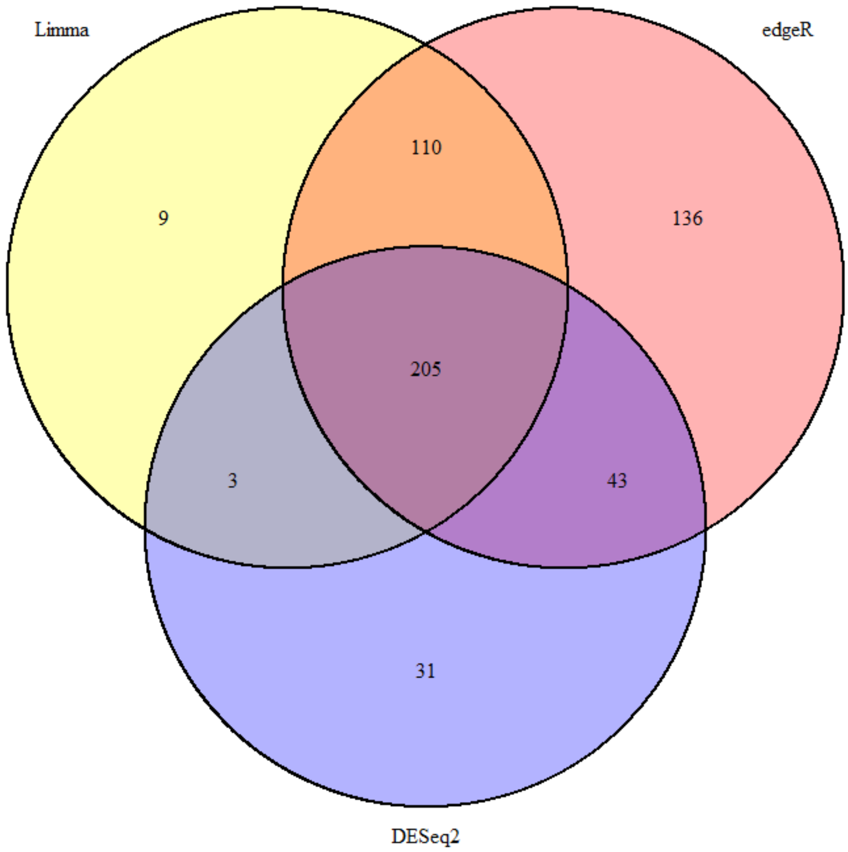

Figure 5.7.Venn-diagram showing overlap in identification of differentially-expressed transcripts between FD-treated vs. control eyes using analysis Model 2, with 3 software packages (edgeR, DEseq2, and Limma)

In addition, the high and low myopia groups were analyzed separately using model 2 (this will be referred to as the "model 2 separate" analysis). In the high myopia group, the paired comparison between treated eyes and control eyes identified 181 transcripts in total by 3 software packages; in the low myopia group, in total 1077 transcripts were found. Comparing these two datasets, there were 48 transcripts (45 genes) overlapped (Figure 5.8).

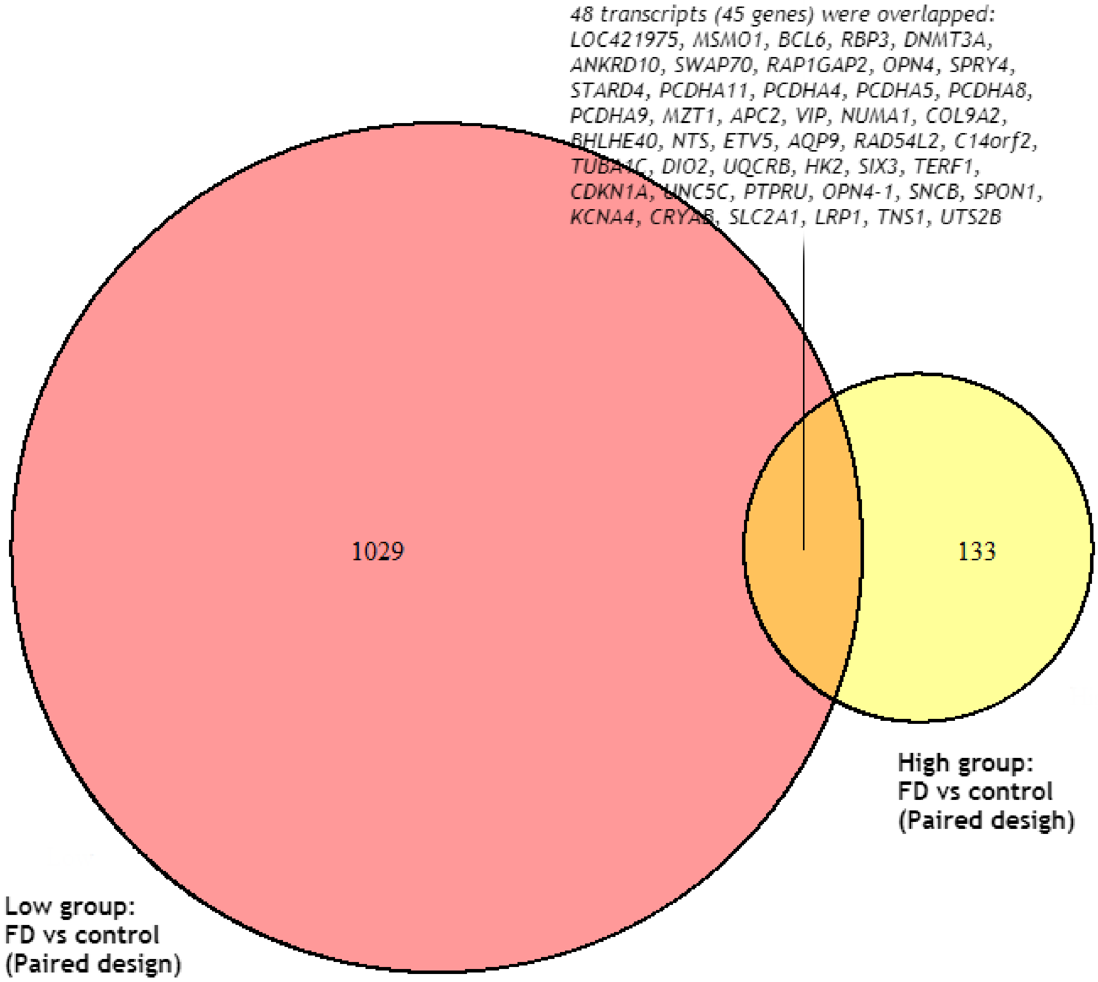

Figure 5.8.Venn-diagram showing overlap in identification of differentially-expressed transcripts between FD-treated vs. control eyes using analysis Model 2, when analyzing high and low group separately.

5.3.6 Results for Model 3

This model incorporated a paired design along with a test for an interaction between treatment (FD vs. control) and group (High vs. Low). A total of 495 transcripts were identified by DESeq2 as showing differential expression between FD-treated and control eyes that differed in High vs. Low chicks. However, Limma failed to identify any transcripts for this analysis, while edgeR only identified 7 transcripts (all of which overlapped with the transcripts found by DEseq2). These 7 transcripts represented 5 genes: *GCG*, *ACSBG2, AQP9, IGFBP4,* and *INSIG1* (Table 5.4). Of the 495

DEseq2 transcripts, 203 transcripts were down-regulated in FD eyes from the High myopia susceptibility group (Appendix 5.2, Figure 5.9).

The candidate gene *PIK3CG* identified from the GWAS was not amongst the set of genes showing evidence of a treatment x group interaction (edgeR: FDR = 0.907; DESeq2: P= 942; Limma: P = 0.861). The other candidate gene from the GWAS, *PRKAR2B*, was not present in the RNAseq annotation files, suggesting that its expression may have been below the detection threshold of my experiment.

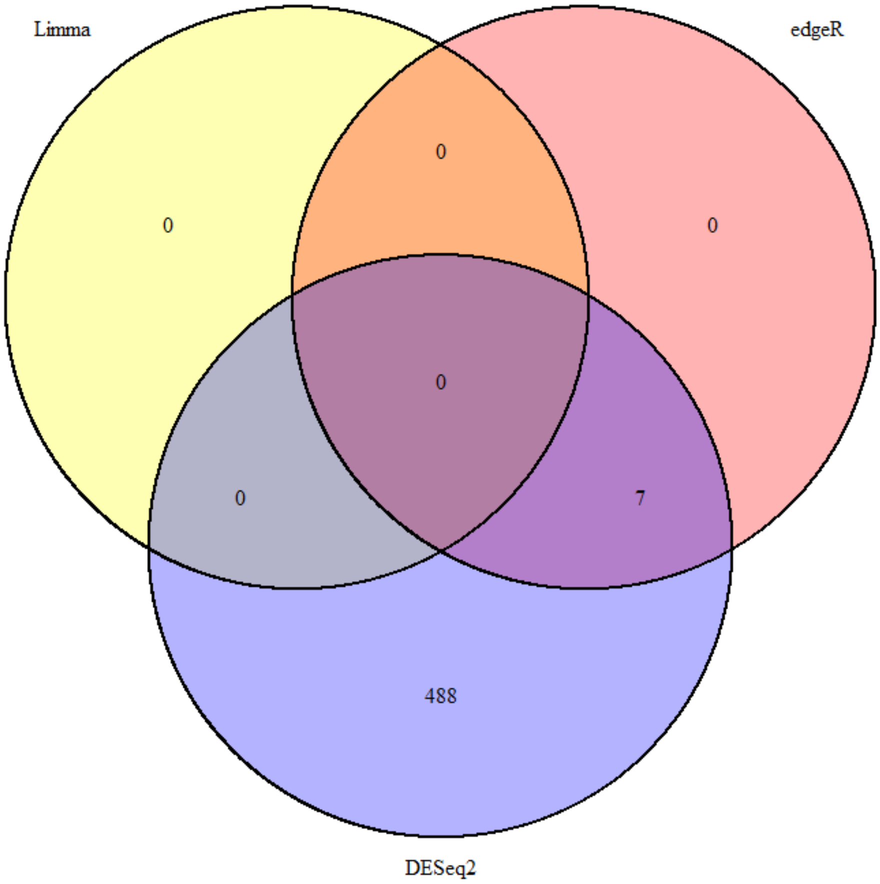

Figure 5.9.Venn-diagram showing transcripts differentially-expressed between FD-treated and control eyes, that also differed in level between High and Low group chicks (interaction between treatment x group, FDR <0.05) using Model 3.

Table 5.4. Transcripts differentially-expressed between FD-treated and control eyes, that also differe group chicks (interaction between treatment x group, FDR <0.05) using Model 3.

Transcript ID	edgeR		DESeq2		Limma		Gene ID	Name
	logFC	**FDR**	**log2FC**	**P-adj**	**logFC**	**P-adj**		
NR_073182	-0.651	0.009	-0.758	2.81E-04	-0.648	0.232	*GCG*	Glucagon
NM_001293238	-0.65	0.009	-0.661	0.002	-0.633	0.232	*AQP9*	Aquaporin 9
NM_001293239	-0.648	0.009	-0.659	0.002	-0.631	0.232	*AQP9*	Aquaporin 9
NM_001012846	0.477	0.009	0.535	3.49E-04	0.476	0.232	*ACSBG2*	acyl-CoA synthe
NM_204353	-0.5	0.011	-0.57	7.94E-04	-0.503	0.232	*IGFBP4*	Insulin like grow
NM_001190165	-0.577	0.016	-0.674	7.94E-04	-0.574	0.232	*GCG*	Glucagon
NM_001030966	0.407	0.037	0.391	0.001	0.407	0.232	*INSIG1*	Insulin induced

LogFC – log (10) scale fold of change; Log2FC – log (2) scale fold of change; P-adj – adjusted P- value.

5.4 Discussion

5.4.1 Retinal gene expression differences induced by form deprivation

5.4.1.1 Comparison between Model 1 and Model 2

Model 1 identified 22 retinal transcripts that were differentially expressed between treated and control eyes after 4 days of FD. The paired design in Model 2 showed greater power (accounting for the covariance in paired eye data that was not explicitly modelled in the independent Model 1 design); it detected 537 transcripts. Except for *LOC420362*, all of the transcripts identified in Model 1 were also identified in Model 2 (Figure 5.10).

From Figure 5.2, it was observed that the variation between individual chicks was greater than the variation between paired eyes. Therefore, a paired eye model (such as model 2) would be expected to perform better than a model in which the eyes were analyzed independently (model 1). This theoretical expectation was confirmed in practice: model 2 detected a larger number of differentially expressed transcripts between FD and control eyes than model 1.

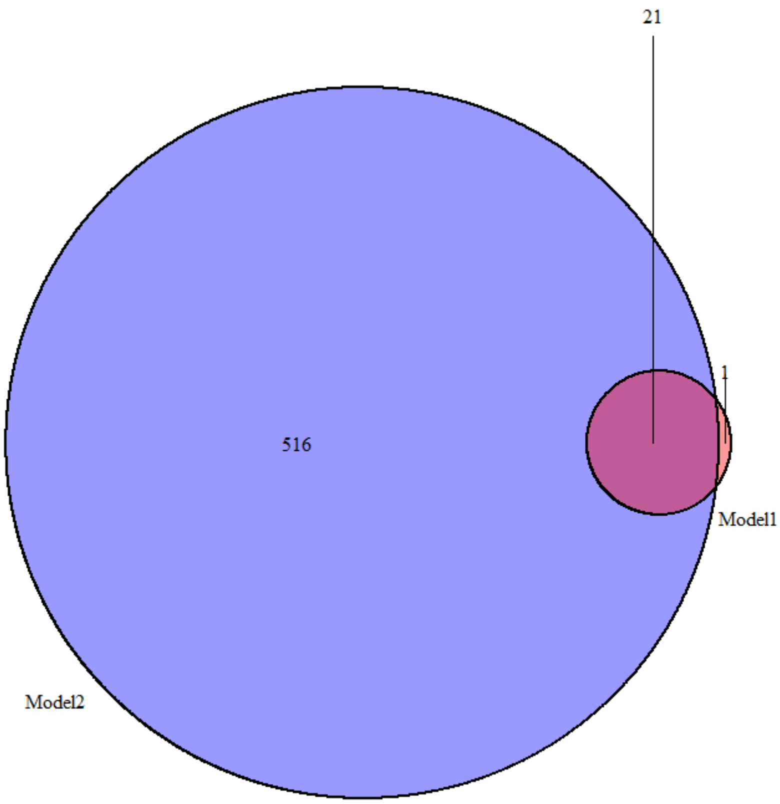

Figure 5.10. Venn-diagram showing genes differentially-expressed between FD-treated and control eyes detected using either Model 1 or Model 2.

5.4.1.2 Comparison with previous findings

For the 538 transcripts detected by either Model 1 or Model 2 in the current study, 94 (17.5%) of them replicated findings from previous experimentally-induced myopia studies that have examined either transcriptomics or proteomics. For example, *VIP, UTS2B and DUSP* were also reported by McGlinn (361) in a study analyzing gene expression in FD chick retina; differential expression of *DIO2, KCNA4* and *OPN4-1* were previously identified in LIM chick model (371); *ATP5C1, MBP* and *UQCRB* replicated Barathi's proteomics study in atropine treated LIM mouse model (372). Full details are presented in Appendix 5.3.

5.4.1.3 Noteworthy genes

Vasoactive intestinal peptide (*VIP*)

Vasoactive intestinal peptide (*VIP*) was found down-regulated in FD-treated chick eyes by McGlinn et al. (361) as was the case in our study. VIP is a peptide hormone from the glucagon family. It causes relaxation of smooth muscle in the gastrointestinal system. Landmark studies have shown that VIP has a role in myopia development. According to Seltner and Stell (373) and Cakmak et al. (374), intravitreal injection of VIP retarded but did not eliminate myopia development in FD eyes of chicks. However, in the FD mouse (375), VIP was not significantly differentially expressed and in FD primate (376), there was an increase of VIP expression in lid-sutured eyes. These contradictory results could be due to differences in the molecular architecture of the emmetropisation system between species, limited statistical power in the latter studies, or differences in experimental conditions, e.g. the precise time-point studied. In the mouse study (375), FD was performed for less than 24 hours, while in the monkey study (376) FD lasted for over 1 month. In contrast, McGlinn et al. used a 3 days FD treatment period. Seltner and Stell (373), and Cakmak et al. (374) performed FD for 7-8 days in their VIP intravitreal injection study.

Sprouty RTK Signaling Antagonist 4 (*SPRY4*)

Another interesting gene is sprouty RTK signalling antagonist 4 (*SPRY4*), which was identified in Model 1 & Model 2. The SPRY4 gene product is a fibroblast growth factor receptor (FGFR) inhibitor and thus regulates the FGF signalling pathway. *FGF* is considered as a candidate myopia susceptibility gene since it can modulate a wide variety of downstream effects, including activation of extracellular matrix-associated genes (377). In a human study, the fibroblast growth factor 10 (*FGF10*) gene was found to be associated with high myopia in both a Chinese (377) and a Japanese cohort(378). In this study, it was found that *SPRY4* gene expression was down-regulated in FD eyes, suggesting reduced inhibition of FGF receptors and therefore enhanced activation of the FGF pathway in the retina.

5.4.2 Retinal gene expression differences between the High and Low myopia susceptibility groups

5.4.2.1 Comparison between Model 1 and Model 3

In Model 1, 21 transcripts were identified as differentially expressed between the high vs. low myopia group chicks; in Model 3, 495 transcripts were identified. None of the identified transcripts overlapped between Model 1 and 3. Therefore, in total, Model 1 and Model 3 discovered 516 potential transcripts that were differentially-expressed between the High and Low myopia groups.

In Model 1, the 'treatment effect' considered both eyes from the same chick as independent samples, and thus, the within-chick variation was not fully accounted for. This would be expected to lead to a reduction in statistical power.

In Model 3, the paired design optimally modelled the variation due to FD; however, due to the limitation of the design caused by the low sample size, it was not possible to directly compare the myopia susceptibility group difference whilst accounting for the paired design. Therefore, an alternative method of including an interaction term corresponding to treatment x myopia group was used. In this model, genes that promoted relatively rapid myopia development in response to FD could be identified.

As mentioned above, a total of 516 transcripts were detected using the High vs. Low myopia group analyses, while a total of 538 transcripts were identified using the FD vs. control eye tests. Comparing these two analyses, there were 44 transcripts in common (Appendix 5.4). This result suggests that these 44 gene products are not only differentially-expressed in response to the FD environment, but also play an active role in the myopia development process, making them especially interesting candidates for further study.

5.4.2.2 Comparison between Model 2 and Model 3

Among the 495 transcripts showing evidence of an interaction effect between treatment (FD vs. control) and group (High vs. Low) using model 3, there were 422 transcripts (448 genes) that were also found in the "model 2 separate" analysis. A detailed comparison of the treatment x group interaction genes identified by these 2 competing methods is presented in Appendix 5.5. The evidence was most consistent for a set of 7 transcripts which consisted of 6 genes (*ANKRD10, OPN4, VIP, AQP9, TUBA1C, and SNCB*).

Separate analysis in model 2 allowed an examination of whether the same genes were differentially expressed in the high and low group chicks. However, using the "model 2 separate" analysis, the sample size in each group dropped by half. Furthermore, the contrast between the high and low group sample in the "model 2 separate" analysis did not consider the expression level of the transcripts, thus it was not a fully quantitative comparison. Model 3 created a matrix for multiple factors, which has been suggested previously for edgeR analyses (365, 379). Although model 3 was testing for treatment x group interactions, the model matrix considered the expression level of every transcript when performing contrasts between conditions. The "model 2 separate" analysis would not be expected to be as powerful as model 3.

5.4.2.3 Comparison with previous findings

When comparing the 516 transcripts found in the High vs. Low myopia group analyses to previously reported candidate myopia genes, there was an overlap of 140 genes (Appendix 5.6). However, none of the studies made a comparison between rapid and slow myopia development samples.

5.4.2.4 Noteworthy genes

Phosphoinositide-3-Kinase Regulatory Subunit 5 (*PIK3R5*)

Phosphoinositide-3-Kinase Regulatory Subunit 5 (*PIK3R5*) is a regulatory subunit of the class I phosphoinositide 3-kinases (*PI3Ks*) gamma complex (Table 5.5). PI3K gamma is a dimeric enzyme, which contains a 110 kD catalytic gamma subunit (such as PIK3CG) and a regulatory subunit of either 55, 87 or 101 kD (such as PIK3R5). During PI3K activation, PIK3R5 recruits PIK3CG from the cytosol to the plasma membrane. Previous studies have also provided evidence of co-localization and phenotypic enhancement effects between PIK3R5 and PIK3CG (379, 380), indicating a strong interaction effect between these two genes.

In the GWAS results, *PIK3CG* was identified as a myopia susceptibly gene; meanwhile, in this transcriptomics study, an up-regulation of *PIK3R5* gene expression in High myopia-susceptibility group chick retinas was observed (Model 1). The converging evidence from these two lines of experimental work argues that PI3K plays a crucial role in myopia development.

***Table 5.5. The PI3K family** (Reproduced from (381)).*

Group		Gene	Protein
class 1	catalytic	*PIK3CA*	PI3K, catalytic, alpha polypeptide
		PIK3CB	PI3K, catalytic, beta polypeptide
		PIK3CG	PI3K, catalytic, gamma polypeptide
		PIK3CD	PI3K, catalytic, delta polypeptide
class 1	regulatory	*PIK3R1*	PI3K, regulatory subunit 1 (alpha)
		PIK3R2	PI3K, regulatory subunit 2 (beta)
		PIK3R3	PI3K, regulatory subunit 3 (gamma)
		PIK3R5	PI3K, regulatory subunit 5
		PIK3R6	PI3K, regulatory subunit 6
class 2	catalytic	*PIK3C2A*	PI3K, class 2, alpha polypeptide
		PIK3C2B	PI3K, class 2, beta polypeptide
		PIK3C2G	PI3K, class 2, gamma polypeptide
class 3	catalytic	*PIK3C3*	PI3K, class 3
	regulatory	*PIK3R4*	PI3K, regulatory subunit 4

GCG, IGFBP4 and INSIG1

Glucagon – Glucagon has been implicated in eye growth and myopia development in several studies (310, 375, 382-387). In the studies conducted by Vessey et al. (385) and Zhu and Wallman (387), myopia development was attenuated by intravitreal injection of glucagon peptide; in Ashby et al.'s study (382), the pre-proglucagon (PPG) transcript level was down-regulated in minus lens-treated and FD-treated chick eyes. In chicks, glucagon-synthesizing amacrine cells have been demonstrated to play an important role in ocular growth regulation (384). However, there is no glucagon-containing amacrine cell type in the human retina, and therefore the relevance of these findings to human myopia is uncertain. Consistent with previous findings, in my study, the expression of glucagon was similarly down-regulated in the FD-treated eyes, especially in the High myopia susceptibility group animals.

IGFBP4 – *IGFBP4* encodes Insulin-like growth factor binding protein 4, which binds insulin-like growth factors (IGFs) I and II. Previous studies in Caucasian, Chinese, Polish and Egyptian individuals found that IGF I polymorphisms were associated with extreme high myopia, and that blood serum IGF I levels were increased in patients with high myopia (388-391). IGFBP4 has been reported to decrease the binding of IGF I to its receptor, thus inhibiting its activity (392, 393). In this study, the down-regulation of *IGGBP4* gene expression in the treated eyes of chicks from the high group suggests increased activity of IGF I in eyes developing myopia.

INSIG1—Insulin-induced gene 1 encodes a protein that regulates lipogenesis and the metabolism of cholesterol and glucose. Although the regulatory mechanism between INSIG1 and insulin is still unclear, studies have demonstrated that *INSIG1* expression could be up-regulated by hypoglycemia (394). This study revealed that the expression of *INSIG1* was decreased in chicks from the High group (perhaps as a consequence of decreased glucagon levels). This could potentially have increased insulin levels locally within the eye, which is known to stimulate myopia development (387, 395). The *GCG*, *IGFBP4* and *INSIG1* genes are all involved in regulating the insulin-signalling axis. Coincident with previous findings, results from this study strongly suggest that the insulin pathway plays a role in myopia development.

COL8A1

COL8A1 encodes one of the two alpha chains of type VIII collagen, a component of the extracellular matrix. COL8A1 is a short chain collagen, which is found in the sclera and is the major component of the basement membrane of the corneal endothelium. Previous studies have indicated that *COL8A1* polymorphisms are associated with myopia development, corneal thickness, glaucoma, AMD and choroidal neovascularization in high myopia (396-398). In this study, the expression of *COL8A1* was up-regulated in the High myopia group FD-treated eyes. Any role for type VIII collagen in the retina was unanticipated, and its relationship to myopia development is not clear.

DCT

Dopachrome tautomerase (*DCT*), which takes part in melanin synthesis, was previously reported to be associated with congenital microcoria, myopia, juvenile open-angle glaucoma (399) and eye colour (400). One prior study identified a down-regulation of *DCT* gene expression in myopic chick retina (314); in another meta-analysis of transcriptome datasets, differentially expressed genes during hyperopia induction were analysed, and *DCT* was found to be down-regulated in the retina during the early stage of hyperopia development (401). However, in this study, DCT was found up-regulated in chicks with high myopia susceptibility.

PMEL

The protein encoded by the *PMEL* gene is a melanocyte-specific type I transmembrane glycoprotein, which is enriched in melanosomes. PMEL exists primarily in pigment cells of the skin and eye. There is no direct evidence linking PMEL with myopia development, however, several studies suggest that melatonin is associated with myopia (402). According to the results from my study, PMEL might influence the melatonin system to result in myopia development.

AQP9

Aquaporins 9 is one member of the water channel family that regulates water transportation across the cell membrane. AQP9 was identified in rat and chick retina (403, 404) and is known to be to be involved in energy metabolism (405) and ganglion cell survival (406). Only one previous study reported that AQP9 was up-regulated in the treated eye of form deprived chicks (404); the opposite was found in my study, i.e. AQP9 gene expression was lower in treated eyes. AQP4 is also implicated in myopia development in chicks (407). More research is needed to understand the role of water transport in the retina during myopia development.

5.4.3 Transcript analysis

During the gene expression process in eukaryotes, the transcribed pre-mRNA may undergo alternative splicing to yield different mature mRNAs isoforms. These isoforms give rise to different *transcripts* when RNAseq reads are mapped back to the genome. In this study, there were instances when more than one transcript from the same gene was differentially expressed. For example, 3 different *PIK3R5* transcripts were differentially expressed in response to FD (Table 5.3) and 2 different *GCG* transcripts (encoding glucagon) showed a treatment x group interaction (Table 5.4). Since alternative splicing varies in different conditions and tissues, and can potentially produce proteins with dissimilar functions (408, 409), it would be of interest to examine the alternatively spliced genes found to be differentially expressed in future work, to find out if the isoforms have different functional consequences. Here, the discovery of differential expression for multiple isoforms of the same gene provides greater confidence that the differential expression is not a false positive finding. The ability to accurately identify and quantify levels of specific mRNA transcripts is an advantage of RNAseq over microarrays.

5.4.4 Comparison of analytical software packages

Three R packages were used to analyse the RNA-Seq data: edgeR, DESeq2, and Limma. Due to the relatively low number of replicate tissue samples, distribution-free rank or permutation-based analysis methods were ruled out. Instead, for small sample sizes - and especially for RNA-seq data - negative binomial (NB) analysis models (as used by edgeR and DESeq2) have become popular and well-established. When estimating the dispersion with these packages, information is ‘shared across all genes’ to obtain more accurate estimates. The main differences between edgeR and

DESeq2 rely on the way how they share the information, in other words, how they estimate the dispersion. For edgeR, it is assumed that all genes have the same dispersion parameter and therefore a common dispersion estimation is carried out for all genes. Subsequently, a gene-wise dispersion estimation is 'squeezed' towards the common one. In contrast, DESeq finds the maximum gene-wise dispersion estimate, and then calculates a dispersion – mean trend. In general, DESeq2 is less powerful, whereas edgeR is more sensitive to outliers (369, 410).

Limma was originally designed for microarray data, however, it can be used for RNA sequencing data analysis if the 'voom' step is used. Differently from edgeR and DESeq2, limma's analytical model is based on the normal distribution. One study (370) made comparisons among these 3 analysis packages under different simulation situations and suggested no single method was optimal under all circumstances. Thus the choice of methods for transcriptome analysis depends on the experimental conditions (see table 5.6).

***Table 5.6.Comparison of edgeR, DESeq2 and limma.** (Modified from(370))*

Method	Features
DESeq2	- Conservative with default settings. Becomes more conservative when outliers are introduced. - Generally low true positive rate. - Poor FDR control with 2 samples/condition, good FDR control for larger sample sizes, also with outliers. - Medium computational time requirement, increases slightly with sample size.
edgeR	- Slightly liberal for small sample sizes with default settings. Becomes more liberal when outliers are introduced. - Generally high true positive rate. - Poor FDR control in many cases, worse with outliers. - Medium computational time requirement, largely independent of sample size.
limma	- Good type I error control, becomes more conservative when outliers are introduced. - Low power for small sample sizes. Medium true positive rate for larger sample sizes. - Good FDR control. Largely unaffected by introduction of outliers. - Computationally fast.

5.5 Conclusion

In this transcriptomics study, a total 538 transcripts were identified from model 1 and model 2 as differentially expressed between FD-treated eyes vs. control eyes, and 516 transcripts were identified as differentially expressed between FD-treated eyes in the High vs. Low myopia groups from model 1 and model 3. There were 44 transcripts that were identified in both sets of analyses. Components of the PI3K pathway and the insulin signalling pathway were the strongest candidates for a role in determining susceptibility to myopia development. In the future, these results need to be validated in an independent sample of chicks (ideally using an independent method such as reverse transcription-PCR).

Chapter 6 Pathway analysis

6.1 Introduction

GWAS and RNA-seq experiments have the potential to identify genetic loci associated with a phenotype, and genes differentially expressed across different phenotypes, respectively. Since the ultimate goal for these types of analysis is to better understand the aetiology or mechanism of a disease (in order to develop effective strategies to treat the condition) adding functional annotations to these results is highly desirable. Gene set or pathway analysis provides such a solution. (For simplicity, the term 'pathway analysis' is used to cover both types of analysis in the remainder of this chapter. However, technically, they are distinct approaches). Based on already known taxonomy data from public repositories such as the Gene Ontology (GO) or Kyoto Encyclopedia of Genes and Genomes (KEGG) databases, genes of interest can be assigned to different meaningful categories. Next, a group of related genes can be tested to assess whether they are significantly associated with a phenotype (411). This approach is known as *knowledge base-driven* pathway analysis (412).

Pathway analyses can be applied to both GWAS and RNA-seq data. In fact, pathway analysis for GWAS was motivated by approaches for gene expression microarray analysis. The statistical hypothesis or principal foundation in pathway analysis is that, if a given disease or phenotype is characterized by a specific biological process, the underlying (co-functioning) genes should be preferentially selected in an omics study (413). There are two main categories of pathway analysis, depending on the algorithm used: firstly, 'self-contained analysis', and secondly 'competitive analysis'. In the self-contained testing approach, only genes in the gene set are considered, and the null hypothesis is that none of these genes is associated with the phenotype. By contrast, in the competitive approach, all genes in the database are considered, and tests are used to assess whether the genes in each gene set are more strongly associated with the phenotype than the other genes. Both GWAS and RNA-seq pathway analyses can employ either approach, the main difference being that, for GWAS data, pathway analysis starts from the level of SNPs while for RNA-seq data, it starts from the level of genes (414).

6.1.1 Pathway analyses for GWAS results

As discussed below, GWAS experiments have three inherent problems that pathway analysis can help to overcome. The first of these is inaccurate mapping. Among SNPs identified by a GWAS, only a small proportion are typically located in the coding regions of genes; in fact, more than 80% of disease-associated SNPs in the NCBI GWAS catalogue are non-coding (415). Secondly, due to LD, the lead GWAS SNP in a region cannot be directly affirmed as the true causal variant. The third limitation of GWA studies is that they are usually underpowered (i.e. the sample size is too small), which means that they are unable to detect SNPs with small effects. Pathway analysis is able to address each of these problems to a certain extent. When mapping SNPs to genes, most pathway analysis tools take up- and down-stream SNPs into consideration, which accounts for sampling variation-induced inconsistency in whether the causal SNP in a region is detected as the lead SNP (416). This also takes account that regulatory variants can be situated several kb away from their target genes (417). Meanwhile, pathway analysis also reduces the multiple testing burden by aggregating SNPs into genes and gene sets. More importantly, by incorporating prior biological evidence, functional variants may be prioritized over less functional variants even if they have similar effect sizes. Thus, the efficiency of revealing new disease-related candidates will be increased (418, 419). For example, in a GWAS comprising 401 patients with Crohn's disease and 433 controls, *IL23R* was identified as a disease-associated gene (420). However, not until a meta-analysis of 3,230 cases and 4,829 controls was carried out did a SNP in another gene (*IL12B*) in the *IL23R* pathway reach the genome-wide significance threshold (421). This example demonstrates that genes in the same functional pathway may interplay with each other and conspire to the mechanism of a disease, but GWAS may not be able to detect every single involved gene owing to limited power. Therefore, pathway analysis may be able to highlight potential candidates that would otherwise go undetected.

6.1.1.1 Features of post-GWAS pathway analysis

Based on the data input format, there are two main approaches to post-GWAS pathway analysis. The first is the 'P-value enrichment approach', which only requires SNP rs ID and P-value data from GWAS summary statistics as input. This approach is easy to use, however it does not consider gene size, which may cause bias. The second approach is the 'raw genotype approach'. This option takes account of LD and gene size in the analysis process, however, its requirement of raw genotype data is restrictive for collaborative GWAS meta-analysis projects, which typically do not permit raw data to be shared (411). Recently, methods have been developed to overcome the requirement for raw genotype data by incorporating LD information from an ancestry-matched reference sample (422).

6.1.1.2 Software

There are many software packages for performing GWAS-based pathway analysis, such as FORGE, JAG, INRICH and MAGMA. In one study comparing the performance of several pathway analysis tools, MAGMA and INRICH showed low type-1 error rates when gene size, density of SNPs and LD between SNPs were considered as confounding factors, and the power of these two tools was similar (414). However, the results from INRICH were strongly dependent on the P-value cut-off threshold chosen, and computation time was longer than MAGMA, on average (423). For this study, therefore MAGMA was chosen for carrying out a post-GWAS pathway analysis.

6.1.2 Pathway analysis for RNA-seq results

Without the requirement of a step to map SNPs to genes, pathway analysis for RNA-seq data is simpler than pathway analysis for post-GWAS results. There are two main methods of pathway analysis for RNA-seq data: over-representation analysis (ORA) approaches and functional class scoring (FCS) approaches.

6.1.2.1 Over-Representation Analysis (ORA)

In ORA approaches, genes are selected to form an input list according to a set of pre-specified criteria, e.g. FDR < 0.05. Then, each pathway (GO annotation, KEGG pathway etc.) is tested to assess whether genes in this pathway are over-represented (enriched) in the predefined gene list. Several tools including DAVID (413), PANTHER (424) and GOEAST (425) implement this method. Among these tools, DAVID is one of the most popular, because it is easy to use, and it has powerful data-mining (functional clustering and functional annotation) capabilities.

All ORA tools extract biological meaning from a given gene list, using annotations applied from different biological perspectives, and report those most likely as output. However, there are some limitations to the ORA approach. First, genes are treated equally and independently in ORA; the degree of association between gene and phenotype is ignored, as is the inter-relationship amongst genes. Second, ORA methods ignore genes that do not reach an arbitrarily-set significance threshold. Third, ORA methods ignore the relationship between different pathways (412).

6.1.2.2 Functional Class Scoring (FCS)

Unlike ORA, the FCS approach takes all genes into consideration. Instead of applying an arbitrary threshold to select genes, they are ranked according to their relationship with the phenotype. The gene-level statistics in the pathway are then summarized into pathway-level statistics, and the statistical significance of that pathway is assessed. Among the tools that apply the FCS approach, Gene Set Enrichment Analysis (GSEA) (426, 427) is one of the most widely used (428-430).

FCS methods include more genes, weight each gene's expression level, and consider the dependence among genes. However, even the FCS approach still neglects the coordination between different pathways. Because of their different strengths and weaknesses, performing both ORA and FCS pathway analysis may increase the power to attribute biological meaning to GWAS and RNA-seq data.

6.2 Methods

6.2.1 Pathway analysis for GWAS

MAGMA was used to perform pathway analysis for GWAS results. The MAGMA workflow was as follows:

i Annotation: Annotation is a step that maps SNPs to the genome and identifies if they fall within genes. SNP information was downloaded from the UCSC Genome Browser. Ensemble Gallus_gallus-4.0 version was selected because the genotyping chip used in my experiments used Gallus_gallus-4.0 as reference. A 5 kb window was applied, i.e. SNPs within a 5kb buffer 5' or 3' to genes were mapped to that gene. Note that certain SNPs mapped to more than 1 gene.

ii Gene analysis: In gene analysis, SNPs are aggregated to the gene level using GWAS summary statistics, and the association between joint markers in the gene and the phenotype is tested. The previous GWAS results in this study (Chapter 4, section 4.3.2, Model 2) were used in this step. Note that the P-values in this GWAS were genomic control-corrected to account for relatedness between samples. To generate P-values for each gene, MAGMA calculates the mean of the χ^2 statistic for all SNPs within each gene. (Note that there were too few unrelated chicks in my GWAS sample to enable the LD between markers to be estimated. Hence, MAGMA was unable to take account of LD when carrying out its gene-based tests).

iii Gene set analysis: In this step, individual genes are grouped into gene sets for further association testing. Based on results from the gene-based analysis (step ii), genes and their corresponding P-values were aggregated according to gene set references. The Molecular Signatures Database (MSigDB) was used as a reference for classifying genes into gene sets (426). A 'competitive' was chosen to perform the gene set analysis.

6.2.2 Pathway analysis for RNA-seq results

In order to maximize the biological information extracted from my previous –omics analyses, both DAVID and GSEA were applied.

6.2.2.1 DAVID

As an ORA approach, DAVID required a gene list as input. In Chapter 5, three analysis packages and two models were used to identify differentially expressed genes between high vs. low myopia-susceptibility chicks (Chapter 5, section 5.3.4.2 and 5.3.6). Since each model and each package has its own advantages and disadvantages, genes identified by any of the three packages in any of the two models were included in the gene list. The workflow was as follows:

- i DEG list submission. The list of differentially-expressed genes was entered; the gene identifier was set as 'Gene symbol' format; species was set as Gallus_gallus; gene background was set as Gallus_gallus;
- ii Select functional annotation categories; GO term, KEGG pathway;
- iii Run Functional annotation chart;
- iv The threshold to select gene sets was: gene sets contain at least 2 genes, the expression analysis systematic explorer (EASE) score < 0.05.

The corresponding Z-score for the DAVID results was generated with the R package '*GOplot*' (431).

6.2.2.2 GSEA

Before running GSEA, gene expression library from RNA-seq was normalized by DESeq2. A phenotype list for the sample was created according to the GSEA manual.

- i The normalized gene expression data and phenotype list were loaded;
- ii Select gene set databases: GO term, KEGG pathway;
- iii Select permutation type: 'gene_set' was selected as the permutation type, with 1000 permutations;
- iv Select gene sets criteria: gene sets with >500 genes or <2 genes were excluded;
- v Run analysis;
- vi Threshold of suggestive significance: FDR < 25%.

6.2.3 Other software packages

'*ClusterProfiler*' (432) was used to create dot plots. '*GOplot*' (431) was used to create circle plots and bubble plots. '*Enrichment Map*' (433) from the Cytoscape package was used to generate the enrichment map, similarity cut off was set as 0.5 (default setting), which will create a connection line if two gene sets have a similarity over 50%.

6.3. Results

6.3.1 MAGMA analysis

6.3.1.1 Annotation

From the GWAS result, summary statistics (Chapter 4, section 4.3.1), 304,936 SNPs were available for annotation. There were 16,844 genes in the Gallus_gallus-4.0 Ensemble annotation file. Amongst the SNPs, 168,244 SNPs (55%) mapped to at least one gene. Amongst all the reference genes, at least one SNP mapped to 14,072 (84%) of the genes.

6.3.1.2 Gene-based analysis

Among the mapped genes, 628 genes (4.4%) had a P-value less than 0.05. None of the genes reached the significance threshold after Bonferroni correction (Appendix 6.1). The top gene was PIK3CG (P = 2.67e-05); 11 SNPs had been mapped to this gene. The top 10 most strongly-associated genes are shown in Table 6.1.

Table 6.1Top 10 genes from MAGMA gene-based analysis.

Gene	CHR	Start BP	Stop BP	Number of SNPs	Z	P
PIK3CG	1	14208410	14246547	11	4.04	2.67e-05
ENSGALT00000006673.4	7	5730049	5902491	15	3.94	4.15e-05
ENSGALT00000039781.2	7	5867755	5878724	3	3.72	9.84e-05
ENSGALT00000021678.3	13	14376043	14389235	5	3.53	2.04e-04
USP40	7	5896675	5938176	15	3.48	2.50e-04
GPR22	1	14513792	14525725	1	3.35	4.03e-04
DOCK9	1	143955154	144047261	15	3.34	4.17e-04
SPSB4	9	6118832	6129579	5	3.28	5.19e-04
OGN	12	3419002	3443509	4	3.13	8.65e-04
PXYLP1	9	6322526	6382838	29	3.12	8.94e-04

CHR –Chromosome number, BP – Base pair, Z – Z score.

6.3.1.3 Gene set analysis

In total, 17,453 gene set definitions from MSigDB were selected as the reference (note that set C1 was removed, since C1 is categorized by human chromosome position, while the gene position in chicks differs from that in humans). However, only 17,439 gene sets (containing 10194 unique genes) were available for use in the analysis because 14 gene sets could not be mapped to any gene. Then, 10,000 permutations for multiple testing corrections were performed and a corrected P-value was given (the significance threshold for permutation was P <1.22e-05).

Among the gene sets, 969 (5.5%) had uncorrected P-values less than 0.05, but none reached the corrected significance threshold of 1.22e-05. The MSigDB classification of the 969 gene sets is shown in Figure 6.1a. Some gene set categories had a higher proportion of sets with p <0.05; specifically, 4.0% of the Hallmark gene sets, 4.9% of the curated gene sets, 3.8% of the motif gene sets, 4.0% of the computational gene sets, 5.3% of the GO gene sets, 8.5% of the oncogenic signatures and 7.1% of the immunologic signatures had P <0.05 (Figure 6.1b).

Including too many irrelevant annotation terms would have increased the type I error rate in the above analysis. For example, the top gene set was 'effector vs. memory CD8 T-cell down' (P = 6.15e-05) from the Immunologic Signatures (C7) category; a set of genes down-regulated in effector CD8 vs. memory CD8 T cells. From past research, there was minimal evidence to suggest a role for the genes in this set in myopia development. Therefore, to focus annotation to pathways and functions that may be more relevant, the KEGG and GO gene sets were analyzed independently.

In gene set analysis using KEGG definitions, 186 gene sets (containing 3,000 unique genes) were used. Permutation tests suggested an empirical multiple testing significance threshold of P <2.92e-04. None of the gene sets had a corrected P-value below the significance threshold. The top 5 gene sets are shown in Table 6.2.

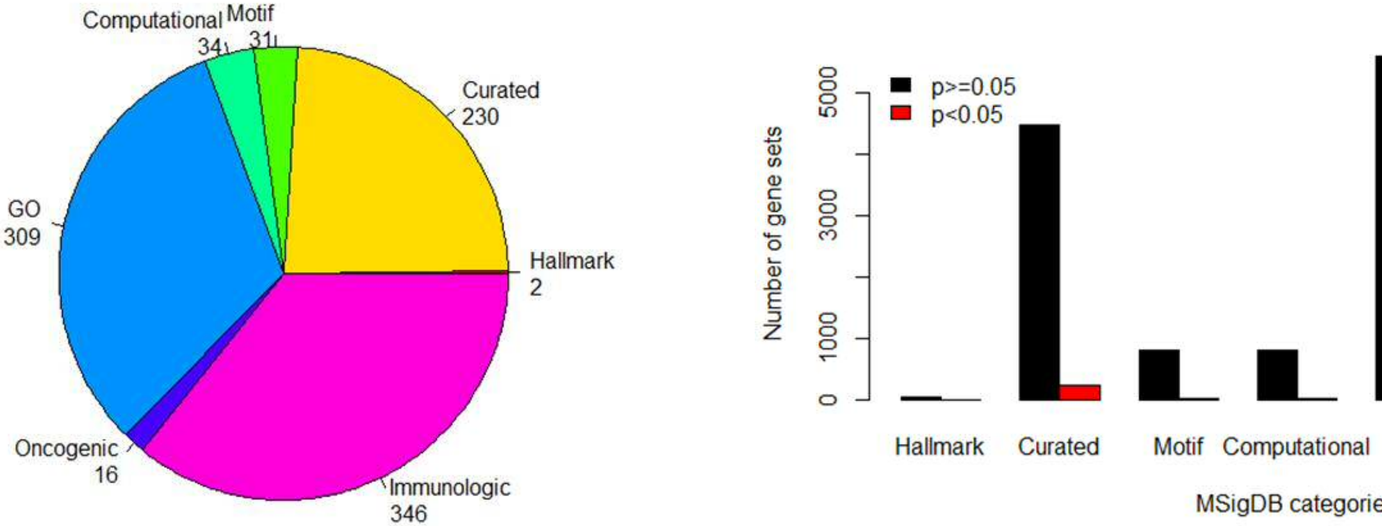

(a)

Figure 6.1.Pathway analysis using MSigDB (except C1) as reference.

(a) Pie chart of 969 gene sets with P <0.05 when using MSigDB (except C1) as reference; (b) Comparison of n sets with p <0.05 (red) and P >= 0.05 (black).

Table 6.2.Top 5 KEGG pathways from pathway analysis using MAGMA

Gene Set (KEGG)	Number of genes	Beta	SE	P	P (Corrected)
Homologous Recombination	22	0.36	0.17	0.02	0.90
Sulfur Metabolism	6	0.50	0.26	0.02	0.97
Circadian Rhythm Mammal	8	0.43	0.22	0.03	0.98
Dorso Ventral Axis Formation	16	0.33	0.18	0.03	0.99
Glycosaminoglycan Degradation	13	0.32	0.18	0.04	1.00

In the GO term analysis, 5,911 gene sets were used for analysis (9,401 unique genes). The empirical significant threshold was p <9.50e-06. Among the 5,911 gene sets, 4,436 of them were derived from the GO Biological Process Ontology, 897 were from the GO Molecular Function Ontology and 578 were from the GO Cellular Component Ontology. None of the gene sets attained the significance threshold after correction for multiple testing. For each GO category, the top three gene sets are shown in Table 6.3.

Table 6.3. Top three gene sets of each GO category from pathway analysis using MAGMA.

	Gene set (GO)	Number of genes	Beta	SE	P	p (Corrected)
BP	Regulation Of Mitotic Cell Cycle	313	0.14	0.04	1.19e-04	0.33
BP	Regulation Of Cell Cycle Process	365	0.13	0.04	2.70e-04	0.59
BP	Bone Development	109	0.22	0.07	4.69e-04	0.76
MF	Sequence Specific DNA Binding	521	0.10	0.03	3.79e-04	0.26
MF	Nucleic Acid Binding Transcription Factor Activity	540	0.09	0.03	1.48e-03	0.67
MF	Double Stranded DNA Binding	386	0.10	0.03	2.29e-03	0.82
CC	Heterochromatin	41	0.31	0.10	1.29e-03	0.47
CC	Cytoplasmic Exosome RNase Complex	12	0.54	0.19	1.92e-03	0.60
CC	Multivesicular Body	17	0.51	0.18	1.94e-03	0.60

BP – Biological Process; MF – Molecular Function; CC – Cellular Component

6.3.2 Results for RNA-Seq data

6.3.2.1 KEGG analysis using DAVID

The 516 transcripts that were differentially expressed between high and low myopia-susceptibility chicks (Chapter 5, section 5.3.4.2 and 5.3.6) yielded 467 genes. Pathway enrichment for 467 genes was analyzed using DAVID. In the 'over-representation' analysis, 178 differentially expressed genes were mapped to the 74 KEGG pathways. 12 pathways had an EASE score (a modified Fisher's exact test P-value from the Expression Analysis Systematic Explorer software program) less than

0.05. However, only 1 pathway – 'Ribosome' – surpassed the Bonferroni correction threshold (P = 8.93e-05). The 'Ribosome' pathway had 3.94 fold of enrichment, and the 19 genes that mapped to this pathway were all down-regulated (Z-score = -4.36). Among the other pathways, 'Oxidative Phosphorylation' and 'Glycolysis/Gluconeogenesis' had relatively low EASE scores. Nine of the 12 top-ranked pathways had a minus Z-score, suggesting the genes in these pathways were generally down-regulated. Details of all the 12 pathways are listed in Table 6.4 and Figure 6.2.

Table 6.4.KEGG pathways with P < 0.05 in DAVID analysis.

KEGG ID	Gene set	Number of genes	EASE (P value)	Fold of Enrichment	Bonf Corr
gga03010	Ribosome	19	8.76e-07	3.94	8.93
gga04530	Tight Junction	14	1.21e-03	2.81	0.12
gga01130	Biosynthesis Of Antibiotics	17	2.66e-03	2.28	0.24
gga00010	Glycolysis / Gluconeogenesis	8	4.15e-03	3.84	0.35
gga00190	Oxidative Phosphorylation	12	6.58e-03	2.55	0.49
gga01200	Carbon Metabolism	10	0.02	2.55	0.79
gga03013	RNA Transport	12	0.02	2.24	0.82
gga04810	Regulation Of Actin Cytoskeleton	14	0.03	1.93	0.94
gga04145	Phagosome	11	0.03	2.15	0.95
gga01230	Biosynthesis Of Amino Acids	7	0.03	2.90	0.96
gga04260	Cardiac Muscle Contraction	7	0.03	2.85	0.97
gga04510	Focal Adhesion	14	0.04	1.86	0.97

Gene Ratio – the number of genes mapped to the particular pathway vs. number of genes mapped to the reference, Z-s
regulated gene -log fold of change for the down-regulated gene)/(total number of genes in the pathway)

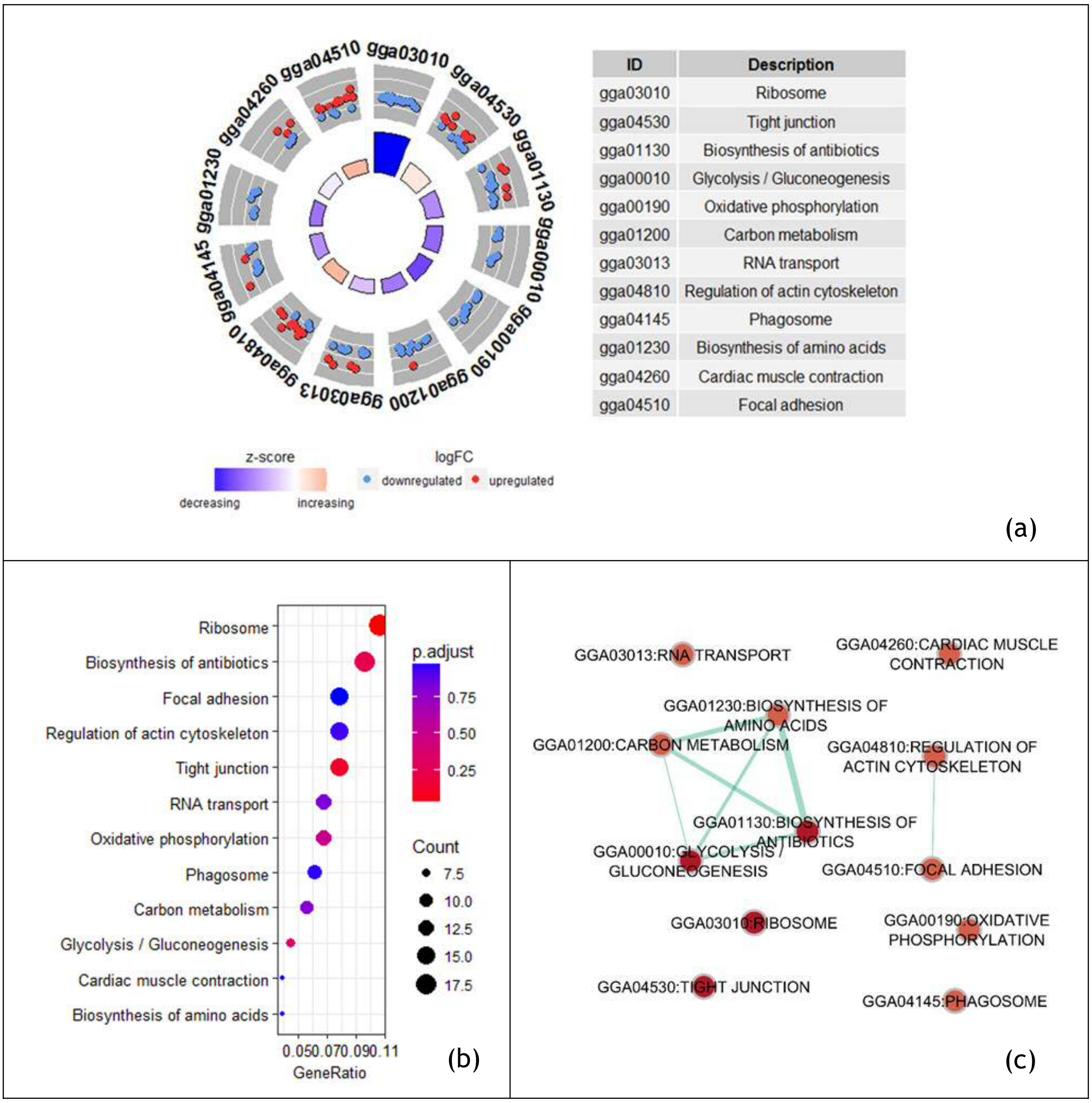

Figure 6.2. KEGG pathways with P < 0.05 in DAVID analysis.

(a) Circle plot of KEGG pathway from the DAVID pathway analysis. The outer circle shows a scatter plot for each term of the logFC (log fold change) of the assigned genes. Red circles denote up-regulation and blue down-regulation. The colours of the inner circle represent Z-scores. (b) Dot plot of DAVID results. The x-axis shows gene ratio of each pathway, dot size shows the number of genes in that pathway, and colour represents the P-value for the pathway (c) Enrichment map of the KEGG pathways most strongly ranked in the DAVID analysis. Red circles represent gene sets that were up-regulated. Connecting lines represent more than 50% of genes overlapped between the two gene sets, with the thickness of the line representing the overlap strength.

6.3.2.2 GO term analysis using DAVID

Altogether, 709 GO terms were linked to at least 2 of the differentially expressed genes, and 72 GO terms had EASE scores that were less than 0.05 (Appendix 6.2). A total of 10 GO terms had EASE P-values below 0.05 after Bonferroni correction. Among the 72 gene sets, 30 were annotated by 'biological processes' terms, 26 were annotated by 'cellular component' terms (7 of which exceeded the corrected significance threshold), and 16 were annotated by 'molecular function' terms (3 of which exceeded the corrected significance threshold) (Figure 6.3a). 42 genes were not able to be mapped to any of the GO terms.

Amongst the 72 gene sets, GO categories 'cytoplasm' (GO:0005737) and 'nucleus' (GO:0005634) had less than a 1.5 fold enrichment, while 'pre-miRNA binding' (GO:0070883) had the greatest enrichment (24.1-fold). The gene ratio ranged from 0.01 to 0.29. GO categories 'dense body' (GO:0097433) and 'mitochondrial respiratory chain complex IV' (GO:0005751) had the smallest gene ratio, while 'extracellular exosome' (GO:0070062) had the largest gene ratio. There were 27 GO terms for genes primarily down-regulated in chicks with a high susceptibility to myopia, and 45 GO terms for genes primarily up-regulated. Z-scores of these terms ranged from -4.24 ('structural constituent of ribosome'; GO:0003735) to 4.24 ('transcription, DNA-templated'; GO:0006351) (Figure 6.3). The interconnection of all 73 GO terms is presented in Figure 6.4. The 10 top-ranked GO terms ($P < 0.05$ after Bonferroni correction) are shown in Table 6.5 and Figure 6.5.

Among the differentially-expressed genes that were used for pathway analysis, the 20 genes that had the largest log fold change and the 20 genes with the smallest log fold change were identified and mapped to the 72 significant GO annotation terms. Only 22 of the selected genes had GO term annotations available; the interconnections between these 22 differentially-expressed genes and their related GO terms are shown in Figure 6.6.

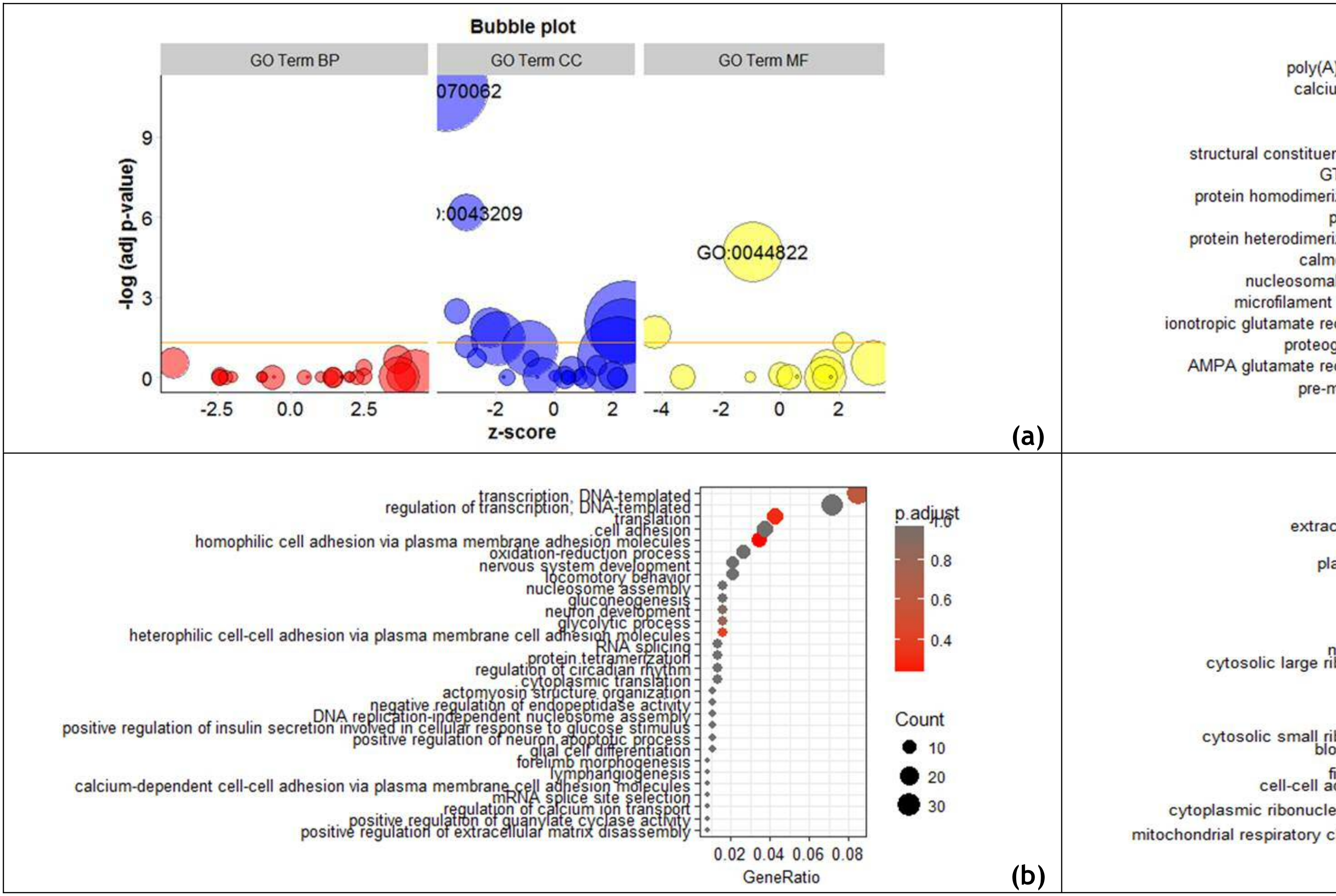

Figure 6.3 GO term with P < 0.05 (Before Bonferroni correction) in DAVID analysis.

(a) Bubble plot of 73 GO terms from the DAVID analysis of DEGs. Red bubbles represent GO terms in the ‘bio represent ‘cellular component’, and yellow represent ‘molecular function’. (b) Corresponding dot plot of th component’, and (d) ‘molecular function’ category.

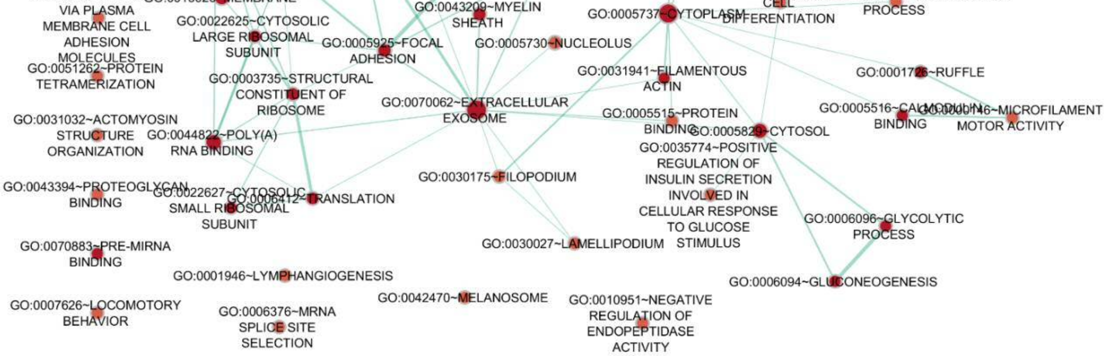

Figure 6.4. Enrichment map of the GO terms with P < 0.05 (Before Bonferroni correction) in DAVID analysis from DAVID results.
Red circles represent gene sets that were up-regulated. Connecting lines represent more than 50% of genes overlap between the two gene sets, the thickness of the line representing the overlap strength.

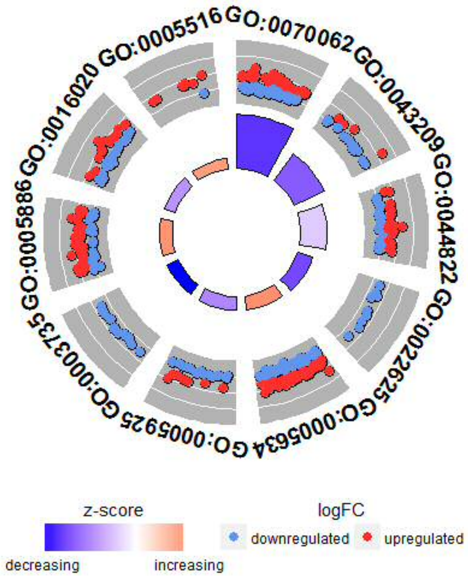

ID	Description
GO:0070062	extracellular exosome
GO:0043209	myelin sheath
GO:0044822	poly(A) RNA binding
GO:0022625	cytosolic large ribosomal subunit
GO:0005634	nucleus
GO:0005925	focal adhesion
GO:0003735	structural constituent of ribosome
GO:0005886	plasma membrane
GO:0016020	membrane
GO:0005516	calmodulin binding

Figure 6.5. Circle plot of GO terms with P < 0.05 (after Bonferroni correction) from the DAVID analysis of differentially-expressed genes.

Table 6.5.GO terms with P <0.05 (after Bonferroni correction) in DAVID analysis of differentially-expressed genes.

GO ID	Gene Set	Number of genes	EASE (P-value)	Fold of Enrichment	Bonferroni correction	Gene Ratio	Z-score
GO:0070062	**Extracellular Exosome**	113	4.60e-14	2.02	1.65E-11	113/389	-3.67
GO:0043209	**Myelin Sheath**	22	1.91e-09	4.99	6.86E-07	22/389	-2.98
GO:0044822	**Poly(A) RNA Binding**	55	4.31e-08	2.19	1.95E-05	55/354	-0.94
GO:0022625	**Cytosolic Large Ribosomal Subunit**	11	9.38e-06	6.05	3.36E-03	11/389	-3.32
GO:0005634	**Nucleus**	107	2.53e-05	1.45	9.06E-03	107/389	2.42
GO:0005925	**Focal Adhesion**	25	3.72e-05	2.58	0.01	25/389	-2.20
GO:0003735	**Structural Constituent Of Ribosome**	18	4.67e-05	3.17	0.02	18/354	-4.24
GO:0005886	**Plasma Membrane**	67	5.11e-05	1.63	0.02	67/389	2.32
GO:0016020	**Membrane**	45	9.41e-05	1.84	0.03	45/389	-1.94
GO:0005516	**Calmodulin Binding**	8	1.09e-04	6.89	0.05	8/354	2.12

Gene Ratio – the number of genes mapped to the particular pathway vs. number of genes mapped to the reference, Z-score = (log fold of change for up-regulated gene –log fold of change for the down-regulated gene)/ (total number of genes in the pathway).

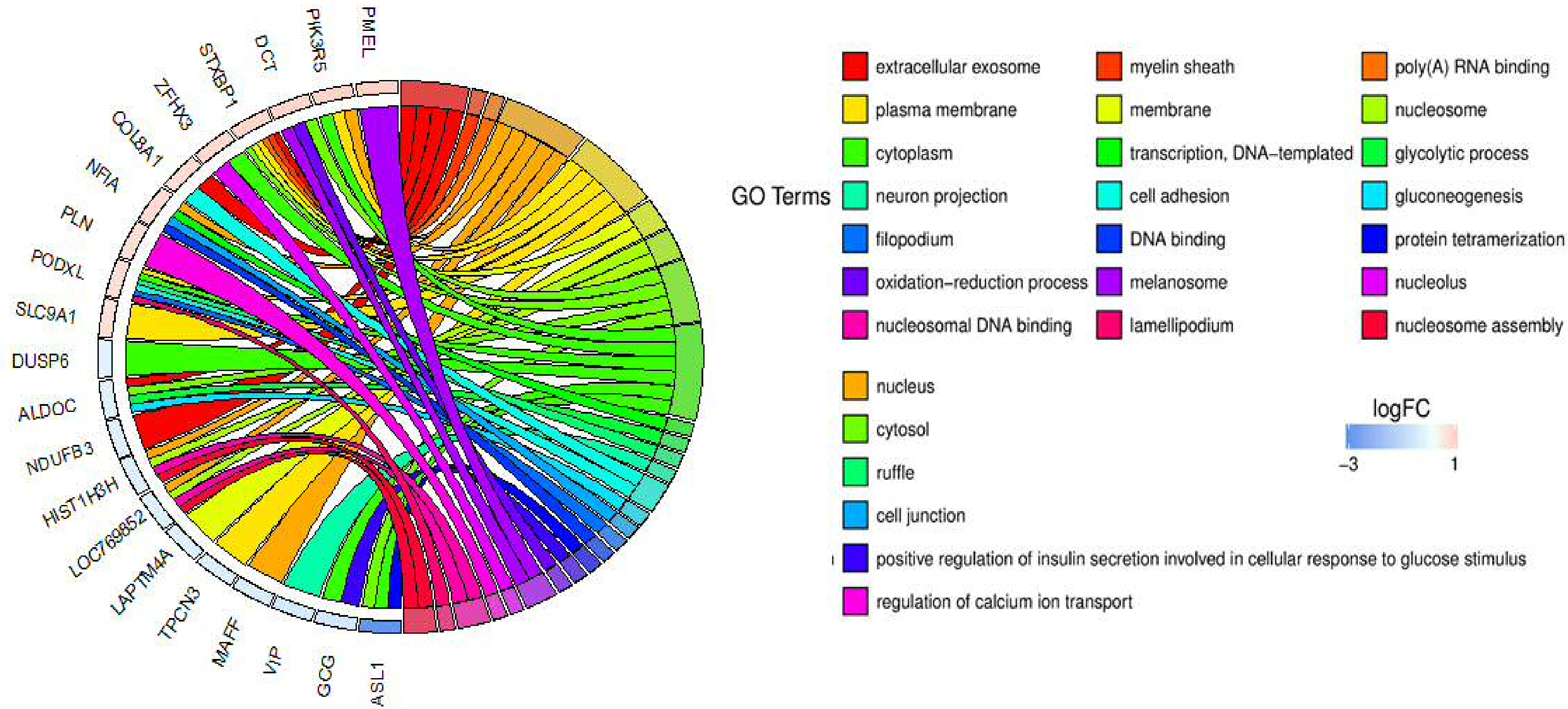

Figure 6.6.Chord plot demonstrating the inter-connections between the 22 largest/smallest changed differentially-expressed genes with the largest/smallest fold-change, and their related GO terms.

6.3.2.3 KEGG analysis using Gene Set Enrichment Analysis (GSEA)

In GSEA, differentially-expressed genes from my high vs. low myopia susceptibility RNA sequencing study were ranked according to their correlation with the myopia susceptibility phenotype using the default 'signal-to-noise ratio' method. Hence, a ranking list was formed. Then, GSEA weighted whether members of a gene set were randomly distributed across the ranking gene list or they tended to occur toward the top (or bottom) of the rank list. Thus, GSEA determined whether any gene set correlated with myopia susceptibility.

Of the 7,341 RNA-seq genes provided as input for GSEA, 5229 mapped to 183 KEGG pathways after applying the exclusion criteria. Among these 183 pathways, 121 pathways were up-regulated in chicks with high-susceptibility to myopia. Of these, 5 pathways exceeded the suggestive threshold, FDR < 0.25, which was considered to be a reasonable threshold for exploratory results. Two of them – the 'Parkinson's Disease' pathway and the 'Oxidative Phosphorylation' pathway – had an FDR q-value <0.05. The other 62 pathways were up-regulated in chicks with low susceptibility to myopia. Of these, only 1 reached FDR <0.25 and none reached FDR <0.05. The normalized enrichment score (NES) ranged from -1.80 to 2.12; the Parkinson's Disease KEGG pathway had the largest NES (Table 6.6, Figures 6.7 and 6.8).

Table 6.6.KEGG with FDR <0.25 in GSEA analysis of differentially-expressed genes.

Gene Set (KEGG)	Count	NES	Nominal P-Val	FDR	Rank At Max	Leading Edge
Parkinsons Disease	53	2.11	0	1.31e-3	1697	tags=74%, list=32%, signal=108%
Oxidative Phosphorylation	60	2.00	0	3.97e-3	1319	tags=55%, list=25%, signal=73%
Ribosome	53	1.85	2.12e-3	0.05	1585	tags=60%, list=30%, signal=86%
Alzheimers Disease	73	1.72	2.02e-3	0.18	1654	tags=60%, list=32%, signal=87%
Huntingtons Disease	79	1.71	0.002	0.15	1319	tags=43%, list=25%, signal=57%
DNA Replication	20	-1.80	0	0.08	1048	tags=50%, list=20%, signal=62%

Annotation - Leading edge: Since not all of the genes in the gene sets will participate in the biological process, the core members that account for the enrichment signal will be extracted by leading edge analysis. Tags - the percentage of genes contributing to the enrichment score; List - The percentage of genes in the ranked gene list before (for positive ES) or after (for negative ES) the peak in the running enrichment score. This gives an indication of where in the list the enrichment score is attained; Signal - The enrichment signal strength that combines the two previous statistics.

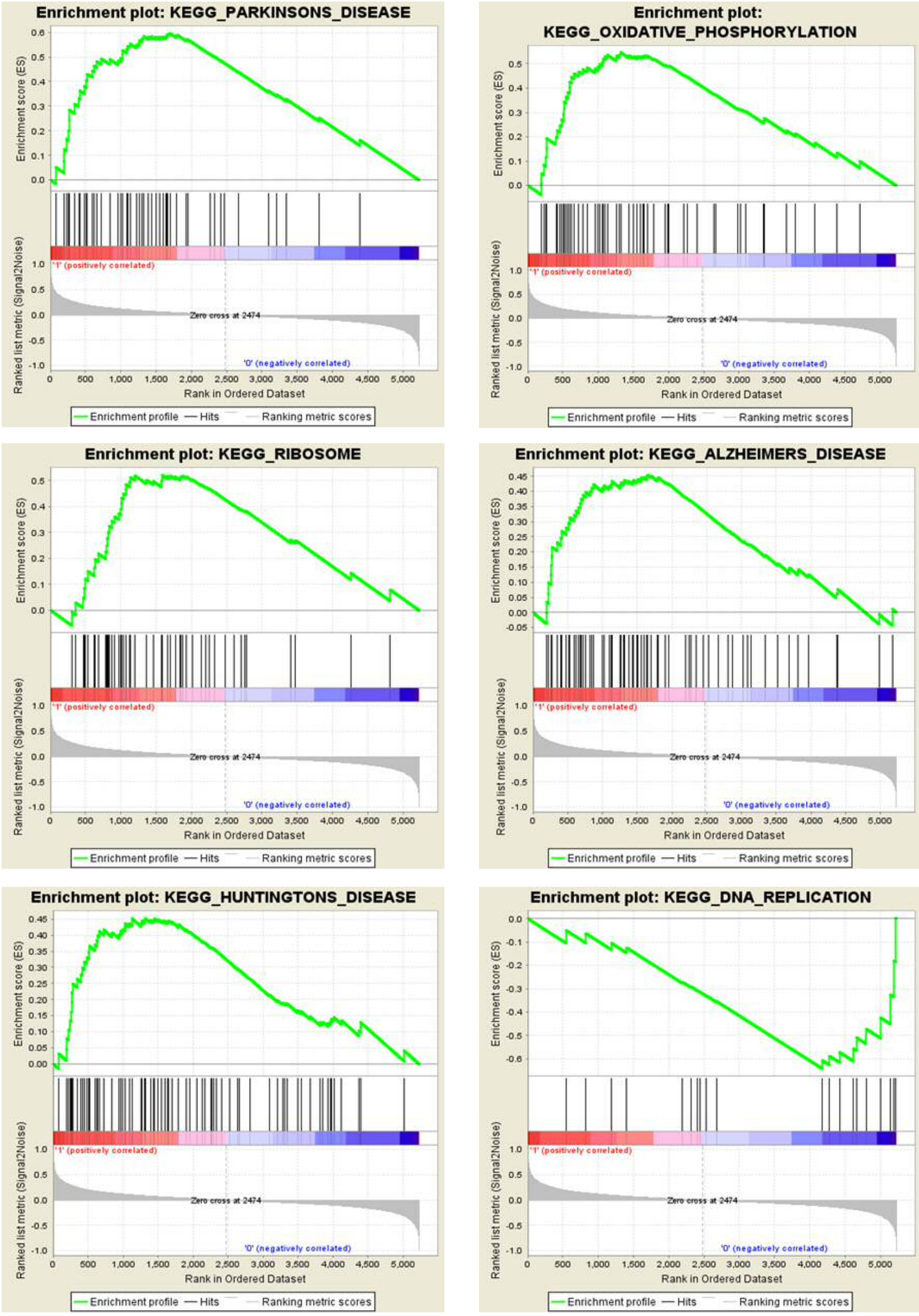

Figure 6.7.Enrichment plot of KEGG with FDR < 0.25 from the GSEA analysis of differentially-expressed genes.

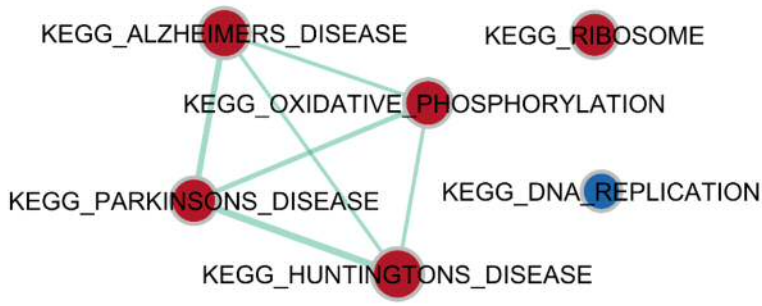

Figure 6.8.Enrichment map of the KEGG pathways from GSEA results.
Red circles represent gene sets that were up-regulated, blue circles represent gene sets that were down-regulated. Connecting lines represent more than 50% of genes overlap between the two gene sets, the thickness of the line representing the overlap strength.

6.3.2.4 GO term analysis using Gene Set Enrichment Analysis (GSEA)

In the enrichment analysis of GO terms, there were 5,765 gene sets that contained more than 2 genes. Of these, 3,198 gene sets (55%) were relatively up-regulated in high-susceptibility chicks, of which 95 gene sets reached FDR <0.25 (Appendix 6.3). The other 2,567 gene sets (45%) were up-regulated in low-susceptibility chicks, of which 10 had an FDR <0.25 (Appendix 6.3). Among the 95 and 10 suggestive gene sets, there were 6 gene sets with an FDR <0.05; these related to ‘inner mitochondrial membrane protein complex’, ‘secondary metabolic process’, ‘multivesicular body’, ‘mitochondrial protein complex’ , ‘terpenoid metabolic process’ and ‘mitochondrial membrane part’ (Table 6.7). The NES for these gene sets ranged from -2.02 to 2.15. The GO terms ‘transcription factor activity direct ligand regulated specific DNA binding’ had the lowest NES and ‘inner mitochondrial membrane protein complex’ had the highest score. The 10 gene sets with the most extreme enrichment scores are shown in Figure 6.9 The interconnections of all the gene sets is shown in Figure 6.10.

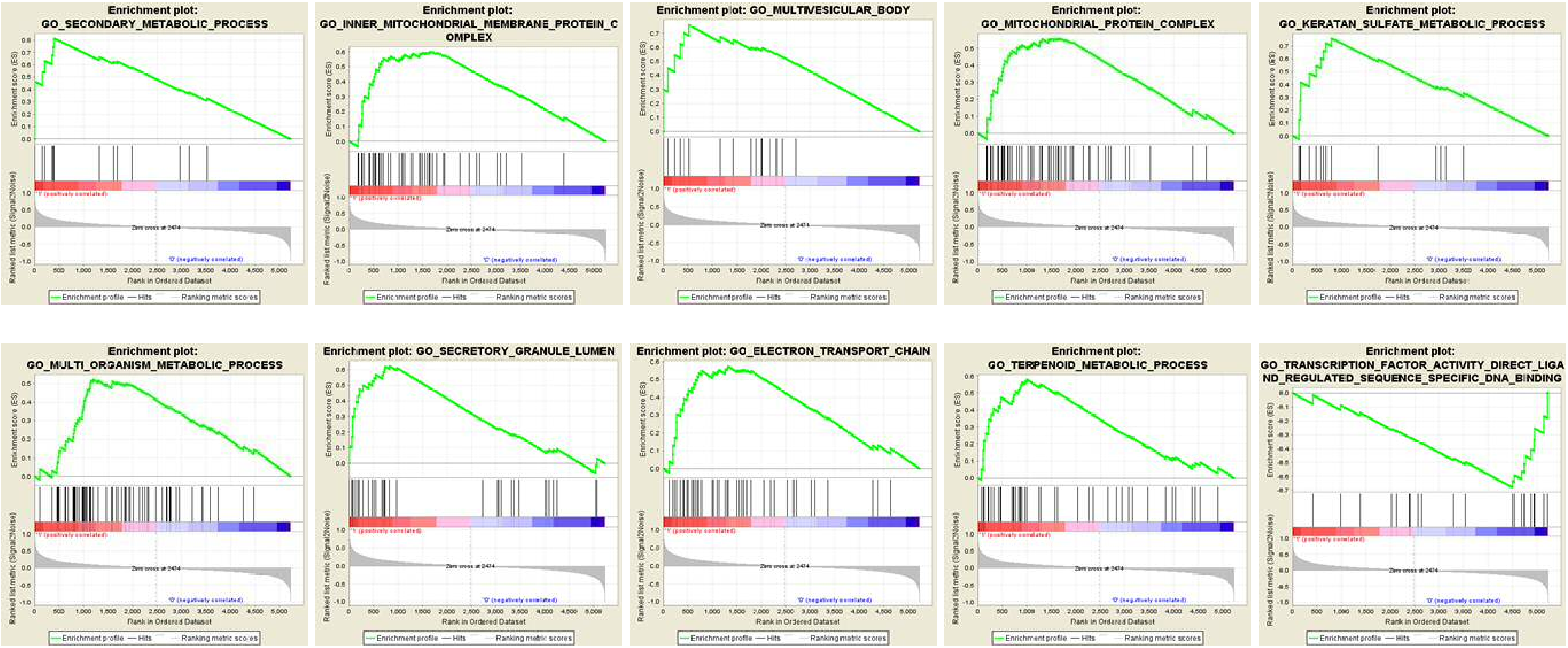

Figure 6.9. Enrichment plot of top 10 GO term from the GSEA analysis of differentially-expressed genes.

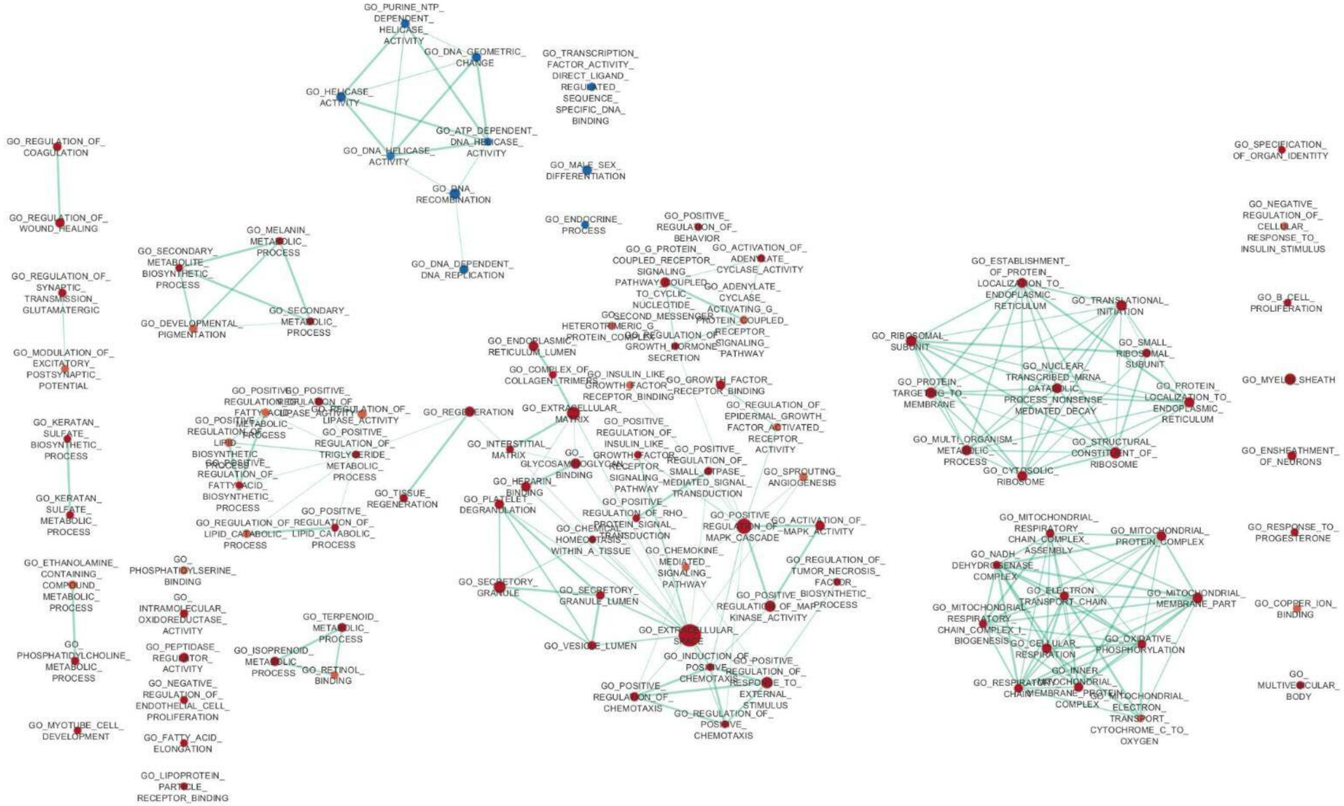

Figure 6.10.Enrichment map of the GO terms from GSEA results.
Red circles represent gene sets that were up-regulated, blue circles represent gene sets that were down-regulated. Connecting lines represent more than 50% of genes overlap between the two gene sets, the thickness of the line representing the overlap strength.

Table 6.7.GO term with FDR <0.05 in GSEA analysis of differentially-expressed genes.

Gene Set (GO)	Count	NESs	Nominal P-Val	FDR Q-Val	Rank At Max	Leading Edge
Inner Mitochondrial Membrane Protein Complex	50	2.11	0	0.02	1654	tags=72%, list=32%, signal=104%
Secondary Metabolic Process	14	2.15	0	0.02	400	tags=50%, list=8%, signal=54%
Multivesicular Body	16	2.08	0	0.02	523	tags=38%, list=10%, signal=42%
Mitochondrial Protein Complex	61	2.04	0	0.03	1654	tags=67%, list=32%, signal=97%
Terpenoid Metaboliprocess	42	1.98	2.01e-3	0.05	1001	tags=52%, list=19%, signal=64%
Mitochondrial Membrane Part	74	1.97	0	0.05	1319	tags=54%, list=25%, signal=71%

6.4 Discussion

Gene set pathway analyses were carried out using both GWAS results and RNA-seq results. In the analyses of GWAS results, no genes or gene sets reached statistical significance. For the RNA-seq results, 2 gene set analysis approaches were used: DAVID and GSEA. In DAVID analysis, 12 KEGG pathways and 73 GO terms had EASE <0.05; In GSEA analysis, 6 KEGG pathways and 105 GO terms reached FDR <0.25.

6.4.1 Gene-based association study

Using MAGMA, SNP-level information was synthesized to gene-level information. The top-ranked gene in the MAGMA analysis was PIK3CG. This was not surprising, since in the GWAS, the top associated SNPs were situated between PIK3CG and PRKAR2B, and the evidence suggested there was only one causal SNP in the region. Due to the lack of LD information for my chick population, the MAGMA results should *not* be considered to add weight to the hypothesis that PIK3CG, rather than PRKAR2B, is likely to be the causal gene associated with high susceptibility to myopia development in FD chicks.

The second strongest signal from the MAGMA analysis was on chromosome 7, implicating the gene *USP40* (ubiquitin specific peptidase 40). In the GWAS study, SNPs in the vicinity of USP40 reached the suggestive significance threshold. In a previous linkage analysis study of a high myopia pedigree, a high myopia locus was mapped to a critical region between markers D2S1279 and D2S2205 on chromosome 2 at q37.1, where UPS40 is located. Thus, *USP40* is a promising candidate gene for high myopia (53).

6.4.2 Gene-set-based association study

Among the potential pathways suggested by pathway analysis, several have been implicated in myopia development in previous studies.

6.4.2.1 Circadian rhythms

The KEGG pathway 'circadian rhythm' was highlighted by the MAGMA analysis, as was the 'regulation of circadian rhythm' pathway by DAVID. In previous studies, circadian rhythms have been shown to influence myopia development. For example, in chicks, both constant light (434, 435) and constant dark (260) result in hyperopia and corneal flattening (436), while tree shrews reared in constant darkness developed a myopic shift (437). Variation in photoperiod (length of the daylight period) also affects the degree of FDM in chicks (438).

There is a hypothesis (439) that, in FD chicks, the lack of normal visual transients might mimic the 'constant conditions' encountered in constant light or constant dark. With reference to this study, chicks highly susceptible to FDM might be especially sensitive to such cues from the diurnal circle.

6.4.2.2 Gene sets relating to extracellular matrix (ECM) and structural remodelling

There were many GO terms enriched for ECM pathways, for example 'glycosaminoglycan degradation', 'positive regulation of extracellular matrix disassembly', 'complex of collagen trimers' and ' keratan sulfate metabolic process'. According to previous studies, glycosaminoglycan synthesis was reduced in the sclera during myopia development (440, 441). It is well known that the ECM is important in determining the biomechanical properties of the sclera and that there are dynamic changes to scleral "creep rate" during myopia development (442).

Several other annotations related to cell structure and adhesion, such as 'cell adhesion', 'focal adhesion', 'calcium-dependent cell-cell adhesion via plasma membrane cell adhesion molecules', 'actomyosin structure organization' and 'positive regulation of Rho protein signal transduction'. This suggests that, during myopia development, cell adhesion may change, or even mediate ECM remodelling. Cell adhesion has previously been implicated in refractive astigmatism (443) and experimentally-induced myopia (444).

6.4.2.3 Energy generation and oxidative stress

Many pathways relating to the respiratory chain and oxidative stress were enriched, for example, 'mitochondrial respiratory chain complex assembly' and 'oxidative phosphorylation'. There could be two possible reasons for this enrichment in energy generation-related terms. First, a difference in energy generation capability may contribute to the degree of axial elongation during FDM, for example, if energy generation is rate-limiting in this process. Thus, chicks that develop high myopia may have greater energy generation capabilities than chicks that develop low myopia under the same FD conditions. Second, a high level of energy generation could be a consequence of fast ocular elongation. The vertebrate retina has a very high demand for oxygen (445). Therefore rapid axial elongation could cause even greater than normal consumption of oxygen and energy. Unfortunately, gene set analysis cannot distinguish between these possible mechanisms.

Oxidative stress could potentially be a negative consequence of myopia development, as previously suggested from microarray studies in form deprived chicks (446) and studies of ocular pulse amplitude in human high myopia (447, 448).

6.4.2.4 Glycometabolism and lipid metabolism

Glucose and lipid metabolism also feature prominently in the pathway annotations, for example: 'Glycolysis and gluconeogenesis', 'glycolytic process', 'positive regulation of insulin secretion involved in cellular response to glucose stimulus', 'positive regulation of triglyceride metabolic process' and 'positive regulation of lipid biosynthetic process'. In one recent study conducted by Yang et al., retinal metabolic changes were analyzed in FD guinea pigs, and the authors concluded that myopia progression was associated with increases in glucose accumulation and decreases in lipid levels (449). These gene sets support those discussed above relating to energy expenditure/generation, as glucose and lipid metabolism provide substrates for the tricarboxylic acid (TCA) cycle. Other potential mechanisms may also link glycometabolism and lipid metabolism to myopia (450).

6.4.2.5 Other terms

In addition to those annotations discussed above, independent but potentially meaningful terms/pathways highlighted by DAVID and/or GSEA analysis included: 'melanin metabolic process', 'melanosome', 'ionotropic glutamate receptor activity' and 'AMPA glutamate receptor activity'.

6.4.3 KEGG and GO

Previous studies of genes differentially expressed in myopia models performed gene set analysis using gene sets derived from KEGG pathways or GO terms. KEGG pathways are a collection of pathway maps that reflect experimental knowledge of metabolism and various other functions of cells and organisms. KEGG contains 6 major categories: metabolism, genetic information processing, environmental information processing, cellular processes, organismal systems, and human diseases and drug development. GO is another widely used annotation reference. Unlike KEGG, which is manually curated by experts, GO terms are generated by a computer. Thus, GO contains more gene sets but has less accuracy than KEGG. GO covers a more comprehensive set of cellular processes, molecular functions and cellular components. Although KEGG and GO cover a wide range of gene set definitions, including different organisms, most of the definitions are based on human studies and human diseases; therefore, since I attempted to map chicken data to the pathways and annotations, care should be taken to confirm their relevance in chickens.

6.4.4 Comparison of pathway analysis methods

Although DAVID and GSEA are both widely used tools, they yielded different results in my study, especially as regards the level of statistical significance. There could be several reasons for the differing results. First, DAVID only took as input genes those that were statistically significant in a previous analysis, while GSEA took all available genes into consideration. For example, regarding the KEGG pathway 'oxidative phosphorylation', which was highlighted by both DAVID and GSEA, in the DAVID analysis, only 8 genes were mapped to the pathway while, in GSEA, 60 genes were mapped. Furthermore, the method of computing Z-scores is different. DAVID took account of accurate fold-change information calculated using a negative binomial model to generate Z-scores, while GSEA used its own ranking list calculation, which is unlikely to be as accurate.

Results from all of these tools should be taken as exploratory rather than definitive. Pathway analysis provides a broader view of genomic and transcriptomics data than do SNP-level or gene-level results, yet at the expense of making more assumptions.

6.5 Limitations

In this study, the pathway information was primarily based on human studies, which may have caused some bias. Also, in the GSEA analysis, to make the results comparable with the DAVID analysis, the minimum number of genes in each gene sets was set as 2, which may have reduced statistical power. Most importantly, however, the use of only 16 RNA samples from 8 animals – while being a larger sample size than most previous gene expression studies in myopia models – will have severely limited statistical power to robustly identify molecular pathways.

Chapter 7 General discussion and future work

To identify myopia susceptibility loci, a GWAS was performed in a sample of chicks with FD-induced myopia. Transcriptomics analysis of chick retina was also performed with the aim of integrating genomic (GWAS) and transcriptomic data (RNA-seq) to pinpoint retinal genes that modulate the signalling pathway linking visual experience to ocular growth. Gene-based and gene set-based analyses were conducted using GWAS and transcriptomics analysis results, with the aim of enhancing the power of each method alone and improving the biological interpretation of the findings.

7.1 Discussion of the key results

Form-deprivation myopia was induced in a large sample of chicks (n=959). It was found that batch-to-batch variation, body weight, sex and a sex-by-body weight interaction were associated with the degree of axial eye elongation and the level of induced myopia (Chapter 3). A GWAS was carried out using 380 chicks (190 selected from each of the phenotype extremes of the myopia susceptibility distribution; i.e. high myopia susceptibility and low myopia susceptibility). Using the form-deprivation-induced increase in axial length (ΔAXL) as the primary outcome of interest, and after controlling for the effects of batch, sex and body weight, the GWAS identified a single genome-wide significant locus on chick chromosome 1 (lead SNP rs317386235) located between the genes *PRKAR2B* and *PIK3CG* (Chapter 4, section 4.3.2). Furthermore, 26 additional SNPs from chromosomes 1, 7 and 12 exceeded the suggestive significance threshold of $P < 1.64e\text{-}05$. Retinal RNA-seq-based transcriptomics analysis was performed for 16 eyes of 8 genotyped chicks; 4 selected as having a high degree of susceptibility to FDM and 4 selected as having a low myopia susceptibility. In a comparison of chicks with a high versus a low level of myopia susceptibility, 516 differentially-expressed genes were identified (FDR <0.05; Chapter 5, section 5.4.2.1). Although neither *PRKAR2B* nor *PIK3CG* were amongst these differentially expressed genes, the *PIK3R5* gene was found to be differentially expressed. Furthermore, the *PIK3CD* (*PI3K* catalytic subunit delta) gene was also identified as being differentially expressed between high and low myopia chicks (Appendix 5.2, section 5.3.6).

Phosphoinositide-3-Kinase Regulatory Subunit 5, encoded by *PIK3R5*, is an interaction partner of PIK3CG, suggesting that signalling through the enzyme PIK3 may partly determine myopia susceptibility. Gene-based analysis (Chapter 6, section 6.3.1.2) also suggested PIK3CG was the gene most strongly associated with the change in axial due to FD. Gene set-based analysis (Chapter 6, section 6.3.1.3) found no overlap between GWAS and RNA sequencing gene sets, but gene sets relating to circadian rhythm, extracellular matrix (ECM) structural remodelling, energy generation, oxidative stress, glycometabolism and lipid metabolism were highlighted at a suggestive significance threshold.

7.2 Pathways controlling myopia susceptibility

My findings implicated several potential pathways that confer a difference in susceptibility to form-deprivation myopia.

7.2.1 Insulin – PI3K – AKT signalling

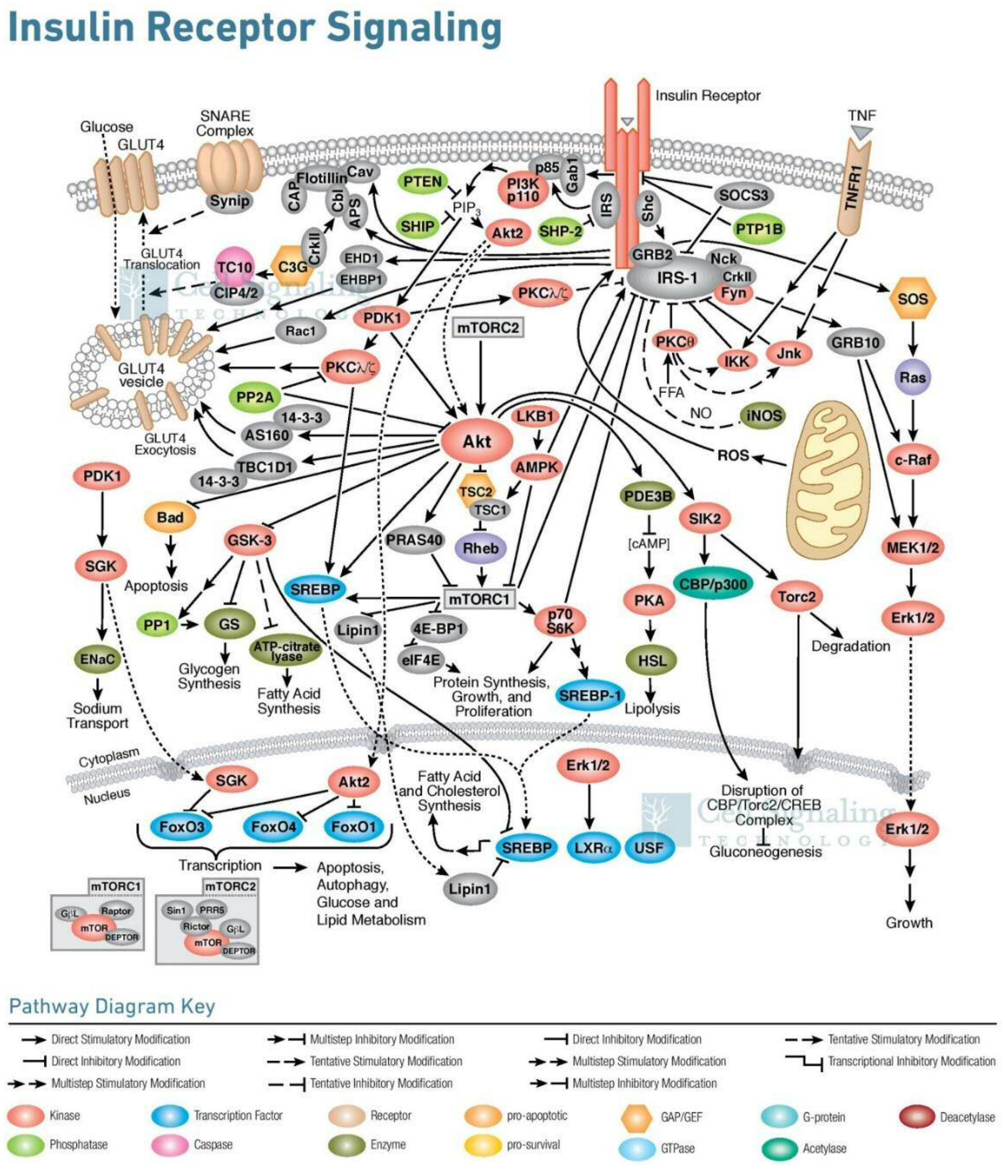

Figure 7.1 The Insulin receptor signalling pathway (451).

In transcriptomics analysis, a down-regulation of glucagon and IGFBP4, and an up-regulation of IGF1R were observed in the retina of chicks with high susceptibility to FD (Chapter 5, section 5.3.6). This suggests an up-regulation of signalling via insulin or an insulin-like growth factor (Figure 7.1). Pathway analysis further suggested glycometabolism and lipid metabolism processes were involved in myopia susceptibility (Chapter 6, section 6.2.4). I speculate that all of these pathways were involved in the fast axial elongation occurring in the eyes of chicks with high susceptibility to FD, since they all relate to cellular metabolism, growth and survival (452). Previous studies had already identified the importance of insulin and insulin-related genes in myopia development (310, 453, 454), although few researchers have investigated the downstream pathways. Nevertheless, one study reported that inhibition of PI3K by Ly294002 could partially block the effect of insulin-induced overcompensation to negative lens wear in chicks (309). This study by Penha et al. (309) demonstrated two findings, first, insulin could accelerate the elongation of axial length under form deprivation situation; second, the effect of insulin exerted its effect through activation of PI3K. These findings suggest the insulin – PI3K pathway might be involved in myopia formation, and, naturally-occurring variants controlling either the expression level or activity of *PI3K* might be associated with myopia susceptibility.

7.2.2 PI3K and scleral extracellular matrix remodelling

The scleral extracellular matrix (ECM) contains collagen fibres, proteoglycans, elastic fibres, and chondrocytes (442). During myopia development, there is a dynamic modulation of the ECM, including a reduction of type I collagen content (441, 455), a decrease in glycosaminoglycan content (441), and an increased expression of ECM-degrading enzymes such as MMP-2 (456, 457). In chicks, proteoglycan synthesis increases after one day of FD and prior to vitreous chamber elongation (458). Several previous studies have identified the involvement of PI3K signalling pathways in the ECM remoulding process. In retinal pigment epithelial cells (459, 460) and the human renal proximal tubular cell line (HKC) (461), the PI3K pathway was activated during ECM remodelling (Figure 7.2) (462).

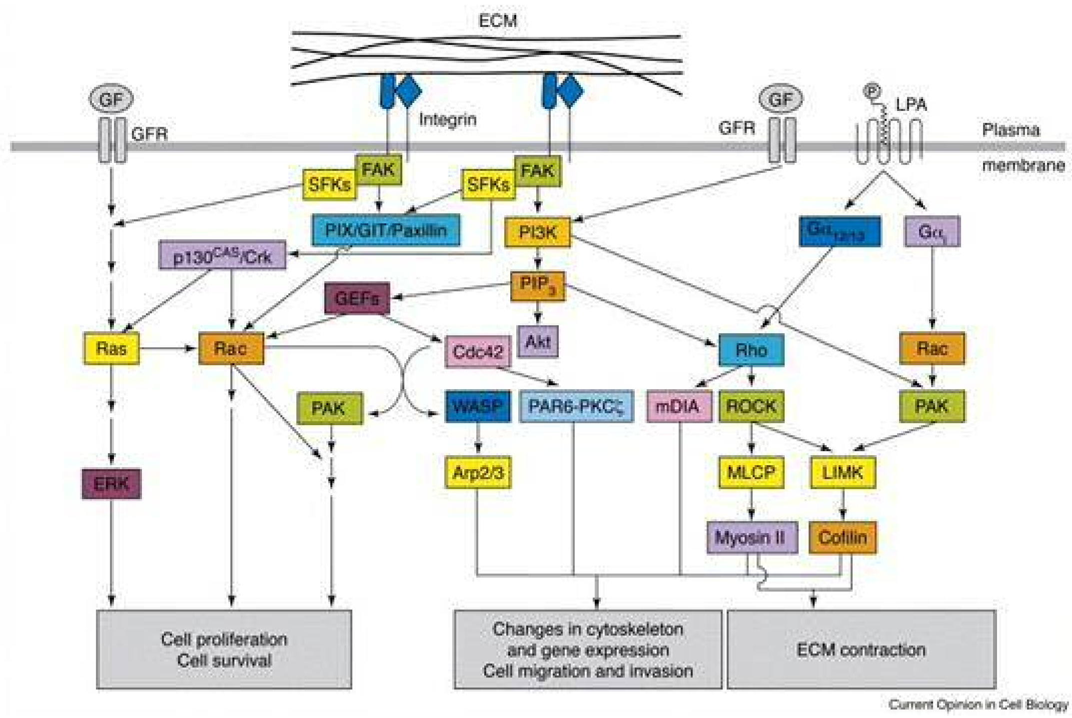

Figure 7.2. Illustration of the PI3K involved ECM remodelling process (462).

However, in this study, due to the limitation of the experimental design, ECM related signals could only be detected if they derived from the retina. In transcriptomics analysis of chicks with high vs. low susceptibility to FD, differentially-expressed genes related to ECM, such as COL8A1, COL12A1, COL5A1, MXRA8, MMP16, CDH13 (cell migration), CDH4, CDH8, ACTG1 and ARHGAP21 were found (Chapter 5, section 5.3.6). Accordingly, in the subsequent pathway analysis, several pathways such as 'glycosaminoglycan degradation', 'positive regulation of extracellular matrix disassembly', 'complex of collagen trimers' and ' keratan sulfate metabolic process' reached a suggestive level of statistical significance (Chapter 6, section 6.3). Considering all of this information together, I hypothesize that during the FD-induced axial elongation process, *PI3K* is involved in extracellular matrix remodelling. Genetic variation in the expression level of PI3KCG might influence the rate of the remodelling process. From my results, it is not possible to infer whether the ECM related genes and pathways detected in retina play a role that is solely restricted to the retina, or if they are in some way connected to – or indicative of – ECM remodelling in the sclera.

7.3 Strengths of the study

This was the first study to perform a GWAS for myopia susceptibility in an animal model of myopia. Compared to conventional GWAS in humans, the current work has several notable features, as described below.

Firstly, in human populations, each individual is exposed to a different set of environmental risk factors. Therefore, detecting a specific gene-environment interaction requires an extremely large sample size (Chapter 4 section 4.1.2). In contrast, in the current experiment, all individuals in this study were exposed to a highly uniform environment; namely, they were treated with a single, specific visual exposure – form deprivation – known to robustly induce myopia. This uniformity was expected to dramatically increase statistical power to detect gene-environment interactions conferring susceptibility to myopia.

Secondly, both refractive error and axial length were measured in the current study. Indeed, the main outcome measure (ΔAXL) was an objectively-assessed ocular parameter that could be measured with high accuracy and reproducibility (463). To maximise the accuracy of quantifying the myopia susceptibility of individual chicks, axial length was recorded in both treated eyes and control eyes, both before and after FD. This enabled me to quantify myopia susceptibility (ΔAXL) in a manner that took account both of the eye size at baseline and the extent of eye growth in the fellow, non-treated eye. By contrast, in human GWAS investigations, the end-point ocular phenotype has generally been assessed, such as the refractive error in adulthood. This approach in human studies neglects the *rate* at which myopia develops. In this study, the use of ΔAXL accounted for baseline axial length before treatment and normal physiological growth, hence it represented a precise measure of susceptibility to FD.

Thirdly, 'systems genetics' is already a well-known concept (341) that has been applied in a prior myopia study (78), however, human studies cannot access retinal tissue from GWAS participants during the critical period when myopia is developing. Using a chick myopia model provided a novel solution to this problem, and allowed a much more complete integration of transcriptomic data with GWAS data, providing the opportunity for a multi-dimensional, systematic assessment of myopia development.

Fourthly, whereas past myopia transcriptomics studies have compared gene expression profiles between FD-treated eyes and control eyes, this study is the first to evaluate how *myopia susceptibility* impacts these treated eye versus control eye differences. When the comparison is between FD eyes and control eyes, it is difficult to know whether differential gene expression has occurred simply as a secondary consequence of having an enlarged, form-deprived eye, or whether the differentially-expressed gene is playing a potentially vital, causal role in signalling the eye to grow. Moreover, the luminance level beneath a goggle is lower than normal, which could confound the results of conventional treated eye versus control eye comparisons. Here, making comparisons between high and low myopia susceptibility chicks removed this potential source of confounding.

7.4 Limitations of the study

Firstly – relatedness of the chick population. The chicks used in this study were obtained from a commercial supplier with a large breeding colony, which was done with the aim of minimizing relatedness between individuals. Nevertheless, kinship analysis showed a moderate level of relatedness amongst the majority of the chicks. Relatedness inflates association test statistics in a systematic manner (quantified by λ_{GC}), and therefore complicates the identification of 'true positive' GWAS signals. Although in this study, genomic control correction and mixed linear models were used to correct for or account for relatedness; both of these correction methods have limitations (Chapter 4, section 4.4.7).

A second important limitation is that chicks are phylogenetically distant from mammals, which makes the findings from chick studies of uncertain relevance to humans. Comparing chick eyes with human eyes, chicken eyes have major differences such as lack of a fovea, a cartilaginous as well as a fibrous layer of the sclera, the presence of both corneal and lenticular accommodation, and a greater diversity of cone photoreceptor cell types (191). Researchers need to be cautious in assuming that findings in chick studies will translate to humans, considering all of these differences.

Thirdly, owing to the relatively small sample size used, my study had limited power to detect genetic variants weakly associated with myopia susceptibility. This was especially true for the transcriptomics analysis in which funds permitted only 8 chicks to be investigated. This factor limited the power to detect differential gene expression, and also eliminated the chance to search for expression QTLs (eQTLs).

Fourthly, form deprivation myopia is rare in humans (it can occur if congenital cataract or corneal opacification is not treated in infancy (464). Typically, children who develop myopia have clear ocular media, and thus the mechanism is different from form deprivation. Hence, another limitation is that the FD model I used does not fully replicate the nature of the cause of myopia in humans. Other myopia models exist, for example, chicks can be raised wearing negative lenses (LIM) or exposed to low ambient light (465). However, since the cause of myopia in children is largely unknown, no animal model can fully recapitulate the human situation.

Finally, no imputation reference panel is available for the chicken, so it was not possible to impute genotypes at sites known to be polymorphic but that were not directly genotyped. Similarly, biological/physiological pathway databases for chickens are also limited in comparison to those available for humans.

7.5 Future work

In this study, a chick GWAS was used for mapping myopia susceptibility QTL, and transcriptomics analysis was used to refine the GWAS findings. Proposed future work to extend this approach would include the following sections.

7.5.1 Expanding the number of genotyped chicks

Only 380 chicks were genotyped in this study. Genotyping the full study cohort of 959 chicks would improve statistical power to detect new genetic loci such as those with a small effect. Alternatively, to reduce costs, instead of performing whole genome genotyping, selected regions showing suggestive evidence of association in the original GWAS could be genotyped to enable fine-mapping to be performed in each selected region.

7.5.2 eQTL analysis and validation of RNA-Seq results

In GWAS analysis, the most strongly associated SNP (rs31738623) was located between the coding regions of the *PRKAR2B* and *PIK3CG* genes, which implied that the SNP might be an eQTL. To test the hypothesis that rs31738623 is a retinal eQTL for the protein encoded by either *PRKAR2B* or *PIK3CG* – or indeed a different nearby gene, would require the expression level of these genes to be quantified in retinal samples from a relatively large number of chicks, e.g. the 380 chicks that were genotyped here. Ideally, I would use RNA-seq to test this hypothesis (since this would allow a search for other eQTLs as well). However, the hypothesis could also be tested by using quantitative RT-PCR to measure the expression level of just the candidate genes in the *PRKAR2B* and *PIK3CG* region, in order to reduce the cost of the experiment.

In the transcriptomic analysis using 8 chicks, hundreds of transcripts showed suggestive evidence (FDR <0.05) of differential expression in response to FD, and dozens of transcripts showed suggestive evidence of a treatment x group (High vs. Low) interaction. To validate these results, it will be necessary to examine retinal samples from an independent sample of chicks. While this could be done using RNAseq again, the use of an independent technique for assessing gene expression, such as quantitative RT-PCR, would provide stronger evidence.

7.5.3 Integration of findings from this study of chicks with human myopia studies

The primary aim of my project was to identify myopia susceptibility genes, so that their role in human myopia development could be examined. There are several potential ways that my findings could be extended to humans. Firstly, I suggest performing a GWAS for the 'rate of myopia progression' in children. Using data from a longitudinal study such as ALSPAC (466), the growth trajectory of refractive error could be quantified using a linear mixed model, and this trait could serve as the phenotype for a GWAS. In the model, the longitudinal records of educational attainment, time spent outdoors, and near work could be adjusted as potential confounding factors. I hypothesize that the comparison between such a 'rate of myopia progression GWAS' in children and my chick study would highlight mechanisms relating to fast versus slow myopia development. Secondly, an inverse pathway analysis could be carried out in a human GWAS dataset. My pathway analysis results implicated the PI3K signalling pathway in regulating visually-guided refractive development. Hence, selecting genes in the PI3K pathway and applying an inverse pathway analysis using human GWAS summary statistics might provide a powerful strategy to detect genetic variants with small but important effects on myopia susceptibility. Thirdly, my results suggest it would be worthwhile to perform a Mendelian Randomization study testing for a causal role of insulin resistance (the 'exposure') on myopia (the 'outcome'). A relationship between insulin resistance and myopia progression has already received support from prior studies (106, 395, 467-469). However, whether myopia and insulin resistance are linked through pleiotropic effects or if instead insulin resistance is a truly causal factor for myopia still needs to be determined. A Mendelian Randomization study would be a feasible method to test this hypothesis. As chicks have also been proposed as a diabetes model (470-472), testing diabetes and myopia in the same chick model may also determine the causal relationship between these two disorders.

References

1. DS. R. The Myopia Myth: The Truth about Nearsightedness and how to Prevent it: International Myopia Prevention Assn.; 1981.
2. Sloane AE. The Myopias: Basic Science and Clinical Management. Archives of Ophthalmology. 1986;104(6):815-.
3. Bennett AG, Rabbetts RB. Bennett and Rabbetts' clinical visual optics: Elsevier Health Sciences; 1998.
4. Sun HP, Li A, Y X, CW P. Secular trends of reduced visual acuity from 1985 to 2010 and disease burden projection for 2020 and 2030 among primary and secondary school students in China. JAMA Ophthalmology. 2015;133(3):262-8.
5. Xiang F, He M, Zeng Y, Mai J, Rose KA, Morgan I. Increases in the prevalence of reduced visual acuity and myopia in Chinese children in Guangzhou over the past 20 years. Eye. 2013;27(12):1353-8.
6. Lin LL, Shih YF, Hsiao CK, Chen CJ. Prevalence of myopia in Taiwanese schoolchildren: 1983 to 2000. Annals of the Academy of Medicine, Singapore. 2004 Jan;33(1):27-33. PubMed PMID: 15008558. Epub 2004/03/11. eng.
7. Tay M, Au EK, Ng C, Lim M. Myopia and educational attainment in 421,116 young Singaporean males. Annals of the Academy of Medicine, Singapore. 1992;21(6):785-91.
8. Dayan YB, Levin A, Morad Y, Grotto I, Ben-David R, Goldberg A, et al. The changing prevalence of myopia in young adults: a 13-year series of population-based prevalence surveys. Investigative Ophthalmology & Visual Science. 2005;46(8):2760-5.
9. Parssinen O. The increased prevalence of myopia in Finland. Acta Ophthalmologica. 2012 Sep;90(6):497-502. PubMed PMID: 21902818.
10. Villarreal MG, Ohlsson J, Abrahamsson M, Sjostrom A, Sjostrand J. Myopisation: the refractive tendency in teenagers. Prevalence of myopia among young teenagers in Sweden. Acta Ophthalmologica Scandinavica. 2000 Apr;78(2):177-81. PubMed PMID: 10794252.
11. Williams KM, Verhoeven VJ, Cumberland P, Bertelsen G, Wolfram C, Buitendijk GH, et al. Prevalence of refractive error in Europe: the European eye epidemiology (E3) Consortium. European Journal of Epidemiology. 2015;30(4):305-15.
12. Sperduto RD, Seigel D, Roberts J, Rowland M. Prevalence of myopia in the United States. Archives of Ophthalmology. 1983 Mar;101(3):405-7. PubMed PMID: 6830491.
13. Vitale S, Ellwein L, Cotch MF, Ferris FL, 3rd, Sperduto R. Prevalence of refractive error in the United States, 1999-2004. Archives of Ophthalmology. 2008 Aug;126(8):1111-9. PubMed PMID: 18695106. Pubmed Central PMCID: 2772054.
14. Vitale S, Sperduto RD, Ferris FL, 3rd. Increased prevalence of myopia in the United States between 1971-1972 and 1999-2004. Archives of Ophthalmology. 2009 Dec;127(12):1632-9. PubMed PMID: 20008719.
15. Attebo K, Ivers RQ, Mitchell P. Refractive errors in an older population: The blue mountains eye study11The authors have no proprietary interest in any of the materials mentioned in this study. Ophthalmology. 1999;106(6):1066-72.
16. Wensor M, McCarty CA, Taylor HR. Prevalence and risk factors of myopia in Victoria, Australia. Archives of Ophthalmology. 1999;117(5):658-63.
17. Rose K, Smith W, Morgan I, Mitchell P. The increasing prevalence of myopia: implications for Australia. Clinical & Experimental Optometry. 2001;29(3):116-20.
18. Jacobsen N, Jensen H, Goldschmidt E. Prevalence of myopia in Danish conscripts. Acta Ophthalmol Scand. 2007 Mar;85(2):165-70. PubMed PMID: 17305729.
19. Koh V, Yang A, Saw SM, Chan YH, Lin ST, Tan MMH, et al. Differences in prevalence of refractive errors in young Asian males in Singapore between 1996–1997 and 2009–2010. Ophthalmic Epidemiology. 2014;21(4):247-55.
20. You QS, Wu LJ, Duan JL, Luo YX, Liu LJ, Li X, et al. Prevalence of myopia in school children in greater Beijing: the Beijing Childhood Eye Study. Acta Ophthalmologica. 2014;92(5).
21. Matamoros E, Ingrand P, Pelen F, Bentaleb Y, Weber M, Korobelnik JF, et al. Prevalence of myopia in France: a cross-sectional analysis. Medicine. 2015;94(45).
22. Naidoo KS, Raghunandan A, Mashige KP, Govender P, Holden BA, Pokharel GP, et al. Refractive error and visual impairment in African children in South Africa. Investigative Ophthalmology & Visual Science. 2003;44(9):3764-70.
23. Pan CW, Zheng YF, Anuar AR, Chew M, Gazzard G, Aung T, et al. Prevalence of Refractive Errors in a Multiethnic Asian Population: The Singapore Epidemiology of Eye Disease Study, Investigative Ophthalmology & Visual Science. 2013;54(4):2590-8.

24. Ip JM, Huynh SC, Robaei D, Kifley A, Rose KA, Morgan I, et al. Ethnic differences in refraction and ocular biometry in a population-based sample of 11–15-year-old Australian children. Eye. 2008;22(5):649-56.
25. Kleinstein RN, Jones LA, Hullett S, Kwon S, Lee RJ, Friedman NE, et al. Refractive error and ethnicity in children. Archives of Ophthalmology. 2003;121(8):1141-7.
26. Pan CW, Ramamurthy D, Saw SM. Worldwide prevalence and risk factors for myopia. Ophthalmic & Physiological Optics. 2012;32(1):3-16.
27. Holden BA, Fricke TR, Wilson DA, Jong M, Naidoo KS, Sankaridurg P, et al. Global prevalence of myopia and high myopia and temporal trends from 2000 through 2050. Ophthalmology. 2016;123(5):1036-42.
28. Tano Y. Pathologic myopia: where are we now? 1. American Journal of Ophthalmology. 2002;134(5):645-60.
29. Vongphanit J, Mitchell P, Wang JJ. Prevalence and progression of myopic retinopathy in an older population. Ophthalmology. 2002;109(4):704-11.
30. Ogawa A, Tanaka M. The relationship between refractive errors and retinal detachment--analysis of 1,166 retinal detachment cases. Japanese Journal of Ophthalmology. 1988;32(3):310-5.
31. Wang NK, Tsai CH, Chen YP, Yeung L, Wu WC, Chen TL, et al. Pediatric rhegmatogenous retinal detachment in East Asians. Ophthalmology. 2005;112(11):1890-5.
32. Jonas JB, Gusek GC, Naumann GO. Optic disk morphometry in high myopia. Graefe's Archive for Clinical and Experimental Ophthalmology. 1988;226(6):587-90.
33. Mitchell P, Hourihan F, Sandbach J, Wang JJ. The relationship between glaucoma and myopia: the Blue Mountains Eye Study. Ophthalmology. 1999;106(10):2010-5.
34. Younan C, Mitchell P, Cumming RG, Rochtchina E, Wang JJ. Myopia and incident cataract and cataract surgery: the Blue Mountains Eye Study. Investigative Ophthalmology & Visual Science. 2002;43(12):3625-32.
35. Hsu WM, Cheng CY, Liu JH, Tsai SY, Chou P. Prevalence and causes of visual impairment in an elderly Chinese population in Taiwan1: The Shihpai Eye Study. Ophthalmology. 2004;111(1):62-9.
36. Iwase A, Araie M, Tomidokoro A, Yamamoto T, Shimizu H, Kitazawa Y. Prevalence and causes of low vision and blindness in a Japanese adult population: the Tajimi Study. Ophthalmology. 2006;113(8):1354-62. e1.
37. Fricke T, Holden B, Wilson D, Schlenther G, Naidoo K, Resnikoff S, et al. Global cost of correcting vision impairment from uncorrected refractive error. Bulletin of the World Health Organization. 2012;90(10):728-38.
38. Cohn HL. The hygiene of the eye in schools: Simpkin, Marshall and Company; 1883.
39. Rose KA, Morgan IG, Smith W, Mitchell P. High heritability of myopia does not preclude rapid changes in prevalence. Clinical & Experimental Ophthalmology. 2002;30(3):168-72.
40. Young TL. The Molecular Genetics of Human Myopia: An Update. Optometry and Vision Science. 2009;86(1):E8.
41. Hawthorne FA, Young TL. Genetic contributions to myopic refractive error: Insights from human studies and supporting evidence from animal models. Experimental Eye Research. 2013;114:141-9.
42. Guggenheim JA, St Pourcain B, McMahon G, Timpson NJ, Evans DM, Williams C. Assumption-free estimation of the genetic contribution to refractive error across childhood. Molecular Vision. 2015;21:621.
43. Guggenheim JA, Zhou X, Evans DM, Timpson NJ, McMahon G, Kemp JP, et al. Coordinated Genetic Scaling of the Human Eye: Shared Determination of Axial Eye Length and Corneal Curvature. Investigative Ophthalmology & Visual Science. 2013;54(3):1715-21.
44. Schwartz M, Haim M, Skarsholm D. X‐linked myopia: Bornholm Eye Disease. Clinical Genetics. 1990;38(4):281-6.
45. Young TL, Ronan SM, Drahozal LA, Wildenberg SC, Alvear AB, Oetting WS, et al. Evidence that a locus for familial high myopia maps to chromosome 18p. The American Journal of Human Genetics. 1998;63(1):109-19.
46. Young TL, Ronan SM, Alvear AB, Wildenberg SC, Oetting WS, Atwood LD, et al. A second locus for familial high myopia maps to chromosome 12q. The American Journal of Human Genetics. 1998;63(5):1419-24.
47. Naiglin L, Gazagne C, Dallongeville F, Thalamas C, Idder A, Rascol O, et al. A genome wide scan for familial high myopia suggests a novel locus on chromosome 7q36. Journal of Medical Genetics. 2002;39(2):118-24.

48. Paget S, Julia S, Vitezica ZG, Soler V, Malecaze F, Calvas P. Linkage analysis of high myopia susceptibility locus in 26 families. Molecular Vision. 2008;14:2566-74.
49. Ciner E, Wojciechowski R, Ibay G, Bailey - Wilson JE, Stambolian D. Genomewide scan of ocular refraction in African - American families shows significant linkage to chromosome 7p15. Genetic Epidemiology. 2008;32(5):454-63.
50. Stambolian D, Ibay G, Reider L, Dana D, Moy C, Schlifka M, et al. Genomewide linkage scan for myopia susceptibility loci among Ashkenazi Jewish families shows evidence of linkage on chromosome 22q12. The American Journal of Human Genetics. 2004;75(3):448-59.
51. Hammond CJ, Andrew T, Mak YT, Spector TD. A susceptibility locus for myopia in the normal population is linked to the PAX6 gene region on chromosome 11: a genomewide scan of dizygotic twins. The American Journal of Human Genetics. 2004;75(2):294-304.
52. Zhang Q, Guo X, Xiao X, Jia X, Li S, Hejtmancik JF. A new locus for autosomal dominant high myopia maps to 4q22-q27 between D4S1578 and D4S1612. Molecular Vision. 2005;11:554-60.
53. Paluru PC, Nallasamy S, Devoto M, Rappaport EF, Young TL. Identification of a novel locus on 2q for autosomal dominant high-grade myopia. Investigative Ophthalmology & Visual Science. 2005;46(7):2300-7.
54. Zhang Q, Guo X, Xiao X, Jia X, Li S, Hejtmancik J. Novel locus for X linked recessive high myopia maps to Xq23–q25 but outside MYP1. Journal of Medical Genetics. 2006;43(5):e20-e.
55. Wojciechowski R, Moy C, Ciner E, Ibay G, Reider L, Bailey-Wilson JE, et al. Genomewide scan in Ashkenazi Jewish families demonstrates evidence of linkage of ocular refraction to a QTL on chromosome 1p36. Human Genetics. 2006;119(4):389-99.
56. Nallasamy S, Paluru PC, Devoto M, Wasserman NF, Zhou J, Young TL. Genetic linkage study of high-grade myopia in a Hutterite population from South Dakota. Molecular Vision. 2007;13:229.
57. Lam CY, Tam PO, Fan DS, Fan BJ, Wang DY, Lee CW, et al. A genome-wide scan maps a novel high myopia locus to 5p15. Investigative Ophthalmology & Visual Science. 2008;49(9):3768-78.
58. Yang Z, Xiao X, Li S, Zhang Q. Clinical and linkage study on a consanguineous Chinese family with autosomal recessive high myopia. Molecular Vision. 2009;15:312.
59. Ma JH, Shen SH, Zhang GW, Zhao DS, Xu C, Pan CM, et al. Identification of a locus for autosomal dominant high myopia on chromosome 5p13.3-p15.1 in a Chinese family. Molecular Vision. 2010 Oct 12;16:2043-54. PubMed PMID: 21042559. Pubmed Central PMCID: Pmc2965568. Epub 2010/11/03. eng.
60. Shi Y, Qu J, Zhang D, Zhao P, Zhang Q, Tam POS, et al. Genetic variants at 13q12. 12 are associated with high myopia in the Han Chinese population. The American Journal of Human Genetics. 2011;88(6):805-13.
61. Shi Y, Li Y, Zhang D, Zhang H, Li Y, Lu F, et al. Exome sequencing identifies ZNF644 mutations in high myopia. PLoS Genetics. 2011;7(6):e1002084.
62. Paluru P, Ronan SM, Heon E, Devoto M, Wildenberg SC, Scavello G, et al. New locus for autosomal dominant high myopia maps to the long arm of chromosome 17. Investigative Ophthalmology & Visual Science. 2003;44(5):1830-6.
63. Tang WC, Yap MK, Yip SP. A review of current approaches to identifying human genes involved in myopia. Clinical and Experimental Optometry. 2008;91(1):4-22.
64. Spielman RS, McGinnis RE, Ewens WJ. Transmission test for linkage disequilibrium: the insulin gene region and insulin-dependent diabetes mellitus (IDDM). The American Journal of Human Genetics. 1993;52(3):506.
65 Li X, Ji BX, Zhu DL, Geng ZC, Chu RY. Studies of the association of pathological myopia in Chinese patients with HLA alleles. Yi Chuan Xue Bao. 1999;27(3):189-94.
66. Han W, Yap MK, Wang J, Yip SP. Family-based association analysis of hepatocyte growth factor (HGF) gene polymorphisms in high myopia. Investigative Ophthalmology & Visual Science. 2006;47(6):2291-9.
67. Han W, Leung KH, Fung WY, Mak JY, Li YM, Yap MK, et al. Association of PAX6 polymorphisms with high myopia in Han Chinese nuclear families. Investigative Ophthalmology & Visual Science. 2009;50(1):47-56.
68. Yanovitch T, Li Y-J, Metlapally R, Abbott D, Viet K-NT, Young TL. Hepatocyte growth factor and myopia: genetic association analyses in a Caucasian population. Molecular Vision. 2009;15:1028.
69. Metlapally R, Li Y-J, Tran-Viet K-N, Abbott D, Czaja GR, Malecaze F, et al. COL1A1 and COL2A1 genes and myopia susceptibility: evidence of association and suggestive linkage to the COL2A1 locus. Investigative Ophthalmology & Visual Science. 2009;50(9):4080-6.
70. Balding DJ. A tutorial on statistical methods for population association studies. Nature Reviews Genetics. 2006;7(10):781-91.

71. Nishizaki R, Ota M, Inoko H, Meguro A, Shiota T, Okada E, et al. New susceptibility locus for high myopia is linked to the uromodulin-like 1 (UMODL1) gene region on chromosome 21q22. 3. Eye. 2009;23(1):222-9.
72. Xiang X, Wang T, Tong P, Li Y, Guo H, Wan A, et al. New ZNF644 mutations identified in patients with high myopia. Molecular Vision. 2014;20:939.
73. Hysi PG, Simpson CL, Fok YK, Gerrelli D, Webster AR, Bhattacharya SS, et al. Common polymorphisms in the SERPINI2 gene are associated with refractive error in the 1958 British Birth Cohort. Investigative Ophthalmology & Visual Science. 2012;53(1):440-7.
74. Mutti DO, Cooper ME, Dragan E, Jones-Jordan LA, Bailey MD, Marazita ML, et al. Vitamin D Receptor (VDR) and Group-Specific Component (GC, Vitamin D–Binding Protein) Polymorphisms in Myopia. Investigative Ophthalmology & Visual Science. 2011;52(6):3818-24.
75. Nakanishi H, Yamada R, Gotoh N, Hayashi H, Yamashiro K, Shimada N, et al. A genome-wide association analysis identified a novel susceptible locus for pathological myopia at 11q24. 1. PLoS Genetics. 2009;5(9):e1000660.
76. Hysi PG, Young TL, Mackey DA, Andrew T, Fernández-Medarde A, Solouki AM, et al. A genome-wide association study for myopia and refractive error identifies a susceptibility locus at 15q25. Nature Genetics. 2010;42(10):902-5.
77. Solouki AM, Verhoeven VJ, Van Duijn CM, Verkerk AJ, Ikram MK, Hysi PG, et al. A genome-wide association study identifies a susceptibility locus for refractive errors and myopia at 15q14. Nature Genetics. 2010;42(10):897-901.
78. Verhoeven VJ, Hysi PG, Wojciechowski R, Fan Q, Guggenheim JA, Höhn R, et al. Genome-wide meta-analyses of multiancestry cohorts identify multiple new susceptibility loci for refractive error and myopia. Nature Genetics. 2013;45(3):314-8.
79. Kiefer AK, Tung JY, Do CB, Hinds DA, Mountain JL, Francke U, et al. Genome-wide analysis points to roles for extracellular matrix remodeling, the visual cycle, and neuronal development in myopia. PLoS Genetics. 2013;9(2):e1003299.
80. Pickrell JK, Berisa T, Liu JZ, Ségurel L, Tung JY, Hinds DA. Detection and interpretation of shared genetic influences on 42 human traits. Nature Genetics. 2016;48(7):709-17.
81. Guo H, Jin X, Zhu T, Wang T, Tong P, Tian L, et al. SLC39A5 mutations interfering with the BMP/TGF-β pathway in non-syndromic high myopia. Journal of Medical Genetics. 2014;51(8):518-25.
82. Jin ZB, Wu J, Huang XF, Feng CY, Cai XB, Mao JY, et al. Trio-based exome sequencing arrests de novo mutations in early-onset high myopia. Proceedings of the National Academy of Sciences. 2017;114(16):4219-24.
83. Sun W, Huang L, Xu Y, Xiao X, Li S, Jia X, et al. Exome Sequencing on 298 Probands With Early-Onset High Myopia: Approximately One-Fourth Show Potential Pathogenic Mutations in RetNet Genes. Investigative Ophthalmology & Visual Science. 2015;56(13):8365-72.
84. Wojciechowski R, Hysi PG. Focusing In on the complex genetics of myopia. PLoS Genetics. 2013;9(4):e1003442.
85. Hirschhorn JN, Lohmueller K, Byrne E, Hirschhorn K. A comprehensive review of genetic association studies. Genetics in Medicine. 2002;4(2):45-61.
86. Yu L, Li ZK, Gao JR, Liu JR, Xu CT. Epidemiology, genetics and treatments for myopia. International Journal of Ophthalmology. 2011;4(6):658-69. PubMed PMID: 22553740. Pubmed Central PMCID: 3340784.
87. Saw SM, Cheng A, Fong A, Gazzard G, Tan DT, Morgan I. School grades and myopia. Ophthalmic & Physiological Optics. 2007 Mar;27(2):126-9. PubMed PMID: 17324201.
88. Muhamedagic L, Muhamedagic B, Halilovic EA, Halimic JA, Stankovic A, Muracevic B. Relation between near work and myopia progression in student population. Materia socio-medica. 2014 Apr;26(2):100-3. PubMed PMID: 24944532. Pubmed Central PMCID: 4035135.
89. Ghosh A, Collins MJ, Read SA, Davis BA, Chatterjee P. Axial elongation associated with biomechanical factors during near work. Optometry and Vision Science. 2014 Mar;91(3):322-9. PubMed PMID: 24413276.
90. Saw SM, Chua WH, Hong CY, Wu HM, Chan WY, Chia KS, et al. Nearwork in early-onset myopia. Investigative Ophthalmology & Visual Science. 2002 Feb;43(2):332-9. PubMed PMID: 11818374.
91. Mutti DO, Zadnik K. Has near work's star fallen? Optometry and Vision Science. 2009;86(2):76-8.
92. Saw SM, Shankar A, Tan SB, Taylor H, Tan DT, Stone RA, et al. A cohort study of incident myopia in Singaporean children. Investigative Ophthalmology & Visual Science. 2006;47(5):1839-44.

93. Jones LA, Sinnott LT, Mutti DO, Mitchell GL, Moeschberger ML, Zadnik K. Parental history of myopia, sports and outdoor activities, and future myopia. Investigative Ophthalmology & Visual Science. 2007;48(8):3524.
94. Mirshahi A, Ponto KA, Hoehn R, Zwiener I, Zeller T, Lackner K, et al. Myopia and level of education: results from the Gutenberg Health Study. Ophthalmology. 2014;121(10):2047-52.
95. Cuellar-Partida G, Lu Y, Kho PF, Hewitt AW, Wichmann HE, Yazar S, et al. Assessing the Genetic Predisposition of Education on Myopia: A Mendelian Randomization Study. Genetic Epidemiology. 2016 Jan;40(1):66-72. PubMed PMID: 26497973.
96. He M, Xiang F, Zeng Y, Mai J, Chen Q, Zhang J, et al. Effect of time spent outdoors at school on the development of myopia among children in China: a randomized clinical trial. JAMA. 2015;314(11):1142-8.
97. Wu PC, Tsai CL, Wu HL, Yang YH, Kuo HK. Outdoor activity during class recess reduces myopia onset and progression in school children. Ophthalmology. 2013 May;120(5):1080-5. PubMed PMID: 23462271. Epub 2013/03/07. eng.
98. Sherwin JC, Reacher MH, Keogh RH, Khawaja AP, Mackey DA, Foster PJ. The association between time spent outdoors and myopia in children and adolescents: a systematic review and meta-analysis. Ophthalmology. 2012 Oct;119(10):2141-51. PubMed PMID: 22809757.
99. Rose KA, Morgan IG, Ip J, Kifley A, Huynh S, Smith W, et al. Outdoor activity reduces the prevalence of myopia in children. Ophthalmology. 2008;115(8):1279-85.
100. Jin JX, Hua WJ, Jiang X, Wu XY, Yang JW, Gao GP, et al. Effect of outdoor activity on myopia onset and progression in school-aged children in northeast China: the Sujiatun Eye Care Study. BMC Ophthalmology. 2015 Jul 9;15:73. PubMed PMID: 26152123.
101. Guggenheim JA, Northstone K, McMahon G, Ness AR, Deere K, Mattocks C, et al. Time outdoors and physical activity as predictors of incident myopia in childhood: a prospective cohort study. Investigative Ophthalmology & Visual Science. 2012 May;53(6):2856-65. PubMed PMID: 22491403. Pubmed Central PMCID: 3367471.
102. Feldkaemper M, Schaeffel F. An updated view on the role of dopamine in myopia. Experimental Eye Research. 2013 Sep;114:106-19. PubMed PMID: 23434455.
103. Lu B, Congdon N, Liu X, Choi K, Lam DS, Zhang M, et al. Associations between near work, outdoor activity, and myopia among adolescent students in rural China: the Xichang Pediatric Refractive Error Study report no. 2. Archives of Ophthalmology. 2009;127(6):769-75.
104. Jones-Jordan LA, Sinnott LT, Graham ND, Cotter SA, Kleinstein RN, Manny RE, et al. The contributions of near work and outdoor activity to the correlation between siblings in the Collaborative Longitudinal Evaluation of Ethnicity and Refractive Error (CLEERE) Study. Investigative Ophthalmology & Visual Science. 2014 Oct;55(10):6333-9. PubMed PMID: 25205866. Pubmed Central PMCID: 4193758.
105. Gardiner PA. Dietary treatment of myopia in children. Lancet. 1958 May 31;1(7031):1152-5. PubMed PMID: 13550953.
106. Cordain L, Eaton SB, Brand Miller J, Lindeberg S, Jensen C. An evolutionary analysis of the aetiology and pathogenesis of juvenile - onset myopia. Acta Ophthalmologica. 2002;80(2):125-35.
107. Lim LS, Gazzard G, Low YL, Choo R, Tan DT, Tong L, et al. Dietary factors, myopia, and axial dimensions in children. Ophthalmology. 2010 May;117(5):993-7 e4. PubMed PMID: 20079928.
108. Edwards MH, Chun CY, Leung SS. Intraocular pressure in an unselected sample of 6- to 7-year-old Chinese children. Optometry and Vision Science. 1993 Mar;70(3):198-200. PubMed PMID: 8483579.
109. Guggenheim JA, Williams C, Northstone K, Howe LD, Tilling K, St Pourcain B, et al. Does vitamin D mediate the protective effects of time outdoors on myopia? Findings from a prospective birth cohort. Investigative Ophthalmology & Visual Science. 2014;55(12):8550-8.
110. Mutti DO. Vitamin D may reduce the prevalence of myopia in Korean adolescents. Investigative Ophthalmology & Visual Science. 2014;55(4):2048-.
111. Choi JA, Han K, Park Y-M, La TY. Low serum 25-hydroxyvitamin D is associated with myopia in Korean adolescents. Investigative Ophthalmology & Visual Science. 2014;55(4):2041-7.
112. Cuellar-Partida G, Williams KM, Yazar S, Guggenheim JA, Hewitt AW, Williams C, et al. Genetically low vitamin D concentrations and myopic refractive error: a Mendelian randomization study. International Journal of Epidemiology. 2017 Jun 06. PubMed PMID: 28586461. Epub 2017/06/07. eng.
113. Mutti DO, Mitchell GL, Moeschberger ML, Jones LA, Zadnik K. Parental myopia, near work, school achievement, and children’s refractive error. Investigative Ophthalmology & Visual Science. 2002;43(12):3633-40.

114. Saw S, Tong L, Chia K, Koh D, Lee Y, Katz J, et al. The relation between birth size and the results of refractive error and biometry measurements in children. British Journal of Ophthalmology. 2004;88(4):538-42.
115. Ojaimi E, Robaei D, Rochtchina E, Rose KA, Morgan IG, Mitchell P. Impact of birth parameters on eye size in a population-based study of 6-year-old Australian children. American Journal of Ophthalmology. 2005;140(3):535. e1-. e.
116. Northstone K, Guggenheim JA, Howe LD, Tilling K, Paternoster L, Kemp JP, et al. Body stature growth trajectories during childhood and the development of myopia. Ophthalmology. 2013;120(5):1064-73. e1.
117. Ip JM, Rose KA, Morgan IG, Burlutsky G, Mitchell P. Myopia and the urban environment: findings in a sample of 12-year-old Australian school children. Investigative Ophthalmology & Visual Science. 2008;49(9):3858-63.
118. Morgan I, Rose K. How genetic is school myopia? Progress in Retinal and Eye Research. 2005;24(1):1-38.
119. O'Donoghue L, Kapetanankis VV, McClelland JF, Logan NS, Owen CG, Saunders KJ, et al. Risk factors for childhood myopia: findings from the NICER study. Investigative Ophthalmology & Visual Science. 2015;56(3):1524-30.
120. Lee YY, Lo CT, Sheu SJ, Yin LT. Risk Factors For and Progression of Myopia in Young Taiwanese Men. Ophthalmic Epidemiology. 2014 (0):1-8.
121. Verhoeven VJ, Buitendijk GH, Rivadeneira F, Uitterlinden AG, Vingerling JR, Hofman A, et al. Education influences the role of genetics in myopia. European Journal of Epidemiology. 2013;28(12):973-80.
122. Myrowitz EH. Juvenile myopia progression, risk factors and interventions. Saudi Journal of Ophthalmology. 2012;26(3):293-7.
123. Rudnicka AR, Owen CG, Richards M, Wadsworth ME, Strachan DP. Effect of breastfeeding and sociodemographic factors on visual outcome in childhood and adolescence. The American Journal of Clinical Nutrition. 2008;87(5):1392-9.
124. Gwiazda J, Deng L, Marsh-Tootle W, Group CS. The Association of Education and Occupation with Myopia in COMET Parents. Optometry and Vision Science. 2011;88(9):1045.
125. Rahi JS, Cumberland PM, Peckham CS. Myopia over the lifecourse: prevalence and early life influences in the 1958 British birth cohort. Ophthalmology. 2011;118(5):797-804.
126. Saw S, Chia K, Lindstrom J, Tan D, Stone R. Childhood myopia and parental smoking. British Journal of Ophthalmology. 2004;88(7):934-7.
127. Saw SM, Tan SB, Fung D, Chia KS, Koh D, Tan DT, et al. IQ and the association with myopia in children. Investigative Ophthalmology & Visual Science. 2004;45(9):2943-8.
128. Lyhne N, Sjolie AK, Kyvik KO, Green A. The importance of genes and environment for ocular refraction and its determiners: a population based study among 20-45 year old twins. British Journal of Ophthalmology. 2001 Dec;85(12):1470-6. PubMed PMID: 11734523. Pubmed Central PMCID: Pmc1723806. Epub 2001/12/06. eng.
129. Jinks JL, Fulker DW. Comparison of the biometrical genetical, MAVA, and classical approaches to the analysis of human behavior. Psychological Bulletin. 1970 May;73(5):311-49. PubMed PMID: 5528333. Epub 1970/05/01. eng.
130. Saw SM, Wu HM, Seet B, Wong TY, Yap E, Chia KS, et al. Academic achievement, close up work parameters, and myopia in Singapore military conscripts. British Journal of Ophthalmology. 2001;85(7):855-60.
131. Chan KY, Cheung SW, Cho P. Orthokeratology for slowing myopic progression in a pair of identical twins. Contact lens & anterior eye : the journal of the British Contact Lens Association. 2014 Apr;37(2):116-9. PubMed PMID: 24144551. Epub 2013/10/23. eng.
132. Zhong Y, Chen Z, Xue F, Miao H, Zhou X. Central and Peripheral Corneal Power Change in Myopic Orthokeratology and Its Relationship With 2-Year Axial Length Change. Investigative Ophthalmology & Visual Science. 2015 Jul;56(8):4514-9. PubMed PMID: 26200489. Epub 2015/07/23. eng.
133. Lam CS, Tang WC, Tse DY, Tang YY, To CH. Defocus Incorporated Soft Contact (DISC) lens slows myopia progression in Hong Kong Chinese schoolchildren: a 2-year randomised clinical trial. British Journal of Ophthalmology. 2014 Jan;98(1):40-5. PubMed PMID: 24169657. Pubmed Central PMCID: Pmc3888618. Epub 2013/10/31. eng.
134. Sun Y, Xu F, Zhang T, Liu M, Wang D, Chen Y, et al. Orthokeratology to Control Myopia Progression: A Meta-Analysis. PloS One. 2015;10(4).

135. Cho P, Cheung SW. Retardation of myopia in Orthokeratology (ROMIO) study: a 2-year randomized clinical trial. Investigative Ophthalmology & Visual Science. 2012;53(11):7077-85.
136. Anstice NS, Phillips JR. Effect of dual-focus soft contact lens wear on axial myopia progression in children. Ophthalmology. 2011;118(6):1152-61.
137. Aller TA, Liu M, Wildsoet CF. Myopia control with bifocal contact lenses: a randomized clinical trial. Optometry and Vision Science. 2016;93(4):344-52.
138. Sankaridurg P, Holden B, Smith E, Naduvilath T, Chen X, de la Jara PL, et al. Decrease in rate of myopia progression with a contact lens designed to reduce relative peripheral hyperopia: one-year results. Investigative Ophthalmology & Visual Science. 2011;52(13):9362-7.
139. Chia A, Chua WH, Cheung YB, Wong WL, Lingham A, Fong A, et al. Atropine for the treatment of childhood myopia: safety and efficacy of 0.5%, 0.1%, and 0.01% doses (Atropine for the Treatment of Myopia 2). Ophthalmology. 2012;119(2):347-54.
140. Yi S, Huang Y, Yu SZ, Chen XJ, Yi H, Zeng XL. Therapeutic effect of atropine 1% in children with low myopia. Journal of American Association for Pediatric Ophthalmology and Strabismus. 2015 Oct;19(5):426-9. PubMed PMID: 26228967. Epub 2015/08/01. eng.
141. Polling JR, Kok RG, Tideman JW, Meskat B, Klaver CC. Effectiveness study of atropine for progressive myopia in Europeans. Eye 2016 Jul;30(7):998-1004. PubMed PMID: 27101751. Pubmed Central PMCID: Pmc4941076. Epub 2016/04/23. eng.
142. Clark TY, Clark RA. Atropine 0.01% Eyedrops Significantly Reduce the Progression of Childhood Myopia. Journal of Ocular Pharmacology and Therapeutics. 2015 Nov;31(9):541-5. PubMed PMID: 26218150. Epub 2015/07/29. eng.
143. Wiesel TN, Raviola E. Myopia and eye enlargement after neonatal lid fusion in monkeys. Nature. 1977;266(5597):66-8.
144. Sherman SM, Norton TT, Casagrande VA. Myopia in the lid-sutured tree shrew (Tupaia glis). Brain Research. 1977 Mar 18;124(1):154-7. PubMed PMID: 843938. Epub 1977/03/18. eng.
145. Wallman J, Turkel J, Trachtman J. Extreme myopia produced by modest change in early visual experience. Science (New York, NY). 1978 Sep 29;201(4362):1249-51. PubMed PMID: 694514. Epub 1978/09/29. eng.
146. Andison ME, Sivak JG, Bird DM. The refractive development of the eye of the American kestrel (Falco sparverius): a new avian model. Journal of Comparative Physiology A. 1992 Jun;170(5):565-74. PubMed PMID: 1507156. Epub 1992/06/01. eng.
147. Troilo D, Judge SJ. Ocular development and visual deprivation myopia in the common marmoset (Callithrix jacchus). Vision Research. 1993 Jul;33(10):1311-24. PubMed PMID: 8333155. Epub 1993/07/01. eng.
148. Verolino M, Nastri G, Sellitti L, Costagliola C. Axial length increase in lid-sutured rabbits. Survey of Ophthalmology. 1999 Oct;44 Suppl 1:S103-8. PubMed PMID: 10548122. Epub 1999/11/05. eng.
149. Tejedor J, de la Villa P. Refractive changes induced by form deprivation in the mouse eye. Investigative Ophthalmology & Visual Science. 2003 Jan;44(1):32-6. PubMed PMID: 12506052. Epub 2002/12/31. eng.
150. McFadden SA, Howlett MH, Mertz JR. Retinoic acid signals the direction of ocular elongation in the guinea pig eye. Vision research. 2004 Mar;44(7):643-53. PubMed PMID: 14751549. Epub 2004/01/31. eng.
151. Shen W, Vijayan M, Sivak JG. Inducing form-deprivation myopia in fish. Investigative Ophthalmology & Visual Science. 2005 May;46(5):1797-803. PubMed PMID: 15851585. Epub 2005/04/27. eng.
152. Schaeffel F, Glasser A, Howland HC. Accommodation, refractive error and eye growth in chickens. Vision Research. 1988;28(5):639-57. PubMed PMID: 3195068. Epub 1988/01/01. eng.
153. Shaikh AW, Siegwart JT, Jr., Norton TT. Effect of interrupted lens wear on compensation for a minus lens in tree shrews. Optometry and Vision Science. 1999 May;76(5):308-15. PubMed PMID: 10375247. Epub 1999/06/22. eng.
154. Howlett MH, McFadden SA. Spectacle lens compensation in the pigmented guinea pig. Vision Research. 2009 Jan;49(2):219-27. PubMed PMID: 18992765. Epub 2008/11/11. eng.
155. Barathi VA, Boopathi VG, Yap EP, Beuerman RW. Two models of experimental myopia in the mouse. Vision Research. 2008 Mar;48(7):904-16. PubMed PMID: 18289630. Epub 2008/02/22. eng.
156. Troilo D, Totonelly K, Harb E. Imposed anisometropia, accommodation, and regulation of refractive state. Optometry and Vision Science. 2009 Jan;86(1):E31-9. PubMed PMID: 19104464. Pubmed Central PMCID: Pmc2702514. Epub 2008/12/24. eng.

157. Shen W, Sivak JG. Eyes of a lower vertebrate are susceptible to the visual environment. Investigative Ophthalmology & Visual Science. 2007 Oct;48(10):4829-37. PubMed PMID: 17898310. Epub 2007/09/28. eng.
158. Wallman J, Adams JI. Developmental aspects of experimental myopia in chicks: susceptibility, recovery and relation to emmetropization. Vision Research. 1987;27(7):1139-63. PubMed PMID: 3660666. Epub 1987/01/01. eng.
159. McBrien NA, Adams DW. A longitudinal investigation of adult-onset and adult-progression of myopia in an occupational group. Refractive and biometric findings. Investigative Ophthalmology & Visual Science. 1997 Feb;38(2):321-33. PubMed PMID: 9040464. Epub 1997/02/01. eng.
160. Curtin BJ. Pathologic myopia. Acta Ophthalmologica. 1988;185:105-6. PubMed PMID: 2853511. Epub 1988/01/01. eng.
161. McBrien NA, Gentle A. Role of the sclera in the development and pathological complications of myopia. Progress in Retinal and Eye Research. 2003 May;22(3):307-38. PubMed PMID: 12852489. Epub 2003/07/11. eng.
162. Hirata A, Negi A. Morphological changes of choriocapillaris in experimentally induced chick myopia. Graefe's Archive for Clinical and Experimental Ophthalmology. 1998 Feb;236(2):132-7. PubMed PMID: 9498124. Epub 1998/03/14. eng.
163. Wildsoet C, Wallman J. Choroidal and scleral mechanisms of compensation for spectacle lenses in chicks. Vision Research. 1995 May;35(9):1175-94. PubMed PMID: 7610579. Epub 1995/05/01. eng.
164. Siegwart JT, Jr., Norton TT. The susceptible period for deprivation-induced myopia in tree shrew. Vision Research. 1998 Nov;38(22):3505-15. PubMed PMID: 9893785. Epub 1999/01/20. eng.
165. von Noorden GK, Lewis RA. Ocular axial length in unilateral congenital cataracts and blepharoptosis. Investigative Ophthalmology & Visual Science. 1987 Apr;28(4):750-2. PubMed PMID: 3557880. Epub 1987/04/01. eng.
166. Ashby R, Ohlendorf A, Schaeffel F. The effect of ambient illuminance on the development of deprivation myopia in chicks. Investigative Ophthalmology & Visual Science. 2009 Nov;50(11):5348-54. PubMed PMID: 19516016. Epub 2009/06/12. eng.
167. Karouta C, Ashby RS. Correlation between light levels and the development of deprivation myopia. Investigative Ophthalmology & Visual Science. 2014 Dec 09;56(1):299-309. PubMed PMID: 25491298. Epub 2014/12/11. eng.
168. Backhouse S, Collins AV, Phillips JR. Influence of periodic vs continuous daily bright light exposure on development of experimental myopia in the chick. Ophthalmic & Physiological Optics. 2013 Sep;33(5):563-72. PubMed PMID: 23668224. Epub 2013/05/15. eng.
169. Smith EL, 3rd, Hung LF, Huang J. Protective effects of high ambient lighting on the development of form-deprivation myopia in rhesus monkeys. Investigative Ophthalmology & Visual Science. 2012 Jan 25;53(1):421-8. PubMed PMID: 22169102. Pubmed Central PMCID: Pmc3292375. Epub 2011/12/16. eng.
170. Ashby RS, Schaeffel F. The effect of bright light on lens compensation in chicks. Investigative Ophthalmology & Visual Science. 2010 Oct;51(10):5247-53. PubMed PMID: 20445123. Epub 2010/05/07. eng.
171. Foulds WS, Barathi VA, Luu CD. Progressive myopia or hyperopia can be induced in chicks and reversed by manipulation of the chromaticity of ambient light. Investigative Ophthalmology & Visual Science. 2013 Dec 09;54(13):8004-12. PubMed PMID: 24222304. Epub 2013/11/14. eng.
172. Smith EL, 3rd, Hung LF, Arumugam B, Holden BA, Neitz M, Neitz J. Effects of Long-Wavelength Lighting on Refractive Development in Infant Rhesus Monkeys. Investigative Ophthalmology & Visual Science. 2015 Oct;56(11):6490-500. PubMed PMID: 26447984.
173. Gawne TJ, Ward AH, Norton TT. Long-wavelength (red) light produces hyperopia in juvenile and adolescent tree shrews. Vision Research. 2017 Aug 29;140:55-65. PubMed PMID: 28801261. Epub 2017/08/13. eng.
174. Di Y, Liu R, Chu R-Y, Zhou X-T, Zhou X-D. Myopia induced by flickering light in guinea pigs: a detailed assessment on susceptibility of different frequencies. International Journal of Ophthalmology. 2013;6(2):115.
175. Crewther SG, Barutchu A, Murphy MJ, Crewther DP. Low frequency temporal modulation of light promotes a myopic shift in refractive compensation to all spectacle lenses. Experimental Eye Research. 2006 Aug;83(2):322-8. PubMed PMID: 16579985. Epub 2006/04/04. eng.
176. Stone RA, Lin T, Laties AM, Iuvone PM. Retinal dopamine and form-deprivation myopia. Proceedings of the National Academy of Sciences. 1989 Jan;86(2):704-6. PubMed PMID: 2911600. Pubmed Central PMCID: Pmc286542. Epub 1989/01/01. eng.

177. Iuvone PM, Tigges M, Stone RA, Lambert S, Laties AM. Effects of apomorphine, a dopamine receptor agonist, on ocular refraction and axial elongation in a primate model of myopia. Investigative Ophthalmology & Visual Science. 1991 Apr;32(5):1674-7. PubMed PMID: 2016144. Epub 1991/04/01. eng.
178. Jiang L, Long K, Schaeffel F, Zhou X, Zheng Y, Ying H, et al. Effects of dopaminergic agents on progression of naturally occurring myopia in albino guinea pigs (Cavia porcellus). Investigative Ophthalmology & Visual Science. 2014 Sep 30;55(11):7508-19. PubMed PMID: 25270191. Epub 2014/10/02. eng.
179. Doi T, Puri P, Bannigan J, Thompson J. HoxB2, HoxB4 and Alx4 genes are downregulated in the cadmium-induced omphalocele in the chick model. Pediatric surgery international. 2010 Oct;26(10):1017-23. PubMed PMID: 20625746. Epub 2010/07/14. eng.
180. Pendrak K, Nguyen T, Lin T, Capehart C, Zhu X, Stone RA. Retinal dopamine in the recovery from experimental myopia. Current Eye Research. 1997 Feb;16(2):152-7. PubMed PMID: 9068946. Epub 1997/02/01. eng.
181. Megaw PL, Morgan IG, Boelen MK. Dopaminergic behaviour in chicken retina and the effect of form deprivation. Australian and New Zealand Journal of Ophthalmology. 1997 May;25 Suppl 1:S76-8. PubMed PMID: 9267633. Epub 1997/05/01. eng.
182. Feldkaemper M, Diether S, Kleine G, Schaeffel F. Interactions of spatial and luminance information in the retina of chickens during myopia development. Experimental Eye Research. 1999 Jan;68(1):105-15. PubMed PMID: 9986748. Epub 1999/02/13. eng.
183. Fischer AJ, McGuire JJ, Schaeffel F, Stell WK. Light- and focus-dependent expression of the transcription factor ZENK in the chick retina. Nature Neuroscience. 1999 Aug;2(8):706-12. PubMed PMID: 10412059. Epub 1999/07/21. eng.
184. Schippert R, Burkhardt E, Feldkaemper M, Schaeffel F. Relative axial myopia in Egr-1 (ZENK) knockout mice. Investigative Ophthalmology & Visual Science. 2007 Jan;48(1):11-7. PubMed PMID: 17197510. Epub 2007/01/02. eng.
185. Howland HC, Howland M, Murphy CJ. Refractive state of the rhinoceros. Vision Research. 1993 Dec;33(18):2649-51. PubMed PMID: 8296461. Epub 1993/12/01. eng.
186. Bracun A, Ellis AD, Hall C. A retinoscopic survey of 333 horses and ponies in the UK. Veterinary Ophthalmology. 2014 Jul;17 Suppl 1:90-6. PubMed PMID: 24636019. Epub 2014/03/19. eng.
187. Murphy CJ, Zadnik K, Mannis MJ. Myopia and refractive error in dogs. Investigative Ophthalmology & Visual Science. 1992 Jul;33(8):2459-63. PubMed PMID: 1634344. Epub 1992/07/01. eng.
188. Mutti DO, Zadnik K, Murphy CJ. Naturally occurring vitreous chamber-based myopia in the Labrador retriever. Investigative Ophthalmology & Visual Science. 1999 Jun;40(7):1577-84. PubMed PMID: 10359340. Epub 1999/06/08. eng.
189. Black J, Browning SR, Collins AV, Phillips JR. A canine model of inherited myopia: familial aggregation of refractive error in labrador retrievers. Investigative Ophthalmology & Visual Science. 2008 Nov;49(11):4784-9. PubMed PMID: 18566472. Epub 2008/06/21. eng.
190. Jiang L, Schaeffel F, Zhou X, Zhang S, Jin X, Pan M, et al. Spontaneous axial myopia and emmetropization in a strain of wild-type guinea pig (Cavia porcellus). Investigative Ophthalmology & Visual Science. 2009 Mar;50(3):1013-9. PubMed PMID: 19029033. Epub 2008/11/26. eng.
191. Schaeffel F, Feldkaemper M. Animal models in myopia research. Clinical & Experimental Optometry. 2015 Nov;98(6):507-17. PubMed PMID: 26769177. Epub 2016/01/16. eng.
192. Schaeffel F, Howland HC. Corneal accommodation in chick and pigeon. Journal of Comparative Physiology. 1987 Mar;160(3):375-84. PubMed PMID: 3572853. Epub 1987/03/01. eng.
193. Troilo D, Wallman J. Changes in corneal curvature during accommodation in chicks. Vision Research. 1987;27(2):241-7. PubMed PMID: 3576984. Epub 1987/01/01. eng.
194. Schmid KL, Wildsoet CF. Effects on the compensatory responses to positive and negative lenses of intermittent lens wear and ciliary nerve section in chicks. Vision Research. 1996 Apr;36(7):1023-36. PubMed PMID: 8736261. Epub 1996/04/01. eng.
195. Chen YP, Hocking PM, Wang L, Povazay B, Prashar A, To CH, et al. Selective breeding for susceptibility to myopia reveals a gene-environment interaction. Investigative Ophthalmology & Visual Science. 2011 Jun 08;52(7):4003-11. PubMed PMID: 21436268. Epub 2011/03/26. eng.
196. Phillips JR. Monovision slows juvenile myopia progression unilaterally. British Journal of Ophthalmology. 2005 Sep;89(9):1196-200. PubMed PMID: 16113381. Pubmed Central PMCID: Pmc1772844. Epub 2005/08/23. eng.

197. Montiani-Ferreira F, Li T, Kiupel M, Howland H, Hocking P, Curtis R, et al. Clinical features of the retinopathy, globe enlarged (rge) chick phenotype. Vision Research. 2003;43(19):2009-18.
198. Troilo D, Li T, Glasser A, Howland HC. Differences in eye growth and the response to visual deprivation in different strains of chicken. Vision Research. 1995;35(9):1211-6.
199. Wallman J, Ledoux C, Friedman MB. Simple devices for restricting the visual fields of birds. Behavior Research Methods. 1978;10(3):401-3.
200. Hodos W, Kuenzel W. Retinal-image degradation produces ocular enlargement in chicks. Investigative Ophthalmology & Visual Science. 1984;25(6):652-9.
201. Irving EL, Callender MG, Sivak JG. Inducing myopia, hyperopia, and astigmatism in chicks. Optometry and Vision Science. 1991 May;68(5):364-8. PubMed PMID: 1852398. Epub 1991/05/01. eng.
202. Papastergiou GI, Schmid GF, Laties AM, Pendrak K, Lin T, Stone RA. Induction of axial eye elongation and myopic refractive shift in one-year-old chickens. Vision Research. 1998;38(12):1883-8.
203. Guggenheim JA, Erichsen JT, Hocking PM, Wright NF, Black R. Similar genetic susceptibility to form-deprivation myopia in three strains of chicken. Vision Research. 2002;42(25):2747-56.
204. Schmid K, Wildsoet C. Breed-and gender-dependent differences in eye growth and form deprivation responses in chick. Journal of Comparative Physiology A: Neuroethology, Sensory, Neural, and Behavioral Physiology. 1996;178(4):551-61.
205. Chen YP. Role of genetics in susceptibility to environmentally-induced myopia: Cardiff University (United Kingdom); 2010.
206. Schmucker C, Schaeffel F. In vivo biometry in the mouse eye with low coherence interferometry. Vision Research. 2004;44(21):2445-56. PubMed PMID: 15358080. Epub 2004/09/11. eng.
207. Glickstein M, Millodot M. Retinoscopy and eye size. Science (New York, NY). 1970 May 01;168(3931):605-6. PubMed PMID: 5436596. Epub 1970/05/01. eng.
208. Glasser A, Howland HC. A history of studies of visual accommodation in birds. The Quarterly Review of Biology. 1996;71(4):475-509.
209. Sakamoto K, Endo K, Suzuki T, Fujimura K, Kurauchi Y, Mori A, et al. P2X7 receptor antagonists protect against N-methyl-D-aspartic acid-induced neuronal injury in the rat retina. European Journal of Pharmacology. 2015;756:52-8.
210. Sloan RC, Rosenbaum M, O'Rourke D, Oppelt K, Frasier CR, Waston CA, et al. High doses of ketamine–xylazine anesthesia reduce cardiac ischemia–reperfusion injury in guinea pigs. Journal of the American Association for Laboratory Animal Science. 2011;50(3):349-54.
211. Arango-Gonzalez B, Schatz A, Bolz S, Eslava-Schmalbach J, Willmann G, Zhour A, et al. Effects of combined ketamine/xylazine anesthesia on light induced retinal degeneration in rats. PLoS One. 2012;7(4):e35687.
212. Schifilliti D, Grasso G, Conti A, Fodale V. Anaesthetic-related neuroprotection. CNS Drugs. 2010;24(11):893-907.
213. Cabral ADM, Kapusta DR, Kenigs VA, Varner KJ. Central α 2-receptor mechanisms contribute to enhanced renal responses during ketamine-xylazine anesthesia. American Journal of Physiology-Regulatory, Integrative and Comparative Physiology. 1998;275(6):R1867-R74.
214. Vucicevic M, Stevanov-Pavlovic M, Stevanovic J, Bosnjak J, Gajic B, Aleksic N, et al. Sex determination in 58 bird species and evaluation of CHD gene as a universal molecular marker in bird sexing. Zoo Biology. 2013 May-Jun;32(3):269-76. PubMed PMID: 22553188. Epub 2012/05/04. eng.
215. Wong T, Foster P, Johnson G, Seah S. Education, socioeconomic status, and ocular dimensions in Chinese adults: the Tanjong Pagar Survey. British Journal of Ophthalmology. 2002;86(9):963-8.
216. Dirani M, Islam A, Baird PN. Body stature and myopia—the genes in myopia (GEM) twin study. Ophthalmic Epidemiology. 2008;15(3):135-9.
217. Wong TY, Foster PJ, Johnson GJ, Klein BE, Seah SK. The relationship between ocular dimensions and refraction with adult stature: the Tanjong Pagar Survey. Investigative Ophthalmology & Visual Science. 2001;42(6):1237-42.
218. Saw SM, Chua WH, Hong CY, Wu HM, Chia KS, Stone RA, et al. Height and its relationship to refraction and biometry parameters in Singapore Chinese children. Investigative Ophthalmology & Visual Science. 2002 May;43(5):1408-13. PubMed PMID: 11980854. Epub 2002/05/01. eng.
219. Zhang J, Hur YM, Huang W, Ding X, Feng K, He M. Shared genetic determinants of axial length and height in children: the Guangzhou twin eye study. Archives of Ophthalmology. 2011;129(1):63-8.
220. Lim LS, Saw S-, Jeganathan VSE, Tay WT, Aung T, Tong L, et al. Distribution and determinants of ocular biometric parameters in an Asian population: the Singapore Malay eye study. Investigative Ophthalmology & Visual Science. 2010;51(1):103-9.
221. Teikari JM. Myopia and stature. Acta Ophthalmologica. 1987;65(6):673-6.

222. Rosner M, Laor A, Belkin M. Myopia and stature: findings in a population of 106,926 males. European Journal of Ophthalmology. 1995;5(1):1-6.
223. Sharma A, Congdon N, Gao Y, Lu Y, Ye Y, Wu J, et al. Height, stunting, and refractive error among rural Chinese schoolchildren: the See Well to Learn Well project. American Journal of Ophthalmology. 2010;149(2):347-53. e1.
224. Jung S-K, Lee JH, Kakizaki H, Jee D. Prevalence of myopia and its association with body stature and educational level in 19-year-old male conscripts in Seoul, South Korea. Investigative Ophthalmology & Visual Science. 2012;53(9):5579-83.
225. Gardiner P. The relation of myopia to growth. Lancet. 1954;263(6810):476-9.
226. Baldwin WR. A review of statistical studies of relations between myopia and ethnic, behavioral, and physiological characteristics. Optometry and Vision Science. 1981;58(7):516-27.
227. Krause U, Krause K, P R. Sex differences in refraction errors up to the age of 15. Acta Ophthalmologica. 1982;60(6):917-26.
228. Šelović A, Juresa V, Ivankovic D, Malcic D, Šelović Bobonj G. Relationship between axial length of the emmetropic eye and the age, body height, and body weight of schoolchildren. American Journal of Human Biology. 2005;17(2):173-7.
229. Wu HM, Gupta A, Newland HS, Selva D, Aung T, Casson RJ. Association between stature, ocular biometry and refraction in an adult population in rural Myanmar: the Meiktila eye study. Clinical & Experimental Optometry. 2007;35(9):834-9.
230. Huang CY, Hou CH, Lin KK, Lee JS, Yang ML. Relationship of lifestyle and body stature growth with the development of myopia and axial length elongation in Taiwanese elementary school children. Indian Journal of Ophthalmology. 2014;62(8):865.
231. Terasaki H, Yamashita T, Yoshihara N, Kii Y, Sakamoto T. Association of lifestyle and body structure to ocular axial length in Japanese elementary school children. BMC Ophthalmology. 2017;17(1):123.
232. Roy A, Kar M, Mandal D, Ray RS, Kar C. Variation of axial ocular dimensions with age, sex, height, BMI-and their relation to refractive status. Journal of Clinical and Diagnostic Research. 2015;9(1):AC01.
233. Wang Q, Klein B, Klein R, Moss SE. Refractive status in the Beaver Dam Eye Study. Investigative Ophthalmology & Visual Science. 1994;35(13):4344-7.
234. Midelfart A, Kinge B, Midelfart S, Lydersen S. Prevalence of refractive errors in young and middle‐aged adults in Norway. Acta Ophthalmologica. 2002;80(5):501-5.
235. Angle J, Wissmann D. The epidemiology of myopia. American Journal of Epidemiology. 1980;111(2):220-8.
236. Hyman L, Gwiazda J, Hussein M, Norton TT, Wang Y, Marsh-Tootle W, et al. Relationship of age, sex, and ethnicity with myopia progression and axial elongation in the correction of myopia evaluation trial. Archives of Ophthalmology. 2005;123(7):977-87.
237. Lundberg K, Suhr Thykjær A, Søgaard Hansen R, Vestergaard AH, Jacobsen N, Goldschmidt E, et al. Physical activity and myopia in Danish children—The CHAMPS Eye Study. Acta Ophthalmologica. 2017.
238. Richter GM, Wang M, Jiang X, Wu S, Wang D, Torres M, et al. Ocular determinants of refractive error and its age-and sex-related variations in the Chinese American Eye Study. JAMA Ophthalmology. 2017.
239. Wong TY, Foster PJ, Ng TP, Tielsch JM, Johnson GJ, Seah SK. Variations in ocular biometry in an adult Chinese population in Singapore: the Tanjong Pagar Survey. Investigative Ophthalmology & Visual Science. 2001;42(1):73-80.
240. He M, Huang W, Li Y, Zheng Y, Yin Q, Foster PJ. Refractive error and biometry in older Chinese adults: the Liwan eye study. Investigative Ophthalmology & Visual Science. 2009;50(11):5130-6.
241. Tan C, Chan Y, Wong TY, Gazzard G, Niti M, Ng TP, et al. Prevalence and risk factors for refractive errors and ocular biometry parameters in an elderly Asian population: the Singapore Longitudinal Aging Study (SLAS). Eye. 2011;25(10):1294.
242. Shimizu N, Nomura H, Ando F, Niino N, Miyake Y, Shimokata H. Refractive errors and factors associated with myopia in an adult Japanese population. Japanese Journal of Ophthalmology. 2003;47(1):6-12.
243. Lee KE, Klein BE, Klein R, Quandt Z, Wong TY. Association of age, stature, and education with ocular dimensions in an older white population. Archives of Ophthalmology. 2009;127(1):88-93.
244. Zhou G, Williams RW. Mouse models for the analysis of myopia: an analysis of variation in eye size of adult mice. Optometry and Vision Science. 1999;76(6):408-18.

245. Brooke MdL, Hanley S, Laughlin S. The scaling of eye size with body mass in birds. Proceedings of the Royal Society of London B: Biological Sciences. 1999;266(1417):405-12.
246. Blaxter JH. The Early Life History of Fish: The Proceedings of an International Symposium Held at the Dunstaffnage Marine Research Laboratory of the Scottish Marine Biological Association at Oban, Scotland, from May 17–23, 1973: Springer Science & Business Media; 2012.
247. Zhou G, Williams RW. Eye1 and Eye2: gene loci that modulate eye size, lens weight, and retinal area in the mouse. Investigative Ophthalmology & Visual Science. 1999;40(5):817-25.
248. Puk O, Dalke C, Favor J, de Angelis MH, Graw J. Variations of eye size parameters among different strains of mice. Mammalian Genome. 2006;17(8):851-7.
249. Murphy CJ, Zadnik K, Mannis M. Myopia and refractive error in dogs. Investigative Ophthalmology & Visual Science. 1992;33(8):2459-63.
250. Kitaya N, Ishiko S, Yoshida A, Mori F, Abiko T, Kagokawa H, et al. Gender differences in tree shrew eyes with growth and experimental myopia. Myopia Updates: Springer; 1998. p. 331-5.
251. Valentini S, Castagnetti C, Musella V, Spinella G. Assessment of Intraocular Measurements in Neonatal Foals and Association with Gender, Laterality, and Body Weight: A Clinical Study. PLoS One. 2014;9(10):e109491.
252. Zhu X, Lin T, Stone RA, Laties AM. Sex differences in chick eye growth and experimental myopia. Experimental Eye Research. 1995;61(2):173-9.
253. Chen YP, Prashar A, Hocking PM, Erichsen JT, To CH, Schaeffel F, et al. Sex, eye size, and the rate of myopic eye growth due to form deprivation in outbred white leghorn chickens. Investigative Ophthalmology & Visual Science. 2010;51(2):651-7.
254. Sng CC, Foo LL, Cheng CY, Allen JC, He M, Krishnaswamy G, et al. Determinants of anterior chamber depth: the Singapore Chinese Eye Study. Ophthalmology. 2012;119(6):1143-50.
255. Leivo MZ, Elson PJ, Tacha DE, Delahunt B, Hansel DE. A combination of p40, GATA-3 and uroplakin II shows utility in the diagnosis and prognosis of muscle-invasive urothelial carcinoma. Pathology. 2016;48(6):543-9.
256. Hongyue W, Jing P, Bokai W, Xiang L, Julia ZZ, Kejia W, et al. Inconsistency between univariate and multiple logistic regressions. Shanghai Archives of Psychiatry. 2017;29(2):124.
257. Scholz K, Messner A, Eppig T, Bruenner H, Langenbucher A. Topography-based assessment of anterior corneal curvature and asphericity as a function of age, sex, and refractive status. Journal of Cataract & Refractive Surgery. 2009;35(6):1046-54.
258. Chen H, Lin H, Lin Z, Chen J, Chen W. Distribution of axial length, anterior chamber depth, and corneal curvature in an aged population in South China. BMC Ophthalmology. 2016 May 1;16(1):47. PubMed PMID: 27138378. Pubmed Central PMCID: PMC4852406. Epub 2016/05/04. eng.
259. Fotedar R, Wang JJ, Burlutsky G, Morgan IG, Rose K, Wong TY, et al. Distribution of axial length and ocular biometry measured using partial coherence laser interferometry (IOL Master) in an older white population. Ophthalmology. 2010 Mar;117(3):417-23. PubMed PMID: 20031227. Epub 2009/12/25. eng.
260. Gottlieb MD, Fugate-Wentzek LA, Wallman J. Different visual deprivations produce different ametropias and different eye shapes. Investigative Ophthalmology & Visual Science. 1987;28(8):1225-35.
261. Saltarelli D, Wildsoet C, Nickla D, Troilo D. Susceptibility to form-deprivation myopia in chicks is not altered by an early experience of axial myopia. Optometry and Vision Science. 2004;81(2):119-26.
262. Troilo D, Nickla DL. The response to visual form deprivation differs with age in marmosets. Investigative Ophthalmology & Visual Science. 2005;46(6):1873-81.
263. Prashar A, Hocking PM, Erichsen JT, Fan Q, Saw SM, Guggenheim JA. Common determinants of body size and eye size in chickens from an advanced intercross line. Experimental Eye Research. 2009;89(1):42-8.
264. Leach N, Wallis N, Lothringer L, Olson J. Corneal hydration changes during the normal menstrual cycle--a preliminary study. The Journal of Reproductive Medicine. 1971;6(5):201.
265. Gupta P, Johar K, Nagpal K, Vasavada A. Sex hormone receptors in the human eye. Survey of Ophthalmology. 2005;50(3):274-84.
266. Dillingham CM, Guggenheim JA, Erichsen JT. Disruption of the centrifugal visual system inhibits early eye growth in chicks. Investigative Ophthalmology & Visual Science. 2013 May 1;54(5):3632-43. PubMed PMID: 23599339. Epub 2013/04/20. eng.
267. Vallortigara G, Regolin L, Bortolomiol G, Tommasi L. Lateral asymmetries due to preferences in eye use during visual discrimination learning in chicks. Behavioural Brain Research. 1996;74(1):135-43.
268. Mench J, Andrew R. Lateralization of a food search task in the domestic chick. Behavioral and Neural Biology. 1986;46(2):107-14.

269. Dogan E, Yanmaz L, Senocak M, Okumus Z. Comparison of propofol, ketamine and ketofol on intraocular pressure in New Zealand white rabbits. Revue de Medecine Veterinaire. 2016;167(1-2):18-21.
270. Yang H, Stone R, Civan M. Effects of anesthesia on mouse IOP: Ketamine vs. ketamine/xylazine. Investigative Ophthalmology & Visual Science. 2004;45(13):5041-.
271. Read SA, Collins MJ, Iskander DR. Diurnal variation of axial length, intraocular pressure, and anterior eye biometrics. Investigative Ophthalmology & Visual Science. 2008;49(7):2911-8.
272. Meng W, Butterworth J, Bradley DT, Hughes AE, Soler V, Calvas P, et al. A Genome-Wide Association Study Provides Evidence for Association of Chromosome 8p23 (MYP10) and 10q21. 1 (MYP15) with High Myopia in the French Population. Investigative Ophthalmology & Visual Science. 2012;53(13):7983-8.
273. Fan Q, Verhoeven VJ, Wojciechowski R, Barathi VA, Hysi PG, Guggenheim JA, et al. Meta-analysis of gene–environment-wide association scans accounting for education level identifies additional loci for refractive error. Nature Communications. 2016;7:11008.
274. Fan Q, Guo X, Tideman JWL, Williams KM, Yazar S, Hosseini SM, et al. Childhood gene-environment interactions and age-dependent effects of genetic variants associated with refractive error and myopia: The CREAM Consortium. Scientific Reports. 2016;6.
275. Wojciechowski R, Yee SS, Simpson CL, Bailey-Wilson JE, Stambolian D. Matrix metalloproteinases and educational attainment in refractive error: evidence of gene–environment interactions in the age-related eye disease study. Ophthalmology. 2013;120(2):298-305.
276. Tkatchenko AV, Tkatchenko TV, Guggenheim JA, Verhoeven VJ, Hysi PG, Wojciechowski R, et al. APLP2 regulates refractive error and myopia development in mice and humans. PLoS Genetics. 2015;11(8):e1005432.
277. Winham SJ, Biernacka JM. Gene – environment interactions in genome – wide association studies: current approaches and new directions. Journal of Child Psychology and Psychiatry. 2013;54(10):1120-34.
278. Van Ijzendoorn MH, Bakermans-Kranenburg MJ, Belsky J, Beach S, Brody G, Dodge KA, et al. Gene-by-environment experiments: a new approach to finding the missing heritability. Nature Reviews Genetics. 2011;12(12):881-.
279. Aschard H, Lutz S, Maus B, Duell EJ, Fingerlin TE, Chatterjee N, et al. Challenges and opportunities in genome-wide environmental interaction (GWEI) studies. Human Genetics. 2012;131(10):1591-613.
280. Karl T, Arnold JC. Schizophrenia: a consequence of gene-environment interactions? Frontiers in Behavioral Neuroscience. 2014;8.
281. Hoffmann TJ, Kvale MN, Hesselson SE, Zhan Y, Aquino C, Cao Y, et al. Next generation genome-wide association tool: design and coverage of a high-throughput European-optimized SNP array. Genomics. 2011 Aug;98(2):79-89. PubMed PMID: 21565264. Pubmed Central PMCID: PMC3146553. Epub 2011/05/14. eng.
282. Dalma – Weiszhausz DD, Warrington J, Tanimoto EY, Miyada CG. The Affymetrix GeneChip® Platform: An Overview. Methods in Enzymology. 2006;410:3-28.
283. Ragoussis J. Genotyping technologies for genetic research. Annual Review of Genomics and Human Genetics. 2009;10:117-33. PubMed PMID: 19453250. Epub 2009/05/21. eng.
284. Perkel J. SNP genotyping: six technologies that keyed a revolution. Nature Publishing Group; 2008.
285. Muir W, Wong G, Zhang Y, Wang J, Groenen M, Crooijmans R, et al. Review of the initial validation and characterization of a 3K chicken SNP array. World's Poultry Science Journal. 2008;64(2):219-26.
286. Groenen MA, Wahlberg P, Foglio M, Cheng HH, Megens H-J, Crooijmans RP, et al. A high-density SNP-based linkage map of the chicken genome reveals sequence features correlated with recombination rate. Genome Research. 2009;19(3):510-9.
287. Elferink MG, van As P, Veenendaal T, Crooijmans RP, Groenen MA. Regional differences in recombination hotspots between two chicken populations. BMC Genomics. 2010;11(1):11.
288. Groenen MA, Megens H-J, Zare Y, Warren WC, Hillier LW, Crooijmans RP, et al. The development and characterization of a 60K SNP chip for chicken. BMC Genomics. 2011;12(1):274.
289. Kranis A, Gheyas AA, Boschiero C, Turner F, Yu L, Smith S, et al. Development of a high density 600K SNP genotyping array for chicken. BMC Genomics. 2013;14(1):59.
290. Fu W, Dekkers JC, Lee WR, Abasht B. Linkage disequilibrium in crossbred and pure line chickens. Genetics Selection Evolution. 2015;47(1):11.

291. Luo C, Qu H, Ma J, Wang J, Li C, Yang C, et al. Genome-wide association study of antibody response to Newcastle disease virus in chicken. BMC Genomics. 2013;14(1):42.
292. Morota G, Abdollahi-Arpanahi R, Kranis A, Gianola D. Genome-enabled prediction of quantitative traits in chickens using genomic annotation. BMC Genomics. 2014;15(1):109.
293. Abdollahi‐Arpanahi R, Pakdel A, Nejati‐Javaremi A, Moradi Shahrbabak M, Morota G, Valente B, et al. Dissection of additive genetic variability for quantitative traits in chickens using SNP markers. Journal of Animal Breeding and Genetics. 2014;131(3):183-93.
294. Gheyas AA, Burt DW. Microarray resources for genetic and genomic studies in chicken: a review. Genesis. 2013;51(5):337-56.
295. Thermo Fisher Scientific. The Axiom™ Genotyping Solution 2017 [cited 2018 17, June]. Available from: http://www.affymetrix.com/products_services/arrays/specific/mirna_array_plate.affx.
296. Scientific TF. Affymetrix Axiom® Automated Target Preparation on Affymetrix® NIMBUS® Target Preparation Instrument Waltham: Thermo Fisher Scientific; 2017 [cited 2017 20 Dec]. Available from: https://www.affymetrix.com/products_services/instruments/specific/axiom_atp.affx#1_1.
297. Chang CC, Chow CC, Tellier LC, Vattikuti S, Purcell SM, Lee JJ. Second-generation PLINK: rising to the challenge of larger and richer datasets. Gigascience. 2015;4(1):1.
298. Consortium WTCC. Genome-wide association study of 14,000 cases of seven common diseases and 3,000 shared controls. Nature. 2007;447(7145):661.
299. Wise AL, Gyi L, Manolio TA. eXclusion: toward integrating the X chromosome in genome-wide association analyses. The American Journal of Human Genetics. 2013;92(5):643-7.
300. König IR, Loley C, Erdmann J, Ziegler A. How to include chromosome x in your genome‐wide association study. Genetic Epidemiology. 2014;38(2):97-103.
301. Gauderman WJ. Sample size requirements for matched case‐control studies of gene‐environment interaction. Statistics In Medicine. 2002;21(1):35-50.
302. Price AL, Zaitlen NA, Reich D, Patterson N. New approaches to population stratification in genome-wide association studies. Nature Reviews Genetics. 2010;11(7):459.
303. Loh PR, Tucker G, Bulik-Sullivan BK, Vilhjalmsson BJ, Finucane HK, Salem RM, et al. Efficient Bayesian mixed-model analysis increases association power in large cohorts. Nature Genetics. 2015 Mar;47(3):284-90. PubMed PMID: 25642633. Pubmed Central PMCID: PMC4342297. Epub 2015/02/03. eng.
304. Kutalik Z, Johnson T, Bochud M, Mooser V, Vollenweider P, Waeber G, et al. Methods for testing association between uncertain genotypes and quantitative traits. Biostatistics (Oxford, England). 2011 Jan;12(1):1-17. PubMed PMID: 20543033. Epub 2010/06/15. eng.
305. Zhou X, Stephens M. Genome-wide efficient mixed-model analysis for association studies. Nature Genetics. 2012;44(7):821-4.
306. Devlin B, Roeder K. Genomic control for association studies. Biometrics. 1999;55(4):997-1004.
307. Reed E, Nunez S, Kulp D, Qian J, Reilly MP, Foulkes AS. A guide to genome-wide association analysis and post-analytic interrogation. Statistics In Medicine. 2015 Dec 10;34(28):3769-92. PubMed PMID: 26343929. Pubmed Central PMCID: PMC5019244. Epub 2015/09/08. eng.
308. Franke T. PI3K/Akt: getting it right matters. Oncogene. 2008;27(50):6473.
309. Penha AM, Burkhardt E, Schaeffel F, Feldkaemper MP. Effects of intravitreal insulin and insulin signaling cascade inhibitors on emmetropization in the chick. Molecular Vision. 2012;18:2608-22. PubMed PMID: 23112573. Pubmed Central PMCID: Pmc3482168. Epub 2012/11/01. eng.
310. Feldkaemper MP, Neacsu I, Schaeffel F. Insulin acts as a powerful stimulator of axial myopia in chicks. Investigative Ophthalmology & Visual Science. 2009;50(1):13-23.
311. Lin HJ, Wei CC, Chang CY, Chen TH, Hsu YA, Hsieh YC, et al. Role of Chronic Inflammation in Myopia Progression: Clinical Evidence and Experimental Validation. EBioMedicine. 2016;10:269-81.
312. Trewhella J. Protein kinase A targeting and activation as seen by small-angle solution scattering. European Journal of Cell Biology. 2006;85(7):655-62.
313. Lorenowicz MJ, Fernandez-Borja M, Hordijk PL. cAMP signaling in leukocyte transendothelial migration. Arteriosclerosis, Thrombosis, and Vascular Biology. 2007;27(5):1014-22.
314. Schippert R, Schaeffel F, Feldkaemper MP. Microarray analysis of retinal gene expression in chicks during imposed myopic defocus. Molecular Vision. 2008;14:1589.
315. Mataruga A, Kremmer E, Müller F. Type 3a and type 3b OFF cone bipolar cells provide for the alternative rod pathway in the mouse retina. Journal of Comparative Neurology. 2007;502(6):1123-37.
316. Parisiadou L, Yu J, Sgobio C, Xie C, Liu G, Sun L, et al. LRRK2 regulates synaptogenesis and dopamine receptor activation through modulation of PKA activity. Nature Neuroscience. 2014;17(3):367-76.

317. Mohammadi Asl J, Tabatabaiefar MA, Galehdari H, Riahi K, Masbi MH, Zargar Shoshtari Z, et al. UGT1A1 gene mutation due to Crigler-Najjar syndrome in Iranian patients: identification of a novel mutation. BioMed Research International. 2013;2013:342371. PubMed PMID: 24286076. Pubmed Central PMCID: PMC3826477. Epub 2013/11/29. eng.
318. Sun L, Li M, Zhang L, Teng X, Chen X, Zhou X, et al. Differences in UGT1A1 gene mutations and pathological liver changes between Chinese patients with Gilbert syndrome and Crigler-Najjar syndrome type II. Medicine 2017 Nov;96(45):e8620. PubMed PMID: 29137095. Epub 2017/11/16. eng.
319. Andrews JS, Futterman S. Metabolism of the retina. 5. The role of microsomes in vitamin A esterification in the visual cycle. Journal of Biological Chemistry. 1964;239:4073-6.
320. Zhong M, Kawaguchi R, Kassai M, Sun H. Retina, retinol, retinal and the natural history of vitamin A as a light sensor. Nutrients. 2012;4(12):2069-96.
321. Seko Y, Shimizu M, Tokoro T. Retinoic acid increases in the retina of the chick with form deprivation myopia. Ophthalmic Research. 1998;30(6):361-7.
322. Mertz J, Howlett M, McFadden S, Wallman J, editors. Retinoic acid from both the retina and choroid influences eye growth. Investigative Ophthalmology & Visual Science; 1999.
323. Bitzer M, Feldkaemper M, Schaeffel F. Visually induced changes in components of the retinoic acid system in fundal layers of the chick. Experimental Eye Research. 2000;70(1):97-106.
324. Mertz JR, Walliam J. Choroidal retinoic acid synthesis: a possible mediator between refractive error and compensatory eye growth. Experimental Eye Research. 2000;70(4):519-27.
325. Sasaki S, Ota M, Meguro A, Nishizaki R, Okada E, Mok J, et al. A single nucleotide polymorphism analysis of the LAMA1 gene in Japanese patients with high myopia. Clinical Ophthalmology 2007;1(3):289.
326. Hayes B, Fitzke F, Hodos W, Holden A. A morphological analysis of experimental myopia in young chickens. Investigative Ophthalmology & Visual Science. 1986;27(6):981-91.
327. Howlett MH, McFadden SA. Form-deprivation myopia in the guinea pig (Cavia porcellus). Vision Research. 2006;46(1):267-83.
328. Qiao-Grider Y, Hung L-F, Kee C-s, Ramamirtham R, Smith EL. Recovery from form-deprivation myopia in rhesus monkeys. Investigative Ophthalmology & Visual Science. 2004;45(10):3361-72.
329. Smith EL, Hung L-F. Form-deprivation myopia in monkeys is a graded phenomenon. Vision Research. 2000;40(4):371-81.
330. Guggenheim JA, McBrien NA. Form-deprivation myopia induces activation of scleral matrix metalloproteinase-2 in tree shrew. Investigative Ophthalmology & Visual Science. 1996;37(7):1380-95.
331. McBrien NA, Cornell LM, Gentle A. Structural and ultrastructural changes to the sclera in a mammalian model of high myopia. Investigative Ophthalmology & Visual Science. 2001;42(10):2179-87.
332. Yang J, Weedon MN, Purcell S, Lettre G, Estrada K, Willer CJ, et al. Genomic inflation factors under polygenic inheritance. European Journal of Human Genetics. 2011;19(7):807.
333. Yu J, Pressoir G, Briggs WH, Bi IV, Yamasaki M, Doebley JF, et al. A unified mixed-model method for association mapping that accounts for multiple levels of relatedness. Nature Genetics. 2006;38(2):203.
334. Yang J, Zaitlen NA, Goddard ME, Visscher PM, Price AL. Advantages and pitfalls in the application of mixed-model association methods. Nature Genetics. 2014;46(2):100-6.
335. Plomin R, Haworth CM, Davis OS. Common disorders are quantitative traits. Nature Reviews Genetics. 2009;10(12):872.
336. Chan Y, Holmen OL, Dauber A, Vatten L, Havulinna AS, Skorpen F, et al. Common variants show predicted polygenic effects on height in the tails of the distribution, except in extremely short individuals. PLoS Genetics. 2011;7(12):e1002439.
337. Li D, Lewinger JP, Gauderman WJ, Murcray CE, Conti D. Using extreme phenotype sampling to identify the rare causal variants of quantitative traits in association studies. Genetic Epidemiology. 2011;35(8):790-9.
338. Guey LT, Kravic J, Melander O, Burtt NP, Laramie JM, Lyssenko V, et al. Power in the phenotypic extremes: a simulation study of power in discovery and replication of rare variants. Genetic Epidemiology. 2011;35(4):236-46.
339. Potkin SG, Turner JA, Guffanti G, Lakatos A, Torri F, Keator DB, et al. Genome-wide strategies for discovering genetic influences on cognition and cognitive disorders: methodological considerations. Cognitive Neuropsychiatry. 2009;14(4-5):391-418.
340. Ward LD, Kellis M. Interpreting noncoding genetic variation in complex traits and human disease. Nature Biotechnology. 2012 Nov;30(11):1095-106. PubMed PMID: 23138309. Pubmed Central PMCID: 3703467.

341. Civelek M, Lusis AJ. Systems genetics approaches to understand complex traits. Nature Reviews Genetics. 2014;15(1):34-48.
342. Kadarmideen HN, Reverter A. Combined genetic, genomic and transcriptomic methods in the analysis of animal traits. CABI review: Perspectives in Agriculture, Eterinary Science, Nutrition and Natural Resources. 2007;2(042):16.
343. Kadarmideen HN, von Rohr P, Janss LL. From genetical genomics to systems genetics: potential applications in quantitative genomics and animal breeding. Mammalian Genome. 2006;17(6):548-64.
344. Sharon-Friling R, Richardson J, Sperbeck S, Lee D, Rauchman M, Maas R, et al. Lens-specific gene recruitment of ζ-crystallin through Pax6, Nrl-Maf, and brain suppressor sites. Molecular and Cellular Biology. 1998;18(4):2067-76.
345. Pinelli M, Carissimo A, Cutillo L, Lai C-H, Mutarelli M, Moretti MN, et al. An atlas of gene expression and gene co-regulation in the human retina. Nucleic Acids Research. 2016:gkw486.
346. Guo L, Frost MR, He L, Siegwart JT, Norton TT. Gene expression signatures in tree shrew sclera in response to three myopiagenic conditions. Investigative Ophthalmology & Visual Science. 2013;54(10):6806-19.
347. Li YI, van de Geijn B, Raj A, Knowles DA, Petti AA, Golan D, et al. RNA splicing is a primary link between genetic variation and disease. Science (New York, NY). 2016;352(6285):600-4.
348. Xu X, Li S, Xiao X, Wang P, Guo X, Zhang Q. Sequence variations of GRM6 in patients with high myopia. 2009.
349. Caminsky NG, Mucaki EJ, Rogan PK. Interpretation of mRNA splicing mutations in genetic disease: review of the literature and guidelines for information-theoretical analysis. F1000Research. 2015;3.
350. Schadt EE, Lamb J, Yang X, Zhu J, Edwards S, GuhaThakurta D, et al. An integrative genomics approach to infer causal associations between gene expression and disease. Nature Genetics. 2005;37(7):710-7.
351. Chun S, Casparino A, Patsopoulos NA, Croteau-Chonka DC, Raby BA, De Jager PL, et al. Limited statistical evidence for shared genetic effects of eQTLs and autoimmune-disease-associated loci in three major immune-cell types. Nature Genetics. 2017 Apr;49(4):600-5. PubMed PMID: 28218759. Pubmed Central PMCID: PMC5374036. Epub 2017/02/22. eng.
352. Norton TT, Essinger JA, McBrien NA. Lid-suture myopia in tree shrews with retinal ganglion cell blockade. Visual Neuroscience. 1994;11(01):143-53.
353. Mcbrien NA, Moghaddam HO, Cottriall CL, Leech EM, Cornell LM. The effects of blockade of retinal cell action potentials on ocular growth, emmetropization and form deprivation myopia in young chicks. Vision Research. 1995;35(9):1141-52.
354. George A, Schmid KL, Pow DV. Retinal serotonin, eye growth and myopia development in chick. Experimental Eye Research. 2005 Nov;81(5):616-25. PubMed PMID: 15949800. Epub 2005/06/14. eng.
355. Wang JC, Chun RK, Zhou YY, Zuo B, Li KK, Liu Q, et al. Both the central and peripheral retina contribute to myopia development in chicks. Ophthalmic & Physiological Optics. 2015 Nov;35(6):652-62. PubMed PMID: 26271934. Epub 2015/08/15. eng.
356. Sheng C, Zhu X, Wallman J. In vitro effects of insulin and RPE on choroidal and scleral components of eye growth in chicks. Experimental Eye Research. 2013 Nov;116:439-48. PubMed PMID: 23994438. Epub 2013/09/03. eng.
357. Rohrer B, Stell WK. Basic fibroblast growth factor (bFGF) and transforming growth factor beta (TGF-beta) act as stop and go signals to modulate postnatal ocular growth in the chick. Experimental Eye Research. 1994 May;58(5):553-61. PubMed PMID: 7925692. Epub 1994/05/01. eng.
358. Nickla DL, Wildsoet C, Wallman J. Compensation for spectacle lenses involves changes in proteoglycan synthesis in both the sclera and choroid. Current Eye Research. 1997 Apr;16(4):320-6. PubMed PMID: 9134320. Epub 1997/04/01. eng.
359. Guo L, Frost MR, Siegwart JT, Jr., Norton TT. Scleral gene expression during recovery from myopia compared with expression during myopia development in tree shrew. Molecular Vision. 2014;20:1643-59. PubMed PMID: 25540576. Pubmed Central PMCID: PMC4265769. Epub 2014/12/30. eng.
360. Ohngemach S, Buck C, Simon P, Schaeffel F, Feldkaemper M. Temporal changes of novel transcripts in the chicken retina following imposed defocus. Molecular Vision. 2004 Dec 28;10:1019-27. PubMed PMID: 15635295. Epub 2005/01/07. eng.
361. McGlinn AM, Baldwin DA, Tobias JW, Budak MT, Khurana TS, Stone RA. Form-deprivation myopia in chick induces limited changes in retinal gene expression. Investigative Ophthalmology & Visual

Science. 2007 Aug;48(8):3430-6. PubMed PMID: 17652709. Pubmed Central PMCID: PMC1983368. Epub 2007/07/27. eng.
362. He L, Frost MR, Siegwart JT, Jr., Norton TT. Gene expression signatures in tree shrew choroid during lens-induced myopia and recovery. Experimental Eye Research. 2014 Jun;123:56-71. Epub 2014/04/20. eng.
363. Industries A. Next Generation Sequencing (NGS) Experimental Design New York: ABM Industries; 2017 [cited 2017 20 Dec]. Available from: https://www.abmgood.com/marketing/knowledge_base/next_generation_sequencing_experimental_design.php.
364. Metzker ML. Sequencing technologies—the next generation. Nature Reviews Genetics. 2010;11(1):31.
365. Robinson MD, McCarthy DJ, Smyth GK. edgeR: a Bioconductor package for differential expression analysis of digital gene expression data. Bioinformatics. 2010;26(1):139-40.
366. Love MI, Huber W, Anders S. Moderated estimation of fold change and dispersion for RNA-seq data with DESeq2. Genome Biology. 2014;15(12):550.
367. Ritchie ME, Phipson B, Wu D, Hu Y, Law CW, Shi W, et al. limma powers differential expression analyses for RNA-sequencing and microarray studies. Nucleic Acids Research. 2015;43(7):e47-e.
368. Chen H, Boutros PC. VennDiagram: a package for the generation of highly-customizable Venn and Euler diagrams in R. BMC Bioinformatics. 2011;12(1):35.
369. Anders S, McCarthy DJ, Chen Y, Okoniewski M, Smyth GK, Huber W, et al. Count-based differential expression analysis of RNA sequencing data using R and Bioconductor. Nature Protocols. 2013;8(9):1765-86.
370. Soneson C, Delorenzi M. A comparison of methods for differential expression analysis of RNA-seq data. BMC Bioinformatics. 2013;14(1):91.
371. Stone RA, McGlinn AM, Baldwin DA, Tobias JW, Iuvone PM, Khurana TS. Image defocus and altered retinal gene expression in chick: clues to the pathogenesis of ametropia. Investigative Ophthalmology & Visual Science. 2011;52(8):5765-77.
372. Barathi VA, Chaurasia SS, Poidinger M, Koh SK, Tian D, Ho C, et al. Involvement of GABA transporters in atropine-treated myopic retina as revealed by iTRAQ quantitative proteomics. Journal of Proteome Research. 2014;13(11):4647-58.
373. Seltner RLP, Stell WK. The effect of vasoactive intestinal peptide on development of form deprivation myopia in the chick: a pharmacological and immunocytochemical study. Vision Research. 1995;35(9):1265-70.
374. Cakmak AI, Basmak H, Gursoy H, Ozkurt M, Yildirim N, Erkasap N, et al. Vasoactive intestinal peptide, a promising agent for myopia? International Journal of Ophthalmology. 2017;10(2):211.
375. Mathis U, Schaeffel F. Glucagon-related peptides in the mouse retina and the effects of deprivation of form vision. Graefe's Archive for Clinical and Experimental Ophthalmology. 2007;245(2):267.
376. Stone RA, Laties AM, Raviola E, Wiesel TN. Increase in retinal vasoactive intestinal polypeptide after eyelid fusion in primates. Proceedings of the National Academy of Sciences. 1988;85(1):257-60.
377. Hsi E, Chen KC, Chang WS, Yu ML, Liang CL, Juo SH. A functional polymorphism at the FGF10 gene is associated with extreme myopia. Investigative Ophthalmology & Visual Science. 2013 May 07;54(5):3265-71. PubMed PMID: 23599340. Epub 2013/04/20. eng.
378. Yoshida M, Meguro A, Okada E, Nomura N, Mizuki N. Association study of fibroblast growth factor 10 (FGF10) polymorphisms with susceptibility to extreme myopia in a Japanese population. Molecular Vision. 2013;19:2321.
379. Chen T-C, Lin K-T, Chen C-H, Lee S-A, Lee P-Y, Liu Y-W, et al. Using an in situ proximity ligation assay to systematically profile endogenous protein–protein interactions in a pathway network. Journal of Proteome Research. 2014;13(12):5339-46.
380. Brock C, Schaefer M, Reusch HP, Czupalla C, Michalke M, Spicher K, et al. Roles of Gβγ in membrane recruitment and activation of p110γ/p101 phosphoinositide 3-kinase γ. The Journal of Cell Biology. 2003;160(1):89-99.
381. Jean S, Kiger AA. Classes of phosphoinositide 3-kinases at a glance. The Company of Biologists Ltd; 2014.
382. Ashby R, Kozulin P, Megaw PL, Morgan IG. Alterations in ZENK and glucagon RNA transcript expression during increased ocular growth in chickens. Molecular Vision. 2010 Apr 13;16:639-49. PubMed PMID: 20405027. Pubmed Central PMCID: Pmc2855734. Epub 2010/04/21. eng.

383. Feldkaemper MP, Burkhardt E, Schaeffel F. Localization and regulation of glucagon receptors in the chick eye and preproglucagon and glucagon receptor expression in the mouse eye. Experimental Eye Research. 2004 Sep;79(3):321-9. PubMed PMID: 15336494. Epub 2004/09/01. eng.
384. Feldkaemper MP, Schaeffel F. Evidence for a potential role of glucagon during eye growth regulation in chicks. Visual Neuroscience. 2002 Nov-Dec;19(6):755-66. PubMed PMID: 12688670. Epub 2003/04/12. eng.
385. Vessey KA, Lencses KA, Rushforth DA, Hruby VJ, Stell WK. Glucagon receptor agonists and antagonists affect the growth of the chick eye: a role for glucagonergic regulation of emmetropization? Investigative Ophthalmology & Visual Science. 2005 Nov;46(11):3922-31. PubMed PMID: 16249465. Pubmed Central PMCID: Pmc1483902. Epub 2005/10/27. eng.
386. Vessey KA, Rushforth DA, Stell WK. Glucagon- and secretin-related peptides differentially alter ocular growth and the development of form-deprivation myopia in chicks. Investigative Ophthalmology & Visual Science. 2005 Nov;46(11):3932-42. PubMed PMID: 16249466. Epub 2005/10/27. eng.
387. Zhu X, Wallman J. Opposite effects of glucagon and insulin on compensation for spectacle lenses in chicks. Investigative Ophthalmology & Visual Science. 2009 Jan;50(1):24-36. PubMed PMID: 18791176. Pubmed Central PMCID: Pmc2755053. Epub 2008/09/16. eng.
388. Mak JY, Yap MK, Fung WY, Ng PW, Yip SP. Association of IGF1 gene haplotypes with high myopia in Chinese adults. Archives of Ophthalmology. 2012;130(2):209-16.
389. Zhang X, Zhou X, Qu X. The association between IGF-1 polymorphisms and high myopia. International Journal of Clinical and Experimental Medicine. 2015;8(6):10158-67.
390. Rydzanicz M, Nowak DM, Karolak JA, Frajdenberg A, Podfigurna-Musielak M, Mrugacz M, et al. IGF-1 gene polymorphisms in Polish families with high-grade myopia. Molecular Vision. 2011 2011(17):11.
391. Zidan HE, Rezk NA, Fouda SM, Mattout HK. Association of Insulin-Like Growth Factor-1 Gene Polymorphisms with Different Types of Myopia in Egyptian Patients. Genetic Testing and Molecular Biomarkers. 2016;20(6):291-6.
392. Mohan S, Nakao Y, Honda Y, Landale E, Leser U, Dony C, et al. Studies on the mechanisms by which insulin-like growth factor (IGF) binding protein-4 (IGFBP-4) and IGFBP-5 modulate IGF actions in bone cells. Journal of Biological Chemistry. 1995;270(35):20424-31.
393. Rees C, Clemmons DR, Horvitz G, Clarke J, Busby W. A Protease-Resistant Form of Insulin-Like Growth Factor (IGF) Binding Protein 4 Inhibits IGF-1 Actions 1. Endocrinology. 1998;139(10):4182-8.
394. Xie Y, Mo Z, Chen K, Yang Y, Xing X, Liao E. Effect of different glucose concentrations on the expressions of insig-1 and insig-2 mRNA during the differentiation of 3T3-L1 cells. Zhong Nan Da Xue Xue Bao. 2008;33(3):238-44.
395. Galvis V, López-Jaramillo P, Tello A, Castellanos-Castellanos YA, Camacho PA, Cohen DD, et al. Is myopia another clinical manifestation of insulin resistance? Medical Hypotheses. 2016;90:32-40.
396. Lu Y, Vitart V, Burdon KP, Khor CC, Bykhovskaya Y, Mirshahi A, et al. Genome-wide association analyses identify multiple loci associated with central corneal thickness and keratoconus. Nature Genetics. 2013;45(2):155-63.
397. Leveziel N, Yu Y, Reynolds R, Tai A, Meng W, Caillaux V, et al. Genetic factors for choroidal neovascularization associated with high myopia. Investigative Ophthalmology & Visual Science. 2012;53(8):5004-9.
398. Springelkamp H, Höhn R, Mishra A, Hysi PG, Khor C-C, Loomis SJ, et al. Meta-analysis of genome-wide association studies identifies novel loci that influence cupping and the glaucomatous process. Nature Communications. 2014;5.
399. Ramprasad VL, Sripriya S, Ronnie G, Nancarrow D, Saxena S, Hemamalini A, et al. Genetic homogeneity for inherited congenital microcoria loci in an Asian Indian pedigree. Molecular Vision. 2005;11:934-40.
400. Sturm RA, Frudakis TN. Eye colour: portals into pigmentation genes and ancestry. Trends in Genetics. 2004;20(8):327-32.
401. Riddell N, Crewther SG. Novel evidence for complement system activation in chick myopia and hyperopia models: a meta-analysis of transcriptome datasets. Scientific Reports. 2017;7(1):9719.
402. Hoffmann M, Schaeffel F. Melatonin and deprivation myopia in chickens. Neurochemistry International. 1996;28(1):95-107.
403. Iandiev I, Biedermann B, Reichenbach A, Wiedemann P, Bringmann A. Expression of aquaporin-9 immunoreactivity by catecholaminergic amacrine cells in the rat retina. Neuroscience Letters. 2006;398(3):264-7.

404. Crewther SG, Giummarra L, Murphy-Edwards MJ. Hifs Seeing The Light-Hypoxia Inducible Factors During Recovery From Form Deprivation Myopia. Investigative Ophthalmology & Visual Science. 2011;52(14):3924-.
405. Dibas A, Yang MH, Bobich J, Yorio T. Stress-induced changes in neuronal Aquaporin-9 (AQP9) in a retinal ganglion cell-line. Pharmacological Research. 2007;55(5):378-84.
406. Miki A, Kanamori A, Negi A, Naka M, Nakamura M. Loss of aquaporin 9 expression adversely affects the survival of retinal ganglion cells. The American Journal of Pathology. 2013;182(5):1727-39.
407. Goodyear MJ, Crewther SG, Murphy MJ, Giummarra L, Hazi A, Junghans BM, et al. Spatial and temporal dissociation of AQP4 and Kir4. 1 expression during induction of refractive errors. Molecular Vision. 2010;16:1610.
408. Graveley BR. Alternative splicing: increasing diversity in the proteomic world. Trends in Genetics. 2001;17(2):100-7.
409. Chen M, Manley JL. Mechanisms of alternative splicing regulation: insights from molecular and genomics approaches. Nature Reviews Molecular cell biology. 2009;10(11):741.
410. Kvam VM, Liu P, Si Y. A comparison of statistical methods for detecting differentially expressed genes from RNA-seq data. American Journal of Botany. 2012;99(2):248-56.
411. Wang K, Li M, Hakonarson H. Analysing biological pathways in genome-wide association studies. Nature Reviews Genetics. 2010;11(12):843-54.
412. Khatri P, Sirota M, Butte AJ. Ten years of pathway analysis: current approaches and outstanding challenges. PLoS Computational Biology. 2012;8(2):e1002375.
413. Huang DW, Sherman BT, Lempicki RA. Systematic and integrative analysis of large gene lists using DAVID bioinformatics resources. Nature Protocols. 2009;4(1):44-57.
414. de Leeuw CA, Neale BM, Heskes T, Posthuma D. The statistical properties of gene-set analysis. Nature Reviews Genetics. 2016;17(6):353-64.
415. Hindorff LA, Sethupathy P, Junkins HA, Ramos EM, Mehta JP, Collins FS, et al. Potential etiologic and functional implications of genome-wide association loci for human diseases and traits. Proceedings of the National Academy of Sciences of the United States of America. 2009;106(23):9362-7.
416. Farh KK-H, Marson A, Zhu J, Kleinewietfeld M, Housley WJ, Beik S, et al. Genetic and epigenetic fine mapping of causal autoimmune disease variants. Nature. 2015;518(7539):337-43.
417. Javierre BM, Burren OS, Wilder SP, Kreuzhuber R, Hill SM, Sewitz S, et al. Lineage-specific genome architecture links enhancers and non-coding disease variants to target gene promoters. Cell. 2016;167(5):1369-84. e19.
418. Hou L, Zhao H. A review of post-GWAS prioritization approaches. Frontiers in Genetics. 2013;4.
419. Cantor RM, Lange K, Sinsheimer JS. Prioritizing GWAS results: a review of statistical methods and recommendations for their application. The American Journal of Human Genetics. 2010;86(1):6-22.
420. Duerr RH, Taylor KD, Brant SR, Rioux JD, Silverberg MS, Daly MJ, et al. A genome-wide association study identifies IL23R as an inflammatory bowel disease gene. Science (New York, NY). 2006;314(5804):1461-3.
421. Barrett JC, Hansoul S, Nicolae DL, Cho JH, Duerr RH, Rioux JD, et al. Genome-wide association defines more than 30 distinct susceptibility loci for Crohn's disease. Nature Genetics. 2008;40(8):955-62.
422. Pasaniuc B, Price AL. Dissecting the genetics of complex traits using summary association statistics. Nature Reviews Genetics. 2017;18(2):117-27.
423. de Leeuw CA, Mooij JM, Heskes T, Posthuma D. MAGMA: generalized gene-set analysis of GWAS data. PLoS Computational Biology. 2015;11(4):e1004219.
424. Thomas PD, Campbell MJ, Kejariwal A, Mi H, Karlak B, Daverman R, et al. PANTHER: a library of protein families and subfamilies indexed by function. Genome Research. 2003;13(9):2129-41.
425. Zheng Q, Wang XJ. GOEAST: a web-based software toolkit for Gene Ontology enrichment analysis. Nucleic Acids Research. 2008;36(suppl_2):W358-W63.
426. Subramanian A, Tamayo P, Mootha VK, Mukherjee S, Ebert BL, Gillette MA, et al. Gene set enrichment analysis: a knowledge-based approach for interpreting genome-wide expression profiles. Proceedings of the National Academy of Sciences. 2005;102(43):15545-50.
427. Mootha VK, Lindgren CM, Eriksson K-F, Subramanian A, Sihag S, Lehar J, et al. PGC-1α-responsive genes involved in oxidative phosphorylation are coordinately downregulated in human diabetes. Nature Genetics. 2003;34(3):267-73.
428. Guttman M, Amit I, Garber M, French C, Lin MF, Feldser D, et al. Chromatin signature reveals over a thousand highly conserved large non-coding RNAs in mammals. Nature. 2009;458(7235):223-7.
429. Houstis N, Rosen ED, Lander ES. Reactive oxygen species have a causal role in multiple forms of insulin resistance. Nature. 2006;440(7086):944-8.

430. Khalil AM, Guttman M, Huarte M, Garber M, Raj A, Morales DR, et al. Many human large intergenic noncoding RNAs associate with chromatin-modifying complexes and affect gene expression. Proceedings of the National Academy of Sciences. 2009;106(28):11667-72.
431. Walter W, Sánchez-Cabo F, Ricote M. GOplot: an R package for visually combining expression data with functional analysis. Bioinformatics. 2015;31(17):2912-4.
432. Yu G, Wang L-G, Han Y, He Q-Y. clusterProfiler: an R package for comparing biological themes among gene clusters. Omics: A Journal of Integrative Biology. 2012;16(5):284-7.
433. Merico D, Isserlin R, Stueker O, Emili A, Bader GD. Enrichment map: a network-based method for gene-set enrichment visualization and interpretation. PloS One. 2010;5(11):e13984.
434. Jensen LS, Matson WE. Enlargement of avian eye by subjecting chicks to continuous incandescent illumination. Science (New York, NY). 1957;125(3251):741-.
435. Lauber JK, McGinnis J. Eye lesions in domestic fowl reared under continuous light. Vision Research. 1966;6(11):619-IN15.
436. Osol G, Schwartz B, Foss DC. The effects of photoperiod and lid suture on eye growth in chickens. Investigative Ophthalmology & Visual Science. 1986;27(2):255-60.
437. Norton TT, Amedo AO, Siegwart JT, Jr. Darkness causes myopia in visually experienced tree shrews. Investigative Ophthalmology & Visual Science. 2006 Nov;47(11):4700-7. PubMed PMID: 17065476. Pubmed Central PMCID: PMC1978105. Epub 2006/10/27. eng.
438. Stone RA, Lin T, Desai D, Capehart C. Photoperiod, early post-natal eye growth, and visual deprivation. Vision Research. 1995 May;35(9):1195-202. PubMed PMID: 7610580. Epub 1995/05/01. eng.
439. Nickla DL. Ocular diurnal rhythms and eye growth regulation: Where we are 50 years after Lauber. Experimental Eye Research. 2013;114:25-34.
440. Moring AG, Baker JR, Norton TT. Modulation of glycosaminoglycan levels in tree shrew sclera during lens-induced myopia development and recovery. Investigative Ophthalmology & Visual Science. 2007;48(7):2947-56.
441. Norton TT, Rada JA. Reduced extracellular matrix in mammalian sclera with induced myopia. Vision Research. 1995;35(9):1271-81.
442. Harper AR, Summers JA. The dynamic sclera: extracellular matrix remodeling in normal ocular growth and myopia development. Experimental Eye Research. 2015;133:100-11.
443. Li Q, Wojciechowski R, Simpson CL, Hysi PG, Verhoeven VJ, Ikram MK, et al. Genome-wide association study for refractive astigmatism reveals genetic co-determination with spherical equivalent refractive error: the CREAM consortium. Human Genetics. 2015 Feb;134(2):131-46. PubMed PMID: 25367360. Pubmed Central PMCID: 4291519.
444. McBrien NA, Metlapally R, Jobling AI, Gentle A. Expression of collagen-binding integrin receptors in the mammalian sclera and their regulation during the development of myopia. Investigative Ophthalmology & Visual Science. 2006 Nov;47(11):4674-82. PubMed PMID: 17065473. Epub 2006/10/27. eng.
445. Sickel W. Electrical and metabolic manifestations of receptor and higher-order neuron activity in vertebrate retina. The Visual System: Springer; 1972. p. 101-18.
446. Riddell N, Giummarra L, Hall NE, Crewther SG. Bidirectional Expression of Metabolic, Structural, and Immune Pathways in Early Myopia and Hyperopia. Frontiers in Neuroscience. 2016;10:390. PubMed PMID: 27625591. Pubmed Central PMCID: Pmc5003873. Epub 2016/09/15. eng.
447. Shih YF, Horng IH, YangCH, Lin LLK, Peng Y, Hung PT. Ocular pulse amplitude in myopia. Journal of Association for Ocular Pharmacology and Therapeutics. 1991;7(1):83-7.
448. Francisco B-M, Salvador M, Amparo N. Oxidative stress in myopia. Oxidative Medicine and Cellular Longevity. 2015;2015.
449. Yang J, Reinach PS, Zhang S, Pan M, Sun W, Liu B, et al. Changes in retinal metabolic profiles associated with form deprivation myopia development in guinea pigs. Scientific Reports. 2017;7(1):2777.
450. Hysi PG, Wojciechowski R, Rahi JS, Hammond CJ. Genome-wide association studies of refractive error and myopia, lessons learned, and implications for the future. Investigative Ophthalmology & Visual Science. 2014 May 29;55(5):3344-51. PubMed PMID: 24876304. Pubmed Central PMCID: Pmc4039381. Epub 2014/05/31. eng.
451. Technology CS. Insulin Receptor Signaling Interactive Pathway Leiden: Cell Signaling Technology; 2016 [cited 2017 20 Dec]. Available from: https://www.cellsignal.com/contents/science-cst-pathways-cellular-metabolism/insulin-receptor-signaling-interactive-pathway/pathways-irs.
452. Boucher J, Kleinridders A, Kahn CR. Insulin receptor signaling in normal and insulin-resistant states. Cold Spring Harbor Perspectives in Biology. 2014;6(1):a009191.

453. Tang Rh, Tan J, Deng Zh, Zhao Sz, Miao Yb, Zhang Wj. Insulin‐like growth factor‐2 antisense oligonucleotides inhibits myopia by expression blocking of retinal insulin‐like growth factor‐2 in guinea pig. Clinical & Experimental Optometry. 2012;40(5):503-11.
454. Kusakari T, Sato T, Tokoro T. Visual deprivation stimulates the exchange of the fibrous sclera into the cartilaginous sclera in chicks. Experimental Eye Research. 2001;73(4):533-46.
455. Gentle A, Liu Y, Martin JE, Conti GL, McBrien NA. Collagen gene expression and the altered accumulation of scleral collagen during the development of high myopia. Journal of Biological Chemistry. 2003 May 09;278(19):16587-94. PubMed PMID: 12606541. Epub 2003/02/28. eng.
456. Rada JA, Brenza HL. Increased latent gelatinase activity in the sclera of visually deprived chicks. Investigative Ophthalmology & Visual Science. 1995 Jul;36(8):1555-65. PubMed PMID: 7601636. Epub 1995/07/01. eng.
457. Rada JA, Perry CA, Slover ML, Achen VR. Gelatinase A and TIMP-2 expression in the fibrous sclera of myopic and recovering chick eyes. Investigative Ophthalmology & Visual Science. 1999 Dec;40(13):3091-9. PubMed PMID: 10586929. Epub 1999/12/10. eng.
458. Rada JA, McFarland AL, Cornuet PK, Hassell JR. Proteoglycan synthesis by scleral chondrocytes is modulated by a vision dependent mechanism. Current Eye Research. 1992 Aug;11(8):767-82. PubMed PMID: 1424721. Epub 1992/08/01. eng.
459. Qin D, Zhang GM, Xu X, Wang LY. The PI3K/Akt signaling pathway mediates the high glucose-induced expression of extracellular matrix molecules in human retinal pigment epithelial cells. Journal of Diabetes Research. 2015;2015:920280. PubMed PMID: 25695094. Pubmed Central PMCID: Pmc4324947. Epub 2015/02/20. eng.
460. Yokoyama K, Kimoto K, Itoh Y, Nakatsuka K, Matsuo N, Yoshioka H, et al. The PI3K/Akt pathway mediates the expression of type I collagen induced by TGF-beta2 in human retinal pigment epithelial cells. Graefe's Archive for Clinical and Experimental Ophthalmology. 2012 Jan;250(1):15-23. PubMed PMID: 21858467. Pubmed Central PMCID: Pmc3262137. Epub 2011/08/23. eng.
461. Hao J, Liu S, Zhao S, Liu Q, Lv X, Chen H, et al. PI3K/Akt pathway mediates high glucose-induced lipogenesis and extracellular matrix accumulation in HKC cells through regulation of SREBP-1 and TGF-beta1. Histochemistry and Cell Biology. 2011 Feb;135(2):173-81. PubMed PMID: 21240525. Epub 2011/01/18. eng.
462. Larsen M, Artym VV, Green JA, Yamada KM. The matrix reorganized: extracellular matrix remodeling and integrin signaling. Current Opinion in Cell Biology. 2006;18(5):463-71.
463. Giers U, Epple C. Comparison of A-scan device accuracy. Journal of Cataract & Refractive Surgery. 1990;16(2):235-42.
464. O'leary D, Millodot M. Eyelid closure causes myopia in humans. Experientia. 1979;35(11):1478-9.
465. Cohen Y, Peleg E, Belkin M, Polat U, Solomon AS. Ambient illuminance, retinal dopamine release and refractive development in chicks. Experimental Eye Research. 2012;103:33-40.
466. Golding J, Pembrey M, Jones R. ALSPAC-the Avon longitudinal study of parents and children. I. Study methodology. Paediatric and Perinatal Epidemiology. 2001;15(1):74-87.
467. Fledelius HC. Myopia and diabetes mellitus with special reference to adult-onset myopia. Acta Ophthalmologica. 1986 Feb;64(1):33-8. PubMed PMID: 3962616. Epub 1986/02/01. eng.
468. Handa S, Chia A, Htoon HM, Lam PM, Yap F, Ling Y. Myopia in young patients with type 1 diabetes mellitus. Singapore medical journal. 2015 Aug;56(8):450-4. PubMed PMID: 26310273. Pubmed Central PMCID: Pmc4545134. Epub 2015/08/28. eng.
469. Jacobsen N, Jensen H, Lund-Andersen H, Goldschmidt E. Is poor glycaemic control in diabetic patients a risk factor of myopia? Acta Ophthalmologica. 2008 Aug;86(5):510-4. PubMed PMID: 18081906. Epub 2007/12/18. eng.
470. Zhang SJ, Li YF, Tan RR, Tsoi B, Huang WS, Huang YH, et al. A new gestational diabetes mellitus model: hyperglycemia-induced eye malformation via inhibition of Pax6 in the chick embryo. Disease Models & Mechanisms. 2016 Feb;9(2):177-86. PubMed PMID: 26744353. Pubmed Central PMCID: Pmc4770145. Epub 2016/01/09. eng.
471. Datar SP, Bhonde RR. Modeling chick to assess diabetes pathogenesis and treatment. The Review of Diabetic Studies : RDS. 2011 Summer;8(2):245-53. PubMed PMID: 22189547. Pubmed Central PMCID: Pmc3280009. Epub 2011/12/23. eng.
472. Biessels GJ. Diabetes: hypoglycemia and dementia in type 2 diabetes: chick or egg? Nature Reviews Endocrinology. 2009 Oct;5(10):532-4. PubMed PMID: 19763124. Epub 2009/09/19. eng.

Appendices

Appendix 5.1. Transcripts differentially expressed (P < 0.05) between FD-treated eye and control eye using analysis Model 2, with 3 software packages.

	edgeR		DESeq2		limma	
Gene ID	**logFC**	**FDR**	**log2FC**	**P-adj**	**logFC**	**P-adj**
VIP	-1.09	2.67e-09	-0.97	4.07e-09	-1.02	0.01
VIP	-1.08	2.67e-09	-0.96	4.07e-09	-1.01	0.01
UTS2B	-0.87	2.01e-07	-0.86	NA	-0.86	3.90e-03
SPON1	-0.35	5.28e-07	-0.33	1.35e-07	-0.35	3.90e-03
HK2	-0.33	6.00e-07	-0.36	6.64e-10	-0.33	0.01
DIO2	-0.39	6.00e-07	-0.34	4.74e-07	-0.39	0.01
NTS	0.40	6.00e-07	0.40	2.19e-06	0.40	0.01
SIX3	-0.28	6.00e-07	-0.27	9.60e-04	-0.28	0.01
DIO2	-0.38	9.03e-07	-0.33	1.18e-06	-0.38	0.01
KCNA4	-0.28	4.36e-06	-0.29	1.34e-03	-0.28	0.01
ACSBG2	0.45	4.91e-06	0.46	5.12e-05	0.45	0.01
UNC5C	-0.31	4.91e-06	-0.32	8.02e-04	-0.31	0.01
TERF1	0.44	4.91e-06	0.39	9.62e-04	0.45	0.01
APC2	-0.30	6.73e-06	-0.30	1.21e-05	-0.30	0.01
OPN4	-0.37	6.73e-06	-0.38	4.45e-05	-0.37	0.01
SWAP70	0.27	1.64e-05	0.25	2.11e-03	0.27	0.01
MSMO1	0.33	4.03e-05	0.36	1.68e-07	0.33	0.01
PTPRU	-0.28	4.03e-05	-0.29	8.02e-04	-0.28	0.01
C14orf2	0.34	4.03e-05	0.34	2.17e-03	0.33	0.02
STARD4	0.30	8.46e-05	0.32	1.21e-05	0.30	0.01
OPN4-1	-0.24	8.46e-05	-0.23	3.30e-03	-0.24	0.01
MZT1	0.27	8.46e-05	0.27	0.01	0.27	0.01
MAFF	-0.56	1.24e-04	-0.53	1.67e-03	-0.55	0.02
RASA4B	-0.28	1.59e-04	-0.28	0.01	-0.28	0.01
GAS2L3	0.72	2.23e-04	0.69	NA	0.74	0.01
NCOA1	-0.33	2.91e-04	-0.35	1.96e-03	-0.33	0.02
SPRY4	-0.89	2.91e-04	-0.82	NA	-0.89	0.02
HDAC7	-0.46	3.21e-04	-0.48	1.65e-03	-0.45	0.02
PCDH19	-0.25	3.39e-04	-0.25	0.01	-0.25	0.02
SPRY4	-0.88	3.39e-04	-0.81	NA	-0.89	0.02
ARL6	0.24	4.21e-04	0.24	4.49e-03	0.24	0.02
RAD54L2	-0.25	5.05e-04	-0.26	2.72e-03	-0.25	0.02
SYT13	-0.24	5.25e-04	-0.22	0.01	-0.24	0.02
PNPLA6	-0.28	5.37e-04	-0.27	0.02	-0.29	0.02
TUBB	-0.28	5.62e-04	-0.28	0.01	-0.28	0.02
ATP13A2	-0.38	5.62e-04	-0.38	0.01	-0.38	0.02
FABP9	0.51	7.82e-04	0.52	2.11e-03	0.52	0.02
CNTN2	-0.27	7.82e-04	-0.28	0.01	-0.27	0.02
UFM1	0.25	8.16e-04	0.27	0.01	0.25	0.02
BRD2	-0.24	8.16e-04	-0.24	0.01	-0.24	0.02
ST8SIA2	-0.31	8.29e-04	-0.30	0.01	-0.31	0.03
RHOT2	-0.31	8.55e-04	-0.29	0.02	-0.31	0.02
TNS1	-0.52	8.99e-04	-0.56	1.67e-03	-0.51	0.02
MGAT3	-0.20	8.99e-04	-0.19	0.01	-0.20	0.01

NPAS2	-0.24	8.99e-04	-0.24	0.01	-0.24	0.02
MRPL53	0.26	8.99e-04	0.27	0.01	0.26	0.02
LMBR1	-0.26	9.53e-04	-0.24	0.03	-0.26	0.03
TGFBI	0.32	9.62e-04	0.33	0.01	0.32	0.02
C7orf73	0.23	9.72e-04	0.20	0.04	0.23	0.02
ADORA2B	-0.28	1.24e-03	-0.25	0.03	-0.29	0.03
FOXP1	-0.38	1.35e-03	-0.40	0.01	-0.38	0.02
P4HB	0.23	1.49e-03	0.23	0.02	0.23	0.02
COX7B	0.23	1.55e-03	0.24	0.01	0.23	0.02
CRYAB	0.56	1.66e-03	0.41	0.01	0.58	0.03
NCAN	-0.39	1.66e-03	-0.36	0.02	-0.39	0.01
DUSP4	-1.06	1.66e-03	-1.00	NA	-1.08	0.03
DNMT3A	-0.27	1.68e-03	-0.31	1.96e-03	-0.27	0.03
ATP6V0D2	0.28	1.73e-03	0.26	0.03	0.28	0.03
GFRA2	-0.27	1.73e-03	-0.25	0.03	-0.27	0.02
RARA	-0.30	1.75e-03	-0.30	0.02	-0.30	0.02
LIMS1	0.21	1.81e-03	0.20	0.04	0.21	0.02
PPAP2B	-0.25	1.82e-03	-0.26	0.03	-0.25	0.03
COX6C	0.21	1.87e-03	0.22	0.01	0.21	0.02
RAP1GAP2	-0.21	1.87e-03	-0.20	0.02	-0.21	0.02
MPC1L	0.21	2.01e-03	0.20	0.03	0.21	0.02
PAN2	-0.25	2.01e-03	-0.25	0.03	-0.26	0.03
GLI2	-0.67	2.01e-03	-0.69	NA	-0.68	0.03
MRPS17	0.21	2.01e-03	0.21	0.04	0.22	0.02
CLU	-0.29	2.06e-03	-0.26	4.31e-03	-0.29	0.02
GMFB	0.21	2.06e-03	0.21	0.04	0.21	0.02
GIT1	-0.32	2.15e-03	-0.33	0.02	-0.32	0.03
LOC421975	0.21	2.26e-03	0.24	1.65e-03	0.21	0.02
RBP3	0.23	2.44e-03	0.25	8.60e-05	0.23	0.02
ETV5	-0.51	2.44e-03	-0.50	1.09e-04	-0.51	0.01
NUMA1	-0.27	2.44e-03	-0.30	1.88e-04	-0.27	0.02
BCL6	-0.24	2.44e-03	-0.24	2.08e-04	-0.24	0.01
UQCRB	0.27	2.44e-03	0.29	2.08e-04	0.27	0.01
CDKN1A	0.33	2.44e-03	0.35	4.42e-04	0.32	0.02
CSRP2	0.32	2.44e-03	0.29	4.42e-04	0.32	0.01
SLC2A1	-0.25	2.44e-03	-0.22	4.51e-04	-0.25	0.01
LRP1	-0.30	2.44e-03	-0.33	4.51e-04	-0.30	0.02
MDH1	0.26	2.44e-03	0.28	4.77e-04	0.26	0.03
MDH1	0.26	2.44e-03	0.28	4.77e-04	0.26	0.03
BHLHE40	-0.29	2.44e-03	-0.29	6.61e-04	-0.29	0.01
GLS2	-0.26	2.44e-03	-0.26	7.98e-04	-0.26	0.01
ME1	0.24	2.44e-03	0.24	7.98e-04	0.24	0.02
RGS16	-0.39	2.47e-03	-0.35	0.03	-0.38	0.02
INPP5K	0.24	2.63e-03	0.22	2.66e-03	0.24	0.02
KCNAB1	-0.21	2.63e-03	-0.17	0.03	-0.21	0.02
TMEM167A	0.23	2.64e-03	0.24	0.02	0.23	0.03
CREBL2	0.25	2.64e-03	0.23	0.05	0.25	0.03
GLI2	-0.65	2.82e-03	-0.68	NA	-0.67	0.03
ELL	-0.24	2.90e-03	-0.23	0.05	-0.24	0.03
SDK2	-0.30	2.93e-03	-0.32	0.01	-0.30	0.04

HDAC4	-0.28	2.93e-03	-0.29	0.01	-0.28	0.03
PDDC1	0.21	2.93e-03	0.20	0.06	0.21	0.02
GORASP1	0.18	2.98e-03	0.19	0.02	0.18	0.02
PRELID3A	0.21	2.98e-03	0.21	0.05	0.21	0.02
KCNIP2	-0.20	3.06e-03	-0.17	0.07	-0.20	0.03
EWSR1	-0.18	3.12e-03	-0.20	0.01	-0.18	0.02
TLN1	-0.21	3.12e-03	-0.22	0.03	-0.21	0.03
PDDC1	0.21	3.12e-03	0.20	0.06	0.21	0.02
LIMK1	-0.37	3.13e-03	-0.32	0.04	-0.37	0.02
ZNF384	-0.24	3.13e-03	-0.23	0.05	-0.25	0.03
KIT	-0.19	3.15e-03	-0.21	0.02	-0.19	0.02
MPHOSPH6	0.24	3.40e-03	0.23	0.04	0.24	0.03
CORO7-PAM16	-0.24	3.41e-03	-0.23	0.04	-0.24	0.03
DHCR7	0.22	3.47e-03	0.24	0.01	0.22	0.03
COL9A2	-0.85	3.54e-03	-0.83	NA	-0.84	0.03
CYB5B	0.23	3.62e-03	0.19	0.07	0.22	0.03
FABP5	0.21	3.80e-03	0.19	0.03	0.21	0.03
SZT2	-0.25	3.95e-03	-0.25	0.02	-0.25	0.03
IGSF11	-0.20	4.03e-03	-0.18	0.06	-0.21	0.03
STK10	-0.21	4.04e-03	-0.24	0.01	-0.21	0.03
DHCR24	0.24	4.11e-03	0.27	0.01	0.24	0.04
LOC107050474	-0.32	4.21e-03	-0.34	0.01	-0.31	0.03
UGT8	0.26	4.29e-03	0.25	0.04	0.25	0.03
COX20	0.26	4.29e-03	0.25	0.04	0.27	0.03
SLC6A9	-0.25	4.51e-03	-0.21	0.01	-0.25	0.03
UNC5B	-0.23	4.51e-03	-0.23	0.05	-0.23	0.03
PCDHGA2	-0.45	4.55e-03	-0.48	0.01	-0.45	0.04
HYAL6	0.28	4.55e-03	0.29	0.02	0.27	0.03
KIAA0907	-0.19	4.64e-03	-0.16	0.06	-0.19	0.03
PCDH8	-0.23	0.01	-0.20	0.08	-0.23	0.03
DPY30	0.21	0.01	0.21	0.05	0.21	0.03
PHOSPHO1	-0.25	0.01	-0.24	0.05	-0.25	0.03
C5H14ORF166	0.21	0.01	0.22	0.02	0.21	0.03
SNRPF	0.29	0.01	0.31	0.02	0.30	0.03
FBXL21	0.19	0.01	0.19	0.02	0.19	0.03
17.5	-0.50	0.01	-0.56	2.72e-03	-0.52	0.03
SSR3	0.20	0.01	0.23	0.01	0.20	0.03
ZNF335	-0.17	0.01	-0.17	0.04	-0.17	0.02
FBXL21	0.19	0.01	0.19	0.02	0.19	0.03
CNGA1	0.23	0.01	0.26	0.02	0.23	0.04
LACTB2	0.23	0.01	0.26	0.02	0.23	0.04
DCTD	0.34	0.01	0.36	0.02	0.32	0.03
CRABP1	0.26	0.01	0.26	0.04	0.27	0.04
PCDHGA2	-0.23	0.01	-0.25	0.01	-0.23	0.04
SMPX	0.78	0.01	0.89	NA	0.77	0.03
SRC	-0.31	0.01	-0.32	0.03	-0.31	0.03
UCHL3	0.18	0.01	0.19	0.04	0.18	0.03
UQCRHL	0.20	0.01	0.21	0.04	0.20	0.03
GPR137B	-0.30	0.01	-0.23	0.07	-0.30	0.03
CAMK2B	-0.39	0.01	-0.42	0.03	-0.39	0.02

TET2	-0.31	0.01	-0.32	0.02	-0.31	0.05
KCNH6	-0.28	0.01	-0.28	0.03	-0.28	0.05
NME3	0.18	0.01	0.19	0.04	0.18	0.03
FBXO32	-0.17	0.01	-0.17	0.07	-0.17	0.03
MAEA	0.19	0.01	0.21	0.02	0.19	0.03
APEH	-0.25	0.01	-0.26	0.04	-0.25	0.04
ZNF609	-0.20	0.01	-0.21	0.02	-0.20	0.03
HSPE1	0.18	0.01	0.16	0.07	0.18	0.03
GNG10	0.27	0.01	0.27	0.05	0.27	0.02
OPTC	-0.33	0.01	-0.31	0.04	-0.32	0.05
LINGO1	-0.17	0.01	-0.15	0.11	-0.17	0.03
TFAP2B	-0.22	0.01	-0.21	0.06	-0.22	0.04
CHCHD4	0.26	0.01	0.25	0.05	0.26	0.03
FABP7	0.34	0.01	0.28	0.05	0.36	0.05
ST3GAL5	0.19	0.01	0.20	0.06	0.19	0.03
MERTK	-0.38	0.01	-0.35	0.07	-0.39	0.02
HBP1	-0.19	0.01	-0.16	0.11	-0.19	0.03
ACTR6	0.20	0.01	0.22	0.01	0.20	0.04
COPS2	0.18	0.01	0.19	0.02	0.18	0.03
ZDHHC5	-0.20	0.01	-0.19	0.08	-0.20	0.04
FOSL2	-0.45	0.01	-0.46	NA	-0.44	0.03
MYH11	-0.34	0.01	-0.37	0.02	-0.34	0.03
HMGCS1	0.21	0.01	0.23	0.01	0.21	0.03
UCHL1	0.26	0.01	0.28	0.01	0.26	0.04
SELENOF	0.20	0.01	0.20	0.04	0.20	0.04
CYCS	0.23	0.01	0.23	0.05	0.23	0.04
FAM103A1	0.24	0.01	0.27	0.01	0.24	0.05
RSL24D1	0.19	0.01	0.18	0.06	0.19	0.04
GLCCI1	-0.18	0.01	-0.19	0.04	-0.18	0.03
FAM103A1	0.23	0.01	0.26	0.01	0.23	0.05
PTK7	-0.18	0.01	-0.18	0.06	-0.18	0.03
MBP	0.24	0.01	0.27	1.68e-03	0.24	0.03
ATP5G3	0.20	0.01	0.22	0.01	0.20	0.04
LAMB2	-0.39	0.01	-0.43	0.02	-0.40	0.03
EMC2	0.20	0.01	0.18	0.05	0.20	0.04
PPP1R12B	-0.38	0.01	-0.36	0.06	-0.37	0.03
PALM	-0.20	0.01	-0.19	0.07	-0.20	0.05
OLA1	0.18	0.01	0.17	0.09	0.18	0.04
IGHMBP2	-0.18	0.01	-0.18	0.09	-0.18	0.03
EIF1AX	0.23	0.01	0.23	0.01	0.23	0.03
HSBP1	0.21	0.01	0.21	0.02	0.21	0.04
MAB21L1	-0.24	0.01	-0.28	0.01	-0.24	0.05
NT5C2	-0.17	0.01	-0.16	0.04	-0.17	0.03
LOC431499	-0.28	0.01	-0.25	0.09	-0.30	0.03
UBE2L3	0.19	0.01	0.21	0.01	0.19	0.04
IL17RD	0.32	0.01	0.31	0.06	0.32	0.03
ATP5G3	0.19	0.01	0.22	0.02	0.19	0.04
XYLT2	-0.21	0.01	-0.22	0.06	-0.21	0.03
PBX1	-0.22	0.01	-0.22	0.06	-0.22	0.05
CSNK1E	-0.18	0.01	-0.17	0.11	-0.18	0.04

ATP5G3	0.19	0.01	0.22	0.02	0.19	0.04
NET1	0.19	0.01	0.21	0.03	0.19	0.05
EFNB1	-0.25	0.01	-0.23	0.08	-0.25	0.04
MTERF3	0.24	0.01	0.27	0.02	0.23	0.03
PER3	-0.24	0.01	-0.26	0.02	-0.24	0.05
FBXL16	-0.32	0.01	-0.33	0.04	-0.32	0.03
SP1	-0.42	0.01	-0.43	0.04	-0.44	0.04
TXNDC12	0.21	0.01	0.22	0.06	0.21	0.04
ODF2	-0.19	0.01	-0.19	0.08	-0.19	0.04
FUNDC1	0.17	0.01	0.16	0.06	0.17	0.03
CKB	0.22	0.01	0.25	4.31e-03	0.22	0.05
WWP2	-0.19	0.01	-0.19	0.09	-0.19	0.04
LZIC	0.16	0.01	0.17	0.04	0.16	0.03
HSP90B1	0.22	0.01	0.18	0.02	0.21	0.03
EPB41	-0.26	0.01	-0.27	0.01	-0.26	0.04
NRBP1	-0.16	0.01	-0.18	0.03	-0.16	0.03
RWDD3	0.20	0.01	0.20	0.09	0.20	0.04
LIN7C	0.18	0.01	0.18	0.01	0.18	0.03
GNRH1	0.29	0.01	0.30	0.04	0.29	0.03
SLC9A1	-0.40	0.01	-0.38	0.04	-0.38	0.06
NLGN3	-0.34	0.01	-0.38	0.02	-0.34	0.05
DCK	0.21	0.01	0.25	0.02	0.21	0.05
RGMA	-0.31	0.01	-0.30	0.06	-0.30	0.03
NDUFB1	0.20	0.01	0.17	0.06	0.20	0.04
ARL8BL	0.23	0.01	0.25	0.04	0.23	0.05
RNF7	0.18	0.01	0.17	0.08	0.18	0.05
HSDL1	0.21	0.01	0.23	0.04	0.21	0.04
FBF1	-0.18	0.01	-0.21	0.02	-0.18	0.04
FN3KRP	0.20	0.01	0.19	0.04	0.20	0.04
LMF2	-0.25	0.01	-0.20	0.11	-0.25	0.05
FUNDC1	0.16	0.01	0.16	0.06	0.16	0.03
ARNT	-0.17	0.01	-0.16	0.10	-0.17	0.04
NREP	0.18	0.02	0.20	7.98e-04	0.18	0.03
DNMT1	-0.25	0.02	-0.28	0.03	-0.25	0.06
ACAT1	0.19	0.02	0.21	0.04	0.19	0.05
GMPR2	-0.17	0.02	-0.18	0.10	-0.18	0.04
NDUFB1	0.19	0.02	0.17	0.07	0.19	0.05
NDUFB1	0.19	0.02	0.17	0.07	0.19	0.05
CNOT8	0.16	0.02	0.16	0.08	0.16	0.04
PNRC1	-0.18	0.02	-0.18	0.01	-0.18	0.02
MAB21L2	-0.33	0.02	-0.29	0.09	-0.32	0.04
SREBF1	-0.28	0.02	-0.29	0.04	-0.29	0.06
TXN2	0.22	0.02	0.22	0.05	0.22	0.06
ZNF692	-0.32	0.02	-0.31	0.07	-0.31	0.03
PHAX	0.16	0.02	0.17	0.05	0.16	0.04
ATG9A	-0.21	0.02	-0.19	0.11	-0.21	0.06
MCFD2	0.20	0.02	0.20	0.04	0.20	0.05
PALM	-0.21	0.02	-0.20	0.09	-0.21	0.06
GABRQ	-0.29	0.02	-0.30	0.05	-0.30	0.05
CD69L	-0.50	0.02	-0.58	0.01	-0.53	0.04

COL2A1	-0.19	0.02	-0.20	0.05	-0.19	0.05
BRINP1	-0.15	0.02	-0.14	0.09	-0.15	0.03
FOS	-0.71	0.02	-0.61	NA	-0.72	0.06
KDM5B	-0.17	0.02	-0.17	0.01	-0.17	0.02
UQCRFS1	0.18	0.02	0.21	0.02	0.18	0.05
GABRQ	-0.29	0.02	-0.30	0.05	-0.30	0.05
H2AFZ	0.17	0.02	0.19	0.07	0.17	0.05
FN1	-0.24	0.02	-0.23	0.08	-0.24	0.06
MAP3K14	-0.18	0.02	-0.18	0.10	-0.18	0.04
RSPO2	-0.65	0.02	-0.59	NA	-0.64	0.04
LSM7	0.26	0.02	0.22	0.11	0.27	0.05
OSTC	0.17	0.02	0.19	0.04	0.17	0.05
ACTN4	-0.17	0.02	-0.20	0.02	-0.17	0.04
PLXNB3	-0.24	0.02	-0.26	0.02	-0.24	0.05
DISP3	-0.19	0.02	-0.19	0.07	-0.19	0.05
GBX2	-0.50	0.02	-0.46	NA	-0.50	0.05
MCTS1	0.20	0.02	0.23	0.04	0.20	0.05
P4HA1	-0.17	0.02	-0.18	0.01	-0.17	0.03
P4HA1	-0.17	0.02	-0.18	0.01	-0.17	0.03
COX4I1	0.21	0.02	0.19	0.03	0.20	0.04
IGFBP4	-0.28	0.02	-0.28	0.05	-0.27	0.07
CLCN7	-0.23	0.02	-0.17	0.14	-0.23	0.06
TWF1	0.17	0.02	0.19	1.03e-03	0.17	0.02
MPP1	-0.16	0.02	-0.15	0.12	-0.16	0.04
KCNA3	-0.40	0.02	-0.38	0.08	-0.40	0.05
CYP51A1	0.18	0.02	0.18	0.05	0.18	0.05
ZNF512B	-0.16	0.02	-0.15	0.12	-0.16	0.05
ZNF341	-0.20	0.02	-0.20	0.11	-0.21	0.04
RNF123	-0.19	0.02	-0.18	0.09	-0.19	0.05
P4HA1	-0.17	0.02	-0.18	0.01	-0.17	0.03
DUSP1	-0.29	0.02	-0.26	0.09	-0.27	0.07
ZNF512B	-0.16	0.02	-0.15	0.12	-0.16	0.05
HSP90AB1	0.18	0.02	0.18	0.10	0.18	0.06
P4HA1	-0.17	0.02	-0.18	0.01	-0.17	0.03
SUB1	0.19	0.02	0.18	0.02	0.19	0.03
RAN	0.21	0.02	0.19	0.04	0.21	0.04
ACADS	-0.18	0.02	-0.18	0.10	-0.17	0.05
PPIF	0.18	0.02	0.21	0.05	0.18	0.05
MST1	-0.77	0.02	-0.73	NA	-0.77	0.06
ECE1	-0.19	0.02	-0.18	0.12	-0.19	0.05
MDGA1	-0.21	0.02	-0.23	0.04	-0.21	0.06
COX7A2	0.17	0.02	0.16	0.06	0.17	0.04
ZNF512B	-0.16	0.02	-0.15	0.12	-0.16	0.05
OAZ1	0.21	0.02	0.20	0.03	0.21	0.05
HDDC2	0.21	0.02	0.20	0.10	0.21	0.05
KCNJ3	-0.32	0.02	-0.29	0.09	-0.31	0.05
RPAP3	0.17	0.02	0.14	0.12	0.17	0.05
TNFRSF21	-0.15	0.02	-0.14	0.10	-0.15	0.04
DCTN1	-0.16	0.02	-0.17	0.01	-0.16	0.03
ISCA1	0.17	0.02	0.19	0.03	0.17	0.05

KRR1	0.18	0.02	0.18	0.10	0.18	0.05
HMGCR	0.20	0.02	0.20	0.03	0.20	0.04
OSBPL2	0.20	0.02	0.16	0.04	0.20	0.04
ASNS	0.20	0.02	0.21	0.08	0.20	0.03
EMC3	0.15	0.02	0.16	0.08	0.15	0.05
COL6A1	-0.37	0.02	-0.41	0.03	-0.38	0.05
TOB1	-0.24	0.02	-0.27	0.03	-0.24	0.07
SCP2	0.20	0.02	0.20	0.04	0.20	0.05
PRKAA2	-0.30	0.02	-0.31	0.05	-0.30	0.07
POLR2L	0.20	0.02	0.21	0.08	0.20	0.04
TAOK3	-0.22	0.02	-0.22	0.09	-0.22	0.05
SEPT2L	0.19	0.02	0.19	0.03	0.19	0.04
CALB1	0.28	0.02	0.21	0.06	0.28	0.07
ABRACL	0.33	0.02	0.33	0.09	0.33	0.03
GAS2	0.35	0.02	0.30	0.10	0.36	0.05
HMGN1	0.20	0.02	0.20	0.04	0.20	0.05
THOC7	0.18	0.02	0.20	0.05	0.18	0.06
FGFR1	-0.18	0.02	-0.18	0.08	-0.18	0.06
GTF2E2	0.19	0.03	0.18	0.11	0.19	0.06
FURIN	-0.22	0.03	-0.22	0.10	-0.22	0.05
SDC3	-0.22	0.03	-0.20	0.13	-0.22	0.06
ID2	0.18	0.03	0.21	0.04	0.18	0.06
PRNP	-0.16	0.03	-0.15	0.04	-0.16	0.03
RER1	0.16	0.03	0.12	0.19	0.16	0.05
MVB12A	-0.17	0.03	-0.16	0.13	-0.17	0.04
MAFK	-0.41	0.03	-0.36	NA	-0.41	0.05
GNAI2	-0.23	0.03	-0.20	0.13	-0.23	0.05
MAGOH	0.20	0.03	0.23	0.04	0.20	0.06
PSMD12	0.21	0.03	0.14	0.15	0.22	0.07
MAGOH	0.20	0.03	0.23	0.04	0.20	0.06
ARID5B	-0.24	0.03	-0.26	0.05	-0.24	0.07
PARK7	0.19	0.03	0.20	0.04	0.19	0.05
MED24	-0.24	0.03	-0.23	0.11	-0.25	0.07
FGL2	0.60	0.03	0.65	NA	0.68	0.05
PCDHA11	-0.45	0.03	-0.58	1.64e-03	-0.45	0.09
LOC100858655	-0.37	0.03	-0.40	0.06	-0.36	0.05
VPS29	0.16	0.03	0.17	0.06	0.16	0.05
ASMT	0.19	0.03	0.20	0.09	0.18	0.07
NEK7	0.15	0.03	0.15	0.10	0.15	0.05
PAK1IP1	0.18	0.03	0.18	0.11	0.18	0.06
GTF2H5	0.16	0.03	0.16	0.06	0.16	0.05
SUCLG1	0.16	0.03	0.17	0.04	0.16	0.05
DLD	0.17	0.03	0.18	0.06	0.17	0.05
SLC16A9	0.34	0.03	0.35	0.10	0.34	0.04
PCDHA4	-0.42	0.03	-0.53	2.11e-03	-0.42	0.08
PSMC1	0.17	0.03	0.17	0.05	0.17	0.05
SLC5A1	-0.70	0.03	-0.78	NA	-0.72	0.07
PTPN9	-0.38	0.03	-0.37	0.10	-0.38	0.04
C2H6orf52	0.16	0.03	0.17	0.10	0.16	0.05
YPEL5	0.18	0.03	0.19	0.02	0.18	0.04

CMPK1	0.15	0.03	0.15	0.07	0.15	0.05
PKP4	-0.14	0.03	-0.14	0.10	-0.14	0.04
ASXL2	-0.15	0.03	-0.14	0.11	-0.15	0.05
CLK2	-0.17	0.03	-0.17	0.12	-0.17	0.05
CALM2	0.22	0.03	0.22	0.03	0.22	0.07
SNX24	0.19	0.03	0.20	0.10	0.18	0.06
YIPF5	0.16	0.03	0.17	0.11	0.16	0.06
CASP3	0.20	0.03	0.19	0.13	0.21	0.05
EEF1AKMT1	0.28	0.03	0.25	0.12	0.29	0.04
PDLIM7	-0.47	0.03	-0.48	NA	-0.47	0.05
RHOBTB1	-0.18	0.03	-0.19	0.08	-0.18	0.07
SORL1	-0.21	0.03	-0.22	0.03	-0.21	0.06
NDUFA10	0.17	0.03	0.17	0.03	0.17	0.04
NSUN2	-0.16	0.03	-0.18	0.08	-0.16	0.05
UQCR10	0.17	0.03	0.20	0.05	0.17	0.07
TESC	-0.46	0.03	-0.53	NA	-0.46	0.04
TWF1	0.15	0.03	0.18	0.05	0.15	0.06
NDUFB5	0.17	0.03	0.17	0.08	0.17	0.06
ZFAND6	0.16	0.03	0.15	0.09	0.16	0.05
NRP2	-0.23	0.03	-0.23	0.11	-0.23	0.06
SLC51A	-0.80	0.03	-0.78	NA	-0.79	0.07
PTN	0.14	0.03	0.15	0.01	0.14	0.05
NME1	0.20	0.03	0.21	0.03	0.20	0.05
MAGI3	-0.17	0.03	-0.18	0.03	-0.17	0.04
SLCO4A1	-0.18	0.03	-0.18	0.12	-0.19	0.06
TMEM41B	0.16	0.03	0.15	0.13	0.16	0.06
PHACTR1	-0.15	0.03	-0.15	0.15	-0.15	0.06
C1D	0.24	0.03	0.25	0.09	0.24	0.05
Sep-09	-0.15	0.03	-0.13	0.11	-0.15	0.05
ACVR2B	-0.23	0.03	-0.22	0.12	-0.22	0.05
LOC421792	0.29	0.03	0.27	0.13	0.29	0.04
DNAJC2	0.15	0.03	0.14	0.18	0.15	0.06
GLI1	-0.29	0.03	-0.32	0.07	-0.29	0.04
C26H6ORF125	0.22	0.03	0.20	0.13	0.22	0.05
HNRNPH3	0.21	0.03	0.19	0.06	0.20	0.06
ALG12	0.13	0.03	0.13	0.13	0.13	0.05
C10H15ORF59	-0.21	0.03	-0.20	0.14	-0.21	0.07
HYDIN	-0.21	0.03	-0.23	0.06	-0.21	0.08
TFCP2	-0.20	0.03	-0.17	0.18	-0.20	0.06
PCDHA5	-0.44	0.03	-0.57	1.68e-03	-0.43	0.10
RFK	0.16	0.04	0.13	0.18	0.16	0.07
ZFAND6	0.16	0.04	0.15	0.09	0.16	0.06
NEURL1	-0.18	0.04	-0.15	0.15	-0.18	0.07
TCF3	-0.19	0.04	-0.19	0.11	-0.19	0.07
PCDHA1	-0.44	0.04	-0.56	1.96e-03	-0.43	0.10
PSMD5	0.16	0.04	0.18	0.06	0.16	0.07
CSPG5	-0.18	0.04	-0.14	0.14	-0.18	0.07
C1D	0.23	0.04	0.24	0.10	0.23	0.05
LOC425783	-0.40	0.04	-0.51	0.01	-0.44	0.06
ACAT2	0.20	0.04	0.24	0.04	0.20	0.07

THY1	-0.19	0.04	-0.16	0.10	-0.19	0.06
NDUFS3	0.18	0.04	0.18	0.11	0.18	0.08
ZFAND6	0.16	0.04	0.15	0.10	0.16	0.06
RPA2	0.17	0.04	0.18	0.10	0.17	0.05
PRPSAP2	0.16	0.04	0.15	0.12	0.16	0.06
TRAPPC2	0.16	0.04	0.17	0.10	0.16	0.07
OARD1	0.18	0.04	0.17	0.15	0.19	0.07
ATP6AP1	0.16	0.04	0.19	0.08	0.16	0.05
DNAJB9	0.15	0.04	0.14	0.18	0.16	0.06
AP1S2	0.16	0.04	0.14	0.06	0.16	0.04
HEATR3	0.15	0.04	0.18	0.04	0.15	0.06
GCLM	0.14	0.04	0.15	0.16	0.15	0.05
PITPNB	0.17	0.04	0.13	0.20	0.17	0.07
CECR2	-0.18	0.04	-0.23	0.03	-0.19	0.07
SNRPA1	0.17	0.04	0.18	0.11	0.17	0.07
MRPS25	0.19	0.04	0.19	0.14	0.19	0.06
LDB1	-0.31	0.04	-0.39	0.01	-0.32	0.07
LHX9	-0.24	0.04	-0.22	0.13	-0.24	0.06
PCDHA9	-0.44	0.04	-0.57	1.67e-03	-0.43	0.11
PCDHA8	-0.44	0.04	-0.57	1.67e-03	-0.43	0.11
TMX4	0.16	0.04	0.16	0.03	0.16	0.04
DUT	0.16	0.04	0.16	0.16	0.16	0.05
PIK3R5	0.17	0.04	0.14	0.22	0.17	0.06
PCDHA3	-0.43	0.04	-0.55	2.11e-03	-0.42	0.11
CCNL2	-0.15	0.04	-0.16	0.07	-0.15	0.05
C12orf75	0.25	0.04	0.24	0.12	0.25	0.05
PCDHA2	-0.43	0.04	-0.55	2.12e-03	-0.42	0.11
SLC31A1	0.18	0.04	0.21	0.06	0.18	0.06
SLC31A1	0.18	0.04	0.21	0.06	0.18	0.06
POLE3	0.20	0.04	0.21	0.09	0.20	0.07
NR2F2	-0.16	0.04	-0.18	0.09	-0.16	0.07
ARPC5	0.16	0.04	0.17	0.11	0.16	0.07
IER3IP1	0.18	0.04	0.19	0.11	0.18	0.05
NSMCE3	0.14	0.04	0.15	0.13	0.14	0.05
AXIN1	-0.16	0.04	-0.17	0.14	-0.16	0.06
SGF29	-0.18	0.04	-0.16	0.16	-0.17	0.08
MYD88	0.19	0.04	0.21	0.09	0.19	0.04
C22H2ORF42	-0.25	0.04	-0.26	0.09	-0.25	0.05
ABCE1	0.16	0.04	0.17	0.04	0.16	0.05
PEX13	0.14	0.04	0.16	0.10	0.14	0.06
POLR2D	0.20	0.04	0.20	0.12	0.20	0.04
RAP1B	0.14	0.04	0.12	0.17	0.14	0.06
KCNN2	-0.27	0.04	-0.26	0.12	-0.27	0.05
DNAJC15	0.16	0.04	0.17	0.13	0.16	0.05
DHFR	0.34	0.04	0.32	0.15	0.36	0.04
ZC3H3	-0.15	0.04	-0.15	0.16	-0.15	0.07
RWDD1	0.25	0.04	0.18	0.20	0.27	0.06
ERH	0.19	0.04	0.15	0.17	0.19	0.08
VEZF1	-0.24	0.04	-0.25	0.09	-0.24	0.09
C5H15ORF57	0.15	0.04	0.16	0.09	0.15	0.06

ALDH1A1	0.28	0.04	0.28	0.11	0.27	0.08
CDC25A	-0.24	0.04	-0.20	0.19	-0.25	0.05
CAPN11	-0.15	0.04	-0.13	0.18	-0.15	0.06
CAPN2	-0.28	0.04	-0.29	0.08	-0.28	0.09
GXYLT1	0.20	0.04	0.20	0.12	0.20	0.06
UQCR11	0.18	0.04	0.20	0.06	0.17	0.08
BLMH	0.16	0.04	0.17	0.09	0.16	0.07
RNF166	-0.16	0.04	-0.14	0.22	-0.16	0.07
HIBADH	0.15	0.04	0.12	0.24	0.15	0.07
EBF1	-0.22	0.04	-0.24	0.10	-0.23	0.06
TFEB	-0.28	0.04	-0.27	0.12	-0.28	0.07
OTUD6A	0.14	0.04	0.14	0.10	0.14	0.06
SSB	0.17	0.04	0.15	0.13	0.17	0.07
CHUK	-0.14	0.04	-0.15	0.12	-0.14	0.07
CAPZA2	0.18	0.04	0.18	0.05	0.18	0.06
PHB	0.18	0.04	0.17	0.13	0.18	0.08
MIR1800	-0.62	0.04	-0.68	NA	-0.61	0.05
BDNF	-0.45	0.04	-0.42	NA	-0.45	0.06
EXFABP	-0.65	0.04	-0.79	NA	-0.63	0.07
GNG13	0.14	0.04	0.15	0.09	0.14	0.06
COPE	0.15	0.04	0.15	0.09	0.15	0.06
ID4	0.16	0.04	0.18	0.10	0.16	0.08
CXCL14	-0.18	0.04	-0.15	0.20	-0.18	0.09
FLII	-0.15	0.05	-0.14	0.14	-0.15	0.07
RPS2	0.16	0.05	0.17	0.04	0.16	0.05
KCNT1	-0.26	0.05	-0.28	0.08	-0.26	0.07
SGK1	-0.17	0.05	-0.14	0.08	-0.17	0.05
DUSP6	-0.25	0.05	-0.22	0.14	-0.25	0.09
C20H20ORF24	0.14	0.05	0.15	0.10	0.14	0.06
DNPEP	-0.17	0.05	-0.16	0.15	-0.17	0.08
TRIM8	-0.22	0.05	-0.23	0.11	-0.23	0.06
ATG4B	0.17	0.05	0.17	0.14	0.17	0.08
HS2ST1	0.17	0.05	0.15	0.15	0.17	0.08
ATOX1	0.17	0.05	0.16	0.17	0.17	0.06
NAB1	-0.22	0.05	-0.24	0.09	-0.22	0.05
STRAP	0.14	0.05	0.13	0.16	0.15	0.07
GID8	0.16	0.05	0.16	0.04	0.16	0.05
WDR24	-0.20	0.05	-0.22	0.10	-0.20	0.06
PTPRG	-0.20	0.05	-0.22	0.04	-0.20	0.07
TNFRSF10B	-0.84	0.05	-0.81	NA	-0.79	0.12
INSIG1	0.21	0.05	0.25	0.02	0.21	0.08
OPN1MSW	-0.23	0.05	-0.20	0.10	-0.23	0.08
PDGFA	-0.51	0.05	-0.48	NA	-0.51	0.07
SCAF4	-0.16	0.05	-0.17	0.12	-0.17	0.08
NHLH2	-0.43	0.05	-0.44	NA	-0.43	0.06
MRPL51	0.19	0.05	0.19	0.13	0.19	0.07
SAP130	-0.28	0.05	-0.35	0.03	-0.28	0.09
EXOC5	0.15	0.05	0.16	0.04	0.15	0.04
SFRP1	0.17	0.05	0.17	0.07	0.17	0.06
ATP6V1D	0.17	0.05	0.18	0.04	0.17	0.06

RAB5B	-0.26	0.05	-0.27	0.12	-0.26	0.04
MAPRE2	-0.15	0.05	-0.14	0.07	-0.15	0.04
TMEM254	0.15	0.05	0.16	0.03	0.15	0.05
SMS	0.15	0.05	0.16	0.05	0.15	0.05
CERK	0.14	0.05	0.13	0.10	0.14	0.05
BTF3L4	0.15	0.05	0.16	0.05	0.15	0.05
TMEM254	0.15	0.05	0.16	0.03	0.15	0.05
GRIN1	-0.14	0.05	-0.13	0.05	-0.14	0.04
PCDHA1	-0.42	0.06	-0.55	3.31e-03	-0.41	0.12
ARL6IP5	0.17	0.06	0.19	0.02	0.17	0.06
CCT2	0.16	0.06	0.18	0.04	0.16	0.06
ARL6IP1	0.18	0.06	0.19	0.04	0.18	0.07
CRISPLD1	0.28	0.06	0.28	0.18	0.27	0.05
GNB1	0.14	0.06	0.14	0.05	0.14	0.06
NDUFB6	0.18	0.06	0.23	0.05	0.17	0.11
CTSC	0.21	0.06	0.19	0.19	0.21	0.05
PRDX1	0.17	0.07	0.18	0.05	0.17	0.07
DHX30	-0.14	0.07	-0.13	0.08	-0.14	0.05
PPP3R1	0.15	0.07	0.15	0.04	0.14	0.05
FDFT1	0.16	0.07	0.18	0.03	0.16	0.07
SETD5	-0.15	0.07	-0.18	0.03	-0.15	0.07
CBX3	0.13	0.07	0.12	0.10	0.13	0.05
TCEB1	0.14	0.07	0.17	0.03	0.14	0.08
SLC15A2	-0.21	0.07	-0.26	0.04	-0.21	0.12
ATP5C1	0.15	0.08	0.17	0.05	0.15	0.07
ATP5C1	0.15	0.08	0.17	0.05	0.15	0.07
ADCYAP1R1	-0.43	0.08	-0.52	0.04	-0.45	0.10
CCT8	0.15	0.08	0.17	0.04	0.15	0.08
CDC42	0.16	0.08	0.18	0.04	0.16	0.08
PCDHA11	-0.16	0.09	-0.20	0.04	-0.16	0.11
PCDHA8	-0.16	0.09	-0.21	0.03	-0.16	0.12
PCDHA5	-0.16	0.09	-0.21	0.03	-0.16	0.12
PCDHA2	-0.17	0.09	-0.22	0.03	-0.17	0.12
PCDHA4	-0.16	0.09	-0.21	0.04	-0.16	0.12
PCDHA3	-0.16	0.10	-0.21	0.04	-0.16	0.12
SKP1	0.14	0.10	0.16	0.04	0.14	0.09
PCDHA13	-0.16	0.10	-0.21	0.04	-0.16	0.12
PCDHA7	-0.16	0.10	-0.21	0.04	-0.16	0.12
PCDHA1	-0.16	0.10	-0.21	0.04	-0.16	0.13
GHITM	0.16	0.10	0.18	0.04	0.16	0.10
AACS	0.14	0.11	0.17	0.02	0.14	0.08
PCDHA9	-0.16	0.11	-0.21	0.04	-0.16	0.14
ASL1	0.74	0.51	0.18	NA	7.12	0.02

Appendix 5.2. Transcripts differentially expressed (P < 0.05) between High vs. Low myopia groups using analysis Model 3, with 3 software packages.

	edgeR		DESeq2		limma	
Gene ID	**logFC**	**FDR**	**log2FC**	**P-adj**	**logFC**	**P-adj**
NOVA1	0.48	0.15	0.66	1.02e-05	0.48	0.23
NOVA1	0.48	0.15	0.66	1.02e-05	0.48	0.23
ALDOC	-0.38	0.18	-0.51	1.02e-05	-0.38	0.23
SRRM1	0.39	0.15	0.53	3.67e-05	0.39	0.23
PROX1	0.45	0.11	0.59	4.73e-05	0.45	0.23
AKAP9	0.27	0.31	0.41	4.73e-05	0.27	0.29
PGAM1	-0.34	0.19	-0.44	5.75e-05	-0.34	0.23
USP34	0.38	0.21	0.53	5.99e-05	0.37	0.24
ANKRD10	0.47	0.17	0.67	5.99e-05	0.47	0.24
TMEM131	0.51	0.06	0.63	6.68e-05	0.51	0.23
CACNA1B	0.44	0.15	0.61	6.68e-05	0.44	0.23
PEBP1	-0.35	0.16	-0.46	6.68e-05	-0.35	0.23
PGK1	-0.31	0.15	-0.36	1.59e-04	-0.32	0.23
MAGI2	0.40	0.19	0.55	1.59e-04	0.40	0.23
ANK3	0.33	0.19	0.45	1.59e-04	0.33	0.23
SNCB	-0.28	0.29	-0.40	1.96e-04	-0.29	0.28
JARID2	0.29	0.29	0.43	1.96e-04	0.29	0.28
ANKRD52	0.61	0.15	0.84	2.29e-04	0.62	0.23
ACACA	0.39	0.15	0.52	2.29e-04	0.39	0.23
KIAA2018	0.57	0.17	0.82	2.29e-04	0.57	0.23
GAPDH	-0.33	0.15	-0.39	2.30e-04	-0.33	0.23
SALL3	0.46	0.14	0.62	2.38e-04	0.46	0.23
KCND3	0.56	0.15	0.75	2.38e-04	0.58	0.23
RALGAPA1	0.35	0.19	0.47	2.38e-04	0.35	0.23
RALGAPA1	0.35	0.19	0.47	2.38e-04	0.35	0.23
RALGAPA1	0.35	0.20	0.47	2.69e-04	0.35	0.23
FASN	0.31	0.22	0.41	2.69e-04	0.31	0.23
GRIA3	0.32	0.28	0.49	2.72e-04	0.32	0.29
CTTNBP2	0.35	0.15	0.44	2.73e-04	0.35	0.23
ATF7IP	0.36	0.18	0.48	2.73e-04	0.36	0.23
GCG	-0.65	9.00e-03	-0.76	2.81e-04	-0.65	0.23
RALGAPA1	0.35	0.20	0.47	2.81e-04	0.35	0.23
RALGAPA1	0.35	0.20	0.46	2.88e-04	0.35	0.23
ACSBG2	0.48	9.00e-03	0.54	3.49e-04	0.48	0.23
RPS3	-0.27	0.19	-0.32	3.49e-04	-0.27	0.23
NBEA	0.29	0.22	0.39	3.49e-04	0.29	0.24
GRIA3	0.32	0.28	0.48	3.49e-04	0.32	0.29
BAZ2B	0.29	0.34	0.45	3.62e-04	0.29	0.31
CHCHD2P9	-0.31	0.15	-0.36	3.68e-04	-0.31	0.23
PKLR	-0.22	0.27	-0.29	3.81e-04	-0.22	0.27
RPRD2	0.50	0.17	0.70	3.88e-04	0.50	0.24
ANKRD26	0.29	0.33	0.46	4.48e-04	0.29	0.32
PABPC1	0.38	0.23	0.55	4.49e-04	0.38	0.27
NME1	-0.28	0.19	-0.34	4.94e-04	-0.29	0.23
PPP1R12A	0.30	0.22	0.41	4.94e-04	0.30	0.23

NLGN4Y	0.42	0.19	0.60	5.25e-04	0.42	0.26
RPS10-NUDT3	-0.26	0.29	-0.35	5.25e-04	-0.26	0.27
TENM2	0.32	0.25	0.44	6.12e-04	0.32	0.25
PBRM1	0.29	0.23	0.43	6.12e-04	0.29	0.26
TUBB4B	-0.28	0.27	-0.37	6.12e-04	-0.28	0.26
ARHGAP21	0.23	0.32	0.32	6.12e-04	0.22	0.27
TET2	0.45	0.11	0.55	6.38e-04	0.45	0.23
CST3	-0.32	0.16	-0.38	6.52e-04	-0.32	0.23
DMD	0.28	0.32	0.41	6.52e-04	0.28	0.30
EEF1A1	-0.22	0.27	-0.29	6.56e-04	-0.22	0.28
ADGRL2	0.31	0.19	0.40	7.16e-04	0.31	0.23
CDH2	0.33	0.19	0.46	7.16e-04	0.33	0.23
FSCN2	-0.29	0.26	-0.39	7.17e-04	-0.29	0.26
GNG11	-0.27	0.32	-0.39	7.33e-04	-0.26	0.30
CALB2	-0.34	0.18	-0.41	7.48e-04	-0.34	0.23
SLIT2	0.34	0.19	0.45	7.62e-04	0.34	0.23
IGFBP4	-0.50	0.01	-0.57	7.94e-04	-0.50	0.23
GCG	-0.58	0.02	-0.67	7.94e-04	-0.57	0.23
NR3C2	0.43	0.17	0.58	7.94e-04	0.44	0.23
EEF1A2	-0.20	0.44	-0.30	7.94e-04	-0.20	0.36
BSG	-0.30	0.15	-0.33	8.08e-04	-0.30	0.23
ATP6V0E2	-0.31	0.17	-0.41	8.08e-04	-0.31	0.23
ATP6V0E2	-0.31	0.18	-0.40	8.08e-04	-0.31	0.23
RYR3	0.38	0.18	0.52	8.08e-04	0.39	0.23
MYO5A	0.31	0.27	0.43	8.08e-04	0.31	0.27
GRIA4	0.30	0.23	0.41	8.59e-04	0.30	0.24
CLTB	-0.23	0.40	-0.34	8.59e-04	-0.23	0.32
CLTB	-0.23	0.40	-0.34	8.59e-04	-0.23	0.32
INSIG1	0.41	0.04	0.39	1.00e-03	0.41	0.23
SOD1	-0.35	0.15	-0.40	1.00e-03	-0.35	0.23
BSG	-0.29	0.15	-0.32	1.00e-03	-0.29	0.23
CNIH1	-0.32	0.15	-0.38	1.00e-03	-0.32	0.23
PCDH15	0.41	0.17	0.54	1.00e-03	0.42	0.23
CNTRL	0.31	0.19	0.42	1.00e-03	0.31	0.23
RPLP0	-0.32	0.19	-0.39	1.00e-03	-0.32	0.23
JMJD1C	0.32	0.19	0.40	1.00e-03	0.32	0.23
EPB41	0.32	0.20	0.41	1.00e-03	0.32	0.23
RPL8	-0.23	0.27	-0.29	1.00e-03	-0.23	0.23
TTC14	0.26	0.25	0.36	1.00e-03	0.26	0.23
PRKDC	0.31	0.22	0.43	1.00e-03	0.31	0.24
GRIA4	0.29	0.25	0.40	1.00e-03	0.29	0.25
PTPRZ1	0.26	0.27	0.35	1.00e-03	0.26	0.25
GNGT2	-0.24	0.26	-0.30	1.00e-03	-0.24	0.26
DDX6	0.29	0.27	0.41	1.00e-03	0.29	0.26
TENM1	0.30	0.27	0.42	1.00e-03	0.30	0.27
PLEKHB1	-0.24	0.31	-0.31	1.00e-03	-0.24	0.27
CELF2	0.31	0.26	0.47	1.00e-03	0.31	0.29
CDK6	0.31	0.29	0.46	1.00e-03	0.31	0.30
HERC2	0.23	0.36	0.35	1.00e-03	0.23	0.32
ACTB	0.29	0.37	0.45	1.00e-03	0.29	0.33

VPS13A	0.25	0.38	0.41	1.00e-03	0.25	0.34
AQP9	-0.65	9.00e-03	-0.66	2.00e-03	-0.63	0.23
AQP9	-0.65	9.00e-03	-0.66	2.00e-03	-0.63	0.23
GCG	-0.56	0.12	-0.69	2.00e-03	-0.56	0.23
SEPP1	-0.36	0.15	-0.38	2.00e-03	-0.36	0.23
NOS2	0.51	0.15	0.69	2.00e-03	0.50	0.23
NRXN3	0.31	0.19	0.38	2.00e-03	0.31	0.23
NRXN3	0.30	0.19	0.38	2.00e-03	0.31	0.23
ANKHD1	0.25	0.26	0.33	2.00e-03	0.25	0.23
RS1	-0.27	0.25	-0.34	2.00e-03	-0.27	0.24
RIMBP2	0.34	0.22	0.45	2.00e-03	0.34	0.24
NFAT5	0.36	0.21	0.48	2.00e-03	0.36	0.24
ATP6V1G1	-0.25	0.27	-0.32	2.00e-03	-0.25	0.24
PTPRS	0.25	0.27	0.34	2.00e-03	0.25	0.24
CA2	-0.21	0.25	-0.26	2.00e-03	-0.21	0.26
DDX6	0.29	0.27	0.40	2.00e-03	0.29	0.26
GNAT2	-0.26	0.28	-0.33	2.00e-03	-0.26	0.27
IGF1R	0.31	0.27	0.44	2.00e-03	0.31	0.27
TUBB2B	-0.30	0.33	-0.42	2.00e-03	-0.30	0.30
GRIA2	0.22	0.40	0.34	2.00e-03	0.22	0.32
GRIA2	0.22	0.40	0.34	2.00e-03	0.22	0.32
ATP6V0B	-0.27	0.35	-0.42	2.00e-03	-0.27	0.34
TOP2B	0.24	0.41	0.38	2.00e-03	0.24	0.35
SRSF5	0.31	0.38	0.51	2.00e-03	0.31	0.37
SKI	0.43	0.11	0.52	3.00e-03	0.43	0.23
MYH15	0.73	0.11	0.88	3.00e-03	0.71	0.23
GPX3	-0.41	0.11	-0.49	3.00e-03	-0.41	0.23
NDUFB8	-0.34	0.12	-0.42	3.00e-03	-0.34	0.23
NCALD	0.39	0.15	0.51	3.00e-03	0.39	0.23
COX4I1	-0.29	0.15	-0.30	3.00e-03	-0.29	0.23
CXCR4	-0.34	0.17	-0.46	3.00e-03	-0.33	0.23
MBNL3	0.35	0.19	0.45	3.00e-03	0.35	0.23
MBNL3	0.35	0.19	0.44	3.00e-03	0.35	0.23
MBNL3	0.35	0.19	0.45	3.00e-03	0.35	0.23
MBNL3	0.35	0.19	0.44	3.00e-03	0.35	0.23
MBNL3	0.34	0.19	0.44	3.00e-03	0.34	0.23
MBNL3	0.35	0.19	0.44	3.00e-03	0.35	0.23
RPL7A	-0.22	0.27	-0.25	3.00e-03	-0.22	0.23
MYLK	0.21	0.33	0.29	3.00e-03	0.21	0.26
MYLK	0.21	0.33	0.29	3.00e-03	0.21	0.26
EIF4A1	-0.26	0.27	-0.33	3.00e-03	-0.26	0.27
CTSB	-0.27	0.29	-0.37	3.00e-03	-0.27	0.28
HIST1H3H	-0.40	0.26	-0.59	3.00e-03	-0.42	0.28
HIST1H2B7	-0.33	0.25	-0.46	3.00e-03	-0.33	0.29
MIA3	0.29	0.28	0.43	3.00e-03	0.29	0.29
RPL15	-0.24	0.33	-0.33	3.00e-03	-0.24	0.29
HIST1H2B7	-0.32	0.26	-0.45	3.00e-03	-0.32	0.29
TPI1	-0.27	0.32	-0.36	3.00e-03	-0.27	0.29
ACTG1	-0.29	0.32	-0.40	3.00e-03	-0.29	0.30
ATP5B	-0.23	0.38	-0.33	3.00e-03	-0.23	0.32

LDHB	-0.20	0.40	-0.28	3.00e-03	-0.20	0.32
ENS-1	0.59	0.08	0.69	4.00e-03	0.58	0.23
LAPTM4A	-0.43	0.08	-0.47	4.00e-03	-0.43	0.23
SREBF1	0.43	0.15	0.54	4.00e-03	0.43	0.23
NAV3	0.39	0.15	0.48	4.00e-03	0.39	0.23
THADA	0.33	0.15	0.43	4.00e-03	0.34	0.23
RALGAPB	0.34	0.16	0.43	4.00e-03	0.34	0.23
SBF2	0.29	0.22	0.36	4.00e-03	0.29	0.23
SLC9A8	0.27	0.23	0.37	4.00e-03	0.27	0.25
CLTA	-0.26	0.30	-0.34	4.00e-03	-0.26	0.27
ITM2A	-0.19	0.40	-0.25	4.00e-03	-0.19	0.32
CKB	-0.22	0.37	-0.30	4.00e-03	-0.22	0.34
PPIA	-0.26	0.38	-0.38	4.00e-03	-0.26	0.34
KCNMA1	0.26	0.40	0.41	4.00e-03	0.26	0.35
ERNI	0.55	0.15	0.68	5.00e-03	0.58	0.23
PODXL	0.56	0.15	0.70	5.00e-03	0.58	0.23
UBN2	0.30	0.17	0.39	5.00e-03	0.30	0.23
FAT3	0.41	0.18	0.55	5.00e-03	0.41	0.23
HARS	-0.29	0.18	-0.35	5.00e-03	-0.29	0.23
ABI1	0.31	0.18	0.42	5.00e-03	0.31	0.23
CARMIL1	0.29	0.19	0.37	5.00e-03	0.29	0.23
COL12A1	0.42	0.21	0.59	5.00e-03	0.45	0.25
HMBOX1	0.42	0.19	0.58	5.00e-03	0.42	0.25
EPHA7	0.33	0.23	0.48	5.00e-03	0.33	0.28
PTPRG	0.27	0.29	0.37	5.00e-03	0.27	0.28
TRPM7	0.27	0.29	0.39	5.00e-03	0.27	0.29
CACNA2D1	0.24	0.36	0.35	5.00e-03	0.25	0.30
VIP	-0.48	0.43	-0.81	5.00e-03	-0.60	0.32
SLC15A2	0.28	0.37	0.45	5.00e-03	0.28	0.36
MIF	-0.21	0.50	-0.36	5.00e-03	-0.21	0.45
SLC38A1	0.32	0.15	0.39	6.00e-03	0.32	0.23
MID1IP1	-0.32	0.16	-0.41	6.00e-03	-0.32	0.23
NDFIP2	0.40	0.17	0.49	6.00e-03	0.40	0.23
SPHKAP	0.26	0.25	0.33	6.00e-03	0.26	0.23
RPL6	-0.23	0.26	-0.26	6.00e-03	-0.23	0.23
TIMP2	-0.28	0.20	-0.36	6.00e-03	-0.28	0.23
SLC8A1	0.25	0.27	0.36	6.00e-03	0.25	0.28
ITPR1	0.25	0.34	0.36	6.00e-03	0.25	0.30
VIP	-0.47	0.44	-0.79	6.00e-03	-0.58	0.33
CCNK	0.46	0.36	0.74	6.00e-03	0.46	0.35
LDHA	-0.20	0.41	-0.29	6.00e-03	-0.20	0.37
HNRNPD	0.27	0.50	0.51	6.00e-03	0.26	0.51
COL5A1	0.33	0.19	0.41	7.00e-03	0.33	0.23
HMGCR	0.24	0.26	0.29	7.00e-03	0.24	0.23
SOBP	0.45	0.27	0.67	7.00e-03	0.45	0.29
RPL4	-0.19	0.37	-0.23	7.00e-03	-0.19	0.29
QSOX1	-0.27	0.31	-0.37	7.00e-03	-0.27	0.29
PHF20L1	0.20	0.42	0.32	7.00e-03	0.20	0.34
MTSS1	0.31	0.19	0.37	8.00e-03	0.31	0.23
EIF3I	-0.26	0.25	-0.33	8.00e-03	-0.26	0.24

CLOCK	0.21	0.30	0.26	8.00e-03	0.21	0.24
CDC42BPA	0.19	0.38	0.27	8.00e-03	0.19	0.29
BRSK1	0.24	0.38	0.37	8.00e-03	0.24	0.33
YWHAG	0.20	0.48	0.33	8.00e-03	0.20	0.40
HIST1H2A4	-0.37	0.15	-0.46	9.00e-03	-0.37	0.23
ANKS1B	0.29	0.19	0.37	9.00e-03	0.29	0.23
RPS4Y1	-0.23	0.27	-0.26	9.00e-03	-0.23	0.23
CLOCK	0.20	0.31	0.26	9.00e-03	0.20	0.24
RAB5C	-0.29	0.23	-0.40	9.00e-03	-0.29	0.27
CNTNAP5	0.31	0.25	0.43	9.00e-03	0.31	0.28
CCSER2	0.23	0.33	0.32	9.00e-03	0.23	0.28
STMN1	-0.27	0.31	-0.35	9.00e-03	-0.27	0.29
CDH4	0.28	0.30	0.41	9.00e-03	0.27	0.32
CLU	-0.23	0.38	-0.32	9.00e-03	-0.23	0.32
LOC776816	-0.18	0.47	-0.27	9.00e-03	-0.18	0.40
ANKRD44	0.21	0.47	0.36	9.00e-03	0.21	0.40
ENO1	-0.14	0.54	-0.22	9.00e-03	-0.14	0.47
PCDHGA2	0.44	0.45	0.75	9.00e-03	0.41	0.48
KIAA0586	0.30	0.23	0.42	0.01	0.30	0.27
RORA	0.21	0.38	0.29	0.01	0.21	0.30
MMP16	0.31	0.15	0.36	0.01	0.31	0.23
NFIA	0.61	0.15	0.82	0.01	0.62	0.23
ERNI	0.53	0.18	0.68	0.01	0.57	0.23
NFIB	0.34	0.18	0.46	0.01	0.34	0.23
CDH13	0.30	0.19	0.38	0.01	0.30	0.23
GUCA1A	-0.29	0.19	-0.33	0.01	-0.29	0.23
SRGAP1	0.25	0.25	0.30	0.01	0.25	0.23
PLN	0.54	0.22	0.73	0.01	0.59	0.24
CDH8	0.20	0.36	0.27	0.01	0.20	0.27
ADIPOR1	-0.27	0.26	-0.38	0.01	-0.27	0.29
KIF2A	0.23	0.37	0.34	0.01	0.23	0.32
RPS29	-0.26	0.37	-0.39	0.01	-0.26	0.34
GRM5	0.35	0.36	0.56	0.01	0.37	0.35
MEIS2	0.24	0.37	0.39	0.01	0.24	0.36
PPP1CC	0.23	0.43	0.36	0.01	0.23	0.37
MPDZ	0.18	0.51	0.29	0.01	0.18	0.41
VTN	-0.16	0.57	-0.28	0.01	-0.16	0.48
TBC1D1	0.30	0.15	0.36	0.01	0.30	0.23
RAN	-0.28	0.17	-0.29	0.01	-0.28	0.23
OPN4	0.28	0.22	0.35	0.01	0.28	0.23
GUCA1B	-0.26	0.23	-0.30	0.01	-0.26	0.23
RPL7	-0.23	0.26	-0.25	0.01	-0.22	0.23
DUSP6	-0.39	0.19	-0.50	0.01	-0.37	0.27
ZFHX3	0.65	0.19	0.94	0.01	0.65	0.27
TENM2	0.29	0.26	0.38	0.01	0.29	0.27
PCDHAC2	0.20	0.37	0.27	0.01	0.20	0.28
NLGN1	0.31	0.25	0.44	0.01	0.31	0.29
B3GNT5	0.72	0.21	1.05	0.01	0.68	0.30
TENM3	0.23	0.36	0.33	0.01	0.23	0.30
WASL	0.26	0.36	0.37	0.01	0.26	0.32

SS2	-0.24	0.40	-0.38	0.01	-0.24	0.39
EEF2	-0.16	0.54	-0.25	0.01	-0.16	0.45
RPL19	-0.24	0.28	-0.28	0.01	-0.24	0.25
SDK2	0.31	0.24	0.41	0.01	0.31	0.27
SLC9A3R1	-0.25	0.35	-0.34	0.01	-0.25	0.32
KPNA3	0.25	0.36	0.39	0.01	0.25	0.36
LIFR	0.34	0.15	0.40	0.01	0.35	0.23
MEF2D	0.77	0.15	1.04	0.01	0.77	0.23
QSER1	0.24	0.25	0.34	0.01	0.24	0.26
SIPA1L1	0.21	0.36	0.29	0.01	0.21	0.28
CHD2	0.18	0.40	0.24	0.01	0.18	0.29
FARP1	0.30	0.30	0.44	0.01	0.30	0.32
FMN1	0.23	0.38	0.36	0.01	0.23	0.35
DIAPH2	0.20	0.47	0.34	0.01	0.20	0.44
LOC769852	-0.41	0.15	-0.49	0.02	-0.42	0.23
BICC1	0.37	0.19	0.50	0.02	0.37	0.23
RPL26L1	-0.23	0.22	-0.24	0.02	-0.23	0.23
TGFB2	0.40	0.25	0.57	0.02	0.41	0.27
SLC8A3	0.22	0.34	0.31	0.02	0.22	0.29
RGS7	0.21	0.40	0.31	0.02	0.21	0.32
CLTC	0.18	0.40	0.26	0.02	0.18	0.33
STRBP	0.17	0.46	0.27	0.02	0.17	0.35
NRXN3	0.40	0.19	0.53	0.02	0.40	0.23
LOC101749238	-0.34	0.19	-0.44	0.02	-0.34	0.24
H3F3B	-0.21	0.29	-0.24	0.02	-0.22	0.25
HRAS	-0.35	0.19	-0.44	0.02	-0.34	0.26
RPS27A	-0.20	0.40	-0.28	0.02	-0.20	0.32
RACK1	-0.18	0.44	-0.25	0.02	-0.18	0.32
GAPVD1	0.19	0.33	0.24	0.02	0.19	0.24
CITED4	-0.20	0.33	-0.24	0.02	-0.20	0.26
ZSWIM8	0.25	0.28	0.32	0.02	0.25	0.26
TRIM2	0.19	0.35	0.26	0.02	0.20	0.27
HIST2H4B	-0.28	0.27	-0.34	0.02	-0.28	0.27
HIST1H46	-0.28	0.27	-0.34	0.02	-0.28	0.27
HIST1H2B8	-0.32	0.25	-0.41	0.02	-0.32	0.28
NEUROD4	0.36	0.15	0.45	0.02	0.36	0.23
MAFF	-0.51	0.19	-0.65	0.02	-0.50	0.23
RPL26L1	-0.24	0.22	-0.23	0.02	-0.24	0.23
EIF3H	-0.23	0.25	-0.27	0.02	-0.23	0.23
ITM2B	-0.20	0.30	-0.22	0.02	-0.20	0.24
ANOS1	0.21	0.30	0.26	0.02	0.21	0.24
BMPR2	0.21	0.31	0.27	0.02	0.21	0.25
EIF2S3	-0.22	0.32	-0.27	0.02	-0.22	0.26
ADAM23	0.24	0.29	0.34	0.02	0.24	0.30
GLG1	0.23	0.36	0.33	0.02	0.23	0.31
PPP2CB	-0.21	0.40	-0.28	0.02	-0.21	0.32
MYH9	0.20	0.37	0.30	0.02	0.20	0.32
UBB	-0.20	0.46	-0.29	0.02	-0.20	0.37
PNISR	0.13	0.75	0.32	0.02	0.13	0.70
CSRP2	-0.30	0.17	-0.28	0.02	-0.30	0.23

RPS28	-0.31	0.18	-0.38	0.02	-0.31	0.23
AGTPBP1	0.27	0.19	0.33	0.02	0.27	0.23
PPP3CB	0.25	0.25	0.31	0.02	0.25	0.23
STAU1	0.21	0.31	0.26	0.02	0.21	0.25
XPO5	0.24	0.27	0.31	0.02	0.24	0.25
COPS8	-0.24	0.26	-0.30	0.02	-0.24	0.26
NCOA1	0.30	0.22	0.40	0.02	0.30	0.27
TLE4	0.30	0.23	0.41	0.02	0.30	0.27
PSMC5	-0.24	0.27	-0.32	0.02	-0.24	0.28
PPIB	-0.25	0.27	-0.34	0.02	-0.25	0.29
SLC25A6	-0.17	0.40	-0.21	0.02	-0.17	0.30
RPL3	-0.16	0.45	-0.22	0.02	-0.16	0.32
LSS	0.33	0.12	0.37	0.02	0.33	0.23
OTX2	0.28	0.17	0.33	0.02	0.28	0.23
HEBP1	-0.32	0.18	-0.39	0.02	-0.32	0.23
LTN1	0.26	0.23	0.29	0.02	0.26	0.23
TOM1L2	0.29	0.25	0.34	0.02	0.29	0.24
MAPK10	0.24	0.27	0.30	0.02	0.24	0.25
MAPK10	0.24	0.27	0.30	0.02	0.24	0.25
HIST1H46L2	-0.30	0.25	-0.36	0.02	-0.30	0.26
CCNRC01	0.20	0.34	0.27	0.02	0.20	0.27
SRI	-0.26	0.25	-0.36	0.02	-0.26	0.27
LEPROT	0.31	0.25	0.43	0.02	0.32	0.29
DGKZ	0.24	0.28	0.34	0.02	0.24	0.29
ARL6IP5	-0.16	0.48	-0.23	0.02	-0.16	0.35
USP28	0.27	0.40	0.46	0.02	0.27	0.37
NDUFV1	-0.24	0.40	-0.36	0.02	-0.23	0.38
AK1	-0.37	0.41	-0.59	0.02	-0.35	0.41
LAMTOR3	-0.27	0.15	-0.30	0.02	-0.27	0.23
TTLL5	0.26	0.17	0.27	0.02	0.26	0.23
RORB	0.25	0.19	0.30	0.02	0.25	0.23
FAM213A	-0.28	0.22	-0.30	0.02	-0.28	0.23
SLC38A2	0.23	0.25	0.25	0.02	0.23	0.23
SELENOT	-0.20	0.36	-0.26	0.02	-0.20	0.29
NCAM1	0.18	0.36	0.23	0.02	0.18	0.29
HSPA2	-0.23	0.35	-0.33	0.02	-0.23	0.32
EIF4A3	-0.19	0.43	-0.27	0.02	-0.19	0.34
CLIP1	0.16	0.48	0.24	0.02	0.16	0.35
SYP	-0.15	0.49	-0.20	0.02	-0.15	0.38
PER2	0.22	0.46	0.34	0.02	0.22	0.39
LBH	-0.14	0.65	-0.24	0.02	-0.14	0.54
TFAP2B	0.31	0.12	0.35	0.02	0.31	0.23
KCNA2	0.30	0.13	0.34	0.02	0.30	0.23
POU2F1	0.49	0.15	0.57	0.02	0.51	0.23
TOMM6	-0.28	0.19	-0.36	0.02	-0.28	0.25
YTHDC1	0.15	0.55	0.25	0.02	0.15	0.43
ENS-1	0.55	0.19	0.68	0.02	0.61	0.23
RPL5	-0.25	0.22	-0.23	0.02	-0.24	0.23
FAM213A	-0.28	0.22	-0.30	0.02	-0.28	0.23
ERNI	0.41	0.27	0.58	0.02	0.46	0.27

HIST1H46L2	-0.29	0.27	-0.36	0.02	-0.29	0.27
GAP43	-0.37	0.27	-0.51	0.02	-0.35	0.31
FSCN1	-0.23	0.35	-0.34	0.02	-0.22	0.35
VPS33B	-0.29	0.15	-0.32	0.02	-0.29	0.23
NUDT16L1	-0.33	0.16	-0.41	0.02	-0.33	0.23
GABRA6	-0.17	0.43	-0.22	0.02	-0.17	0.32
MYH10	0.16	0.50	0.25	0.02	0.17	0.37
KDM3A	0.23	0.46	0.36	0.02	0.23	0.40
DPF3	0.32	0.22	0.42	0.03	0.32	0.27
STXBP1	0.74	0.25	1.11	0.03	0.74	0.30
NR2C1	0.29	0.27	0.43	0.03	0.29	0.30
SYNGR1	-0.19	0.36	-0.26	0.03	-0.19	0.31
UBE2E3	0.31	0.15	0.33	0.03	0.31	0.23
AKAP2	0.20	0.28	0.24	0.03	0.21	0.23
NDUFA4	-0.24	0.26	-0.28	0.03	-0.24	0.23
KCNH6	0.34	0.19	0.42	0.03	0.34	0.25
NCAM1	0.18	0.37	0.22	0.03	0.18	0.29
RPS6	-0.19	0.40	-0.24	0.03	-0.19	0.31
CHD1	0.17	0.43	0.25	0.03	0.17	0.32
SMARCA2	0.15	0.48	0.23	0.03	0.16	0.34
ZCCHC6	0.16	0.47	0.25	0.03	0.16	0.35
SERINC1	-0.15	0.55	-0.24	0.03	-0.16	0.45
LOC422214	-0.32	0.15	-0.36	0.03	-0.32	0.23
SIRT6	-0.34	0.18	-0.42	0.03	-0.34	0.23
SAP18	-0.23	0.31	-0.31	0.03	-0.23	0.31
PHB	-0.31	0.15	-0.35	0.03	-0.31	0.23
LPP	0.48	0.25	0.64	0.03	0.50	0.25
PIK3CD	0.38	0.26	0.52	0.03	0.37	0.29
SCG5	-0.27	0.34	-0.35	0.03	-0.27	0.32
ANAPC10	0.39	0.34	0.59	0.03	0.39	0.32
TUBA1C	-0.25	0.40	-0.38	0.03	-0.25	0.39
VSNL1	-0.15	0.54	-0.22	0.03	-0.15	0.41
C12ORF57	-0.39	0.15	-0.45	0.03	-0.38	0.23
SOX5	0.23	0.22	0.30	0.03	0.23	0.23
SZT2	0.26	0.22	0.32	0.03	0.26	0.25
MELTF	0.33	0.20	0.43	0.03	0.34	0.26
EDF1	-0.22	0.30	-0.28	0.03	-0.22	0.29
SNAP25	-0.20	0.40	-0.25	0.03	-0.20	0.32
TOX3	0.43	0.36	0.65	0.03	0.44	0.32
TMSB4X	-0.17	0.46	-0.23	0.03	-0.17	0.34
SLC17A6	0.45	0.34	0.72	0.03	0.45	0.35
SUGP2	0.16	0.48	0.24	0.03	0.16	0.36
GHITM	-0.17	0.51	-0.25	0.03	-0.17	0.40
AP2M1	-0.13	0.61	-0.20	0.03	-0.13	0.50
DICER1	0.41	0.24	0.59	0.03	0.41	0.28
FUT9	0.37	0.26	0.53	0.03	0.37	0.28
NACA	-0.25	0.31	-0.33	0.03	-0.25	0.31
LUC7L3	0.12	0.69	0.25	0.03	0.12	0.59
REPS1	0.32	0.15	0.38	0.03	0.32	0.23
ST8SIA2	-0.31	0.21	-0.37	0.03	-0.31	0.26

HIGD1C	-0.22	0.30	-0.28	0.03	-0.22	0.29
MDGA1	0.24	0.31	0.34	0.03	0.24	0.31
LOC107053055	0.46	0.27	0.70	0.03	0.47	0.32
IQGAP2	0.20	0.47	0.31	0.03	0.20	0.39
MGEA5	0.18	0.55	0.31	0.03	0.18	0.47
ACLY	0.22	0.25	0.27	0.03	0.22	0.24
LOC772071	0.21	0.29	0.29	0.03	0.21	0.28
ANO5	0.26	0.27	0.37	0.03	0.27	0.29
TOX3	0.43	0.37	0.65	0.03	0.44	0.34
COX6A1	-0.27	0.17	-0.31	0.03	-0.27	0.23
FNDC3A	0.22	0.27	0.30	0.03	0.22	0.27
RAB18	-0.22	0.36	-0.26	0.03	-0.22	0.29
PARD3	0.24	0.30	0.33	0.03	0.24	0.31
MLF2	-0.20	0.40	-0.27	0.03	-0.20	0.32
SCAF11	0.17	0.45	0.25	0.03	0.17	0.34
PER3	0.23	0.37	0.34	0.03	0.23	0.35
C4orf48	-0.15	0.50	-0.21	0.03	-0.15	0.35
RAB3GAP2	0.17	0.47	0.26	0.03	0.17	0.36
HSPA8	-0.16	0.49	-0.22	0.03	-0.16	0.42
COX6A1	-0.27	0.17	-0.31	0.04	-0.27	0.23
CELF1	0.20	0.29	0.28	0.04	0.20	0.27
PGRMC1	-0.18	0.38	-0.22	0.04	-0.18	0.28
RPS27A	-0.18	0.43	-0.25	0.04	-0.18	0.34
RPSAP58	-0.16	0.47	-0.21	0.04	-0.16	0.34
ATP1B3	-0.15	0.53	-0.22	0.04	-0.15	0.40
TM2D3	-0.31	0.18	-0.37	0.04	-0.31	0.24
TM2D3	-0.31	0.19	-0.37	0.04	-0.30	0.24
PCDH1	0.28	0.22	0.35	0.04	0.28	0.26
UQCR11	-0.22	0.31	-0.32	0.04	-0.22	0.32
USP7	0.38	0.33	0.58	0.04	0.38	0.32
ECHS1	-0.35	0.12	-0.38	0.04	-0.35	0.23
DROSHA	0.28	0.15	0.33	0.04	0.28	0.23
CNBP	-0.23	0.27	-0.24	0.04	-0.23	0.23
CHUNK-1	0.41	0.22	0.51	0.04	0.40	0.27
MICALL1	0.48	0.15	0.53	0.04	0.47	0.23
MBNL1	0.28	0.19	0.35	0.04	0.28	0.23
MBNL1	0.27	0.19	0.35	0.04	0.28	0.23
MBNL1	0.28	0.19	0.36	0.04	0.29	0.23
HIST1H2A4	-0.34	0.27	-0.46	0.04	-0.34	0.29
XPO1	0.29	0.40	0.48	0.04	0.29	0.36
SNRNP200	0.19	0.46	0.28	0.04	0.19	0.37
MDH1	-0.18	0.50	-0.25	0.04	-0.18	0.39
MDH1	-0.18	0.50	-0.25	0.04	-0.18	0.39
SLC9A1	0.56	0.15	0.62	0.04	0.56	0.23
TCP1	-0.21	0.37	-0.25	0.04	-0.21	0.29
PCDHA3	0.16	0.59	0.30	0.04	0.15	0.54
NDUFB3	-0.41	0.15	-0.43	0.04	-0.39	0.23
MBNL1	0.27	0.19	0.35	0.04	0.27	0.23
ZDHHC8	0.31	0.19	0.39	0.04	0.31	0.23
MBNL1	0.27	0.19	0.34	0.04	0.27	0.23

PCGF5	0.26	0.19	0.33	0.04	0.26	0.23
HIST1H2A4L3	-0.34	0.26	-0.45	0.04	-0.34	0.28
RPS15	-0.21	0.38	-0.28	0.04	-0.21	0.32
TALDO1	-0.21	0.39	-0.27	0.04	-0.21	0.32
PCDHA13	0.15	0.59	0.30	0.04	0.15	0.54
RMND5A	0.19	0.40	0.29	0.04	0.19	0.35
AQP1	-0.38	0.36	-0.55	0.04	-0.32	0.41
OXCT1	0.14	0.55	0.24	0.04	0.14	0.44
OPCML	0.51	0.19	0.62	0.04	0.50	0.23
ATM	0.19	0.43	0.26	0.04	0.19	0.33
PCM1	0.13	0.57	0.21	0.04	0.13	0.44
ARR3	-0.14	0.58	-0.23	0.04	-0.14	0.49
SLC24A5	0.24	0.29	0.35	0.04	0.24	0.30
ERP29	-0.14	0.55	-0.21	0.04	-0.14	0.42
GNAI3	-0.27	0.23	-0.29	0.04	-0.27	0.23
RPS12	-0.22	0.25	-0.21	0.04	-0.22	0.23
DCX	0.22	0.25	0.29	0.04	0.22	0.26
BNIP3L	-0.17	0.44	-0.20	0.04	-0.17	0.33
RPL17	-0.17	0.47	-0.23	0.04	-0.17	0.35
VAV3	0.15	0.54	0.26	0.04	0.15	0.46
DCX	0.22	0.25	0.29	0.05	0.22	0.26
YTHDF3	0.20	0.27	0.27	0.05	0.21	0.26
SPTBN1	0.10	0.80	0.26	0.05	0.10	0.75
EHMT1	0.21	0.30	0.25	0.05	0.21	0.25
MYSM1	0.17	0.40	0.25	0.05	0.17	0.34
LARGE1	0.19	0.44	0.28	0.05	0.19	0.36
RPL13	-0.17	0.48	-0.23	0.05	-0.17	0.36
MEF2A	0.15	0.51	0.22	0.05	0.15	0.37
SAP130	0.30	0.47	0.50	0.05	0.29	0.45
PRPF19	-0.19	0.53	-0.32	0.05	-0.18	0.50
WAPL	0.12	0.65	0.22	0.05	0.12	0.52
HMGN2P46	-0.26	0.22	-0.32	0.05	-0.26	0.25
YBX3	-0.19	0.36	-0.21	0.05	-0.19	0.26
CHD7	0.41	0.26	0.57	0.05	0.41	0.28
ASCC3	0.21	0.32	0.28	0.05	0.21	0.30
SPATS2L	0.29	0.15	0.32	0.05	0.29	0.23
PSMA7	-0.22	0.29	-0.28	0.05	-0.22	0.29
SEC24A	0.23	0.26	0.29	0.05	0.23	0.26
G0S2	-0.30	0.22	-0.37	0.05	-0.30	0.27
PHTF2	0.27	0.28	0.36	0.05	0.27	0.30
PRRG1	0.22	0.31	0.31	0.05	0.22	0.31
TUBA1C	-0.27	0.40	-0.40	0.05	-0.28	0.35
PSAP	-0.14	0.48	-0.19	0.05	-0.15	0.39
TMEM59	-0.15	0.56	-0.22	0.05	-0.15	0.44
ATP6V0D1	-0.12	0.71	-0.22	0.05	-0.12	0.60
CANX	0.12	0.75	0.28	0.05	0.12	0.69
MIR3526	-0.36	0.18	-0.42	0.05	-0.37	0.23
NECAB3	-0.30	0.20	-0.36	0.05	-0.29	0.26
NEGR1	0.20	0.37	0.29	0.05	0.20	0.34
ARL6IP1	-0.19	0.45	-0.25	0.05	-0.19	0.35

Appendix 5.3. Common differentially expressed genes between comparisons for treated vs. control and previous studies.

Gene	Model. 1	Model. 2	Author	Year	Method	Species	Tissue
FOS		Yes	Brand	2007	Microarray	Mouse	Retina
ALDH1A1		Yes	McGlinn	2007	Microarray	Chick	Retina/RPE
ASL1		Yes	McGlinn				
CDKN1A		Yes	McGlinn				
COPS2		Yes	McGlinn				
CTSC		Yes	McGlinn				
DHCR7		Yes	McGlinn				
DHFR		Yes	McGlinn				
DUSP4	Yes	Yes	McGlinn				
GAS2		Yes	McGlinn				
GCLM		Yes	McGlinn				
GNG10		Yes	McGlinn				
GXYLT1		Yes	McGlinn				
ID4		Yes	McGlinn				
IL17RD		Yes	McGlinn				
MCFD2		Yes	McGlinn				
NTS		Yes	McGlinn				
PTN		Yes	McGlinn				
SWAP70		Yes	McGlinn				
TCEB1		Yes	McGlinn				
UTS2B	Yes	Yes	McGlinn				
VIP	Yes	Yes	McGlinn				
ETV5		Yes	Schippert	2008	Microarray	Chick	Retina
ID2		Yes	Schippert				
ATP6V0D2		Yes	Ashby	2010	Microarray	Chick	Amacrine cell layer
C26H6ORF125		Yes	Ashby				
GNG13		Yes	Ashby				
GTF2H5		Yes	Ashby				
NT5C2		Yes	Ashby				
AACS		Yes	Stone	2011	Microarray	Chick	Retina/RPE
ABRACL		Yes	Stone				
ACTR6		Yes	Stone				
ADCYAP1R1		Yes	Stone				
ALG12		Yes	Stone				
ARL6		Yes	Stone				
ARNT		Yes	Stone				
ATG4B		Yes	Stone				
BDNF		Yes	Stone				
CALB1		Yes	Stone				
CCNL2		Yes	Stone				
CDC42		Yes	Stone				

CLCN7		Yes	Stone				
CXCL14		Yes	Stone				
CYB5B		Yes	Stone				
DIO2	Yes	Yes	Stone				
FN3KRP		Yes	Stone				
FOSL2		Yes	Stone				
GLCCI1		Yes	Stone				
GMFB		Yes	Stone				
GORASP1		Yes	Stone				
GPR137B		Yes	Stone				
GTF2E2		Yes	Stone				
H2AFZ		Yes	Stone				
HNRNPH3		Yes	Stone				
HSBP1		Yes	Stone				
HSP90AB1		Yes	Stone				
KCNA4	Yes	Yes	Stone				
LIMS1		Yes	Stone				
LOC421792		Yes	Stone				
LSM7		Yes	Stone				
MAGI3		Yes	Stone				
MRPL51		Yes	Stone				
MZT1		Yes	Stone				
NAB1		Yes	Stone				
NDUFA10		Yes	Stone				
NPAS2		Yes	Stone				
NSUN2		Yes	Stone				
OARD1		Yes	Stone				
OLA1		Yes	Stone				
OPN4		Yes	Stone				
OPN4-1	Yes	Yes	Stone				
OSBPL2		Yes	Stone				
PDDC1		Yes	Stone				
PER3		Yes	Stone				
POLE3		Yes	Stone				
PTPRG		Yes	Stone				
RNF166		Yes	Stone				
RSPO2		Yes	Stone				
SSR3		Yes	Stone				
SZT2		Yes	Stone				
TCF3		Yes	Stone				
TET2		Yes	Stone				
TMEM167A		Yes	Stone				
UFM1		Yes	Stone				
ZNF335		Yes	Stone				
CKB		Yes	Bertrand	2006	2D GE, MS	Chick	Retina

CRYAB	Yes	Zhou	2010	2D GE, MS	Guinea Pig	Posterior Sclera
PRDX1	Yes	Zhou				
COL6A1	Yes	Frost	2012	2D GE, MS	Tree Shrew	Sclera
CRABP1	Yes	Frost				
CCT8	Yes	Frost				
ATP5C1	Yes	Barathi	2014	iTRAQ	Mouse	Retina
MBP	Yes	Barathi				
UQCRB	Yes	Barathi				

Appendix 5.4 Common differentially expressed genes between comparisons for treated vs. control and comparisons for high vs. low.

Transcript ID	Gene symbol
NM_001001604	*ST8SIA2*
NM_001006171	*ARL6IP1*
NM_001006395	*MDH1*
NM_001012605	*ARL6IP5*
NM_001012846	*ACSBG2*
NM_001012882	*NCOA1*
NM_001030577	*COX4I1*
NM_001030697_2	*PIK3R5*
NM_001030966	*INSIG1*
NM_001031217	*GHITM*
NM_001031301	*SAP130*
NM_001044643	*SLC9A1*
NM_001044647	*MDGA1*
NM_001044653	*OPN4*
NM_001111133_2	*PCDHA3*
NM_001111136	*PCDHA13*
NM_001168004	*EPB41*
NM_001177309	*VIP*
NM_001177735	*PHB*
NM_001190802	*UQCR11*
NM_001204761	*NME1*
NM_001277766	*SZT2*
NM_001277794	*TET2*
NM_001289779	*PER3*
NM_001305113	*KCNH6*
NM_001316891	*MDH1*
NM_001319028	*SLC15A2*
NM_204126	*SREBF1*
NM_204204	*UGT8*
NM_204314	*PTPRG*
NM_204353	*IGFBP4*
NM_204354	*DUSP6*
NM_204485	*HMGCR*
NM_204538	*SDK2*
NM_204757	*MAFF*
NM_204895	*TFAP2B*
NM_204900	*CLU*
NM_205208	*CSRP2*
NM_205258	*RAN*
NM_205280	*MBP*
NM_205310	*CKB*
NM_205366	*VIP*
NM_205429	*17.5*
NM_205501	*ASL1*

Appendix 5.5. Venn-diagram showing overlap in differentially-expressed transcripts identified by "model 2 separate" (i.e. FD treated vs. control eyes in high group; FD treated vs. control eyes in low group) and by model 3 (an analysis testing for an interaction between FD treatment and high vs. low group).

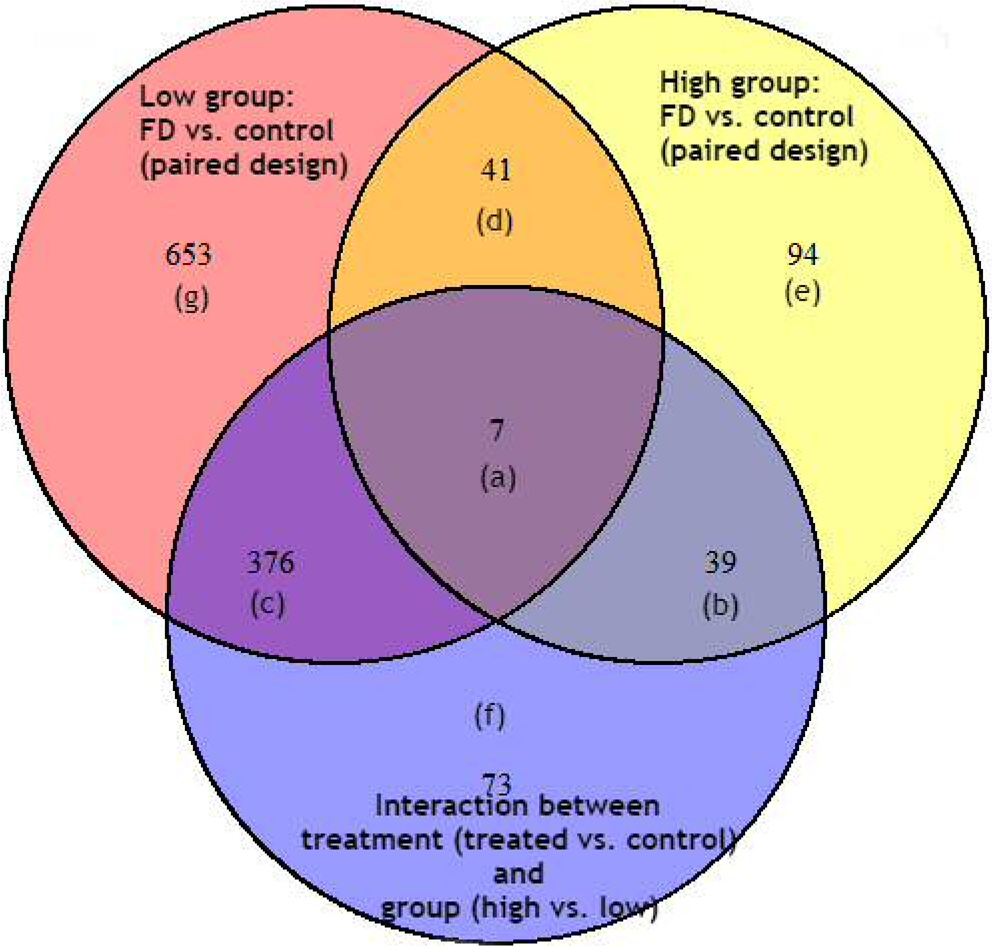

The overlapped **genes** are listed

(a) ANKRD10, OPN4, VIP, AQP9, TUBA1C, SNCB

(b) ST8SIA2, SLC9A3R1, LSS, OXCT1, PLEKHB1, ACSBG2, HEBP1, INSIG1, HIST1H2A4, GPX3, FSCN1, GCG, BSG, ALDOC, SYNGR1, TBC1D1, ECHS1, RPS29, HIST1H2A4L3, LOC101749238, XPO1, RPS28, MIF, QSOX1, TIMP2, IGFBP4, DUSP6, HMGCR, CXCR4, GNAT2, MAFF, CLU, VTN, PKLR

(c) TMSB4X, BMPR2, CDH2, CDH13, GRIA2, STMN1, TENM2, RACK1, RPL7A, LARGE1, SOX5, CDH4, TUBB2B, PROX1, HARS, ARL6IP1, PPP1CC, EDF1, CHCHD2P9, PHTF2, RPL3, EIF2S3, DDX6, RPL7, RAB18, DROSHA, YTHDF3, MDH1, TCP1, HMGN2P46, LOC422214, NDUFB8, TMEM59, TTC14, SELENOT, LAMTOR3, RPL4, RPSAP58, ACTG1, GUCA1B, CDK6, ANAPC10, CELF1, EHMT1, ITM2A, MBNL3, ARL6IP5, TMEM131, SNRNP200, ATF7IP, FNDC3A, STAU1, JARID2, REPS1, NCOA1, SBF2, ANKRD44, MYSM1, RPRD2, ANKRD52, COX4I1, CLTB, EIF4A3, STRBP, NDFIP2, RPS3, RALGAPB, RPL19, MTSS1, HIGD1C, ADIPOR1, LBH, TGFB2, SERINC1, PNISR, LAPTM4A, YTHDC1, TALDO1, DGKZ, SRSF5, CCNK, GHITM, SAP130, ATP5B, YWHAG, SRRM1, USP28, LUC7L3, PGAM1, LPP, NDUFV1, PABPC1, MEF2D, SEPP1, CNIH1, SLC24A5, ZDHHC8, SLC9A8, PHF20L1, ABI1, MGEA5, CLTA, SKI, AQP1, KIAA0586, SLC9A1, MDGA1, PCDH15, PCDH1, COPS8, CNTNAP5, CHD7, SLC8A1, AP2M1, HIST1H2B7, LOC772071, SRGAP1, CLTC, TUBB4B, SRI, ENS-1, ERNI, NLGN1, ARR3, CTTNBP2, THADA, SOBP, CCNRC01, PCDHAC2, PCDHA3, PCDHA13, FAT3, GRIA3, GRIA4, B3GNT5, NCAM1, RS1, ADAM23, NR3C2, NAV3, CARMIL1, RAB3GAP2, EIF3I, PPIA, EPB41, SLC17A6, NLGN4Y, ITPR1,

CACNA2D1, ARHGAP21, SPHKAP, TRPM7, PHB, FSCN2, ADGRL2, UQCR11, G0S2, FAM213A, KPNA3, SUGP2, ZSWIM8, TENM3, RGS7, PEBP1, NFAT5, PTPRZ1, QSER1, USP34, CDC42BPA, WASL, BICC1, CCSER2, WAPL, MAGI2, JMJD1C, BRSK1, SLC38A1, NOVA1, MICALL1, ANKHD1, AKAP2, NME1, PCDHGA2, ANKS1B, FARP1, NBEA, HERC2, MPDZ, RPS10-NUDT3, SLIT2, TOM1L2, PODXL, NRXN3, PGRMC1, ERP29, ANK3, RPL26L1, TOX3, ATP6V0E2, RALGAPA1, COX6A1, MIA3, ATP6V0B, XPO5, ATP6V1G1, HMBOX1, RPL8, UBN2, SZT2, TET2, KIAA2018, VPS13A, RPS12, GNG11, CHD2, HIST1H3H, ANKRD26, RPS27A, PER3, CLOCK, RORA, SCG5, PSMC5, ZFHX3, SLC8A3, C4orf48, UBB, TM2D3, NDUFA4, GNGT2, NDUFB3, GAP43, KCNH6, RPL15, SLC38A2, STXBP1, CNTRL, LOC776816, MAPK10, SLC15A2, EEF1A1, MYLK, LOC107053055, SREBF1, GRM5, RPL6, LDHB, DIAPH2, KCNMA1, SLC25A6, TLE4, RIMBP2, CELF2, PER2, CACNA1B, GAPDH, SAP18, PTPRG, KCND3, KCNA2, USP7, OTX2, RAB5C, PCM1, SDK2, EIF4A1, LIFR, RPL5, PSMA7, DPF3, SALL3, PRKDC, BAZ2B, OPCML, MYH15, COL5A1, MEIS2, PSAP, CHUNK-1, NEGR1, TENM1, MEF2A, TFAP2B, CNBP, CHD1, NOS2, PGK1, RPLP0, RPL13, HSPA8, COL12A1, IGF1R, SOD1, TOP2B, EPHA7, ITM2B, RORB, RPS4Y1, AK1, ENO1, PPP1R12A, PPP2CB, SMARCA2, NCALD, FASN, PBRM1, MMP16, MELTF, CSRP2, RPS6, VSNL1, RAN, NFIB, NFIA, LDHA, HRAS, H3F3B, DMD, MYO5A, CKB, CALB2, CA2, CTSB, SYP, YBX3, PTPRS, PLN, ANOS1, TPI1, SNAP25, POU2F1, MYH9, GLG1, CST3, ACACA, ATP1B3, VAV3, RYR3, AKAP9, MID1IP1, MIR3526

(d) LOC421975, MSMO1, BCL6, RBP3, DNMT3A, SWAP70, RAP1GAP2, SPRY4, STARD4, PCDHA11, PCDHA4, PCDHA5, PCDHA8, PCDHA9, MZT1, APC2, NUMA1, COL9A2, BHLHE40, NTS, ETV5, RAD54L2, C14orf2, DIO2, UQCRB, HK2, SIX3, TERF1, CDKN1A, UNC5C, PTPRU, OPN4-1, SPON1, KCNA4, CRYAB, SLC2A1, LRP1, TNS1, UTS2B

(e) CFDP1, EGF, SUCLG2, CORO7-PAM16, AACS, MTERF3, DHFR, TANGO2, YPEL2, ATP6V0D2, AZIN1, DNPEP, DEPDC1, BCL2L1, MON1A, TWF1, TFEB, KDM5B, DHCR24, SGF29, DCTN1, CTSA, AOX1, WWP2, EWSR1, LOC395100, OLFML3, HIST1H101, GADD45A, FOSL2, CYP51A1, FGL2, NA, DUSP1, FBF1, CDK5, FADS2, PALM, SQLE, P4HA1, COQ8A, DHCR7, RHOBTB1, KCNMB4, JUP, UCKL1, SIRT5, GAS2L3, RGS16, TWF1, CREBL2, RASA4B, ELN, C10H15ORF59, FAM136A, STK10, PFKL, EGR1, MAB21L2, ILK, GIT1, KIT, THY1, NR2F2, COL2A1, AIP, OPTC, SGK1, IL17RD, RARA, RGMA, NA, CXCL14, CSPG5, ANGPT2, DUSP4, MERTK, GFRA4, GBX2, ADORA2B, GFRA2, AANAT, NA, SDC3, KCNJ3, HMGCS1, EXFABP, OPN1LW, FOS, FGFR1

(f) UBE2E3, SPATS2L, LOC769852, NEUROD4, VPS33B, C12ORF57, NUDT16L1, TTLL5, SIRT6, GUCA1A, AGTPBP1, MBNL1, MBNL1, MBNL1, MBNL1, MBNL1, PCGF5, TOMM6, NECAB3, GNAI3, LTN1, DICER1, HIST1H2B8, PPP3CB, LEPROT, HIST1H46L2, ACLY, DCX, DCX, EIF3H, SEC24A, PIK3CD, FUT9, PPIB, NR2C1, ANO5, HIST1H46L2, HIST2H4B, HIST1H46, PARD3, NACA, PRRG1, ASCC3, CITED4, GAPVD1, HSPA2, TRIM2, CDH8, SIPA1L1, ACTB, KIF2A, RPS15, FMN1, SS2, MLF2, RMND5A, ATM, GABRA6, BNIP3L, EEF1A2, SCAF11, KDM3A, ZCCHC6, IQGAP2, RPL17, CLIP1, MYH10, HNRNPD, PRPF19, EEF2, ATP6V0D1, CANX, SPTBN1

(g) *ST3GAL5, SDC2, RTN1, P3H2, CYB5A, LOC414835, CDHR1, LIMS1, GSTA2, CAPZA2, ZYX, CCT8, CNTN2, SERPINI1, NFASC, MRPS11, MAP2K1, HSDL1, UQCRFS1, GPI, PPP2CA, SKP1, C13H5ORF15, GET4, UBE2L3, SEPT2L, RANBP1, TMED2, XBP1, ACADS, NOL11, CCT6A, PSMC2, RPAP3, SLC25A3, PHC1, FKBP4, AP1S2, TRAPPC2, SUCLA2, SPRYD7, RTFDC1, RER1, SDF4, PGD, ZDHHC18, NUDC, LSM7, COPE, FABP5, OTUD6A, EIF3E, ARF1, GTPBP4, HIBADH, CNDP2, PSME4, MCFD2, LOC421792, LMBRD1, CHMP1B, ABCE1, OSTC, DCTD, COPS4, DCK, RPL7L1, ASAH1, NUCB2, API5, ERH, EIF2S1, PSMA3, ACTR10, PSMC6, ASNSD1, BIN1, ZNF326, NDUFB5, ANP32E, OAT, GOLGA7, TMEM175, AP3S1, SLC25A46, SYNGR3, VPS29, YWHAH, RNF5, GID8, AP1M1, TCEB1, YPEL5, PSMB1, MPP1, RNF141, TMED5, RPL30, TRAPPC3, TMEM41B, CD82, GLRX5, SUB1, MRPL51, PNRC1, CCT2, CCT5, GPM6A, EXOC5, HNRNPH3, SEC62, MAEA, MGAT3, MAGI3, RBM10, HAGH, RAB14, ODF2, CNOT4, POLDIP3, SCAF4, GNB1, ELL, GLCCI1, SCCPDH, TMEM30A, SLC25A14, TMEM164, GTF2E2, SUCLG1, CHUK, NEURL1, HSPD1, SELENOF, STX7, PAN2, FOXP1, SELENOK, ERBB4, KCNA3, CRABP1, NPAS2, MESDC2, HEATR3, CYB5B, APEH, IMPDH2, CLCN7, NRF1, NET1, SNAP29, SETD1A, BG8, BRD2, NUP188, SET, DLD, DNAJB9, NELL2, KRR1, ST13P5, CHMP2B, CBR3, EIF1AX, PDCL3, ABCC4, UFM1, SRSF6, EIF6, AURKAIP1, ATP13A2, MEAF6, AGO3, AHCYL1, OARD1, PTBP1, FBXO32, GMPR2, RPRD1A, MAPRE2, TIMM17B, SERTAD2, CRIPT, GPR137B, LIN7C, RWDD1, OSTM1, ASXL2, GGA3, SEC31A, SGCB, ANGEL1, GMFB, UNC5B, TRIM8, NDUFA10, GLS2, PLEKHA3, OLA1, PSMD14, VTG2, SLC6A9, BTF3L4, RNF7, PPP1R2, KIAA0907, MRPL28,*

MED24, TBL1XR1, H2AFZ, HDAC7, TXN2, SLC30A5, DCTN3, BRIX1, FYB, MAP1LC3B, ZMAT2, MPC1L, PCMT1, CCT7, ARPC5, ZC3H3, IRF5, LOC431499, BG8, VDAC1, ATG9A, VEZF1, ZNF512B, LY75-CD302, SMARCB1, PITPNB, AGO4, ACP1, FDFT1, FNIP1, ZDHHC5, PRKAA2, MRPS26, SPECC1L, CYCS, HMGN4, ZNF384, UBN1, USP48, PFN2, UCHL1, CD69L, NCAPD2, RHOT2, GNRH1, PHB2, EVI2A, ARL1, ATP5I, GTF2H5, NDUFA5, THOC7, ADCYAP1R1, PCDH19, PCDH8, ZNF692, HSP90AA1, PCDHA1, PCDHA12, PCDHA2, PCDHA7, HSBP1, PNPLA6, TMEM167A, CHCHD4, FN3KRP, SCOC, TXNRD3, PPAP2B, CECR2, MEIS1, PSMD4, OAZ2, C12orf75, NDUFS3, ABLIM1, HYDIN, NFASC, GABRQ, DYNC1LI1, ODC1, CTSV, LAMTOR5, NLGN3, SSB, SUGP1, SRSF3, EAPP, EMC3, YIPF5, MRPS17, MRPS33, COX6C, EMC2, P4HB, FN1, COX7A2, DPY30, DISP3, NDUFAF2, TMX4, HIPK3, CFAP36, PLCB4, TTBK1, DACH1, ROCK1, ZC3H8, MRPL53, FABP9, C5H15ORF57, PDDC1, CDC25A, XPOT, SYT13, PHF21A, RNF111, GNG10, C2H6orf52, PLD5, NOTCH2, RPL32, FNDC3B, ARL8BL, TIAL1, TSPAN3, PLXNB3, GPR158, RPL9, LOC427025, ZNF512B, RAB1B, TBX3, C26H6ORF125, GLI2, PRDX1, ISCA1, ATP2A2, PTN, FUNDC1, LOC407092, FAM103A1, CNOT1, MPHOSPH6, RPS2, SLIT1, SNRPF, PHF5A, CHMP5, LACTB2, PPP1R7, ATP6V1D, NCBP2, SSR3, ZFAND6, NDUFB6, ZFAND6, CNRIP1, FAM192A, HYPK, NDUFA8, RPL27A, COX20, UQCRHL, RPL12, PSKH1, SLC51A, COPS9, SYAP1, NDUFB1, CWC15, SEC13, ATP5G3, LOC425783, ALYREF, DHRS3, HDDC2, DHRS7C, IL16, RPL38, SETD5, WBP2, RAB40B, RCAN1, FZR1, MRPS35, ZNF341, ATP5C1, REXO2, MPC2, PCP4, SLCO4A1, FBXL16, TMEM254, NME3, BEND7, INPP5K, TXNDC12, MARC1, LOC417414, TICRR, FAXDC2, MYO9B, RSL24D1, RCN2, ZNF609, RCN2, GNB5, RNF123, NDUFA1, C7orf73, COX7B, COX17, SPTSSA, COA5, PIGY, ARL6, RELN, SORL1, RPL11, SCP2, LOC420362, UCHL5, MAGOH, AGO1, P2RY14, GPR83-L, IGSF11, NLRC5, SCN5A, SRPRB, WBP2NL, ZEB2, PIP5K1C, RSPO2, C8B, RPL24, SDK1, PDIA3, BASP1, NRG1, NHLH1, PTPRO, ACTN1, LIMK1, LAMB2, LMBR1, ACO2, ARNT, PCBD2, UGT8, CBL, SOD2, RPS17, DAB1, IMPG1, KCNIP2, RPL35, BRCA2, ID4, NRP2, HSP90B1, CAMK2A, ME1, HDAC4, LEPR, MAGOH, DPF2, TNKS, PPP3R1, CSNK1E, PSMB7, YBX1, PDE6G, PHACTR1, FGFRL1, CCNL2, HS2ST1, DPYSL2, HNRNPH2, RGS9BP, TLN1, SH3GL1, SH3GL2, MAB21L1, FET1, DYRK1A, SFRP1, KCNT1, NSG1, FKBP1B, ALDH1A1, GJD2, PARK7, SP1, PTPRJ, ACTR6, ALDH1A3, SNCG, ZBTB7A, GNAT1, TLL1, RHOA, SALL1, CASP3, PPP1R12B, NCAN, PBX1, RDX, EBF1, SOUL, NEUROG2, NHLH2, KCNN2, MTCH2, UCHL3, PHOSPHO1, RBPMS2, LSAMP, SCD, HMGB1, KCNAB1, RHOB, OAZ1, PSMC1, FMOD, ID2, CALM2, PSMA1, EFNB1, TGFBI, CDC42, RREB1, LRPAP1, HSPE1, LDB1, TSN, TFAP2A, HDLBP, GFRA1, BLMH, HMGN1, COL6A1, PPP1CB, ACTN4, GLRX, NTRK3, ALCAM, EFNA5, LRP8, MST1, CNGA1, RAB2A, SNRPE, NPM1, NFIC, MYH11, TNR, MBP, HMGB3, COL9A3, FABP7, TUBB, GOT1, RPLP1, HNRNPAB, MYL12A, ASMT, GABRG2, RNF13, C5H14ORF166, NREP, INHBA, LOC396380, ISL1, IFNA3, 17.5, BG2, SRC, PRNP, RBP4, HMGB2, OPN1MSW, HSPA5, GLUL, CALB1, CAPZA1, GOT2, APOA1, AGRN, POPDC2, CCT4, CG-16, EPHB2, DNMT1, HSP90AB1, GRIN1, PLA2R1, ATG4B, NDUFC2, PCDH10, PCDHGC3, AMY1AP, MIR1728, MIR1768, ATP2A2, FUNDC1, RPL12, COPS9, ATP5G3, TMEM254, UCHL5

Appendix 5.6. Common differentially expressed genes between comparisons for high vs. low and previous studies.

Gene ID	Model 1	Model 3	Author	Year	Method	Species	Tissue
BICC1		Yes	Verhoeven	2013	microarray	Human	Retinal/RPE/ photoreceptors / choroid.
RORB		Yes	Verhoeven				
PCGF5		Yes	Brand	2007	Microarray	Mouse	Retina
REPS1		Yes	Brand				
ASCC3		Yes	McGlinn	2007	Microarray	Chick	Retina/RPE
ASL1	Yes		McGlinn				
DCX		Yes	McGlinn				
G0S2		Yes	McGlinn				
LBH		Yes	McGlinn				
LOC422214		Yes	McGlinn				
RGN	Yes		McGlinn				
TOX3		Yes	McGlinn				
VIP		Yes	McGlinn				
WASL		Yes	McGlinn				
CNTRL		Yes	Schippert	2008	Microarray	Chick	Retina
DCT	Yes		Schippert				
GCG		Yes	Schippert				
GNAT2		Yes	Schippert				
HERC2		Yes	Schippert				
MYLK		Yes	Schippert				
NLGN1		Yes	Schippert				
QSER1		Yes	Schippert				
RALGAPA1		Yes	Schippert				
SPTBN1		Yes	Schippert				
TRPM7		Yes	Schippert				
CST3		Yes	Rada	2009	Microarray	Chick	Retina/RPE/choro id
GAPDH		Yes	Rada				
HSPA8		Yes	Rada				
RPLP0		Yes	Rada				
AP2M1		Yes	Ashby	2010	Microarray	Chick	Amacrine cell layer
COL8A1	Yes		Ashby				
CHD7		Yes	Ashby				
CLTA		Yes	Ashby				
DPF3		Yes	Ashby				
GRIA3		Yes	Ashby				
NEGR1		Yes	Ashby				
NFAT5		Yes	Ashby				
OTX2		Yes	Ashby				

RPL7		Yes	Ashby				
RPS15		Yes	Ashby				
SEPP1		Yes	Ashby				
UBB		Yes	Ashby				
AGTPBP1		Yes	Stone	2011	Microarray	Chick	Retina/RPE
CCSER2		Yes	Stone				
GRIA4		Yes	Stone				
KCNMA1		Yes	Stone				
AKAP9		Yes	Stone				
ANK3		Yes	Stone				
ANKHD1		Yes	Stone				
ANKS1B		Yes	Stone				
ARHGAP21		Yes	Stone				
B3GNT5		Yes	Stone				
BAZ2B		Yes	Stone				
CACNA2D1		Yes	Stone				
CDC42BPA		Yes	Stone				
CDH13		Yes	Stone				
CDK6		Yes	Stone				
CELF1		Yes	Stone				
CLIP1		Yes	Stone				
CLOCK		Yes	Stone				
DICER1		Yes	Stone				
DMD		Yes	Stone				
DROSHA		Yes	Stone				
EDF1		Yes	Stone				
EIF4A3		Yes	Stone				
ENO1		Yes	Stone				
EOGT	Yes		Stone				
EPHA7		Yes	Stone				
ERP29		Yes	Stone				
FARP1		Yes	Stone				
FAT3		Yes	Stone				
FMN1		Yes	Stone				
FNDC3A		Yes	Stone				
FUT9		Yes	Stone				
GAPVD1		Yes	Stone				
GRM5		Yes	Stone				
HARS		Yes	Stone				
HMBOX1		Yes	Stone				
ITPR1		Yes	Stone				
JMJD1C		Yes	Stone				
KDM3A		Yes	Stone				
KIAA0586		Yes	Stone				
KIAA2018		Yes	Stone				

LSS	Yes	Stone				
MAGI2	Yes	Stone				
MIA3	Yes	Stone				
MPDZ	Yes	Stone				
MYH10	Yes	Stone				
MYO5A	Yes	Stone				
NBEA	Yes	Stone				
NOS2	Yes	Stone				
OPN4	Yes	Stone				
PCDH1	Yes	Stone				
PCDH15	Yes	Stone				
PER3	Yes	Stone				
PHTF2	Yes	Stone				
PSMC5	Yes	Stone				
PTPRG	Yes	Stone				
PTPRZ1	Yes	Stone				
RAB3GAP2	Yes	Stone				
RIMBP2	Yes	Stone				
RPS27A	Yes	Stone				
SCAF11	Yes	Stone				
SIRT6	Yes	Stone				
SLC38A2	Yes	Stone				
SNAP25	Yes	Stone				
SPATS2L	Yes	Stone				
SPHKAP	Yes	Stone				
SRI	Yes	Stone				
SZT2	Yes	Stone				
TENM2	Yes	Stone				
TET2	Yes	Stone				
TMEM131	Yes	Stone				
TRIM2	Yes	Stone				
TTC14	Yes	Stone				
USP34	Yes	Stone				
USP7	Yes	Stone				
VPS13A	Yes	Stone				
XPO5	Yes	Stone				
ZDHHC8	Yes	Stone				
ZFHX3	Yes	Stone				
CKB	Yes	Bertrand	2006	2D GE, MS	Chick	Retina
PGAM1	Yes	Lam	2007	2D GE, MS	Chick	Retina
TUBB2B	Yes	Lam				
AK1	Yes	Zhou	2010	2D GE, MS	Guinea Pig	Posterior Sclera
EIF3I	Yes	Zhou				
PGK1	Yes	Zhou				
RACK1	Yes	Zhou				

ACTB		Yes	Frost	2012	2D GE, MS	Tree Shrew	Sclera
COL12A1		Yes	Frost				
PEBP1		Yes	Frost				
TPI1		Yes	Frost				
CRYBA2	Yes		Li	2012	2D GE, MS	Mouse	Retina
CLTC		Yes	Barathi	2014	iTRAQ	Mouse	Retina
FSCN1		Yes	Barathi				
LDHA		Yes	Barathi				
MBP	Yes		Barathi				
RPL4		Yes	Barathi				
STXBP1		Yes	Barathi				
CNIH1		Yes	Barathi				

Appendix 6.1 Gene-based analysis by MAGMA (with P < 0.05)

GENE	CHR	START	STOP	ZSTAT	P
PIK3CG	1	14208410	14246547	4.04	2.67e-05
ENSGALT00000006673.4	7	5730049	5902491	3.94	4.15e-05
ENSGALT00000039781.2	7	5867755	5878724	3.72	9.84e-05
ENSGALT00000021678.3	13	14376043	14389235	3.53	2.04e-04
USP40	7	5896675	5938176	3.48	2.50e-04
GPR22	1	14513792	14525725	3.35	4.03e-04
DOCK9	1	143955154	144047261	3.34	4.17e-04
SPSB4	9	6118832	6129579	3.28	5.19e-04
OGN	12	3419002	3443509	3.13	8.65e-04
PXYLP1	9	6322526	6382838	3.12	8.94e-04
KCNK16	3	28436386	28453914	3.12	9.08e-04
TSPAN5	4	59387903	59420610	3.09	9.92e-04
KIF6	3	28290092	28442362	3.07	0.001
gga-mir-1690	1	83228226	83238330	3.07	0.001
FOLH1	1	186840640	186881181	3.02	0.001
ENSGALT00000044890.1	10	12637496	12648801	2.97	0.002
ENSGALT00000032906.3	7	30705685	30717735	2.92	0.002
GPC4	4	3745510	3792904	2.90	0.002
CHRDL2	1	194986363	195015253	2.83	0.002
TCEANC2	8	24033682	24046647	2.82	0.002
ENSGALT00000011411.4	1	15230834	15286162	2.82	0.002
CHRNA5	10	3125408	3140905	2.82	0.002
FGF20	4	62870509	62884757	2.82	0.002
WBP11	1	47911129	47929400	2.81	0.002
SYF2	23	2356271	2368540	2.81	0.003
DYRK1A	1	106533437	106564176	2.77	0.003
PUS7	1	13783330	13814208	2.74	0.003
FCHSD2	1	194312764	194453987	2.71	0.003
ANO4	1	47287274	47469213	2.69	0.004
ENSGALT00000044937.1	2	95939287	95949385	2.68	0.004
TGFBI	13	14290425	14514385	2.68	0.004
ITPA	8	4683298	4696874	2.68	0.004
HBP1	1	14351758	14372631	2.67	0.004
TOP2B	2	38415563	38487069	2.67	0.004
ENSGALT00000017057.3	8	20799323	20812546	2.67	0.004
ENSGALT00000045541.1	23	2349968	2369999	2.67	0.004
HYAL3	12	3226619	3238209	2.67	0.004
KCTD15	11	10163413	10221329	2.66	0.004
TMEM59	8	24025292	24043522	2.65	0.004
PLD4	5	51688868	51710952	2.65	0.004
ENSGALT00000011337.4	17	3550763	3566244	2.64	0.004
H2A-VIIId	1	47919628	47930018	2.64	0.004
ILDR1	1	82607953	82635949	2.63	0.004

OGDH	22	4022420	4053078	2.61	0.005
CNDP2	2	91848634	91872910	2.59	0.005
DET1	10	12637749	12657973	2.58	0.005
ENSGALT00000044097.1	1	13811697	13821797	2.58	0.005
COG5	1	14364254	14558213	2.58	0.005
VAMP4	8	4689855	4712280	2.54	0.006
ENSGALT00000014522.4	17	922030	938004	2.53	0.006
ENSGALT00000044588.1	11	10914215	10928303	2.53	0.006
ATPAF1	8	20739186	20759041	2.52	0.006
PEPD	11	9799381	9930979	2.52	0.006
RNF121	1	193345969	193366446	2.51	0.006
PKIB	3	60682660	60748857	2.51	0.006
ENSGALT00000021778.4	1	48012423	48023082	2.51	0.006
RINT1	1	13805272	13827128	2.50	0.006
MOB3C	8	20721721	20742106	2.50	0.006
SCL	8	20805414	20818774	2.50	0.006
PLEKHG7	1	44466026	44494240	2.49	0.006
CYBA	11	17888778	17900490	2.48	0.007
MAML3	4	28841110	28925597	2.48	0.007
ENSGALT00000043354.1	7	6061699	6071767	2.48	0.007
CLSTN2	9	5561976	5866817	2.48	0.007
CCDC69	13	12336372	12349594	2.48	0.007
ENSGALT00000006953.4	13	12339790	12353418	2.48	0.007
FAM73B	17	5453245	5477221	2.48	0.007
HTRA3	4	80433629	80466899	2.47	0.007
SMAD5	13	14422580	14440845	2.47	0.007
ENSGALT00000030959.3	2	94083924	94218373	2.46	0.007
H2A-VIIIc	1	48005461	48032267	2.45	0.007
ENSGALT00000043224.1	1	48005778	48016912	2.45	0.007
ANXA4	22	3983992	4003235	2.45	0.007
gga-mir-1803	2	92558596	92568685	2.44	0.007
ENTPD8	17	912233	928564	2.44	0.007
ENSGALT00000007165.4	6	11130324	11142516	2.44	0.007
SPOCK1	13	13901201	14168956	2.44	0.007
RAP1GDS1	4	59293213	59392366	2.43	0.008
ENSGALT00000014517.3	17	928055	953197	2.42	0.008
SS18L2	11	10370343	10392067	2.41	0.008
gga-let-7j	26	1586917	1597000	2.40	0.008
gga-let-7k	26	1587117	1597200	2.40	0.008
EF1Aa	3	80908075	80921878	2.40	0.008
HYDIN	11	1532249	1646091	2.39	0.008
EXOC8	3	39092130	39108582	2.39	0.008
MYLK	7	26669969	26864021	2.39	0.008
gga-mir-1816	2	88285497	88295602	2.39	0.008
ENSGALT00000008831.4	7	6592660	6626009	2.38	0.009

gga-mir-214	8	4622232	4632342	2.38	0.009
CNGB3	2	122948407	122987927	2.38	0.009
PPARa	1	71406619	71447947	2.38	0.009
NDUFA10	7	6547330	6597902	2.37	0.009
ZAR1	1	173854595	173866411	2.37	0.009
ENSGALT00000027578.4	1	173858588	174007319	2.37	0.009
RHD	23	2337637	2354134	2.37	0.009
TBX3	15	12202813	12224746	2.37	0.009
MICU3	4	62815273	62874495	2.36	0.009
gga-mir-1555	1	144180922	144191008	2.36	0.009
MFSD10	4	81831411	81864788	2.36	0.009
GTF2F2	1	166960969	167062679	2.36	0.009
gga-mir-383	4	63590604	63600677	2.36	0.009
KXD1	28	3652471	3664967	2.36	0.009
GPR146	14	2315567	2336815	2.35	0.009
LDLRAD1	8	24018107	24030375	2.35	0.009
FAM193A	4	82044671	82102810	2.35	0.009
DRD3	1	82392144	82417833	2.35	0.009
ETS2	1	107162342	107185491	2.34	0.010
GLIS1	8	23799848	23905621	2.34	0.010
DSP	2	64606441	64645267	2.33	0.010
PDZK1IP1	8	20789710	20804010	2.33	0.010
PHYKPL	13	13609746	13626757	2.33	0.010
EDF1	17	545446	558619	2.33	0.010
gga-mir-6600	2	5785772	5795882	2.33	0.010
ENSGALT00000033803.3	9	5937141	5949259	2.33	0.010
TMEM57	23	2320806	2341889	2.32	0.01
ENSGALT00000002125.4	10	2102248	2119518	2.32	0.01
FKBP8	28	3655482	3670804	2.32	0.01
STOML1	10	2110124	2123216	2.31	0.01
EFCAB10	1	13816810	13828862	2.30	0.01
gga-mir-199-2	8	4616375	4626483	2.30	0.01
PKHD1	3	107225219	107466810	2.29	0.01
NEK3	1	169682935	169706053	2.28	0.01
GORAB	8	4864944	4884119	2.28	0.01
TMEM203	17	944677	955088	2.28	0.01
IL17RD	12	8530419	8600065	2.27	0.01
SMPX	1	118545326	118563867	2.27	0.01
TSHR	5	40037539	40095213	2.27	0.01
XKR5	3	107100044	107114160	2.27	0.01
gga-mir-1579	6	2159857	2169924	2.26	0.01
FKBP14	2	34420409	34435988	2.26	0.01
SLC2A13	1	14911516	15059085	2.26	0.01
GPER1	14	2348428	2361256	2.25	0.01
RAD54L	8	20466190	20494383	2.25	0.01

ENSGALT00000044503.1	3	107098313	107108845	2.25	0.01
PPIB	10	801483	812487	2.24	0.01
AMBP	17	630093	645394	2.23	0.01
VPS8	9	2958832	3035421	2.23	0.01
CRLF1	28	3646444	3658912	2.23	0.01
AHNAK2	5	51706520	51741637	2.23	0.01
MAMDC4	17	549236	570821	2.22	0.01
KCNK1	3	38001260	38041746	2.22	0.01
TPT1	1	167053419	167071619	2.22	0.01
SGPL1	6	11109346	11189726	2.22	0.01
SNX22	10	802605	814314	2.22	0.01
ENSGALT00000013424.3	15	12192003	12203222	2.22	0.01
DNM3	8	4509808	4683962	2.21	0.01
gga-mir-1783	12	8790544	8800645	2.21	0.01
HMX3	6	31008802	31019912	2.21	0.01
GPR15	1	82589872	82600979	2.21	0.01
BRCA2	1	173815723	173862456	2.20	0.01
SLC19A2	1	83051656	83075746	2.20	0.01
ANKRD6	3	74948169	74990332	2.20	0.01
C15orf61	10	18425851	18437733	2.19	0.01
MOCOS	2	84807788	85030689	2.19	0.01
irx2	2	86619613	86636727	2.19	0.01
EIF4E	4	59492315	59535000	2.19	0.01
ENSGALT00000007184.4	6	11134585	11155803	2.18	0.01
GPX3	13	12372502	12384482	2.18	0.01
PALD1	6	11091826	11115392	2.18	0.01
ENSGALT00000017926.4	3	38130387	38179625	2.18	0.01
SOCS6	2	93538028	93572247	2.17	0.01
KCTD4	1	166990126	167000900	2.17	0.01
PDE6H	1	47819918	47838585	2.17	0.01
ZNF385C	27	4758259	4802776	2.17	0.02
SNORD71	11	19219873	19229960	2.17	0.02
DMBX1	8	20560275	20588037	2.16	0.02
FARP1	1	144147282	144339650	2.16	0.02
KIAA0355	11	10371829	10408785	2.16	0.02
ATXN7L1	1	13826429	13903855	2.16	0.02
CRISP1	3	108315647	108338075	2.16	0.02
N4BP2L1	1	173803325	173825489	2.16	0.02
METTL13	8	4677861	4692818	2.16	0.02
ENSGALT00000008462.3	9	6269494	6291125	2.16	0.02
PHLPP2	11	19233987	19273628	2.15	0.02
NPTXR	1	50622426	50654375	2.15	0.02
GDPD5	1	194093030	194261622	2.14	0.02
CPA6	2	115180936	115278389	2.14	0.02
CFAP99	4	82156952	82214841	2.14	0.02

EFCAB11	5	42887401	42952303	2.14	0.02
ENSGALT00000010583.3	12	3232732	3244576	2.14	0.02
TBCEL	24	3553095	3576802	2.13	0.02
MADPRT	1	193342494	193354021	2.13	0.02
PSME3	27	5055693	5072398	2.13	0.02
EEA1	1	44492301	44567796	2.12	0.02
ENSGALT00000036276.2	12	3480320	3503864	2.12	0.02
TAT	11	19275393	19294813	2.12	0.02
ENSGALT00000010200.3	13	14402282	14421685	2.12	0.02
DOLK	17	5322458	5409262	2.12	0.02
ENSGALT00000044726.1	17	5310360	5320455	2.12	0.02
MVD	11	17890873	17903830	2.11	0.02
MRPL37	8	24059756	24073753	2.11	0.02
RABL6	17	576462	634223	2.11	0.02
ENSGALT00000030452.3	1	82528507	82553223	2.11	0.02
UBAC2	1	143793560	143889756	2.11	0.02
GABBR2	2	87951517	88383890	2.11	0.02
ARL4C	7	5649087	5659666	2.11	0.02
ENSGALT00000007414.4	6	11370532	11506581	2.10	0.02
NUFIP1	1	166899654	166932469	2.10	0.02
ENSGALT00000025631.4	2	124066733	124095805	2.10	0.02
TWF2	12	2940887	2963336	2.10	0.02
SOX14	9	3702359	3713061	2.10	0.02
CHRNB4	10	3098511	3121708	2.10	0.02
TMEM59L	28	3638256	3655421	2.09	0.02
ITGB3	27	2297639	2324626	2.09	0.02
ENSGALT00000034196.1	14	2340371	2352987	2.09	0.02
ENSGALT00000005098.4	11	19350608	19365270	2.09	0.02
MRPL46	10	12662220	12674762	2.08	0.02
RUNX3	23	2404725	2445882	2.08	0.02
RGS7	3	35233581	35476485	2.08	0.02
ENSGALT00000039842.2	15	1909171	1948298	2.08	0.02
ENSGALT00000031457.3	11	19111727	19124502	2.08	0.02
CHST4	11	19295002	19306139	2.08	0.02
OCC-1	1	54137066	54163684	2.08	0.02
NAALAD2	1	186808785	186850023	2.08	0.02
KCNK17	3	28448896	28483662	2.08	0.02
HERC1	10	3428413	3533542	2.08	0.02
RFTN2	7	9748088	9783093	2.07	0.02
NEK2	3	21499435	21516540	2.07	0.02
gga-mir-1739	5	38511932	38522025	2.07	0.02
ENSGALT00000043438.1	4	79577075	80002954	2.07	0.02
SLMAP	12	8741152	8826988	2.07	0.02
ENSGALT00000042402.1	1	140637264	140647385	2.07	0.02
IQCH	10	18363139	18431597	2.07	0.02

FGF14	1	142466031	142611517	2.07	0.02
SNX1	10	804666	825365	2.07	0.02
Epm2a	3	45764622	45816385	2.07	0.02
IL17C	11	17885559	17897594	2.07	0.02
ENSGALT00000026953.4	3	108469780	108481823	2.06	0.02
ENSGALT00000044305.1	2	92802128	92812236	2.06	0.02
PITPNB	15	7525399	7552053	2.06	0.02
gga-mir-6684	12	11067267	11077377	2.06	0.02
RGMA	10	14161476	14188190	2.06	0.02
NCOA4	6	2244005	2262782	2.06	0.02
gga-mir-6687	3	80907032	80917142	2.06	0.02
ENSGALT00000032174.3	4	48573788	48584482	2.06	0.02
GABARAPL2	11	19342940	19361180	2.06	0.02
PHPT1	17	560838	572461	2.05	0.02
C9orf172	17	563201	575706	2.05	0.02
COL22A1	2	144137254	144379426	2.05	0.02
NR2C2AP	28	3328910	3341777	2.05	0.02
TTC28	15	7549368	7676872	2.05	0.02
FOXN3	5	42661772	42850899	2.05	0.02
cOpn5L2	3	108442860	108457107	2.05	0.02
ENSGALT00000009756.4	15	8029377	8047034	2.05	0.02
noxa1	17	897673	920909	2.05	0.02
LRRC9	5	54540270	54570985	2.04	0.02
ZFAND2A	14	2367452	2380530	2.04	0.02
TRIM42	9	5900651	5919210	2.04	0.02
ENSGALT00000001342.4	11	19358499	19374931	2.04	0.02
ENSGALT00000022354.4	2	94282865	94304074	2.04	0.02
RAB33B	4	28772868	28789884	2.04	0.02
CCDC51	12	11248812	11263331	2.03	0.02
CNOT7	4	62753273	62782681	2.03	0.02
WASF2	23	1949482	1985118	2.03	0.02
ENSGALT00000028011.4	1	194082351	194099501	2.03	0.02
DTL	3	21359604	21391867	2.03	0.02
ENSGALT00000031356.3	1	193357030	193369866	2.03	0.02
ENSGALT00000025078.4	4	79996880	80100152	2.03	0.02
ENSGALT00000008986.4	12	8632491	8706433	2.03	0.02
FAH	10	12054479	12075953	2.03	0.02
IL9	13	14557899	14570599	2.03	0.02
PLS1	9	9970583	10018804	2.03	0.02
AP1G1	11	19190951	19242680	2.03	0.02
ENSGALT00000044263.1	3	47964054	47974166	2.03	0.02
DHX38	11	19145948	19166411	2.02	0.02
gga-mir-6714	14	12383338	12393448	2.02	0.02
BTG1	1	44266337	44278899	2.02	0.02
ISM2	5	38519086	38532515	2.02	0.02

C6orf132	26	3131185	3153471	2.01	0.02
FAM135B	2	143850748	144043521	2.01	0.02
DLC1	4	63974466	64204133	2.01	0.02
DHODH	11	19157774	19171255	2.01	0.02
PHIP	3	78921378	79021040	2.00	0.02
ZDHHC2	4	62782143	62819535	2.00	0.02
APOV1	1	82604205	82617227	2.00	0.02
gga-mir-1649	3	21189284	21199382	2.00	0.02
TRPC1	9	10010076	10041192	2.00	0.02
gga-mir-1577	9	4937396	4947481	2.00	0.02
TNIP1	13	12362917	12381206	2.00	0.02
EFHC1	3	107125487	107152698	2.00	0.02
QTRTD1	1	82419530	82441617	1.99	0.02
TMEM66	4	48641934	48659556	1.99	0.02
EED	1	189664528	189690501	1.99	0.02
FAM110D	23	3148761	3161554	1.99	0.02
IST1	11	19161597	19178788	1.99	0.02
TMX3	2	94230831	94268036	1.99	0.02
CALM1	5	43130795	43148958	1.99	0.02
ENSGALT00000044604.1	3	78140678	78150769	1.99	0.02
SGK3	2	114928091	114973853	1.99	0.02
TRMT10A	4	59619812	59638939	1.99	0.02
gga-mir-6612	24	4774926	4785036	1.98	0.02
ESCO2	3	104785087	104805567	1.98	0.02
ENSGALT00000000913.4	11	18371039	18383680	1.98	0.02
NIP7	11	18373689	18385054	1.98	0.02
B3GALT5	1	107439586	107451093	1.98	0.02
ENSGALT00000039237.2	6	22933413	22946166	1.98	0.02
IBTK	3	77654754	77722628	1.98	0.02
ENSGALT00000036939.2	1	82518358	82536728	1.98	0.02
VAPA	2	98222824	98259555	1.98	0.02
LRP8	8	23556279	23715577	1.98	0.02
LPGAT1	3	21422205	21485741	1.98	0.02
ZDHHC23	1	82454932	82471590	1.97	0.02
CALN1	19	950426	1066274	1.97	0.02
C20H20ORF43	20	12309418	12339709	1.97	0.02
ZNF821	11	19170525	19191003	1.97	0.02
DENND6A	12	8717033	8746878	1.97	0.02
HNRNPA2B1	2	32312344	32332887	1.97	0.02
TK2	11	10901479	10922656	1.96	0.02
PFKP	2	11349184	11400733	1.96	0.02
HES6	9	4937247	4953675	1.96	0.03
MKI67	6	32885713	32915556	1.96	0.03
ADAT1	11	19317211	19347909	1.95	0.03
RNF166	11	17895343	17911187	1.95	0.03

ENSGALT00000034106.3	9	10082483	10093628	1.95	0.03
ARSI	13	12498422	12512422	1.95	0.03
CCDC14	7	26875823	26894311	1.95	0.03
B4GALT4	1	80031446	80066032	1.95	0.03
TFAP2C	20	12277245	12296290	1.95	0.03
ENSGALT00000017045.4	8	20778470	20795800	1.95	0.03
HMX2	6	31013103	31028370	1.95	0.03
IMPA1	2	121257378	121282486	1.94	0.03
ZFHX3	11	18931950	19036832	1.94	0.03
CBLN2	2	92622799	92635335	1.94	0.03
ENSGALT00000031456.3	11	19136567	19150768	1.94	0.03
CD8B	4	85435287	85451044	1.94	0.03
NUP43	3	47484108	47503142	1.94	0.03
MRPL14	3	29727267	29746085	1.94	0.03
TIMP3	1	53053720	53096132	1.94	0.03
FAM81A	10	6211547	6232549	1.94	0.03
CENPP	12	3328635	3457411	1.94	0.03
CCDC79	11	10795309	10819201	1.94	0.03
RFXANK	28	3328910	3347226	1.94	0.03
IGFBP7	4	48576285	48600158	1.94	0.03
CRABP2	25	463702	475859	1.94	0.03
PPDPF	20	9363434	9375742	1.94	0.03
SNORA84	12	3500490	3510625	1.94	0.03
GPALPP1	1	166922077	166947984	1.94	0.03
CKAP2	1	169696517	169715954	1.94	0.03
C18orf63	2	91916175	91939799	1.93	0.03
MN1	15	7483964	7526455	1.93	0.03
gga-mir-6584	2	93539764	93549874	1.93	0.03
IRAK1BP1	3	79035636	79056664	1.93	0.03
TSHZ1	2	91337032	91351101	1.93	0.03
gga-mir-6640	3	21530493	21540603	1.93	0.03
CNDP1	2	91814975	91842036	1.93	0.03
gga-mir-1625	15	7563814	7573894	1.93	0.03
gga-mir-1688	10	864889	874960	1.93	0.03
WDR77	26	3149032	3161732	1.93	0.03
ENSGALT00000017904.3	3	37618858	37675716	1.92	0.03
FAM96B	11	10650811	10663144	1.92	0.03
TBC1D9B	13	12754005	12781256	1.92	0.03
MBTPS2	1	118497827	118540488	1.92	0.03
UQCRH	8	20493969	20505444	1.92	0.03
ENSGALT00000016586.4	8	19811838	19828208	1.92	0.03
ERGIC2	1	14772555	14805582	1.92	0.03
PGM2L1	1	195081449	195125846	1.92	0.03
F5	1	83005007	83051065	1.91	0.03
ANXA6	13	12345518	12367997	1.91	0.03

ENSGALT00000045881.1	1	49127164	49137271	1.91	0.03
gga-mir-1581	1	49128040	49138126	1.91	0.03
PPM1M	12	2959625	2975401	1.91	0.03
ENSGALT00000042082.1	2	84972747	84982825	1.91	0.03
ADAM11	27	1251094	1271189	1.90	0.03
WDYHV1	2	137617324	137637958	1.90	0.03
ZFYVE28	4	82204991	82355777	1.90	0.03
KCNK12	3	8578545	8603351	1.90	0.03
C3H2ORF43	3	101604617	101724052	1.90	0.03
DNAJC24	5	5009652	5051383	1.90	0.03
RPS16	1	39674924	39690489	1.89	0.03
POLD3	1	195024321	195063322	1.89	0.03
RBP3	6	17523349	17547877	1.89	0.03
HYKK	10	3146804	3161695	1.89	0.03
CHST8	11	10011611	10149234	1.89	0.03
gga-mir-1699	11	18928028	18938125	1.89	0.03
SEC22B	8	4125592	4144427	1.89	0.03
ENSGALT00000034796.2	10	2094479	2105748	1.88	0.03
TMCC3	1	45032003	45081411	1.88	0.03
ISLR2	10	2099513	2111613	1.88	0.03
MEF2BNB	28	3337691	3356021	1.88	0.03
CHRM3	3	35722537	35882494	1.88	0.03
C10orf54	6	11470430	11489506	1.88	0.03
FAT2	13	12263216	12324359	1.88	0.03
ENSGALT00000003144.3	6	2129546	2160479	1.88	0.03
CDCP2	8	24040804	24054407	1.88	0.03
STRA6	10	2084887	2102471	1.88	0.03
MAP6	1	194002332	194038028	1.87	0.03
SLC45A4	2	145617307	145660804	1.87	0.03
DMRTB1	8	23764010	23783972	1.87	0.03
LTC4S	13	12822840	12836848	1.87	0.03
ENSGALT00000016927.4	4	35930706	35940859	1.87	0.03
TACC1	22	2379464	2404036	1.87	0.03
FKBP9	2	48578320	48604111	1.87	0.03
RRNAD1	25	454757	466809	1.87	0.03
TUSC3	4	63223828	63347046	1.86	0.03
OTOGL	1	39685269	39786595	1.86	0.03
ZC3H12C	1	178900487	178931969	1.86	0.03
APOB	3	101875366	101921760	1.86	0.03
ELL	28	3661227	3705318	1.86	0.03
SLCO2A1	9	4058858	4093360	1.85	0.03
IRF2BP2	3	37703941	37714703	1.85	0.03
MGRN1	14	12344366	12401724	1.85	0.03
SSBP3	8	24069036	24129115	1.85	0.03
ACOT11	8	24126386	24145486	1.85	0.03

RREB1	2	64730014	64859227	1.85	0.03
ENSGALT00000018675.4	7	22066157	22094594	1.85	0.03
CHST2	9	10146973	10159431	1.84	0.03
FOXO6	23	1186629	1241092	1.84	0.03
ENSGALT00000014677.4	17	500643	513199	1.84	0.03
INTS7	3	21381043	21413216	1.84	0.03
LDLRAP1	23	2302618	2328671	1.84	0.03
HOXA1	2	32786505	32798226	1.84	0.03
MDN1	3	74848140	74951896	1.84	0.03
RNF25	7	21954844	21968533	1.84	0.03
RYK	9	3980680	4042412	1.84	0.03
CHRM4	5	22939470	22950943	1.84	0.03
SLC30A1	3	21525531	21541494	1.84	0.03
TRMU	1	15515695	15537337	1.83	0.03
UBE3D	3	77399160	77454989	1.83	0.03
gga-mir-6661	4	82208018	82218128	1.83	0.03
ZIC1	9	11390946	11405537	1.83	0.03
ALK	3	8089159	8389451	1.83	0.03
ENSGALT00000045050.1	3	104568756	104579824	1.83	0.03
PTGDS	17	504033	516024	1.83	0.03
CACHD1	8	26972491	27066474	1.83	0.03
CTU2	11	17902682	17916287	1.83	0.03
TBC1D16	18	9840356	9875528	1.82	0.03
ENSGALT00000010863.4	9	2940064	2953848	1.82	0.03
ENSGALT00000000929.3	11	18375394	18387865	1.82	0.03
GPR183	1	143832082	143852582	1.82	0.03
NDOR1	17	946104	972412	1.82	0.03
BOC	1	82670888	82701983	1.82	0.03
NARS2	1	191803031	191926160	1.82	0.03
ENSGALT00000025383.2	2	93243440	93254914	1.82	0.03
ADRA1A	22	3929594	3954175	1.82	0.03
KBP	21	1451790	1471358	1.81	0.03
TLR4	17	3561453	3576907	1.81	0.03
SLC29A1	3	29632258	29659613	1.81	0.03
SLC17A8	1	47107356	47146991	1.81	0.04
RP9	2	48608434	48625142	1.81	0.04
ATP2B1	1	43268705	43310815	1.81	0.04
EXOC6B	4	89397350	89589157	1.81	0.04
KIFAP3	8	4977259	5044415	1.81	0.04
Dkk-1	6	9759379	9771014	1.80	0.04
ST3GAL6	1	83609755	83661869	1.80	0.04
ENSGALT00000030645.3	1	44269202	44282390	1.80	0.04
PCMT1	3	47498536	47542193	1.80	0.04
ENSGALT00000001296.3	11	19267174	19279159	1.80	0.04
ENSGALT00000010438.4	12	11244995	11258626	1.80	0.04

ENSGALT00000019911.4	2	48622591	48638397	1.80	0.04
ASB14	12	8622513	8640443	1.80	0.04
ENSGALT00000021485.4	2	85456254	85640911	1.80	0.04
PTDSS1	2	126611010	126650632	1.80	0.04
ENSGALT00000040015.2	27	4642053	4660682	1.80	0.04
SERINC1	3	60759155	60783623	1.80	0.04
GPR18	1	143869786	143885033	1.79	0.04
METTL11B	8	4942463	4969307	1.79	0.04
HSP90AB1	3	29625921	29641756	1.79	0.04
GPI	11	10445874	10476700	1.79	0.04
ENSGALT00000005719.3	14	1584934	1597226	1.79	0.04
SRSF11	8	27908699	27930763	1.78	0.04
ENSGALT00000044719.1	1	54169608	54209367	1.78	0.04
MRPL24	25	453647	464713	1.78	0.04
POLR2B	4	48590102	48619515	1.78	0.04
UBE4A	24	4387699	4571947	1.78	0.04
SPRTN	3	39088468	39135259	1.78	0.04
SASH1	3	46925246	47054931	1.78	0.04
CHST15	6	31377329	31430438	1.78	0.04
CCR7	27	4462062	4481841	1.78	0.04
IGSF9B	24	2422010	2469846	1.78	0.04
PHEX	1	118324958	118426519	1.78	0.04
LARP1	13	11373039	11395962	1.78	0.04
SGCZ	4	63464830	63824243	1.78	0.04
NSDHL	4	11226921	11247461	1.77	0.04
LACTB2	2	116450966	116478097	1.77	0.04
ENSGALT00000042339.1	1	194193786	194203866	1.77	0.04
TRAF2	17	526954	552794	1.77	0.04
ITM2C	9	4861583	4886692	1.77	0.04
MTG2	20	8099921	8114585	1.77	0.04
CDC5L	3	108474341	108516164	1.77	0.04
GPD2	7	35560239	35610889	1.77	0.04
PANK4	21	1430526	1464981	1.77	0.04
DAAM2	3	28088814	28290437	1.77	0.04
cdk6	2	22838080	22967940	1.76	0.04
ENSGALT00000033720.3	9	4778952	4791016	1.76	0.04
ATP6V1D	5	28240790	28258755	1.76	0.04
BFSP1	3	11358003	11386764	1.76	0.04
TMEM41A	9	3146884	3158694	1.76	0.04
COG1	18	9253690	9272198	1.76	0.04
SC5D	24	3520334	3534948	1.76	0.04
Ex-FABP	17	496841	509845	1.75	0.04
STK36	7	21943534	21964693	1.75	0.04
WDR43	3	8483900	8516828	1.75	0.04
gga-mir-1635	21	1736923	1747030	1.75	0.04

ITGBL1	1	142609260	142757083	1.75	0.04
DHX58	27	4817591	4831644	1.75	0.04
MAGOH2	8	23545023	23556699	1.74	0.04
NSUN4	8	20496439	20510675	1.74	0.04
ENSGALT00000037436.2	5	51840059	51859861	1.74	0.04
ZBTB10	2	120778327	120814194	1.74	0.04
PDIK1L	23	3157644	3173327	1.74	0.04
RTN1	5	54587266	54693712	1.74	0.04
COL23A1	13	13573333	13611087	1.74	0.04
ENSGALT00000028290.4	25	470092	483012	1.74	0.04
gga-mir-2126	1	14562819	14572965	1.74	0.04
BCAP29	1	14562865	14596310	1.74	0.04
DAAM1	5	54634542	54787177	1.74	0.04
ENSGALT00000017050.4	8	20766031	20785775	1.74	0.04
SPR	4	89385873	89398991	1.74	0.04
DYNC1LI2	11	10812083	10846597	1.74	0.04
EFCAB7	8	26743610	26767766	1.74	0.04
ALOX5AP	1	174330142	174349760	1.74	0.04
OSTC	4	37148758	37162890	1.74	0.04
gga-mir-6658	4	1169076	1179186	1.74	0.04
DUS4L	1	14548187	14568663	1.74	0.04
LRRC41	8	20482709	20503624	1.74	0.04
BDKRB2	5	45616377	45647975	1.73	0.04
DNAJB11	9	3856049	3878808	1.73	0.04
C11orf24	5	15651186	15666708	1.73	0.04
DNAJC6	8	27181949	27222638	1.73	0.04
gga-mir-1596	1	5673878	5683968	1.73	0.04
EDN2	23	945278	960659	1.73	0.04
RYR2	3	36493790	36666068	1.73	0.04
DHCR24	8	24152605	24170747	1.73	0.04
SNORD53_SNORD92	3	8492971	8511580	1.73	0.04
ENSGALT00000031254.3	2	12957516	12968530	1.72	0.04
COL8A1	1	83656752	83753442	1.72	0.04
TOM1L1	18	5781850	5812221	1.72	0.04
RPRML	27	2293588	2303924	1.72	0.04
KCNK9	2	144599863	144688639	1.72	0.04
KLHL3	13	13813619	13856076	1.72	0.04
JKAMP	5	54714446	54730149	1.72	0.04
MYOC	8	4702986	4715477	1.72	0.04
ATAD2	2	137581975	137626986	1.71	0.04
USP28	24	4413800	4442648	1.71	0.04
ENSGALT00000034299.3	14	1573945	1593403	1.71	0.04
ADHFE1	2	114782386	114804160	1.71	0.04
SFT2D1	3	42142562	42167710	1.71	0.04
ENSGALT00000003257.4	6	2255606	2282212	1.71	0.04

ENSGALT00000039707.2	17	5307125	5321669	1.71	0.04
PSAP	6	11505432	11535618	1.71	0.04
NPPB	21	5572061	5584681	1.71	0.04
PLCL1	7	9817435	9948072	1.70	0.04
IARS	12	3499494	3599440	1.70	0.04
PROKR2	3	11267176	11286262	1.70	0.04
MDK	5	22942433	22953426	1.70	0.04
TOP1	20	5175401	5247581	1.70	0.04
NME7	1	83099917	83182722	1.70	0.04
TRPM2	9	4694123	4717793	1.70	0.04
SLC13A1	1	22189830	22223981	1.70	0.04
WNT11B	4	1176325	1188490	1.70	0.04
SHISA5	12	3237718	3258873	1.70	0.04
PRSS35	3	77125272	77142465	1.70	0.04
COL21A1	3	86626542	86713701	1.70	0.04
ENSGALT00000007125.3	4	1169206	1181630	1.70	0.04
EIF2S1	5	28230900	28250721	1.70	0.04
GluR1/A	13	11641222	11758641	1.70	0.04
USPL1	1	174345050	174368188	1.70	0.04
MTO1	3	80923944	80941582	1.70	0.04
MYEOV2	9	4719225	4732052	1.70	0.04
gga-mir-1608	9	4718168	4728261	1.69	0.05
PPP1R17	2	49062175	49090386	1.69	0.05
DOK5	20	12593229	12638483	1.69	0.05
HNRNPAB	13	13619725	13636823	1.69	0.05
DST	3	86244529	86550594	1.69	0.05
CASP10	7	10919384	10937701	1.69	0.05
SSR1	2	64705799	64725473	1.69	0.05
KIAA1407	1	82431524	82460764	1.69	0.05
ENSGALT00000002009.2	28	2585048	2603927	1.69	0.05
ENSGALT00000037006.2	3	86276184	86288796	1.68	0.05
PHLDA3	26	762672	773044	1.68	0.05
NBR2	27	5168808	5178871	1.68	0.05
C12orf40	1	15056969	15074520	1.68	0.05
PLEKHG1	3	47790130	47938046	1.68	0.05
SYT6	26	3746476	3783467	1.68	0.05
MTERF3	2	126592211	126620684	1.68	0.05
LRP11	3	47533736	47611787	1.68	0.05
T	3	42228585	42246528	1.68	0.05
TRIP12	9	9528375	9583184	1.68	0.05
RAB11FIP2	6	28998776	29052647	1.68	0.05
SNW1	5	38629499	38656966	1.68	0.05
UBALD1	14	12391925	12409682	1.68	0.05
gga-mir-1575	4	28993677	29003781	1.67	0.05
gga-mir-6574	9	7099152	7109259	1.67	0.05

RNF213	18	9766939	9823172	1.67	0.05
ENSGALT00000041141.2	16	473530	484889	1.67	0.05
ENSGALT00000022016.4	16	473725	485245	1.67	0.05
RPS6KC1	3	20971410	21071009	1.67	0.05
COX20	3	34034071	34048740	1.67	0.05
PODN	8	23446382	23482433	1.67	0.05
ENSGALT00000040808.2	6	10378542	10394962	1.67	0.05
HGF/SF	1	10466387	10539407	1.67	0.05
TRAK2	7	10957319	10985326	1.67	0.05
CYB5RL	8	24049756	24068868	1.67	0.05
ERG	1	106939607	107013750	1.67	0.05
MAP3K6	23	1925453	1941866	1.67	0.05
L3HYPDH	5	54718689	54731778	1.67	0.05
NEK5	1	169661483	169690951	1.67	0.05
ENSGALT00000045685.1	4	85444697	85463910	1.67	0.05
KARS	11	19304961	19327126	1.67	0.05
GPRIN2	6	2236233	2248572	1.67	0.05
CPNE8	1	15301093	15407789	1.67	0.05
BECN1	27	5050738	5065519	1.66	0.05
ABCD2	1	15075339	15131895	1.66	0.05
CLDN25	24	4409651	4420344	1.66	0.05
PRKCQ	1	3554594	3600000	1.66	0.05
TMED8	5	38474796	38490414	1.66	0.05
MRPS11	10	12658654	12672185	1.66	0.05
FBXO32	2	137639050	137673702	1.66	0.05
MCMDC2	2	114965566	114984273	1.66	0.05
CACNG1b	18	7188266	7206862	1.66	0.05
TGM4	2	43738130	43758642	1.66	0.05
ENSGALT00000044541.1	8	28723160	28739974	1.66	0.05
CCDC101	8	28724100	28738351	1.66	0.05
AP3B2	10	858777	879957	1.66	0.05
SOX10	1	50906764	50926215	1.66	0.05
CUL2	2	12967706	13027987	1.66	0.05
ENSGALT00000043826.1	1	41512811	41522930	1.66	0.05
MYCN	3	98773413	98785948	1.65	0.05
ATRIP	12	3274855	3295698	1.65	0.05
GCNT7	20	12318249	12332049	1.65	0.05
ZMYND11	2	9786127	9899465	1.65	0.05
KLHL29	3	103279323	103645841	1.65	0.05
ENSGALT00000016958.4	8	20512454	20532586	1.65	0.05
LIPH	9	3148811	3170001	1.65	0.05
ZNF800	1	20639894	20664015	1.65	0.05
FOXL2	9	5195074	5205992	1.65	0.05
CTNNAL1	2	88494506	88562002	1.65	0.05
KCNS3	3	99917983	99947855	1.65	0.05

Appendix 6.2 GO terms had EASE scores that were less than 0.05 (DAVID).

Category	Term	Count	Fold of Enrichment	P-Value	Bonferroni
CC	extracellular exosome	113	2.02	4.60e-14	1.65e-11
CC	myelin sheath	22	4.99	1.91e-09	6.86e-07
MC	poly(A) RNA binding	55	2.19	4.31e-08	1.95e-05
CC	cytosolic large ribosomal subunit	11	6.05	9.38e-06	3.36e-03
CC	nucleus	107	1.45	2.53e-05	0.01
CC	focal adhesion	25	2.58	3.72e-05	0.01
MC	structural constituent of ribosome	18	3.17	4.67e-05	0.02
CC	plasma membrane	67	1.63	5.11e-05	0.02
CC	membrane	45	1.84	9.41e-05	0.03
MC	calmodulin binding	8	6.89	1.09e-04	0.05
BP	homophilic cell adhesion via plasma membrane adhesion molecules	13	3.75	1.54e-04	0.21
CC	nucleosome	9	5.41	2.02e-04	0.07
BP	translation	16	3.04	2.27e-04	0.30
CC	cytosol	48	1.73	2.29e-04	0.08
BP	heterophilic cell-cell adhesion via plasma membrane cell adhesion molecules	6	8.97	3.66e-04	0.43
CC	cytoplasm	104	1.36	5.39e-04	0.18
CC	cytosolic small ribosomal subunit	7	6.46	5.80e-04	0.19
CC	filamentous actin	6	8.16	6.19e-04	0.20
BP	transcription, DNA-templated	32	1.91	6.43e-04	0.63
MC	calcium ion binding	32	1.89	7.67e-04	0.29
MC	RNA binding	19	2.37	1.04e-03	0.37
BP	glycolytic process	6	7.18	1.13e-03	0.82
CC	ruffle	8	4.81	1.17e-03	0.34
BP	neuron development	6	6.52	1.80e-03	0.94
CC	neuron projection	12	3.04	1.86e-03	0.49
BP	cell adhesion	14	2.60	2.75e-03	0.99
BP	gluconeogenesis	6	5.74	3.27e-03	0.99
MC	protein heterodimerization activity	10	3.26	3.29e-03	0.78
BP	cytoplasmic translation	5	7.48	3.63e-03	1.00
CC	cell junction	13	2.57	4.65e-03	0.81
MC	pre-miRNA binding	3	24.10	4.98e-03	0.90
BP	locomotory behavior	8	3.68	5.49e-03	1.00
BP	regulation of transcription, DNA-templated	27	1.75	6.28e-03	1.00
BP	glial cell differentiation	4	9.57	6.93e-03	1.00

CC	cytoplasmic ribonucleoprotein granule	4	9.40	7.46e-03	0.93
CC	filopodium	6	4.70	8.11e-03	0.95
MC	protein binding	11	2.62	8.76e-03	0.98
BP	positive regulation of neuron apoptotic process	4	8.70	9.24e-03	1.00
MC	AMPA glutamate receptor activity	3	18.08	9.69e-03	0.99
BP	positive regulation of extracellular matrix disassembly	3	17.94	9.84e-03	1.00
CC	synapse	9	2.91	0.01	0.99
BP	regulation of circadian rhythm	5	5.44	0.01	1.00
BP	positive regulation of guanylate cyclase activity	3	14.35	0.02	1.00
MC	DNA binding	28	1.58	0.02	1.00
BP	protein tetramerization	5	4.78	0.02	1.00
CC	mitochondrial respiratory chain complex IV	3	12.93	0.02	1.00
MC	GTPase activity	11	2.31	0.02	1.00
MC	protein homodimerization activity	11	2.31	0.02	1.00
BP	positive regulation of insulin secretion involved in cellular response to glucose stimulus	4	6.38	0.02	1.00
MC	proteoglycan binding	3	12.05	0.02	1.00
BP	oxidation-reduction process	10	2.39	0.02	1.00
CC	cytoskeleton	9	2.56	0.02	1.00
CC	melanosome	5	4.46	0.02	1.00
BP	nervous system development	8	2.73	0.03	1.00
CC	dense body	3	11.08	0.03	1.00
CC	blood microparticle	6	3.45	0.03	1.00
CC	cell-cell adherens junction	5	4.17	0.03	1.00
CC	nucleolus	24	1.57	0.03	1.00
MC	ionotropic glutamate receptor activity	3	10.33	0.03	1.00
BP	DNA replication-independent nucleosome assembly	4	5.63	0.03	1.00
BP	mRNA splice site selection	3	10.25	0.03	1.00
BP	regulation of calcium ion transport	3	10.25	0.03	1.00
MC	nucleosomal DNA binding	4	5.36	0.04	1.00
BP	negative regulation of endopeptidase activity	4	5.32	0.04	1.00
BP	RNA splicing	5	3.86	0.04	1.00
CC	lamellipodium	8	2.52	0.04	1.00
MC	microfilament motor activity	3	9.04	0.04	1.00

BP	lymphangiogenesis	3	8.97	0.04	1.00
BP	calcium-dependent cell-cell adhesion via plasma membrane cell adhesion molecules	3	8.97	0.04	1.00
BP	forelimb morphogenesis	3	8.97	0.04	1.00
BP	actomyosin structure organization	4	5.04	0.04	1.00
BP	nucleosome assembly	6	2.99	0.05	1.00

Appendix 6.3 GO terms had FDR that were less than 0.25 (GSEA).

NAME	SIZE	NES	FDR
GO_INNER_MITOCHONDRIAL_MEMBRANE_PROTEIN_COMPLEX	50	2.11	0.02
GO_SECONDARY_METABOLIC_PROCESS	14	2.15	0.02
GO_MULTIVESICULAR_BODY	16	2.08	0.02
GO_MITOCHONDRIAL_PROTEIN_COMPLEX	61	2.04	0.03
GO_TERPENOID_METABOLIC_PROCESS	42	1.98	0.05
GO_MITOCHONDRIAL_MEMBRANE_PART	74	1.97	0.05
GO_ELECTRON_TRANSPORT_CHAIN	46	1.98	0.05
GO_SECRETORY_GRANULE_LUMEN	32	1.98	0.06
GO_PLATELET_DEGRANULATION	49	1.95	0.06
GO_MULTI_ORGANISM_METABOLIC_PROCESS	69	1.98	0.06
GO_KERATAN_SULFATE_METABOLIC_PROCESS	14	1.99	0.07
GO_ESTABLISHMENT_OF_PROTEIN_LOCALIZATION_TO_ENDOPLASMIC_RETICULUM	62	1.93	0.07
GO_ISOPRENOID_METABOLIC_PROCESS	47	1.93	0.07
GO_OXIDATIVE_PHOSPHORYLATION	41	1.93	0.07
GO_MITOCHONDRIAL_RESPIRATORY_CHAIN_COMPLEX_ASSEMBLY	32	1.91	0.08
GO_MITOCHONDRIAL_RESPIRATORY_CHAIN_COMPLEX_I_BIOGENESIS	24	1.91	0.08
GO_DNA_DEPENDENT_DNA_REPLICATION	40	-1.97	0.09
GO_TRANSCRIPTION_FACTOR_ACTIVITY_DIRECT_LIGAND_REGULATED_SEQUENCE_SPECIFIC_DNA_BINDING	22	-2.02	0.10
GO_NADH_DEHYDROGENASE_COMPLEX	22	1.89	0.10
GO_VESICLE_LUMEN	38	1.89	0.10
GO_KERATAN_SULFATE_BIOSYNTHETIC_PROCESS	11	1.88	0.10
GO_ENSHEATHMENT_OF_NEURONS	43	1.88	0.10
GO_NEGATIVE_REGULATION_OF_ENDOTHELIAL_CELL_PROLIFERATION	16	1.87	0.10
GO_POSITIVE_REGULATION_OF_BEHAVIOR	10	1.87	0.10
GO_MELANIN_METABOLIC_PROCESS	8	1.86	0.11
GO_DNA_GEOMETRIC_CHANGE	46	-1.92	0.12
GO_RESPIRATORY_CHAIN	40	1.84	0.12
GO_LIPOPROTEIN_PARTICLE_RECEPTOR_BINDING	10	1.85	0.12
GO_POSITIVE_REGULATION_OF_RHO_PROTEIN_SIGNAL_TRANSDUCTION	6	1.84	0.12
GO_REGULATION_OF_SYNAPTIC_TRANSMISSION_GLUTAMATERGIC	24	1.85	0.13
GO_PURINE_NTP_DEPENDENT_HELICASE_ACTIVITY	33	-1.94	0.13
GO_SPECIFICATION_OF_ORGAN_IDENTITY	7	1.85	0.13
GO_ACTIVATION_OF_MAPK_ACTIVITY	57	1.83	0.13
GO_MALE_SEX_DIFFERENTIATION	54	-1.97	0.14
GO_SECONDARY_METABOLITE_BIOSYNTHETIC_PROCESS	7	1.82	0.14
GO_RIBOSOMAL_SUBUNIT	86	1.83	0.14
GO_ATP_DEPENDENT_DNA_HELICASE_ACTIVITY	16	-1.92	0.14
GO_COMPLEX_OF_COLLAGEN_TRIMERS	9	1.82	0.15
GO_NUCLEAR_TRANSCRIBED_MRNA_CATABOLIC_PROCESS_NONSENSE_MEDIATED_DECAY	63	1.81	0.15
GO_DNA_RECOMBINATION	77	-1.87	0.15
GO_INDUCTION_OF_POSITIVE_CHEMOTAXIS	5	1.81	0.16
GO_HELICASE_ACTIVITY	54	-1.87	0.16

GO_PHOSPHATIDYLCHOLINE_METABOLIC_PROCESS	22	1.80	0.16
GO_GROWTH_FACTOR_RECEPTOR_BINDING	50	1.79	0.17
GO_POSITIVE_REGULATION_OF_MAP_KINASE_ACTIVITY	93	1.79	0.17
GO_REGULATION_OF_POSITIVE_CHEMOTAXIS	10	1.79	0.17
GO_MYELIN_SHEATH	95	1.79	0.17
GO_POSITIVE_REGULATION_OF_FATTY_ACID_BIOSYNTHETIC_PROCESS	7	1.78	0.17
GO_POSITIVE_REGULATION_OF_LIPASE_ACTIVITY	29	1.79	0.17
GO_HEPARIN_BINDING	56	1.78	0.18
GO_REGULATION_OF_GROWTH_HORMONE_SECRETION	6	1.80	0.18
GO_POSITIVE_REGULATION_OF_FATTY_ACID_METABOLIC_PROCESS	13	1.78	0.18
GO_POSITIVE_REGULATION_OF_TRIGLYCERIDE_METABOLIC_PROCESS	6	1.77	0.18
GO_ENDOCRINE_PROCESS	14	-1.88	0.18
GO_CYTOSOLIC_RIBOSOME	66	1.78	0.18
GO_SMALL_RIBOSOMAL_SUBUNIT	34	1.77	0.18
GO_DNA_HELICASE_ACTIVITY	26	-1.88	0.19
GO_EXTRACELLULAR_SPACE	349	1.77	0.19
GO_POSITIVE_REGULATION_OF_SMALL_GTPASE_MEDIATED_SIGNAL_TRANSDUCTION	18	1.76	0.20
GO_STRUCTURAL_CONSTITUENT_OF_RIBOSOME	96	1.76	0.20
GO_ETHANOLAMINE_CONTAINING_COMPOUND_METABOLIC_PROCESS	28	1.76	0.20
GO_CELLULAR_RESPIRATION	68	1.73	0.20
GO_POSITIVE_REGULATION_OF_CHEMOTAXIS	44	1.73	0.20
GO_PROTEIN_TARGETING_TO_MEMBRANE	86	1.73	0.21
GO_REGULATION_OF_LIPASE_ACTIVITY	36	1.75	0.21
GO_G_PROTEIN_COUPLED_RECEPTOR_SIGNALING_PATHWAY_COUPLED_TO_CYCLIC_ NUCLEOTIDE_SECOND_MESSENGER	60	1.74	0.21
GO_SPROUTING_ANGIOGENESIS	22	1.73	0.21
GO_SECRETORY_GRANULE	111	1.74	0.21
GO_MITOCHONDRIAL_ELECTRON_TRANSPORT_CYTOCHROME_C_TO_OXYGEN	9	1.74	0.21
GO_ACTIVATION_OF_ADENYLATE_CYCLASE_ACTIVITY	16	1.75	0.21
GO_B_CELL_PROLIFERATION	6	1.74	0.21
GO_TISSUE_REGENERATION	23	1.74	0.21
GO_ADENYLATE_CYCLASE_ACTIVATING_G_PROTEIN_COUPLED_RECEPTOR_SIGNALING _PATHWAY	19	1.75	0.21
GO_MODULATION_OF_EXCITATORY_POSTSYNAPTIC_POTENTIAL	10	1.72	0.21
GO_EXTRACELLULAR_MATRIX	134	1.74	0.21
GO_MYOTUBE_CELL_DEVELOPMENT	7	1.72	0.21
GO_RESPONSE_TO_PROGESTERONE	17	1.75	0.21
GO_POSITIVE_REGULATION_OF_LIPID_CATABOLIC_PROCESS	9	1.73	0.21
GO_REGULATION_OF_LIPID_CATABOLIC_PROCESS	19	1.72	0.21
GO_TRANSLATIONAL_INITIATION	80	1.74	0.21
GO_POSITIVE_REGULATION_OF_INSULIN_LIKE_GROWTH_FACTOR_RECEPTOR_SIGNALI NG_PATHWAY	5	1.72	0.21
GO_POSITIVE_REGULATION_OF_RESPONSE_TO_EXTERNAL_STIMULUS	98	1.73	0.21
GO_REGULATION_OF_COAGULATION	31	1.74	0.22
GO_HETEROTRIMERIC_G_PROTEIN_COMPLEX	16	1.72	0.22
GO_CHEMICAL_HOMEOSTASIS_WITHIN_A_TISSUE	5	1.71	0.22
GO_INTRAMOLECULAR_OXIDOREDUCTASE_ACTIVITY	22	1.71	0.22

GO_REGULATION_OF_TUMOR_NECROSIS_FACTOR_BIOSYNTHETIC_PROCESS	5	1.71	0.23
GO_PROTEIN_LOCALIZATION_TO_ENDOPLASMIC_RETICULUM	70	1.71	0.23
GO_PEPTIDASE_REGULATOR_ACTIVITY	54	1.71	0.23
GO_RETINOL_BINDING	7	1.71	0.23
GO_COPPER_ION_BINDING	18	1.69	0.23
GO_REGULATION_OF_EPIDERMAL_GROWTH_FACTOR_ACTIVATED_RECEPTOR_ACTIVITY	9	1.69	0.23
GO_REGULATION_OF_WOUND_HEALING	49	1.69	0.23
GO_POSITIVE_REGULATION_OF_LIPID_BIOSYNTHETIC_PROCESS	25	1.69	0.23
GO_NEGATIVE_REGULATION_OF_CELLULAR_RESPONSE_TO_INSULIN_STIMULUS	12	1.69	0.23
GO_PHOSPHATIDYLSERINE_BINDING	13	1.70	0.23
GO_INTERSTITIAL_MATRIX	4	1.69	0.24
GO_DEVELOPMENTAL_PIGMENTATION	23	1.69	0.24
GO_INSULIN_LIKE_GROWTH_FACTOR_RECEPTOR_BINDING	6	1.70	0.24
GO_GLYCOSAMINOGLYCAN_BINDING	70	1.69	0.24
GO_REGENERATION	68	1.70	0.24
GO_POSITIVE_REGULATION_OF_MAPK_CASCADE	186	1.69	0.24
GO_ENDOPLASMIC_RETICULUM_LUMEN	64	1.70	0.24
GO_CHEMOKINE_MEDIATED_SIGNALING_PATHWAY	6	1.70	0.24
GO_FATTY_ACID_ELONGATION	6	1.70	0.24